

**APPLICATION OF NANO BASE LUBRICANTS IN MACHINING
PROCESS FOR PERFORMANCE IMPROVEMENT**

MOHD SAYUTI BIN AB KARIM

**DISSERTATION SUBMITTED IN FULFILLMENT
OF THE REQUIREMENT FOR THE DEGREE
OF DOCTOR OF PHILOSOPHY**

**FACULTY OF ENGINEERING
UNIVERSITY OF MALAYA
KUALA LUMPUR**

2013

UNIVERSITY OF MALAYA
ORIGINAL LITERARY WORK DECLARATION

Name of candidate: **Mohd Sayuti bin Ab Karim**

Registration/Matric No.: **KHA100005**

Name of Degree: Doctor of Philosophy (Ph.D)

Title of Project Paper/Research Report/Dissertation/Thesis ("This Work"): **Application of Nano Base Lubricants in Machining Process for Performance Improvement**

Field of Study: Manufacturing Engineering

I do solemnly and sincerely declare that:

- (1) I am the sole author/writer of this work
- (2) This work is original
- (3) Any use or any work in which copyright exists was done by way of fair dealing and for permitted purposes and any excerpt or extract from, or reference to or reproduction of any copyright work has been disclosed expressly and sufficiently and the title of the work and its authorship have been in this work;
- (4) I do not have any actual knowledge nor do I ought reasonably to know that the making of this work constitutes an infringement of any copyright work;
- (5) I hereby assign all and every rights in the copyright to this work to this University of Malaya (UM), who henceforth shall be owner of the copyright in this work and that any reproduction or use in any form or by any means whatsoever is prohibited without written consent of UM having been first had and obtained;
- (6) I am fully aware that if in the course of making this work I have infringed any copyright whether internationally or otherwise, I may be subject to legal action or any other action as may be determined by UM.

Candidate Signature

Date:

Subscribed and solemnly declare before,

Witness's Signature

Name:

Date:

Designation:

ABSTRACT

For the various manufacturing industries, particularly aerospace and automotive applications, producing high-quality metal-based products is very important. During the turning and milling operations of metal workpieces, product quality is among the criteria with the potential to be improved by using a suitable lubrication system. The capability of the CNC milling process to produce complex shapes provides noteworthy advantages owing to its wide variety of parameter setups. In practice, the effectiveness of lubrication systems should be increased to enhance product quality. However, it is feasible to improve machining quality by introducing nanoparticles to the base lubricant, which becomes a nano-based lubricant. Nanoparticles within the lubricant reduce the friction at the tool-workpiece interface by means of rolling and sliding actions. In this research, nano-based lubricants containing SiO_2 , MoS_2 and carbon onion nanoparticles were developed by mixing each of these types of particles with ordinary mineral oil. By using the $L_{16}(4)^4$ orthogonal array experimental design for machining parameter optimization in the hard turning process, improvements of 10.48%, 10.48%, 8.52%, 8.22% and 10.55% for cutting force, power consumption, surface roughness, chip thickness and cutting temperature were gained, respectively, as opposed to the smallest values obtained in the preliminary experiments. Subsequently, upon implementing the $L_{16}(4)^3$ orthogonal array experimental design to the hard turning process with SiO_2 nano-based lubricant, power consumption was reduced by 37.19% compared with an ordinary lubrication system. From the Fuzzy logic approach, surface roughness and tool wear were found to be reduced by 23% and 15% when SiO_2 nano-based lubricant was employed in the hard turning process rather than an ordinary lubrication system. On the other hand, implementing the $L_{16}(4)^3$ orthogonal array design of experiment with SiO_2 nano base lubricant for the milling process reduced cutting force, surface roughness and cutting temperature by 25.02%, 26.28% and 29.34%

respectively, compared with ordinary lubrication. Alternatively, to investigate the effect of different types of nano-based lubricant in milling, the $L_{16}(4)^3$ orthogonal array experimental design was utilized with a MoS_2 nano-based lubricant. The outcome represents 2.62%, 2.56% and 0.04% enhanced cutting force, surface roughness and cutting temperature respectively, in contrast to the lowest values obtained from the initial experiments. Furthermore, performance enhancement in the milling process was additionally investigated by applying carbon onion nano-based lubricant in light of its tribological properties. The results signify that cutting force and surface roughness were reduced by 21.99% and 46.32% respectively, in the presence of optimum carbon onion in the lubrication system as opposed to using an ordinary lubrication system.

ABSTRAK

Dalam industri pembuatan, pengeluaran produk berasaskan logam dengan kualiti dan produktiviti yang tinggi adalah penting terutamanya dalam bidang aeroangkasa dan automotif. Dalam proses larik dan kisar, kualiti produk adalah salah satu kriteria yang boleh diperbaiki dengan cara mengaplikasikan sistem pelinciran yang sesuai. Pemesinan dengan menggunakan mesin larik dan kisar berasaskan CNC untuk menghasilkan produk khas yang rumit menjadi satu kelebihan yang perlu diberi perhatian bagi proses pengeluaran berasaskan logam kerana pelbagai parameter mesin yang boleh dikawal. Dalam amalan biasa, keberkesanan sistem pelinciran perlu ditambah untuk meningkatkan kualiti produk. Namun, kualiti pemesinan masih boleh dipertingkatkan dengan memperkenalkan sistem pelinciran asas nano yang bertindak sebagai elemen pelicin diantara muka cip alat pemotongan dan bahan pemesinan. Dalam kajian ini, pelincir berasaskan nano SiO_2 , MoS_2 dan Carbon Onion telah dibangunkan oleh dengan mencampurkan masing-masing bersama pelincir mineral biasa menjadi satu sistem pelinciran berasaskan nano untuk mengkaji peningkatan daya pemotong dalam operasi pemesinan CNC. Dengan menjalankan $L_{16}(4)^4$ reka bentuk eksperimen susunan ortogon untuk mengoptimumkan parameter proses pemesinan bahan keras, peningkatan sebanyak 10.48 %, 10.48 %, 8.52 %, 8.22 % dan 10.55 % untuk daya pemotongan, penggunaan kuasa, kekasaran permukaan, ketebalan cip dan suhu pemotongan telah diperolehi secara masing-masing setelah ia dibandingkan dengan nilai yang paling kecil yang diperolehi daripada eksperimen awal. Pada langkah berikutnya, apabila melaksanakan $L_{16}(4)^3$ reka bentuk eksperimen susunan ortogon dalam proses pemesinan bahan keras untuk mengoptimumkan parameter pelincir berasaskan SiO_2 nano, penggunaan kuasa boleh dikurangkan sebanyak 37.19%, berbanding dengan sistem pelinciran biasa. Dari pendekatan 'Fuzzy logic', kekasaran permukaan dan kadar kerosakan mata alat boleh

dikurangkan sebanyak 23% dan 15% dengan penggunaan pelincir berasaskan SiO₂ nano dalam proses pemesinan bahan keras berbanding dengan sistem pelinciran biasa. Sebaliknya, pelaksanaan rekabentuk eksperimen L₁₆(4)³ susunan ortogon dengan pelincir berasaskan SiO₂ nano untuk proses pemesinan kasar telah mengurangkan kuasa memotong, kekasaran permukaan dan suhu pemotongan sehingga 25.02%, 26.28% dan 29.34% secara masing-masing berbanding dengan sistem pelinciran biasa. Selain itu, untuk mengkaji kesan terhadap berlainan jenis pelincir berasaskan nano dalam proses pemesinan kasar, reka bentuk eksperimen L₁₆(4)³ susunan ortogon telah diplikasikan menggunakan pelincir berasaskan MoS₂ nano. Hasilnya, pengurangan sebanyak 2.62%, 2.56% dan 0.04% pada daya pemotongan, kekasaran permukaan dan suhu pemotongan dapat diperolehi secara masing-masing berbanding dengan nilai yang paling kecil yang diperolehi daripada eksperimen awal. Untuk tambahan, peningkatan prestasi dalam proses pemesinan kasar juga dikaji menggunakan pelincir berasaskan karbon onion kerana sifat tribologi yang bagus. Hasil yang diperolehi menggambarkan bahawa daya pemotongan dan kekasaran permukaan dapat dikurangkan sebanyak 21.99% dan 46.32% secara masing-masing dengan kehadiran carbon onion yang optimum dalam sistem pelinciran berbanding system pelinciran biasa.

ACKNOWLEDGMENT

I would like to express my sincere gratitude to everyone who provided essential guidance, encouragement, support, conscientiousness, advice and help to carry out my thesis project.

First of all, I would like to express my deepest appreciation, sincere thanks and gratitude to both of my supervisor Dr. Ahmed Sarhan and Prof. Mohd Hamdi Abd Shukor. I deeply appreciate their contributions, precious time to monitor, guidance, direction and funding to accomplish the whole project.

I gratefully acknowledge my all friends for their input, cooperation and concern especially Mr. Bizhan, Mr. Ooi, Mr. Ng and Mr. Saleem. Sincerest thanks to all individuals and authorities who helped me in time of needs.

Finally, I would like to extend my deepest gratitude to my beloved parents, wife, sons and family members for their unconditional love and regular moral support. The support helped me to maintain my determination at high level all the way throughout the project.

CONTENTS

ABSTRACT	iii
ABSTRAK.....	v
ACKNOWLEDGMENT	vii
LIST OF FIGURES	xiii
LIST OF TABLES	xxi
LIST OF EQUATIONS	xxiv
LISTS OF ABBREVIATION	xxv
CHAPTER 1 INTRODUCTION	
1.1 Introduction	1
1.2 Importance of the study.....	3
1.3 Problem statement	4
1.4 Research motivation	4
1.5 Objectives.....	5
1.6 Scope of study	6
1.7 Research Methodology.....	6
1.8 Arrangement of thesis content	10
CHAPTER 2 LITERATURE REVIEW	
2.1 Introduction	12
2.2 Computer numerical control (CNC) machining process.....	14
2.3 Lubrication system	15
2.3.1 Ordinary lubrication system.....	15
2.3.2 Minimal Quantity Lubricant	17
2.4 Nano base lubricant.....	19

2.4.1 Nano base lubricant performance.....	19
2.4.2 Nano base lubricant in machining to improve environmental issues...	23
2.4.3 Nano base lubricant in machining to improve cutting force	24
2.4.4 Nano base lubricant in machining to improve cutting temperature	27
2.4.5 Nano base lubricants in machining to improve tool wear	28
2.4.6 Nano base lubricants in machining to improve surface roughness	32
2.4.7 Nano base lubricants in machining to improve surface morphology...	34
2.5 Conclusion.....	36

CHAPTER 3 METHODOLOGY

3.1 Introduction	38
3.2 Nano base lubricant preparation.....	39
3.2.1 Lubricant oil	39
3.2.2 SiO ₂ nanoparticles	40
3.2.3 MoS ₂ nanoparticles	40
3.2.4 Carbon onion nanoparticles.....	41
3.2.5 Nano base lubricant preparation method.....	42
3.3 Experimental design.....	44
3.4 Experimental set up	47
3.4.1 Experimentation for optimization the cutting parameters in hard turning process	47
3.4.2 Experimentation for SiO ₂ nano base lubricant in hard turning process	52
3.4.3 Experimentation for SiO ₂ and MoS ₂ nano base lubricant in milling process	53

3.4.4 Experimental set up for carbon onion nano base lubricant in milling process	56
3.5 Measuring Instrument	58
3.5.1 Measuring cutting force	58
3.5.2 Measuring surface roughness	59
3.5.3 Measurement of cutting temperature	60
3.5.4 Measuring Tool wear	61
3.5.5 Surface morphology	62

CHAPTER 4 RESULTS, DATA ANALYSIS AND DISCUSSIONS

4.1 Introduction	64
4.2 $L_{16}(4)^4$ orthogonal array design of experiment for machining parameter optimization in hard turning process	65
4.2.1 Cutting force and power consumption	65
4.2.2 Surface roughness	75
4.2.3 Chip thickness ratio	80
4.2.4 Cutting temperature	82
4.3 $L_{16}(4)^3$ orthogonal array design of experiment in hard turning with SiO_2 nano base lubricant	87
4.3.1 Cutting force and power consumption	87
4.3.2 Surface roughness	92
4.3.3 Tool wear	96
4.4 Fuzzy logic approach in determining the effect of SiO_2 nano base lubricant on tool wear and surface roughness in hard turning	99
4.4.1 Fuzzy Logic Analysis	99
4.4.1 (i) Membership functions for input and output fuzzy variables	99

4.4.1(ii) Structure of fuzzy rules	101
4.4.1 (iii) Defuzzification.....	102
4.4.1 (iv) Investigating fuzzy model accuracy and error	104
4.5 $L_{16}(4)^3$ orthogonal array design of experiment in milling with SiO_2 nano base lubricant.....	107
4.5.1 Cutting force and power consumption	107
4.5.2 Surface roughness	115
4.5.3 Cutting temperature.....	119
4.5.4 Morphological analysis	128
4.5.4 (i) The morphology of the machined surface.....	131
4.5.4 (ii) The formation and growth of the protective SiO_2 thin film on the machined surface.....	132
4.5.4 (iii) Surface elemental mapping.....	135
4.5.4 (iv) Material migration during machining.....	137
4.6 Fuzzy logic approach in determining the effect of SiO_2 nano base lubricant on cutting force and surface roughness in milling process	139
4.6.1 Introduction	139
4.6.2 Data analysis and discussions	139
4.6.2 (i) Membership functions for input and output fuzzy variables.....	140
4.6.2 (ii) Structure of Fuzzy Rules	142
4.6.2 (iii) Defuzzification	143
4.6.2 (iv) Investigate the accuracy of the fuzzy model	146
4.6.3 Summary	151
4.7 $L_{16}(4)^3$ orthogonal array design of experiment in milling with MoS_2 nano base lubricant.....	152

4.7.1 Cutting force.....	152
4.7.2 Surface roughness	157
4.7.3 Cutting temperature.....	161
4.7.4 Morphological analysis	168
4.7.4 (i) FESEM analysis	168
4.7.4 (ii) XRD analysis.....	172
4.8 Reduction in cutting force and surface roughness of Al-2017-T4 alloy by using carbon onion nano base lubricant	175
4.8.1 Introduction	175
4.8.2 Data analysis and discussions	175
4.8.3 Summary	181
4.6 Discussions.....	183
CHAPTER 5 CONCLUSIONS	
5.1 Conclusions	188
5.2 Future works.....	189
REFERENCES	190
LIST OF PUBLICATION	199
PATENTS	200
AWARDS	200

LIST OF FIGURES

Figure 1.1 Distribution of the manufacturing cost in the European automotive industries (Nasir., 1998)	2
Figure 1.2 Research flow chart	9
Figure 2.1 The basic process and parameters in machining process.....	12
Figure 2.2 Evaluation of product quality in machining process	13
Figure 2.3 Factors and benefit for effective lubrication.....	17
Figure 2.4 Variation of thrust force with machining under (a) wet, (b) dry and (c) nano base lubricant assisted machining (Reddy et al., 2010)	25
Figure 2.5 Variation of tool temperature with machining time for (a) HSS and (b) carbide tool (Damera & Pasam, 2008).....	28
Figure 2.6 Variation of flank wear with machining time of carbide tool (Damera & Pasam, 2008)	29
Figure 2.7 Surface roughness (R_a) for different lubricants (HSS Tool)(Damera & Pasam, 2008)	33
Figure 2.8 The variation of surface roughness for dry hard turning and nano base lubricants assisted hard turning at different cutting speed (Dilbag & Rao, 2008).....	33
Figure 2.9 Variation of surface roughness for dry hard turning and nano base lubricants assisted hard turning at different cutting speed	34
Figure 3.1 Overall research plan for nano base lubricant research	39
Figure 3.2 Transmission electron microscopy (TEM) image of carbon onion	42
Figure 3.3 The nano base lubricant preparation process	44
Figure 3.4 Experimental set up	48
Figure 3.5 Okuma LB15 CNC lathe.....	48

Figure 3.6 Geometries of TaeguTec mixed ceramic tool (TaeguTec, 2011)	49
Figure 3.7 Geometries of Sandvik Coromant PDJNL25-25M-15 tool holder	49
Figure 3.8 Experimental set-up	54
Figure 3.9 The workpiece and tool paths	55
Figure 3.10 Schematic drawing of the nozzle	56
Figure 3.11 The experimental set up	56
Figure 3.12 The tool geometry	56
Figure 3.13 The workpiece and tool paths	58
Figure 3.14 Raytek Infrared Thermometer	61
Figure 3.15 Dino Lite Digital microscope	61
Figure 3.16 Tool flank wear measurement by using Somotech light microscope	62
Figure 3.17 Zeiss Gemini field emission scanning electron microscope (FESEM)	63
Figure 4.1 An example of measured cutting forces at cutting speed of 50 m/min, feed rate: 0.15 mm/rev and depth of cut 0.4 mm and MQL lubrication modes	65
Figure 4.2 TPM response graph for cutting force	67
Figure 4.3 S/N response graph for cutting force	68
Figure 4.4 Cutting force components which occurs during metal cutting in turning	71
Figure 4.5 The power consumption of the cutting tool for both lubrication modes.....	72
Figure 4.6 Graph of TPM response for surface roughness.....	76
Figure 4.7 Graph of S/N ratio response for surface roughness	77
Figure 4.8 TPM response graph for chip thickness ratio	81

Figure 4.9 TPM response graph for cutting temperature	83
Figure 4.10 S/N ratio response graph for cutting temperature	84
Figure 4.11 An example of measured cutting forces in X, Y and Z-axis direction after 20 seconds of cutting at a speed of 120 m/min, feed rate of 0.15 mm/rev and depth of cut of 0.5 mm by using (a) ordinary lubrication system and (b) SiO ₂ nano base lubricant	88
Figure 4.12 Variation of cutting performance at different concentration of SiO ₂	88
Figure 4.13 Variation in cutting forces for both modes of lubrication	89
Figure 4.14 The specific energy required at the cutting tool for both lubrication modes.....	90
Figure 4.15 The power required at the cutting tool for both lubrication modes	90
Figure 4.16 An example of surface roughness at 120 m/min cutting speed, 15 mm/rev feed and 0.5 mm depth of cut (nanoparticle concentration: 0.0 wt%, air pressure: 1 bar and nozzle angle 15°)	92
Figure 4.17 An example of measured surface roughness at 120m/min cutting speed, 15mm/rev feed rate and 0.5 mm depth of cut by using (a) ordinary lubricant and (b) nano base lubricant containing 0.2 wt% SiO ₂	93
Figure 4.18 An example of measured surface roughness for both lubrication modes at 120m/min cutting speed, 15mm/rev feed and 0.5 mm depth of cut by using (a) ordinary lubricant and (b) nano base lubricant containing 0.2 wt% SiO ₂	94
Figure 4.19 Surface roughness at different control factors (a) S/N response graph and (b) TPM response graph	95

Figure 4.20 An example of tool wear at 120 m/min cutting speed, 15 mm/rev feed and 0.5 mm depth of cut (Concentration: 0.0 wt%, air pressure: 1 bar and nozzle angle 15°)	96
Figure 4.21 Tool wear at different control factors (a) S/N response graph and (b) TPM response graph	98
Figure 4.22 Membership function for the input variables (a) nanoparticle concentration, (b) air pressure and (c) nozzle angle	100
Figure 4.23 Membership function for the output variable of (a) tool wear and (b) surface roughness	101
Figure 4.24 The predicted tool wears obtained by fuzzy logic in relation to (a) change of lubrication pressure and SiO ₂ concentration and (b) nozzle angle and lubrication pressure	103
Figure 4.25 The predicted surface roughness obtained by fuzzy logic in relation to (a) change of SiO ₂ concentration and nozzle angle and (b) lubrication pressure and nozzle angle	104
Figure 4.26 TPM and S/N response graphs of cutting force at different control factors (a) concentration of the nanoparticles, control factor A, (b) air pressure, control factor B and (c) nozzle orientation, control factor C	109
Figure 4.27 The cutting forces for both modes of lubrication	112
Figure 4.28 Reduction in cutting force	112
Figure 4.29 Changes in specific energy during the cutting process for both modes of lubrication	113
Figure 4.30 Requirement of power at the cutting tool for both lubrication modes	113
Figure 4.31 Reduction in power consumption for both lubrication modes	114

Figure 4.32 TPM and S/N response graphs of surface roughness at different control factors (a) concentration of the nanoparticles, control factor A, (b) air pressure, control factor B and (c) nozzle orientation, control factor C.....	116
Figure 4.33 TPM and S/N response graphs of cutting temperature at different control factors (a) concentration of the nanoparticles, control factor A, (b) air pressure, control factor B and (c) nozzle orientation, control factor C.....	120
Figure 4.34 Illustration of (a) cutting forces in the X, Y and Z-axis directions and (b) surface roughness at 5000 min ⁻¹ cutting speed, 100 mm/min feed rate and 5 mm depth of cut using 0.2 wt% nanoparticles in the lubricant.....	129
Figure 4.35 Effects of SiO ₂ nanoparticles on (a) cutting force, (b) cutting temperature and (c) surface roughness.....	130
Figure 4.36 FESEM image on the surface machined by nano base lubricants containing SiO ₂ nanoparticles of (a) 0 wt%, (b) 0.2 wt%, (c) 0.5 wt% and (d) 1.0 wt%.....	133
Figure 4.37 Energy dispersive X-Ray (EDX) analysis on the surface machined by nano base lubricants containing SiO ₂ nanoparticles of (a) 0 wt%, (b) 0.2 wt%, (c) 0.5 wt% and (d) 1.0 wt%.....	134
Figure 4.38 Surface elemental mapping of the samples machined by nano base lubricants containing SiO ₂ nanoparticle of (a) 0.2 wt%, (b) 0.5 wt% and (c) 1.0 wt%	135

Figure 4.39 Elemental mapping and EDX spectroscopy on a machined surface at 8 mm depth of cut, 5000 min ⁻¹ cutting speed and 100 mm/min feed rate	138
Figure 4.40 Membership function for inputs variables (a) nanoparticle concentration, (b) air pressure and (c) Nozzle angle	141
Figure 4.41 Membership function for the output variables of (a) cutting force, (b) cutting temperature and (c) surface roughness	142
Figure 4.42 The predicted cutting force by fuzzy logic in relation to lubrication parameters (a) air pressure and SiO ₂ concentration and (b) SiO ₂ concentration and nozzle angle	144
Figure 4.43 The predicted cutting temperature by fuzzy logic in relation to lubrication parameters (a) air pressure and SiO ₂ concentration and (b) SiO ₂ concentration and nozzle angle	145
Figure 4.44 The predicted surface roughness by fuzzy logic in relation to lubrication parameters (a) SiO ₂ concentration and air pressure and (b) SiO ₂ concentration and nozzle angle	146
Figure 4.45 Comparison of the predicted and measured values of Al-6061-T6 alloy during milling operation (a) cutting force, (b) cutting temperature and (c) surface roughness	148
Figure 4.46 <i>S/N</i> response graphs of cutting force for (a) nanoparticles concentration <i>A</i> , (b) air pressure <i>B</i> and (c) nozzle orientation <i>C</i>	154
Figure 4.47 The contribution diagram and cumulative contribution for cutting force	156
Figure 4.48 <i>S/N</i> response graphs of surface roughness for (a) nanoparticles concentration <i>A</i> , (b) air pressure <i>B</i> and (c) nozzle orientation <i>C</i>	158

Figure 4.49 The contribution diagram and cumulative contribution for surface roughness.....	160
Figure 4.50 <i>S/N</i> response graphs of cutting temperature for (a) nanoparticles concentration <i>A</i> , (b) air pressure <i>B</i> and (c) nozzle orientation <i>C</i>	162
Figure 4.51 The contribution diagram and cumulative of contribution for cutting temperature.....	164
Figure 4.52 FESEM on samples (a), (b), (c) and (d) which machined with 0, 0.2, 0.5 and 1.0 wt% concentration of MoS ₂ respectively.....	171
Figure 4.53 The presence of nanoparticle reduce the tool-workpiece in contact.....	172
Figure 4.54 X-ray Diffraction (XRD) on samples (a), (b) and (c) under machining with 0.2, 0.5 and 1 wt % concentration of MoS ₂ nanoparticles ,respectively	173
Figure 4.55 Cutting force of the Al-2017-T4 alloy machined nano base lubricants containing carbon onion (a) 0 wt%, (b) 0.5 wt%, (c) 1.0 wt% and (d) 1.5 wt%.....	176
Figure 4.56 Surface roughness of the Al-2017-T4 alloy machined nano base lubricants containing carbon onion (a) 0 wt%, (b) 0.5 wt%, (c) 1.0 wt% and (d) 1.5 wt%.....	178
Figure 4.57 Effects of carbon onion nanoparticles in the lubricant during CNC end milling of Al-2017-T4 alloy (a) cutting force and (b) surface roughness.....	179
Figure 4.58 Stereoscopic three dimensional photographs of the Al-2017-T4 alloy surface during CNC end milling by using nano base lubricant containing carbon onion of (a) 0 wt%, (b) 0.5 wt%, (c) 1.0 wt% and (d) 1.5 wt%	181

Figure 4.59 Primary and secondary shear zone.....	183
Figure 4.60 Merchant circle of cutting mechanism.....	184
Figure 4.61 Shear zones distribution metal cutting process.....	185
Figure 4.62 Shear zones area in metal cutting process	185
Figure 4.63 Friction in cutting mechanism	186
Figure 4.64 Rolling and sliding action of the nanoparticles at the tool-chip interface	187

LIST OF TABLES

Table 3.1 The properties of ECOCUT SSN 322 lubricant oil	39
Table 3.2 Mechanical properties of SiO ₂	40
Table 3.3 Standardized L ₁₆ (4) orthogonal array, the sixteen experiments with detail of the combination levels.....	46
Table 3.4 Factors and experimental condition levels.....	47
Table 3.5 Control factors and experimental condition levels.....	47
Table 3.6 Physical properties of TaeguTec DNGA 150608 mixed ceramic tool.....	49
Table 3.7 Chemical compositions of AISI4140 alloy steel.....	50
Table 3.8 Properties of Mobilcut 102 water soluble cutting fluid.....	50
Table 3.9 Characteristics of ECOCUT HSG 905 S	51
Table 3.10 Specifications of adjustable spot cooler vortex tube 3825.....	51
Table 3.11 Mechanical properties of AISI4140 steel.....	52
Table 3.12 Experimental conditions.....	53
Table 3.13 Mechanical properties of aluminium (Al6061-T6).....	54
Table 3.14 The mechanical properties of Duralumin AL-2017	57
Table 3.15 Measuring instrument to evaluate the experimental response	58
Table 3.16 Specifications for surface roughness measurements.....	60
Table 3.17 K-Type Testo 925 thermocouple specification	60
Table 3.18 Specifications of Raytek Infrared thermometer	61
Table 4.1 TPM and S/N ratio for cutting force	66
Table 4.2 TPM and S/N Response data for cutting force.....	67
Table 4.3 Pareto ANOVA analysis for cutting force	69
Table 4.4 TPM and S/N ratio for surface roughness.....	75
Table 4.5 TPM and S/N response data for surface roughness	76

Table 4.6 Pareto ANOVA analysis for surface roughness	78
Table 4.7 TPM and S/N ratio for chip thickness ratio	80
Table 4.8 TPM response for chip thickness ratio	80
Table 4.9 TPM and S/N ratio for cutting temperature	82
Table 4.10 TPM and S/N response data for cutting temperature	83
Table 4.11: Pareto ANOVA analysis for cutting temperature	85
Table 4.12 Measured value of surface roughness	92
Table 4.13 The calculated S/N and TPM response for surface roughness	95
Table 4.14 The response of tool wear	96
Table 4.15 The calculated of S/N and TPM response data for tool wear	97
Table 4.16 Fuzzy linguistic and abbreviation of variables for each parameter	99
Table 4.17 The basis of Mamdani Fuzzy logic	102
Table 4.18 The accuracy and error of the fuzzy logic model prediction	105
Table 4.19 The TPM and S/N ratio values for cutting force	107
Table 4.20 The TPM and S/N response data for cutting force	108
Table 4.21 Interaction data analysis for cutting force	110
Table 4.22 Pareto ANOVA analysis for cutting force	111
Table 4.23 The calculated (S/N) ratio and TPM values for surface roughness.	115
Table 4.24 The TPM and S/N response data for surface roughness	115
Table 4.25 Interaction data analysis for surface roughness	117
Table 4.26 Pareto ANOVA analysis for surface roughness	118
Table 4.27 The calculated TPM and S/N ratio for cutting temperature	119
Table 4.28 The TPM and S/N response data for cutting temperature	119
Table 4.29 Interaction data analysis for cutting temperature	121
Table 4.30 Pareto ANOVA analysis for cutting temperature	122

Table 4.31 Elemental composition of the surfaces machined by nano base lubricants containing different amount of SiO ₂ nanoparticles	134
Table 4.32 Fuzzy linguistic and abbreviation of variables for each parameter.....	140
Table 4.33 Basis of Mamdani fuzzy logic for cutting force, cutting temperature and surface roughness	143
Table 4.34 The input parameters for the accuracy and error prediction of the fuzzy logic model	147
Table 4.35 The prediction of the accuracy and error of the fuzzy logic model	147
Table 4.36 The measured values of cutting force	152
Table 4.37 The S/N response data for cutting force.....	153
Table 4.38 Interaction data analysis for cutting force	155
Table 4.39 Pareto ANOVA analysis for cutting force	156
Table 4.40 The measured values of surface roughness	157
Table 4.41 The S/N response data for surface roughness	157
Table 4.42 Interaction data analysis for surface roughness.....	159
Table 4.43 Pareto ANOVA analysis for surface roughness.....	160
Table 4.44 The measured values of cutting temperature.....	161
Table 4.45 The S/N response data for cutting temperature.....	161
Table 4.46 Interaction data analysis for cutting temperature	163
Table 4.47 Pareto ANOVA analysis for cutting temperature	164
Table 4.48 The average cutting force and surface roughness of Al-2017-T4 alloy machined by carbon onion nano base lubricant	175

LIST OF EQUATIONS

$F_c = Fx_2 + Fy_2$...Equation 3.1 59
$S_A = (A_1 - A_2)^2 + (A_1 - A_3)^2 + (A_2 - A_3)^2 + (A_3 - A_4)^2$...Equation 4.1 68
$P = FcVc \quad (\text{Watt})$...Equation 4.2 70
$E_c = \frac{F_c V_c}{f d_a d_r} \quad (\text{J/mm}^3)$...Equation 4.3 89
$e_i = \left(\frac{ R_m - R_p }{R_m} \right) \times 100\%$...Equation 4.4 105
$A = \frac{1}{N} \sum_{i=1}^N \left(1 - \frac{ R_m - R_p }{R_m} \right) \times 100\%$...Equation 4.5 105

LISTS OF ABBREVIATION

CNC	Computer Numerical Control
MQL	Minimal Quantity Lubricant
DLC	Diamond-Like Carbon
SiO ₂	Silicone Dioxide
TPM	Target Performance Measure
S/N	Signal to Noise
MoS ₂	Molybdenum disulfide
HSS	High Speed Steel
HV	Vickers Hardness
F _x	Cutting Force, X-direction
F _y	Cutting Force, Y-direction
F _z	Cutting Force, Z-direction
F _c	Cutting Force
F _t	Tangential Force
F _r	Radial Force
R _a	Surface Roughness
E _c	Specific Energy
P	Power
V _c	Cutting Speed
d_a	Axial Depth of Cut
d_r	Radial Depth of Cut

CHAPTER 1 INTRODUCTION

1.1 Introduction

Metal based products are very popular due to their excellent mechanical properties such as hardness and toughness. Hence, the metal based products are considered as a common material for many purposes. As for an example, the hardened steel is commonly used for critical mechanical components in automotive industries to build the crank shaft, bearing and gears. On the other hand, aluminium alloys (Al-2017-T4 and Al-6016-T6) are referred to the group of “Aerospace Alloys” for their practical applications in aviation industries. In manufacturing of metal based products, turning and milling are considered as an important process due to its capability to machine these kinds of materials to make variety of complicated shapes.

In metal cutting process, scientists and engineers have made great efforts to improve the inherently poor thermal conductivities of traditional fluids, such as water, oil and ethylene glycol. There are two main functions of cutting fluids, which include lubricating and cooling. The lubricating emphasis on high degree of lubricity and its function is to reduce the friction (Rao & Srikant, 2006) and adhesion between the workpiece, chip and tool. While the cooling requires excellent heat transfer characteristics and it is essential to cool the tool, workpiece or other parts of the machine efficiently during machining (Fratila, 2009; Weinert et al., 2004).

However, the usage of conventional flooding operation during machining has become a huge liability because of hazardous wastes and economy. Figure 1.1 presents the distribution of manufacturing cost in the European automotive industries (Nasir., 1998). From this figure it can be seen that the cost of the lubrication system can reach as high as 16.9% compared to other cost.

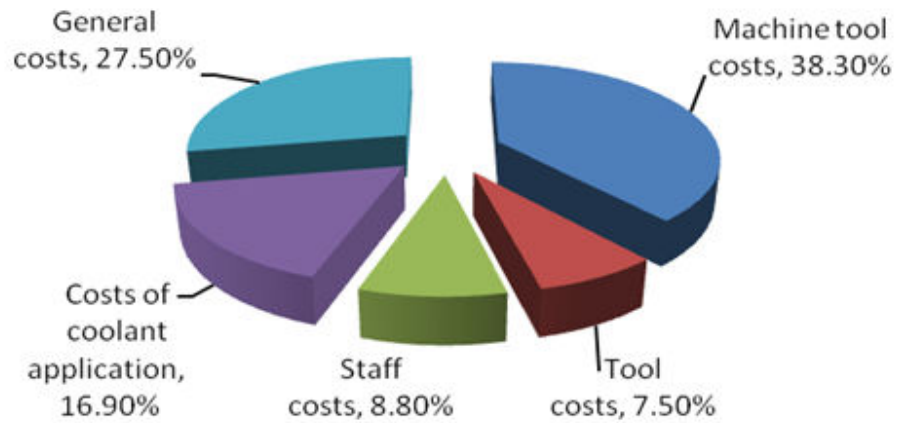


Figure 1.1 Distribution of the manufacturing cost in the European automotive industries (Nasir., 1998)

Therefore, in order to improve the machining processes in metal cutting operation, it is clear that a multi-pronged approach must be used. At present, many efforts are being undertaken to develop advanced machining processes by using less lubricant. In this research work, the development of nano base lubricant is explored in metal cutting process. The nano base lubricant is developed to sustain in the high temperatures during machining process in addition with non-toxicity, easy application, less lubricant and economic feasibility. As an example, silicone dioxide (SiO_2) and carbon onion nanoparticles are successfully incorporated into nano base lubricant to improve the tribological properties in sliding bearing. However, the application of nano base lubricant during machining (turning and milling process) of metal based product is not clear and not yet established. For the development of more advanced machining processes, the implication of nano base lubricant towards performance improvement in metal cutting process is studied in this research work.

1.2 Importance of the study

The search for performance improvement in machining process is always a challenge in the manufacturing industries. The performance improvement in machining process greatly depends on the effectiveness of the lubrication system. This study is important since it covers the following aspects:

- Development of SiO_2 , MoS_2 and carbon onion nano base lubricants for performance improvement in machining process
- $L_{16}(4)^4$ orthogonal array design of experiment machining parameter optimization in hard turning process
- $L_{16}(4)^3$ orthogonal array design of experiment in hard turning process with SiO_2 nano base lubricant
- Fuzzy logic approach in determining the effect of SiO_2 nano base lubricant on tool wear and surface roughness in hard turning process
- $L_{16}(4)^3$ orthogonal array design of experiment in milling process with SiO_2 nano base lubricant
- Fuzzy logic approach in determining the effect of SiO_2 nano base lubricant on cutting force and surface roughness in milling process
- $L_{16}(4)^3$ orthogonal array design of experiment in milling process with MoS_2 nano base lubricant
- Performance improvement in milling process by application of carbon onion nano base lubricant

1.3 Problem statement

Though the significance of lubrication in machining process is widely recognized, the usage of conventional flooding process during machining has become a huge liability. The Environmental Protection Agency regulates the disposal lubricant waste, and many countries and communities have classified them as hazardous material. In economic terms, it is reported that the cost related to the lubrication and cutting fluid can reach up to 17% of the total production cost which is normally higher than that the cost of cutting tool equipments (Nasir., 1998). At present, many efforts have been taken to develop advanced machining processes by using less lubricants and more improvement and advances is required in this field for better and healthy living style (Sreejith & Ngoi, 2000).

The capability of the computer numerical control (CNC) for turning and milling operation makes a noteworthy advantage during batch production of metal based product. However, the demand for high quality focuses attention on the surface finishing of the product because it represents the appearance, function and reliability. The improvement of machining process also focus on less cost, reduction on power consumption, less lubricant consumption in addition with environmental concern. Moreover, the tribological characteristic of machining process requires improvement on the friction characteristic at the tool-chip interface by introducing correct application of lubricants.

1.4 Research motivation

In engineering applications, high precision materials with accurate dimension are developed by using different machining process. The CNC turning and milling machine is capable to produce a wide variety of complicated shape by setting proper parameters compared to other machining processes. Improper cutting process results product with inferior surface finish, appearance, function and reliability. To overcome this problem, the friction between the tool and workpiece should be reduced by improving the effectiveness

of existing lubrication systems. It is expected that introducing nanoparticles in the base lubricant can reduce the cutting force, cutting temperature and surface roughness with better performance in machining process. It is believed that the rolling and sliding actions of nanoparticles at the tool-chip interface reduces the coefficient of friction significantly.

1.5 Objectives

In order to improve the performance of machining process by application of nano base lubricants, this study embarks on the following objectives:

1. To develop SiO_2 , MoS_2 and carbon onion nano base lubricants for performance improvement in machining process
2. To optimize the machining parameters in hard turning process by using $L_{16}(4)^4$ orthogonal array design of experiment
3. To optimize the lubrication parameters in hard turning process by using $L_{16}(4)^3$ orthogonal array design of experiment
4. To determine the effect of SiO_2 nano base lubricant on tool wear and surface roughness in hard turning process by using Fuzzy logic approach
5. To optimize the lubrication parameters in milling process by using $L_{16}(4)^3$ orthogonal array design of experiment with SiO_2 nano base lubricant
6. To determine the effect of SiO_2 nano base lubricant in milling process on cutting force and surface roughness by using Fuzzy logic approach
7. To optimize the lubrication parameters in milling process by using $L_{16}(4)^3$ orthogonal array design of experiment with MoS_2 nano base lubricant
8. To improve the performance in milling process on cutting force and surface roughness with carbon onion nano base lubricant

1.6 Scope of study

In this research, three types of nano base lubricant containing SiO₂, MoS₂ and carbon onion nanoparticles were investigated during metal cutting process. Several parameters of the nano base lubricant were varied during the experimentation including the concentration of nanoparticles in the lubricant. In this research, both turning and milling process were utilized in order to determine the effectiveness of the nano base lubricants in machining process. The workpiece materials were selected from the hardened and ductile categories of metal since these are the common materials used in industrial practice. To improve the performance in machining process, the measurements were conducted to evaluate the cutting force, cutting temperature, surface roughness, tool wear, chip formation and surface morphology by using appropriate measuring equipment. After the experimental results were collected, various analyses were conducted to ensure the performance improvements were obtained in machining process.

1.7 Research Methodology

The detailed research methodology of this work is categorized into several stages as in the research flow chart is presented in the Figure 1.2. The initial stage of the research was literature review, field visit and setup of the experiments which are discussed below.

a. Literature review and field visit

The information for characterizing the nano base lubricant during machining process was gathered at this stage. The preliminary data were collected from the various sources, such as, preliminary experimentation, reported publication etc. The literature review and field visit from related research is taken into consideration because of the following reasons.

- Analyzing the existing problems, setting problem statements and objectives
- Collecting preliminary data, locating the major variables and parameters

- Prediction of result towards achieving the objectives
- Conduct experiments to optimize cutting parameters in hard turning process

b. Experimental set up for SiO₂ and MoS₂ nano base lubricant system

At this stage, the appropriate experimental design was identified to ensure the experimentation is capable to be conducted. Several steps of experimentation were conducted by using the recommended parameters.

- Producing SiO₂ and MoS₂ nano base lubricant having different concentrations of nanoparticles
- Selection of the workpiece material and cutting tools
- Implementation of the nano base lubricant in turning and milling process
- Usage of measuring equipment to evaluate the response

c. Experimental set up for carbon onion nano base lubricant

At this stage, the suitable experimental design was identified to ensure the experimentation is capable to conduct. Several steps of experimentation were conducted by using the recommended parameter.

- Producing carbon onion nano base lubricant having different concentrations of nanoparticles
- Selection of the workpiece material and cutting tools
- Implementation of the nano base lubricant in milling process
- Usage measuring equipment to evaluate the response

d. Data collection

All data from the experimentation were collected for the analysis purposes for better understanding the behaviors of nano base lubricants.

e. Data analysis

All data were analyzed by using various techniques to explain the facts and mechanism including response analysis, pareto ANOVA, fuzzy logic approach and interaction analysis.

f. Report writing

In this final stage, all information were gathered in a systematic format and a report is written together with the details of experimentation and confirmation test.

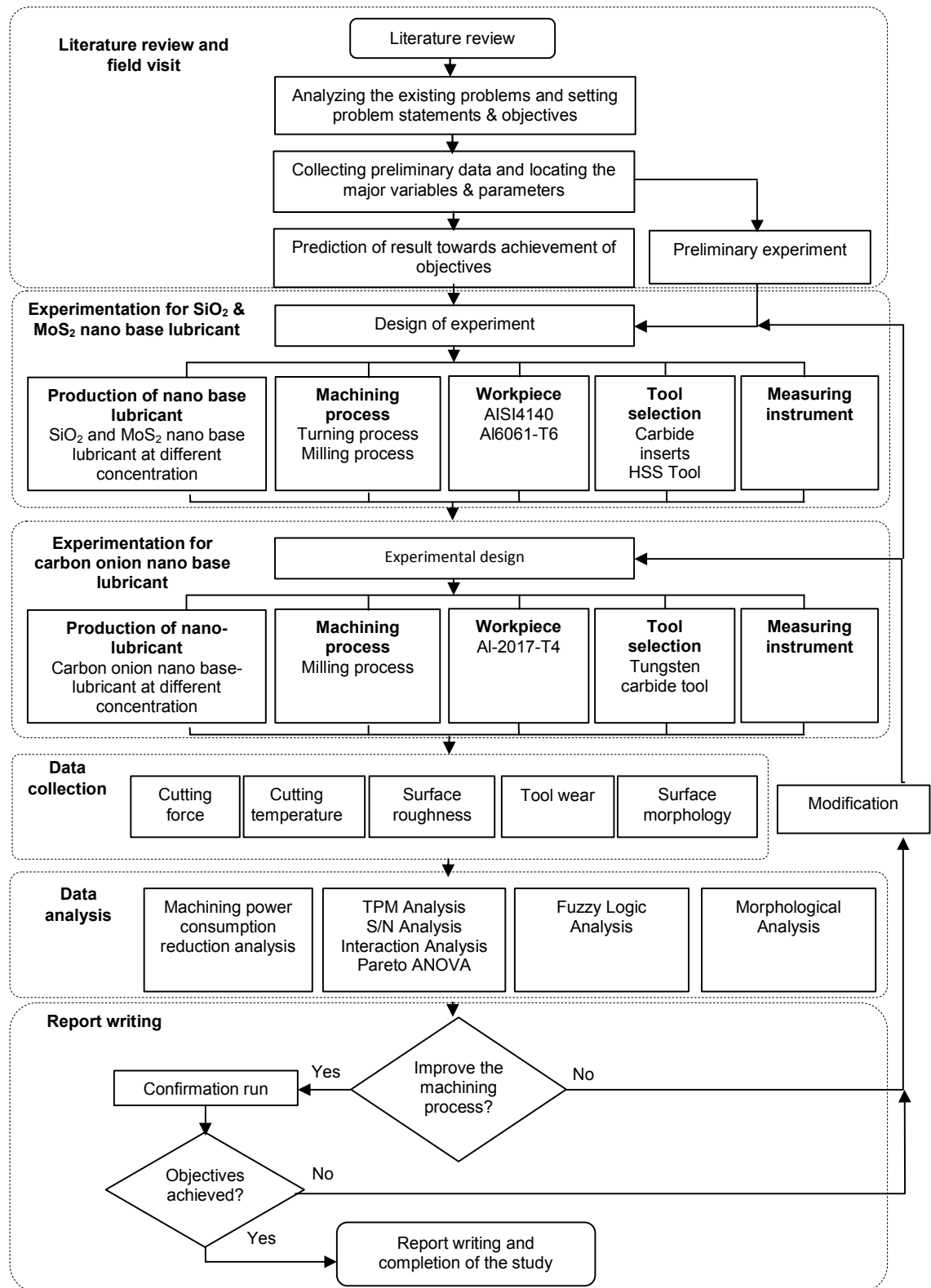


Figure 1.2 Research flow chart

1.8 Arrangement of thesis content

This thesis comprises of five chapters and is organized to explain the background of the study, literature review, methodology, results together with discussion and conclusions. The details of the chapters are summarized below:

Chapter 1 provides a general view on the background and gives the scenario of the problems to be investigated as a motivation of this study. Next, the objectives of this study are identified. It also states the scopes and gives a brief methodology this was used to solve the problems.

Chapter 2 presents the literature review on all issue related to nano base lubricant. The relevance and similar concepts reported by previous researchers are highlighted. This helps to understand the subject matter presented in this work. Most importantly, the research gap is realized for establishing the problem statement, objectives, scopes and research methodology.

Chapter 3 describes the research methodology used in this study which consists of experimental design, experimental setups, procedures, materials and apparatus used for conducting the experiments and collecting data. The variables, procedures of experiment and data collection techniques are clearly outlined. The detail of operating parameters and specifications of all equipment are also included.

Chapter 4 exhibits the findings and results obtained from the experiments. Optimization of nano base lubricants containing SiO_2 , MoS_2 and carbon onion nanoparticles in turning and milling process is presented in this chapter. The obtained data is analyzed and discussed to ensure the improvements of the machining process were obtained.

Chapter 5 concludes the findings of this study. Lastly, recommendations for further considerations and future research works pertaining to this project are suggested and proposed.

CHAPTER 2 LITERATURE REVIEW

2.1 Introduction

In manufacturing industries a huge number of metal cutting and shaping operations are involved during processing and production. The demand for better product quality demands higher productivity in addition with more features in a single component. This situation evolves more challenges in manufacturing a product by machining, particularly in the area of liberalization and global cost competitiveness. These circumstances insist high material removal rate, high stability and long life of a single cutting tools (Reddy et al., 2010).

Cutting parameters are playing a very important role during machining and it should be wisely selected with the proper selection of parameters in order to produce the product with desired quality. In general, the key parameters which greatly affect the machining performance are cutting tool variable, workpiece/material variable, cutting condition and lubrication type. Figure 2.1 shows the basic parameters in machining process.

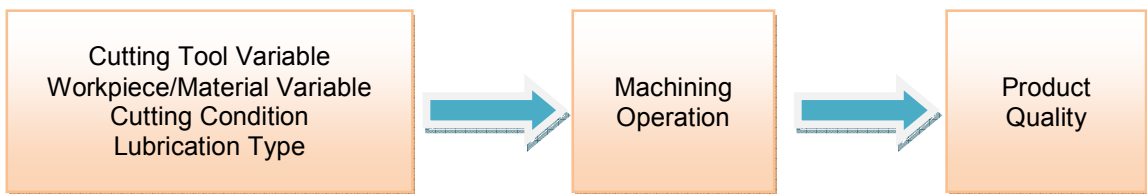


Figure 2.1 The basic process and parameters in machining process

The product quality can be evaluated by investigating several features such as surface roughness, cutting force, cutting temperature, chip formation, and tool wear as it is shown in the Figure 2.2. Out of these parameters, surface roughness is the most important design feature and it is usually used to measure the quality in machining process. Cutting force is another important feature that should be reduced during machining process since it

leads to undesirable vibrations resulting in poor surface finish (Reddy & Rao, 2006). During machining, the friction between tool and workpiece creates plastic deformation in the machining zone which generates heat. The temperature at the contact zone between the tool and workpiece rises at a fast rate due to rapid accumulation of heat. This phenomenon directly affects quality of products of dimensional accuracy and surface finish. It is possible to reduce the tool wear by lowering the heat generation during the machining process through the reduction of coefficient of friction. In general, the quality, efficiency, effectiveness, and overall economy of a machining process largely depend on the machinability characteristic of the tool and workpiece material. In details, the machinability is characterized by:

- i. The cutting temperature, which affects the product quality and tool performance
- ii. Pattern and mode of chip formation
- iii. Magnitude of cutting force, which affect power requirement, dimensional accuracy and vibration
- iv. Surface finish
- v. Tool wear and tool life.

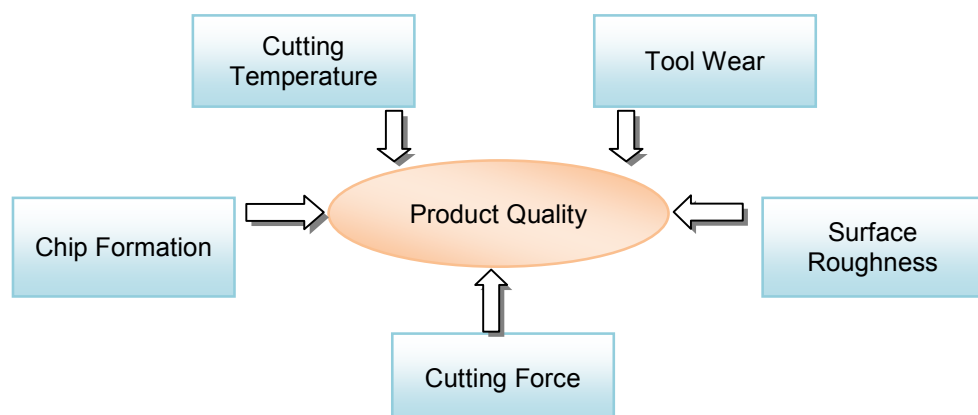


Figure 2.2 Evaluation of product quality in machining process

Previously it is mentioned that a huge amount of heat is generated during metal cutting process due to plastic deformation of workpiece material, friction at the tool-chip interface and friction between the clearance face of the tool and workpiece (Reddy & Rao, 2006). The turning process is widely used as a metal removal process in manufacturing industries which is associated with high cutting forces and high temperature (Reddy & Nouari, 2011). Products with higher feed and depth of cut requires higher machining and are inherently associated with high cutting force, higher cutting temperature with large amount of heat velocity (Reddy et al., 2010). On the other hand, temperature of the end milling cutting tool is not constant and undergoes a heat cycle during the intermittent cutting. It is found that the heat cycle is one of the main reasons for tool failure because of wear or fracture. The distribution of temperature and the peak temperature of cutting tool are also very important factors for tool failure (Ueda et al., 2001).

Hence, lubrication becomes a critical component to minimize the effects of cutting forces and temperature on cutting tool and workpiece during machining process. Dimensional instability and uncertain failure of cutting tools caused by high temperature can be minimized by using proper lubrication. On the other hand the surface finish and accuracy of the product is also affected by the heat generated in machining process which can be reduced by proper lubrication (Reddy et al., 2010).

2.2 Computer numerical control (CNC) machining process

The computer numerical control (CNC) machining process is one of the most advanced machining processes which involves computer aided machining tools. The CNC is commonly used in material removal machining process such as turning and milling. A computer program named G-code is used to control the movement of the tool by using numerical method based on the design and the shape of final product. The G-code is developed from computer aided design (CAD) data by using computer aided manufacturing

(CAM) program. By using this program, the machine tool can be controlled in terms of speed, feed rate, depth of cut and tool path. CNC aided machining process results more precise, repetitive and reliable compare to other manual process.

Requirements for high precision from machining process, a number of complicated shapes with varieties are required to be developed. In CNC milling machine, a variety of set-up parameters can be controlled which makes the machining process superior compared to other manual machining processes. The capability of CNC aided milling machine is noteworthy to make complicated products for batch production.

2.3 Lubrication system

2.3.1 Ordinary lubrication system

The tribological characteristic of machining process can be improved by introducing cutting fluid at the machining zone. Application of cutting fluids at the machining zone influences the performance of machining because of its lubrication and cooling action (Reddy et al., 2010; Tönshoff & Denkena, 2013). Cutting fluid also helps to dissipate the heat generated at the machining zone. As for example, in grinding process cutting fluid is used to protect workpiece and wheel from damages such as thermal burn, residual stress, phase transformation and microcracks. However, implementation of cutting fluid raises some techno-environmental problem like environmental pollution, water contamination, health issue to the operators etc (Reddy & Rao, 2005; Reddy & Rao, 2006; Tan et al., 2002; Venkata Rao, 2011).

Conventional cutting fluid in grinding has raised some issues in advanced machining process due to their restricted accessibility of coolants at the machining zone and their insufficient heat transfer rate (Alberts et al., 2009). In addition, conventional cutting fluids also incur a major portion of the total manufacturing cost (Sreejith & Ngoi, 2000). Some researchers estimated that the cost required for cutting fluid is frequently

higher than the cost of cutting tools. This is due to the reason that many of these fluids are health hazard, hence raising major environmental concerns. So the management and recycling process of these cutting fluids are relatively higher than other parts and processes in the industries (Tan et al., 2002). Therefore, industrial practitioners are looking for cutting fluids which possess both functions in order to reduce severe friction and wear, and hence improve the tribological action of cutting fluids (Ginzburg et al., 2002; Liu et al., 2004; Thottackkad et al., 2012; Zhou et al., 1999).

Moreover, the development of governmental pollution preventing initiatives and increasing consumer focus on industrial regulations has put increased pressure on industries to minimize the use of cutting fluids (Reddy & Rao, 2006). Therefore, the use of less cutting fluids during machining has become the prime priority to minimize all these adverse factors (Sharma et al., 2009).

In other words, industries are struggling to achieve an eco-friendly and sustainable manufacturing process. For this reason the fluid maintenance, fluid life, waste management and health issue of the workers are emphasized (Reddy et al., 2010). Moreover more intense research is required towards the elimination of cutting fluids even though many techniques and equipment have been developed for fluid maintenance and waste disposal. On the other hand, researches in the direction of dry machining, cryogenic cooling, minimal quantity lubricant (MQL) and solid lubricants should be carried out. Effective lubrication minimizes the friction between tool and workpiece which reduces the heat generation to some extent. Factors and benefits for effective lubrication are depicted in Figure 2.3.

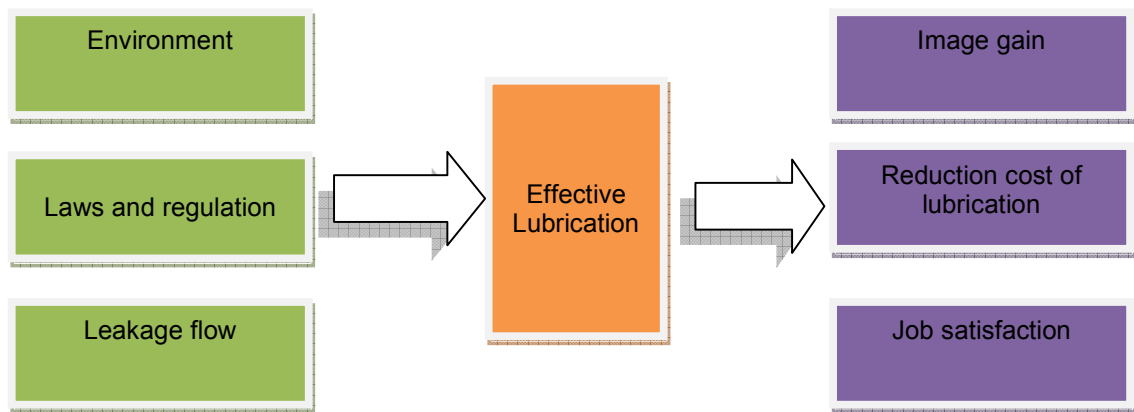


Figure 2.3 Factors and benefit for effective lubrication

In high-speed machining process, conventional cutting fluid often fails to penetrate into the chip-tool interface and thus cannot exercise its characteristic effectively. Insufficient heat transfer rate of the cutting fluids reduces the cutting speed due to the requirement of long time for cooling. To solve this problem, high pressure jet of soluble oil can be effectively applied at the tool-chip interface since it can reduce the cutting temperature and thus improve the tool life (Dhar et al., 2007).

Applying cutting fluids in a metal cutting process can reduce the tool wear and improve the surface quality of the product. However, cutting fluids has negative effects as well such as environment pollution, health issue and high cost. Therefore, there is an increasing demand to reduce the amount of cutting fluid in industries during machining. To serve that purpose, a minimal-cutting-fluid technique is studied in this research.

2.3.2 Minimal Quantity Lubricant

Industries and researchers are searching an alternative to reduce the amount of cutting fluids in metal cutting process to obtain better safety, reduce environmental pollution and gain economical benefits. Beside this, the determination of minimal quantity lubrication (MQL) provides some advantages in terms of reducing the tool wear (Hadad,

2010). It is reported that application of MQL to the tool rake and tool flank increases the tool life (Attanasio et al., 2006).

Researcher concluded that MQL machining combined with the mixture-supply system provides almost the same performance as conventional machining with flood lubrication (Dixit et al., 2012; Tawakoli et al., 2011). This finding is also supported by researchers with further conclusion that the requirement of cutting force in MQL technique is less than dry cutting and flood cooling (Aoyama, 2002; Dhar et al., 2007; Kelly & Cotterell, 2002; Rahman et al., 2002). It is found that the MQL technique is very effective at low speed, low feed rate and low depth of cut in comparison with flood cooling (Shen et al., 2008). Investigation on the different lubrication conditions during low-speed milling concluded that mineral oil spray in form of mist prevents the adhesion of work material on the machined surface and reduces the severity of abrasive wear (Liew, 2010). In another word it can be say that MQL technique reduces the rate of tool wear, dimensional inaccuracy and surface roughness by reducing the temperature at cutting zone and introducing favorable changes in tool-chip and work-tool interaction (Tawakoli et al., 2010).

It is reported that the cutting fluid is applied at the tool-chip interface in a form of narrow, pulsed jet with high velocity at a rate of 2 ml/min. The performance of machining with pulsed-jet application was studied in high-speed milling of hardened steel and the results were compared with dry machining and machining with flood application. The results clearly showed that the pulsed-jet application reduces the cutting force and tool wear, increases tool life and improves the surface finish, especially at high cutting velocity compared to dry machining and machining with flood application (Sadeghi et al., 2010). Moreover, the amount of cutting fluid consumed in pulsed-jet application (2 ml/min) is a drastic reduction compared to flood application. Additional benefit in pulsed-jet application

is that no harmful oil mist is generated during operation. In conclusion, the pulsed-jet application can be applied to mill hardened steel using ball end mills which reduces the negative effects on the environment, improves machining performances, and consequently reduces total production cost (Tawakoli et al., 2009; Thepsonthi et al., 2009).

The cooling process during machining plays a very important role and many operations cannot be carried out efficiently without proper cooling system. Application of a coolant in a cutting process increases the tool life and dimensional accuracy, decrease cutting temperatures, surface roughness and the amount of power consumptions and thus improve the quality of a given system (Lathkar & Bas, 2000; Tawakoli et al., 2010).

2.4 Nano base lubricant

2.4.1 Nano base lubricant performance

In the modern age of time, nanotechnology have become the most regarded and revolutionary technology and its application have become very wide. Investigations on tribological properties of nanoparticles containing lubricant have been conducted to improve performance in machining process (Bhaduri et al., 2010; Chang et al., 2006; Deng et al., 2006; Erdemir et al., 1997; Gopal & Rao, 2004; Greenberg et al., 2003; JX et al., 2006; Krishna & Rao, 2008; Mukhopadyay et al., 2007; Prihandana et al., 2009; Reddy et al., 2010; Reddy & Rao, 2005; Reddy & Rao, 2006; Vamsi Krishna et al., 2012; Wu et al., 2007).

Nano base lubricant system is defined as a new kind of engineering material that consists of nanometer sized particles dispersed in a base fluid. This is an effective method to reduce the friction between two contact surfaces under certain condition (Demas et al., 2012). The requirements of a nano base lubricant are: it must be able to sustain the high machining temperatures during processing, must be non-toxic, easy to be applied and cost effective (Deshmukh & Basu, 2006).

Several types of nanoparticles can be used in nano base lubricant system including graphite, boron nitride, molybdenum disulfide and tungsten disulfide. Graphite and molybdenum disulfide nanoparticles are commonly used in the nano base lubricant system because of their lubrication properties, morphology and crystal structure. For example, graphite possesses hexagonal arrangement of carbons which forms a stable planar lattice due to strong covalent bonds. The effectiveness of the nano base lubrication depends on the morphology and crystal structure of the base lubricant and nanoparticles, dispersion characteristics of the nanoparticles at the tool-workpiece interface, size of the particles and quantity (Alberts et al., 2009).

Due to high performance of the nano base lubricants, it is expected that labor and materials associated with preserving lubricant and equipment will be minimized. Health and environmental concern need to be addressed when dealing with lubricant materials. In addition, the productivity in a machining industry can be increased through cost reduction by reducing the usage of cutting fluid, and thus saving the environment in addition with improved machining properties.

As an example, the rolling and sliding is the dominant mechanism of fullerene to reduce the friction between two surfaces under certain loading conditions (Rapoport et al., 2002). When the fullerenes debris are transferred in between two rubbing surfaces, the dominant friction mechanism of fullerenes are observed (Rapoport et al., 2003). The role of fullerene based nanofluids in ball bearings can be divided into two steps. The first step is the rolling and protective effect which enhances the lubrication efficiency (Lee et al., 2009). The combination of rolling and sliding actions of fullerenes in ball bearing reduces a significant amount friction coefficient.

In the second step the surface modification is occurred by the abrasion of fullerene nanoparticles which significantly enhance the lubrication property. Physical analysis of

nanofluid showed that the nanoparticles can penetrate into the rubbing surfaces and impose a large effect on elastohydrodynamic lubrication (Peng et al., 2009). Under single trust bearing tester, it is seen that the friction coefficient of fullerene nanofluid is less than pure oil and the extreme pressure of nanofluid is two times higher than that of pure oil (Lee et al., 2009). Hence it can be concluded that fullerene nanofluid improve the lubrication performance by increasing the viscosity and preventing the contact between the rubbing surfaces.

It is expected that smaller and spherical nanoparticles will possess superior rolling action with lower affinity towards the metal surface, decrease contact temperature, higher elasticity and higher chemical resilience. Smaller particles can provide stable lubricants which can reduce wear, friction, noise, heat generation and vibration and extend the life of moving parts. Consequence of all these benefits provides longer equipment operation periods, higher efficiency and extended maintenance intervals. A higher affinity towards adhesion is observed for the smaller particles. On the other hand, large particles have more tendency towards agglomeration and the most importantly it is difficult to enter the interface between tool and workpiece (Alberts et al., 2009).

The spherical shaped nanoparticles increase the effectiveness of rolling mechanism during friction. Spherical nanoparticles also act as a spacer which eliminates direct asperities contact between two contact surfaces. Nevertheless, it can be a third body material from the fractured particles to the base fluid (Wu et al., 2007). It is well documented that, boric acid (nano base lubricant) is used as a lubricant in turning process. The variations, cutting force, tool wear, tool temperature and surface roughness have been studied under different machining conditions and the results indicate that there is considerable improvement in the machining performance with boric acid assisted machining (Damera & Pasam, 2008).

Previously the machinability of nano base lubricants containing graphite and molybdenum disulphide (MoS_2) nanoparticles were characterized in terms of cutting force, tool wear, chip thickness, machining dimension, and surface finish of the workpiece. Graphite and molybdenum disulphide are considered as effective lubricant additives due to their lamellar structure. There are several materials which are suitable for nano base lubricants including boron nitride (Erdemir et al., 1999), polytetrafluoroethylene (PTFE), talc, calcium fluoride, cerium fluoride and tungsten disulphides (Sharma et al., 2009). The appropriate ratio of nanoparticles and base fluid can be estimated by selecting the desired lubrication properties of cutting fluid (Alberts et al., 2009; Xiaodong et al., 2007). The three most commonly used nano base lubricants are:

- Graphite - Used in air compressors, foodstuff industry, railway track joints, open gear, ball bearings, machine-shop works etc. Graphite is also common for lubricating locks.
- Molybdenum disulfide (MoS_2) - Used in joints and space vehicles.
- Hexagonal boron nitride - Used in space vehicles. This material is called "white graphite".

The lubricating properties of nanofluids are attributed from the layered structure in the molecular level having weak bonding between layers. Such layers are able to slide on each other with a minimal applied force. Thus these materials possess low frictional properties. Nanoparticles also act as tiny ball bearings in a sliding contact and facilitate the relative movements between two contacting surfaces, thereby leading to lower friction and wear (Greenberg et al., 2003).

2.4.2 Nano base lubricant in machining to improve environmental issues

Lubricants are meant to reduce the friction at the tool-chip interface during machining. But in service not all lubricants have same performance. For instance, high quality and fully synthetic variants of lubricants reduce the friction better than normal mineral oils. As soon as the friction is reduced during machining, less energy is converted to frictional heat. In a consequence, the cutting force is also reduced due to less energy dissipation. This lowers the operating temperature and reduces the vibration level which provides the opportunity to drive the machine at low power and thus the output is enhanced. With proper lubricating system the energy saving can reach as high as 15%. In some cases the saving is much more depending on the other machining and cutting factors (Thepsonthi et al., 2009).

Upgrading the lubrication system is essential for less energy consumption during machining. High quality lubricants are more expensive but much more economic than conventional lubricants. Considering the high energy costs and energy taxes, the use of high quality lubricants usually pays for itself which can be estimated from the lower energy bills. Moreover, the high quality lubricant requires up to 5 times less amount compared to conventional lubricants. On the other hand, high quality lubricants produce less hazardous materials posing less threat to the environment (Khettabi et al., 2013).

For ultra clean environment, nanoparticles are suitable since they are free from routine maintenance (Krajnik et al., 2011). As an example, graphite and boric acid has no pathogenic clinical history which indicates that they are free from hazard (Nageswara Rao & Vamsi Krishna, 2008). Besides, nano base lubricants are not forbiddingly expensive since they can be reused. Hence, nano base lubricants are efficient in term of economical issues (Nageswara Rao & Vamsi Krishna, 2008). However, safety precaution should be taken into consideration since the nanoparticles are very small and tiny material that they can get into human body quite easily, either by inhalation or transdermally.

2.4.3 Nano base lubricant in machining to improve cutting force

Cutting force is the most fundamental, and one of the most significant parameters in machining operation. As an example, in milling processes cutting force can be a cause for parts and tool deflections which may result the violation of tolerance (Budak, 2006). Therefore the maximum force is estimated during tool design and cutter geometry is optimized to minimize the production cost and time. Hence, the measurement of cutting force is important in machining process in order to achieve high accuracy and productivity and it could provide the basis information for process planning as well (Budak, 2006; Reddy & Rao, 2006)

Recent investigation on cutting force shows that the turning process of steel with cemented carbide tool can be obtained at lower cutting force in the presence of nano base lubricants (a mixture of graphite and boric acid with SAE 40 oil) compared to the conventional machining process (Krishna & Rao, 2008). The effectiveness of nano base lubricants appears to be better compared to dry and wet machining process by minimizing the frictional effect between tool and workpiece which in turn reduces the cutting force. In general, the cutting force increases with increasing the surface area for machining. However, the extent of cutting force is varied depending on the type and concentration of the particles.

Nano base lubricant can be envisaged as the rolling of billions of miniature ball bearings. Hence, the cutting force and friction between the contact surface is greatly reduced (X.Tao et al., 1996). From Figure 2.4 it can be seen that graphite nanoparticles containing nano base lubricant minimizes the frictional effects at the tool and workpiece interface to a great extent compared to that of wet and dry machining. As a result, the energy requirement is also reduced and thereby presence of such lubricants enhances the machinability. Graphite is considered to be a good ingredient for nano base lubricant

because of its sliding characteristics at the interface, which contributes to the reduction of friction force. The substantial reduction in cutting forces during nano base lubricant assisted machining is attributed from the formation of the thin film lubricants at the interface which reduces the shear strength of material at the machining zone. (Kalita et al., 2012; Reddy et al., 2010).

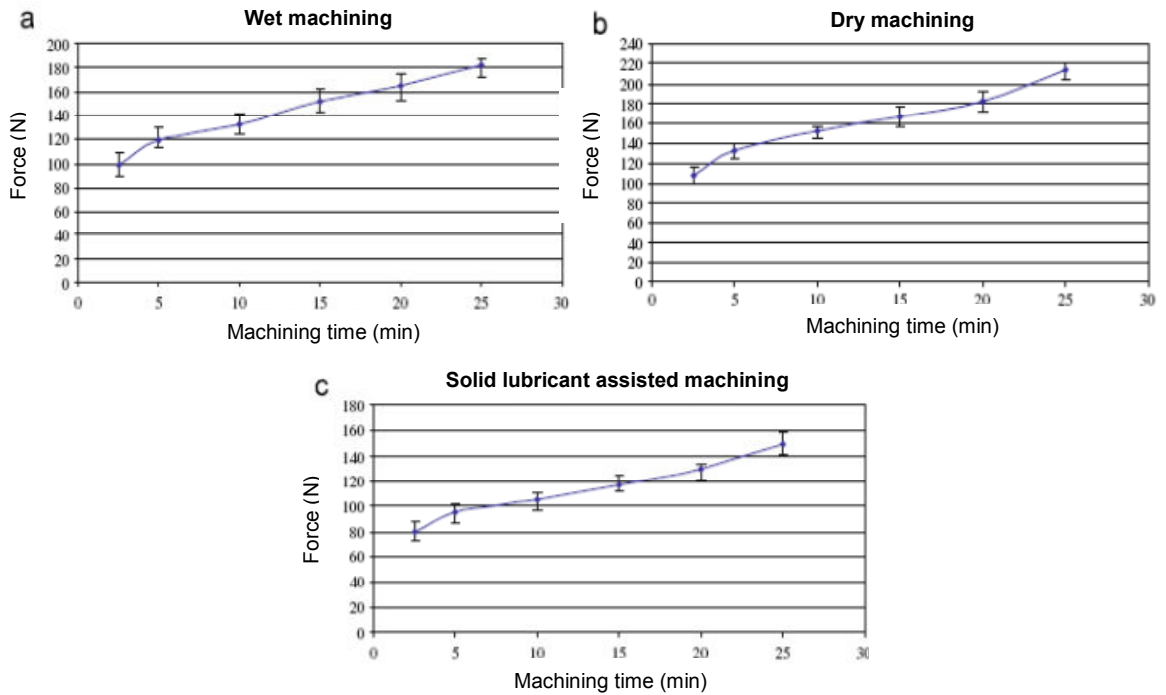


Figure 2.4 Variation of thrust force with machining under (a) wet, (b) dry and (c) nano base lubricant assisted machining (Reddy et al., 2010)

In another study, the coefficient of friction at tool-chip interface in dry cutting of hardened steel and cast iron by using $\text{Al}_2\text{O}_3/\text{TiC}/\text{CaF}_2$ ceramic tool was reduced compared to $\text{Al}_2\text{O}_3/\text{TiC}$ with CaF_2 nano base lubricant (Deng et al., 2006). Another researcher used automated feeder to supply nano base lubricant to the machining zone to increase the effectiveness of machining process especially to improve the morphology and crystal structures of the nano base lubricant particles. It is reported that, the cutting force, surface quality and specific energy is considerably improved by using nano base lubricants (Reddy & Rao, 2006).

For grinding process, investigation were conducted by using graphite as a solid lubricating medium to reduce the heat generation at the cutting zone (Shaji & Radhakrishnan, 2002). Also the development of nano base lubricant moulded grinding wheel with various bonding and lubricants is also reported in attempting to improve the solid lubrication method (Shaji & Radhakrishnan, 2003; Shen, 2008). Recently, a research has been conducted to investigate the feasibility of nanoparticles aided lubrication in diamond turning of RB-SiC. The result shows that nanoparticles provide an effective lubrication for high performance ultra precision cutting of hard materials (Yan et al., 2010). On the other hand, thick paste of powder lubricant made from water soluble oil is reported to serve as the general purpose of grease and it is found that the cutting force is reduced successfully (S.Shaji & V.Radhakrishnan, 2002).

In a research, the performance of graphite in nano base lubricant is evaluated while grinding SiC to reduce the heat generation at the grinding zone. The results show that the tangential force component considerably reduce the specific energy requirement (Gopal & Rao, 2004). In general, higher plasticity in the nanoparticle results in better lubrication performance. This phenomenon is due to the micro fracture/deformation characteristics of the particles. An extremely thin film is generated at the interface due to the fracture/deformation of particles which reduces the direct contact among the asperities between the cutting tool and workpiece (Yan et al., 2010).

Particle size also plays a significant role in affecting the lubrication performance. The smaller particles are considered to be the better than the larger particles due to their capability to penetrate easily at the tool-workpiece interface. In another words, smaller particles facilitate the accessibility to the cutting zone (Yan et al., 2010). At the early stage of cutting, when the tool and workpiece surface are smooth it is important to utilize the smaller nanoparticles. The lubrication performance of solid particles might depend on the

micro fracture/deformation characteristics of the particles. Through the fracture/deformation of the particles, an extremely thin film of nano base lubricant is generated at the interface which significantly reduces the direct contact among the asperities between the cutting tool and the workpiece (Yan et al., 2010).

2.4.4 Nano base lubricant in machining to improve cutting temperature

The high temperature at the cutting zone results in dimensional deviations, fast oxidation, corrosion, thermal stress, residual stresses and microcracks on the workpiece. Thermal burn and phase transformation also exist due to the heat generation during machining (Alberts et al., 2009). For this reason, heat generation generally considered a critical issue in term of workpiece quality. Therefore, the heat generated at the cutting zone must be effectively controlled to ensure good surface finish during machining (Reddy & Rao, 2006).

Cutting fluid is a critical component to deal the excess heat generation during machining. Figure 2.5 compares the tool temperature measured at the nodal point at different time intervals for dry, powder and coolant machining. It is seen that heat generation is lower in case of boric acid assisted (nano base lubricant) machining compared to dry machining. The lubricating action of the nano base lubricants reduces the frictional forces between tool-chip interfaces (Kalita et al., 2012). For this reason the heat generation is reduced in case of nano base lubricants compared to dry and wet machining. The thin film formation of on the surface of the workpiece is significantly depends on temperatures variation of the temperature on cutting tool that presents during the machining process. Though the difference in temperatures while machining with cutting fluid or boric acid is not much, the nonpolluting nature of boric acid is a clear advantage and a critical parameter in making the choice (Damera & Pasam, 2008).

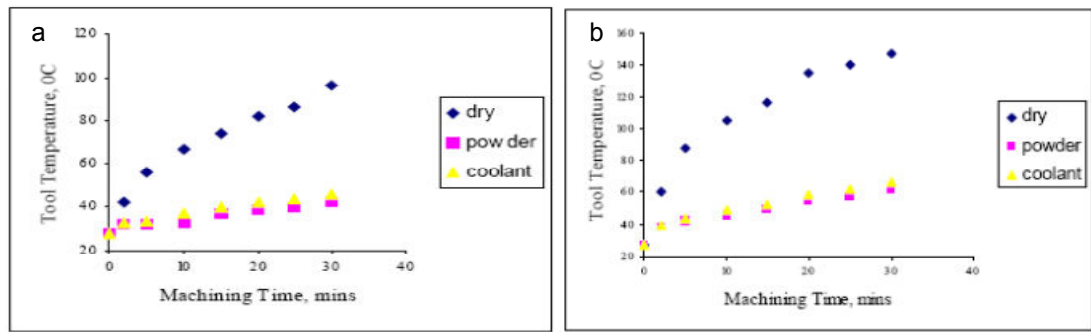


Figure 2.5 Variation of tool temperature with machining time for (a) HSS and (b) carbide tool (Damara & Pasam, 2008)

Various nanoparticles, such as multi-walled carbon nanotube (MWCNT), fullerene, copper oxide, silicon dioxide and silver are used to produce nanofluids for enhancing the thermal conductivity and lubrication properties. Ethylene glycol, mineral oil, silicon oil and poly- α -olefin oil (PAO) is used as a base fluid. The thermal conductivity and kinematic viscosity of the nanofluids are crucial to investigate the thermo-physical properties of nanofluids. It has been observed that, the thermal conductivity of nanofluid increases with increasing the concentration of particles (Hwang et al., 2006).

In the recent research, the base fluid is mixed with the nanoparticles and the Brownian motion of the nanoparticles are modeled, analyzed and compared with existing experimental data from the literatures. The results from simulation indicate that this mixing has a significant influence on the effective thermal conductivity of nanofluids (Li & Peterson, 2007). The thermal conductivity of the nano base lubricants seems to be decreased with increasing the nanoparticles content (Krishna et al., 2009; Reddy et al., 2010).

2.4.5 Nano base lubricants in machining to improve tool wear

The efficiency of cutting and the resultant surface finish is greatly affected by the tool wear. Cutting tools may fail prematurely, randomly and catastrophically by mechanical breakage and plastic deformation under adverse machining conditions caused by intensive

pressure, uneven temperature distribution and/or dynamic loading at the tip of cutting edge particularly if the tool material lacks strength, hot-hardness and fracture toughness. However, for a given tool and workpiece in optimum machining conditions, the tool failure mode is mostly gradual wear. The wear of carbide tool is assessed from the actual machining time as it is shown in Figure 2.6 for wet, dry and nano base lubricant assisted machining. The gradual increase of tool wear under all environments indicates steady machining without any premature failure by chipping or fracturing. Figure 2.6 also shows that the increase of tool wear is decreased by nano base lubricant assisted machining. The cause behind the reduction in tool wear may be attributed from the reduction in temperature by nano base lubricant, which helps to reduce abrasion wear by retaining tool hardness, adhesion and diffusion. Hence the strength and wear resistance of a cutting tool can be retained, which leads to a significant improvement of tool life (Damera & Pasam, 2008; Reddy et al., 2010).

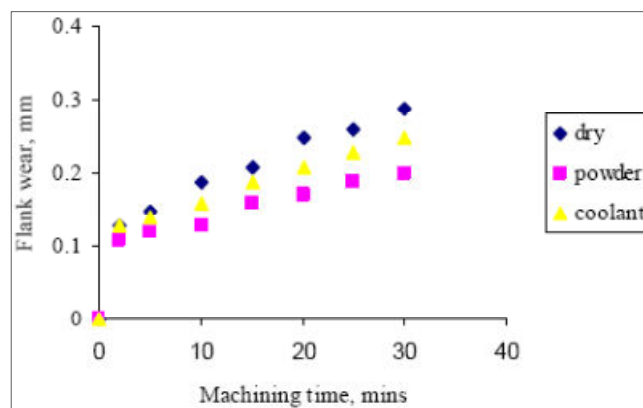


Figure 2.6 Variation of flank wear with machining time of carbide tool (Damera & Pasam, 2008)

Tool wear characteristics are altered when nano base lubricant assisted machining is employed. The variation in tool wear characteristic depends on the type and concentration of nanoparticles. The existence of scratch marks on the tool surface is caused by the scratching of the nanoparticle grain and/or of thermal-chemical reactions between

nanoparticles and tool material. Also, the extend of cutting force should be taken into consideration to determine the tool wear under certain condition.

In boric acid assisted machining, for a given tool-chip combination the flank wear is observed to be considerably less. The chip slides against the tool rake face at a high speed and induces high cutting temperature during cutting process. The nano base lubricant is expected to melt and smear to create a thin film of lubricant on the rake face of the tool in such high cutting temperatures. Due to the low coefficient of friction and sliding action, a substantial reduction of flank wear is observed. The reduction of flank wear is also due to the low shear resistance at the tool and workpiece interface. Due to the lamellar structure the nano base lubricant possesses three important properties: low friction coefficient, sliding between layers and low shear resistance. Therefore, the effectiveness of lubricating action of this lamellar particles mainly depends on the combinations of cutting conditions and tool-workpiece combination (Damera & Pasam, 2008).

In a research the sliding wear tests on cemented carbide tool was carried out in presence of nano base lubricants containing ceramic nanoparticles. From the results it was seen that the ceramic composites exhibits a self-lubricating property both in the case of sliding wear tests and in machining processes. The scanning electron microscopy suggested that a self-tribofilm was consistently formed on the wear surfaces from nano base lubricants containing CaF_2 . The coefficient of friction was significantly reduced due to the presence of self-tribofilm which was formed by the releasing and smearing of CaF_2 containing nano base lubricants on the wear surface. As a consequence it can be said that the nano base lubricants containing ceramic nanoparticles protect the tool from severe wear by brittle microfracture (Jianxin et al., 2007).

To optimize the nano base lubricant, it is seen that lubricants containing 20% of boric acid in SAE 40 provides better performance for a selected tool-workpiece

combination and cutting conditions. However, not much change is observed when the boric acid content is beyond 20%. This suggests that the sliding nature of nano base lubricants is decreased at high viscosity (Krishna et al., 2009). A method has been proposed to adjust the adhesive conditions at the interface between particles and tool or particles and workpiece to reduce the tool wear. Based on the simulation, the tool wear is significantly changed with the change in adhesive strength at these interfaces (Yan et al., 2010).

It is reported that the mechanism of tool wear resistance and reduction of friction is influenced by the colloidal effect, rolling effect, protective films and third body characteristic. The colloidal nanoparticles can penetrate to the tool-workpiece elastohydrodynamic contact by the mechanism of mechanical entrapment. The colloids also form a thin layer of boundary film which is at least two or three times thicker than the size of the nanoparticles in rolling contact at low speed (Wu et al., 2007). At different colloid of nanoparticles, the deposition of tribochemical reaction product is also produced during the friction process. In other words, it results wear resistance boundary films and decreases the shearing stress (Wu et al., 2007).

To demonstrate the machining and wear performance of patterned carbide tool coated with TiN, turning operation was performed on hardened 4340 steel in presence of nano base lubricant containing indium nanoparticles. The results showed that the flank wear was effectively reduced by the incorporation of indium nanoparticles into the lubricant during machining (Guleryuz et al., 2009).

In some instances, nanoparticles concentration is also an important factor to affect the friction and wear (Reddy & Rao, 2006). Some researchers found that low concentration of nanoparticles is sufficient to improve the tribological properties. There are different optimum concentrations for different types of nanoparticles for obtaining the best tribological properties for a given material. It is also reported that flank wear can be

reduced by employing nano base lubricant assisted machining compared to wet and dry machining process. Nano base lubricants containing ceramic nanoparticles are also found to be effective during machining of hardened AISI52100 steel at high cutting speed (Singh & Rao, 2008).

2.4.6 Nano base lubricants in machining to improve surface roughness

Surface roughness influences the functional characteristics of the workpiece such as compatibility, fatigue resistance and surface friction (Reddy & Rao, 2006). In the end milling, the surface roughness is influenced by process parameters, tool geometry, and heat generated during machining operation (Reddy & Rao, 2005). In general, increased wear at the tool flank deteriorates the surface finish (Choi & Liu, 2009; Sarhan et al., 2001).

Figure 2.7 compares the surface roughness of a machined surface in dry, wet and boric acid nano base lubricant machining conditions. The results indicate that the surface finish is improved in the presence of boric acid assisted nano base lubricant compared to dry and wet machining process. The reduction in the cutting forces and the decrement of surface roughness for the presence of boric acid could be a reason for improved surface finish. It is also reported that the lubricating action of the boric acid reduces the frictional forces at the tool and workpiece interface (Erdemir, 1991; Erdemir et al., 1991). This decreases the temperatures evolution at the cutting zone which in turn reduces the tool wear thus resulting improved surface finish (Damera & Pasam, 2008).

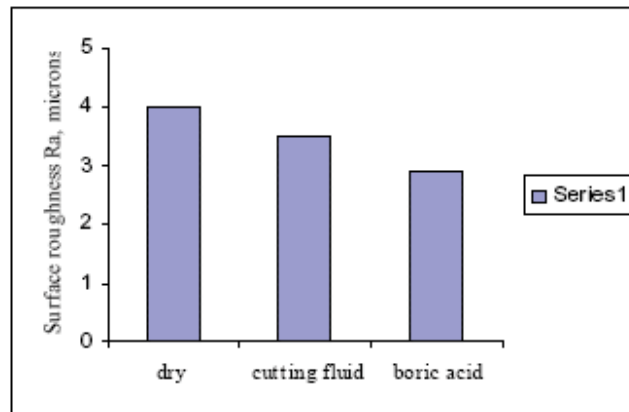


Figure 2.7 Surface roughness (R_a) for different lubricants (HSS Tool)(Damera & Pasam, 2008)

The surface roughness for dry hard turning and nano base lubricants assisted hard turning at different cutting speed is shown in Figure 2.8. It can be seen that nano base lubricant assisted hard turning produces low values of surface roughness compared to dry hard turning. Among the two variants of the nano base lubricant assisted machining, presence of molybdenum disulphide shows better results compared to graphite (Dilbag & Rao, 2008).

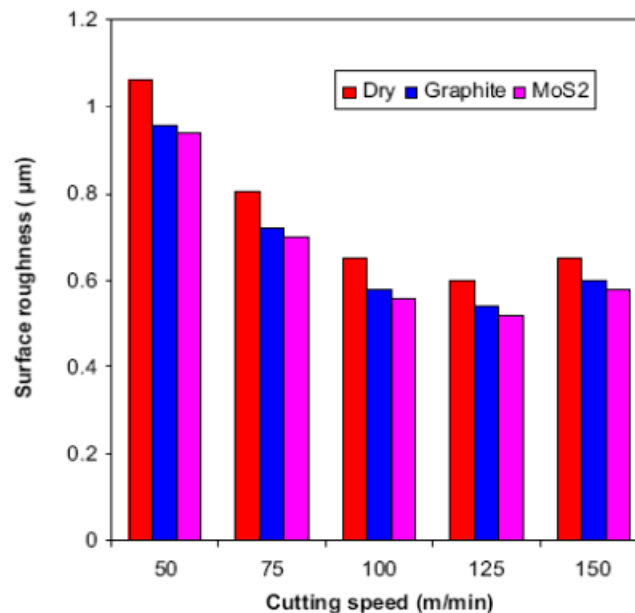


Figure 2.8 The variation of surface roughness for dry hard turning and nano base lubricants assisted hard turning at different cutting speed (Dilbag & Rao, 2008)

At high cutting speed, presence of nano base lubricants containing ceramic nanoparticles such as molybdenum disulphide are more effective during machining of AISI52100 steel. The variation of surface roughness at different cutting speed is shown in Figure 2.9 for dry hard turning and nano base lubricants assisted hard turning. It is seen that nano base lubricants reduces the surface roughness (Dilbag & Rao, 2008). Presence of nano base lubricants reduces the surface roughness even at high temperatures. It is assumed that the layered lattice structures of the nanoparticles contribute to these phenomena. The strong adhesions of molybdenum disulfide provide better surface roughness compared to graphite.

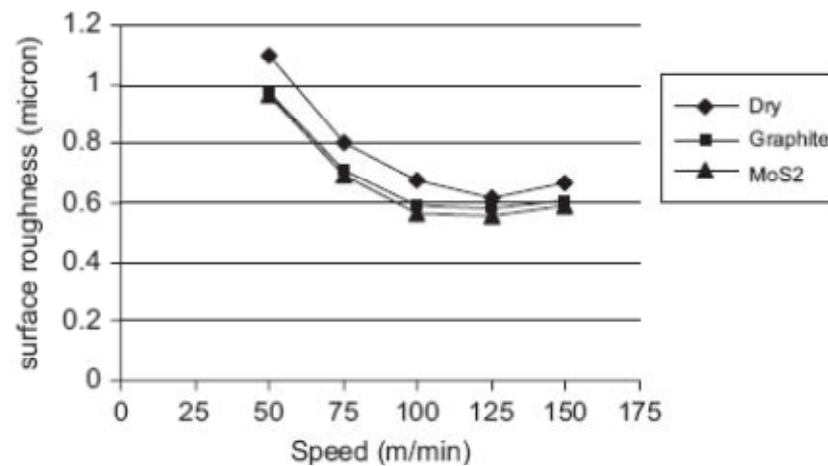


Figure 2.9 Variation of surface roughness for dry hard turning and nano base lubricants assisted hard turning at different cutting speed

(Singh & Rao, 2008)

2.4.7 Nano base lubricants in machining to improve surface morphology

Nanoparticles suspended lubricants have been identified as an advances in modern technology which can sustain and provide lubricity over a wide range of temperatures (Nakamura et al., 2000). Besides, several types of nanoparticles such as MoS₂ and graphite have been used by the researchers in order to reduce the friction between the contacts at the surfaces (He et al., 2010; Lee et al., 2009). The effectiveness of nano base lubricants depends on the morphology, crystal structure , size and quantity of the nanoparticles as well

as the feeding procedure of the lubricant at the tool-workpiece interface (Alberts et al., 2009; Hirata et al., 2004).

The physical analysis of nanofluids shows that the dispersed nanoparticles can easily penetrate into the rubbing surfaces and have the effect of elastohydrodynamic lubrication (Peng et al., 2009). Under a single trust bearing tester, researchers found that the frictional coefficient of a nanofluid containing fullerene is lower than pure oil and can sustain two times higher pressure than that of pure oil. Hence, it can be concluded that fullerene containing nanofluids improve the lubrication performance by increasing the viscosity and preventing contact between the metal surfaces (Lee et al., 2009).

It is observed that the surface roughness obtained in nano base lubricant assisted machining is lower than that of wet and dry machining. Nano base lubricant assisted machining provides better quality due to their layered structure which allows them to form a thin sliding film on the surface (Reddy et al., 2010). It is worthy to note that nanoparticles can also provide the quasi-hydrodynamic lubrication. According to the reported result, a film is required to be formed for assisting the tribological mechanism. This film protects the direct contact of rubbing surfaces and greatly reduced the frictional force at the contacts between two surfaces. (Qiu et al., 2001). At a high cutting speed, the chip slides against the tool rake face at high cutting temperature. Consequences from that, the nano base lubricant melts and smears and creates a thin lubricant film on the rake face of the tools which reduces the coefficient of friction and sliding action (Nageswara Rao & Vamsi Krishna, 2008).

2.5 Conclusion

A wide variety nanoparticle has been used in the base lubricants by researchers to achieve better machining performance. It is well documented that silicon dioxide (SiO_2) nanoparticles are hard, brittle, and cheap material which is easily available in the markets. It has very good mechanical properties especially in term of hardness (Vickers hardness - $1,000 \text{ kgf. mm}^{-2}$). It is also possible to achieve very small sizes of SiO_2 in the range from 5 nm to 100 nm. It is reported that nanoparticles dispersed in the mineral oil acts as a combination of rolling and sliding bearings at the tool-chip interface which significantly reduces the coefficient of friction. Therefore, the cutting force is obtained to be lower in the nanolubrication system compared to the pure mineral oil (Sarhan et al., 2011). The reduction of cutting force leads better performance in machining process (Sarhan & Matsubara, 2011). However the application of SiO_2 nanoparticles dispersed in pure mineral oil is not reported yet for improving the machining performance.

On the other hand, molybdenum disulfide (MoS_2) is widely used in lubricants, composite materials and grease due to their perfect lubricity. The weak Van der Waals force result easy sliding between two S–Mo–S layers. Compared with bulk MoS_2 , nano-sized MoS_2 usually has better tribological properties (Hu et al., 2011). Also MoS_2 nanoparticles is a well identified hard and brittle material which can be easily found in market having a wide range of size. Graphite and MoS_2 are one of the most common lubricants due to their layered morphology and crystal structure. Their morphology consists of a hexagonal arrangement of carbon atoms which forms planar lattices structure due to strong covalent bonds. Parallel planes stay together due to weak inter-layer bonding, mainly by Van der Waals force. The application of MoS_2 nanoparticles suspended mineral oil has not been well investigated as a cutting fluid especially in terms of machined surface quality and morphology.

Over the last decades, carbon onion has been successfully developed with high tribological properties. Carbon onion consists of concentric graphitic shells containing fullerene (C_{60}) and carbon nanotubes (Hirata et al., 2004). It is well proven that carbon onion can provide the similar lubrication as graphite in ambient air. Carbon onion is expected to possess favorable properties, which are desirable for solid lubrication due to its unique structure. It is also proven that carbon onion can be used as a solid additive in grease as a replacement of MoS_2 from a number of commercially available lubricants (Street et al., 2004).

In line with the previous research work, the investigation of optimum SiO_2 , MoS_2 and carbon onion for nano base lubricants is required to focus to improve the performance in machining process. Other parameters such as the concentration of nano base lubricant, nozzle angle and carrier air pressure needs to be optimized.

The overall performance of machining by using nano base lubricants is found to be better than ordinary lubrication. Improvement in machining process would results better product quality. The details presented in this research work provide a scientific basis for developing nano based lubrication system to address recent industrial requirement.

CHAPTER 3 METHODOLOGY

3.1 Introduction

Overall plan of this research is illustrated Figure 3.1. These research plans were specially designed to achieve the objectives which are stated earlier. In order to develop SiO₂, MoS₂ and carbon onion nano base lubricant for metal cutting processes, a proper technique was identified to improve the performance in machining process. Variation of several parameters of the nano base lubricant including different concentrations was studied. In this research, both turning and milling process were utilized to determine the effectiveness of the nano base lubrication in machining process. The workpiece material was selected from the ductile and hardened categories of metal which are commonly used in industrial practice. To determine the product quality, investigations were conducted to obtain the cutting force, cutting temperature, tool wear, surface roughness and morphology by using appropriate equipment. Then further analysis and discussions were carried out to achieve a concrete conclusion for better understanding of the role of nanoparticles in the nano base lubricant.

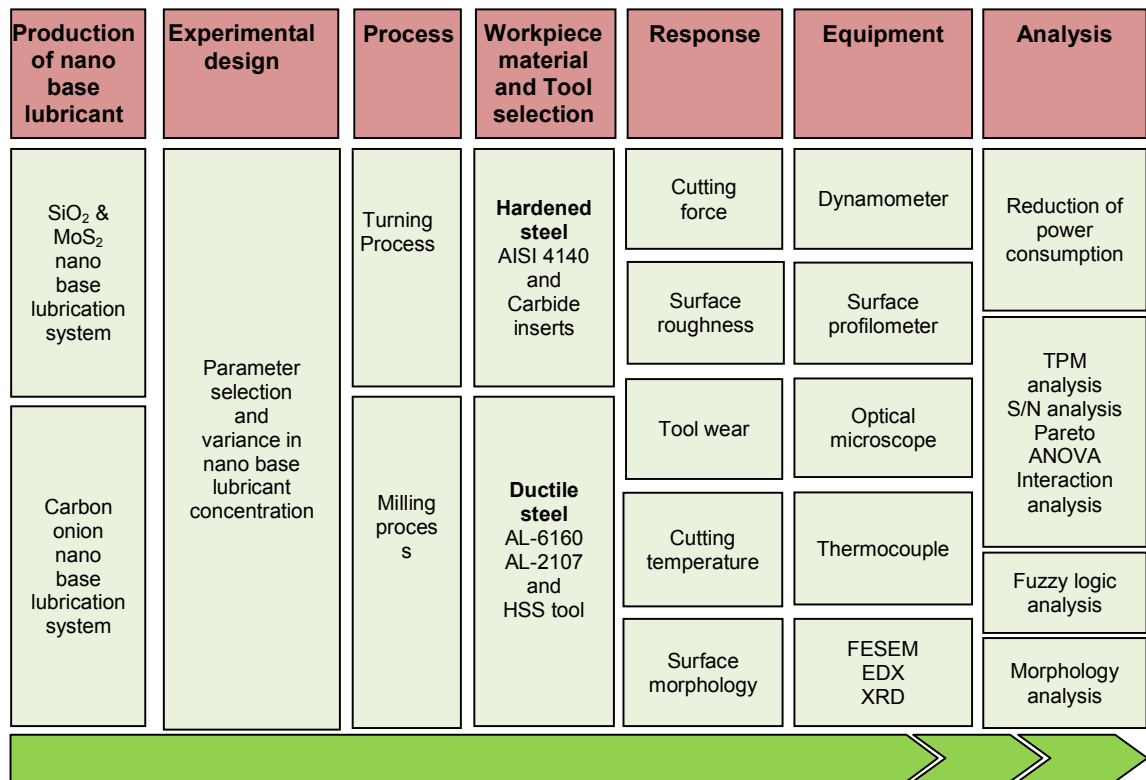


Figure 3.1 Overall research plan for nano base lubricant research

3.2 Nano base lubricant preparation

3.2.1 Lubricant oil

To prepare the SiO₂ and MoS₂ nano base lubricant, the ECOCUT SSN 322 having 40.2 cSt viscosity at 40°C (FUCHS and Alumaticut) was used as a base lubricant. ECOCUT SSN 322 is free from phenol, chlorine and other additives. The properties of Shell Dromus BL lubricant oil is shown in Table 3.1.

Table 3.1 The properties of ECOCUT SSN 322 lubricant oil

Properties	Value	Test method
Appearance	B & C	Visual
Colour	L0.5	ASTM D 1500
Specific gravity at 60/60 °F (°C)	0.828	ASTM D 1298
Flash point COC (°C)	152.0	ASTM D 92
Viscosity at 40 °C (cSt)	5.0	ASTM D 445
Copper corrosion/24 h at 100 °C	1a	ASTM D 130
Pour point (°C)	-15.0	ASTM D 97
Foam test seq. 1 (ml)	15/0	ASTM D 892
TAN (mgKOH/g)	0.2	ASM D 664

For carbon onion nano base lubricant, alumicut type of lubricant oil was selected as a base lubricant. Alumicut type of lubricant has good lubrication characteristic for non-ferrous workpiece specially aluminium. The coefficient of friction between aluminium workpiece and cutting tool is relatively low in presence of alumicut type of lubricants. It appears in clear form with a pH value of 6.9. Alumicut lubricant adheres with the workpiece to eliminate galling, gouging and tearing from the material in addition with restricts the metal chip pile-up at the cutting junction which considerably extend the longevity of the tool.

3.2.2 SiO₂ nanoparticles

SiO₂ nanoparticles are well known as a hard and brittle material and it can be easily found in the market at an affordable price. These nanoparticles have very good mechanical properties, especially hardness (Vickers hardness - 1,000 kgf. mm⁻²). A wide variety of size of SiO₂ is achievable ranging from 5 nm to 100 nm. Table 3.2 presents the mechanical properties of SiO₂.

Table 3.2 Mechanical properties of SiO₂

Properties	SiO ₂
Structure	Amorphous
Melting Point (deg C)	Approx. 1600
Density (g/cm ³)	2.2
Refractive Index	1.46
Dielectric Constant	3.9
Dielectric Strength	10 ⁷
Thermal conductivity at 300K (W/cm-deg K)	0.014

3.2.3 MoS₂ nanoparticles

Molybdenum disulfide (MoS₂) is widely used in lubricants, composite materials and grease due to their perfect lubricity. The weak Van der Waals force result easy sliding

between two S–Mo–S layers. Compared with bulk MoS₂, nano-sized MoS₂ usually has better tribological properties (Hu et al., 2011). Also MoS₂ nanoparticles is a well identified hard and brittle material which can be easily found in market having a wide range of size. MoS₂ is one of the most common used as lubricants due to their layered morphology and crystal structure.

3.2.4 Carbon onion nanoparticles

Carbon onion consists of concentric graphitic shells containing fullerene (C₆₀) and carbon nanotubes (Hirata et al., 2004). It is well proven that the performance of carbon onions during machining is as similar as graphite in ambient air. Carbon onion is expected to possess favorable properties, which are desirable for solid lubrication due to their unique structure. It is also reported that carbon onion can be used as a solid additive in grease as a replacement of MoS₂ form a number of commercially available lubricants (Street et al., 2004).

Carbon onions are defined as quasi-spherical nanoparticles consisting of a structure similar to fullerene enclosed in concentric graphitic shells. Carbon onion possesses better physical and tribological properties compared to other carbon nanostructures due to their high symmetry in the structure. In this research, carbon onion nanoparticles were produced from the heat treatment of carbon black (Cabot R250 from Cabot Corporation) in a resistance heat furnace using a graphite crucible under He atmosphere. The carbon onions were obtained by inductive heating at 2000°C for 15 minute and used without any further treatment (e.g. purification). Figure 3.2 shows the transmission electron microscopy (TEM) image of carbon onion having average size of 5 to 20 nm.

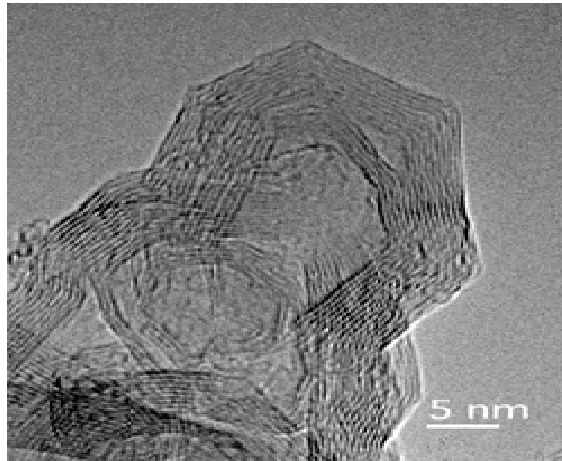


Figure 3.2 Transmission electron microscopy (TEM) image of carbon onion
(Hirata et al., 2004)

3.2.5 Nano base lubricant preparation method

Figure 3.3 presents the nano base lubricant preparation process. Two types of nano base lubricants were developed in this research, namely SiO_2 nano base lubricant and carbon onion nano base lubricant.

(a) Preparation SiO_2 nano base lubricant

The nano base lubricant was prepared by adding silicon dioxide nanoparticles (0.2, 0.5, and 1.0 wt%) into the ECOCUT SSN 322 lubricant oil. The average particle size of the SiO_2 nanoparticles was 5-15 nm. The mixture was stirred in a stirring followed by sonication (240 W, 40 kHz, 500 W) for 48 hours in order to suspend the particles in the mixture homogeneously.

(b) Preparation MoS_2 nano base lubricant

The nano-lubricants were prepared by mixing MoS_2 nanoparticles (average particle size of 20-60 nm) with the mineral oil followed by sonication (240W, 40kHz, 500W) for 48 hours in order to suspend the nanoparticles in the mixture homogeneously.

(c) Preparation of carbon onion nano base lubricant

To reduce the friction at the tool-chip interface, alumaticut types of lubricant was chosen. 0.0, 0.5, 1.0 and 1.5 wt% of carbon onion was mixed with alumaticut oil followed by sonication using Sono Bright ultrasonic (240 V, 40 kHz, 500 W) for 48 hours in order to suspend the particles in the mixture homogeneously. Usage of carbon onions more than 1.5 wt% in base oil results agglomeration. More investigations are required to solve the mixing problem of carbon onions in alumaticut. The preparation of carbon black nano base lubricant was also developed in a similar method of carbon onion nano base lubricant.

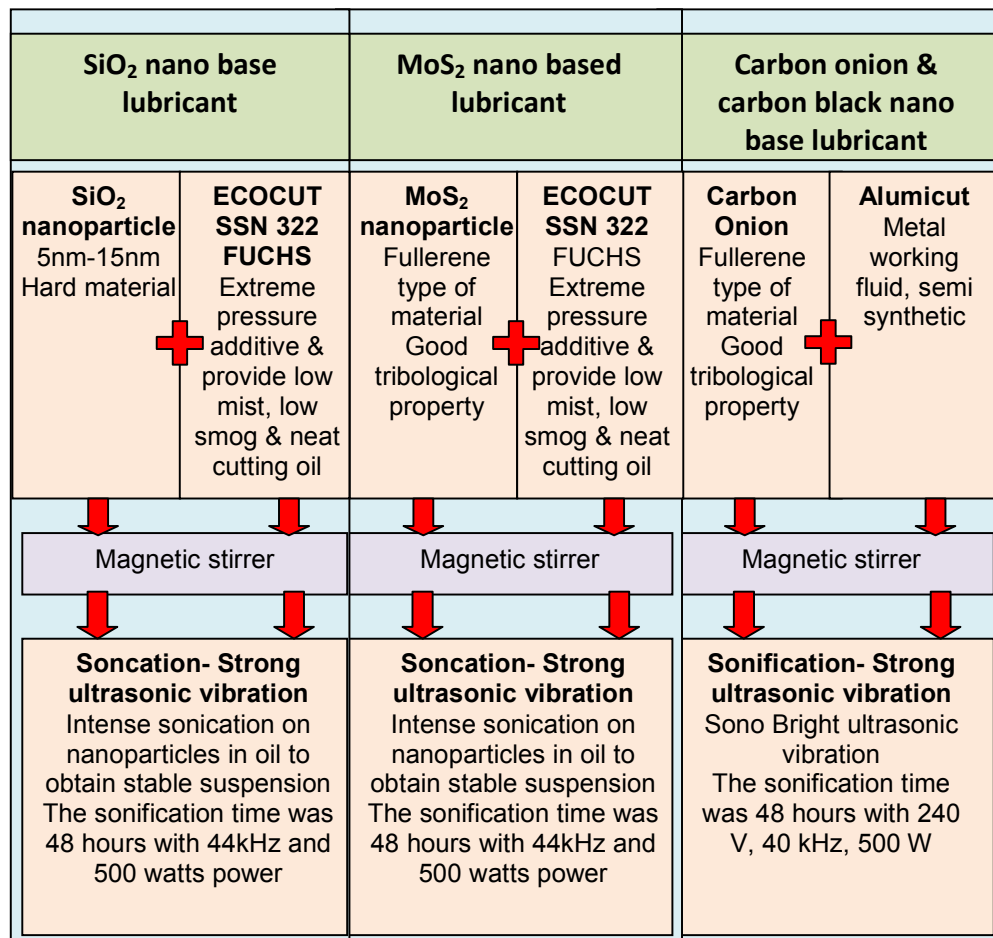


Figure 3.3 The nano base lubricant preparation process

3.3 Experimental design

In line with the previous research work, investigations on optimum amount of SiO₂ MoS₂ and carbon onion nanoparticles in nano base lubricant for turning and milling process is the main focus of this research. Improvement of the machined surface by reducing the cutting force and cutting temperature with the aid of nano base lubricant is another focus. The conventional method to determine the optimal values of these parameters is to use the “trial and error” approach. Since “trial and error” approach is very time consuming for huge number of experiments, a reliable systematic approach is required to optimize these parameters.

The optimization method utilized in this study is called the Taguchi optimization method. Taguchi optimization method was developed by Dr. Genichi Taguchi where a set of methodologies is taken under consideration having minimum variances (Prabhu & Vinayagam, 2012; Sayuti et al., 2011 ; Zhang et al., 2007). In Taguchi optimization method multiple factors can be considered at once. Moreover, this method seeks nominal design points to improve the yield and reliability of a product which are not sensitive to the variations related to production and/or environment. By using the Taguchi optimization method, industries are able to reduce production time for a given product and therefore the reducing costs with more profit (Ghani et al., 2004; Hamdan et al., 2011).

Taguchi optimization method provides a systematic application in design and analysis of experiments and it is used for designing and improving the product quality. Furthermore, it has become a powerful tool for improving the productivity during research and development with costs reductions (Hsiao et al., 2008; Sayuti et al., 2011). The steps in the Taguchi optimization method include: selecting the orthogonal array (OA) according to the numbers of controllable factors, running experiments based on the OA, analyzing data, identifying the optimum parameters, and conducting confirmation runs with the optimal levels of all the parameters.

The most important stage in Taguchi optimization method is the selecting of control factors and identifying the OA. Running experiments based on the identified OA is the second crucial step. To point out the non-significant variables for a system maximum possible factors should be included in the experiment.

The standardized Taguchi optimization method designed for $L_{16}(4)$ orthogonal array was used to optimize both machining parameters and nano base lubricant parameters for the lowest cutting force, lowest cutting temperature, least tool wear and best surface finish. The standard orthogonal array consists of sixteen experiments with three control factors

and four different experimental conditions for each factor. The standardized $L_{16}(4)$ orthogonal array, the sixteen experiments with detail of the combination levels are specified in Table 3.3, while Table 3.4 presents the factors and experimental condition levels for hard turning process. The 16 experiments were carried out in a random sequence to eliminate any other invisible factors, which might also contribute to the responses.

Table 3.3 Standardized $L_{16}(4)$ orthogonal array, the sixteen experiments with detail of the combination levels

Exp. no.	Control factors and levels (<i>i</i>)			
	A	B	C	D
1	<i>i</i> = 1	1	1	1
2	<i>i</i> = 1	2	2	2
3	<i>i</i> = 1	3	3	3
4	<i>i</i> = 1	4	4	4
5	<i>i</i> = 2	1	2	3
6	<i>i</i> = 2	2	1	4
7	<i>i</i> = 2	3	4	1
8	<i>i</i> = 2	4	3	2
9	<i>i</i> = 3	1	3	4
10	<i>i</i> = 3	2	4	3
11	<i>i</i> = 3	3	1	2
12	<i>i</i> = 3	4	2	1
13	<i>i</i> = 4	1	4	2
14	<i>i</i> = 4	2	3	1
15	<i>i</i> = 4	3	2	4
16	<i>i</i> = 4	4	1	3

In optimizing the cutting parameters in hard turning process, the experimental conditions for cutting speed, feed rate and depth of cut were assigned by the tool manufacturer. The lubrication mode was decided by reviewing the literature and considering the availability of cooling equipment. This orthogonal array was chosen to determine and optimize the cutting parameters, namely surface roughness, cutting force, cutting temperature and chip formation.

Table 3.4 Factors and experimental condition levels

Symbol	Factor	Experimental condition level			
		1	2	3	4
A	Cutting speed, v (m/min)	50	115	180	245
B	Feed rate, f (mm/rev)	0.05	0.10	0.15	0.20
C	Depth of cut, a_p (mm)	0.20	0.30	0.40	0.50
D	Lubrication mode	Dry	Flood	MQL	Chilled air

The parameters for optimizing the nano base lubricant during milling process are nanoparticles concentration, nozzle angle and carrier air pressure (hereafter called control factors) were shown in Table 3.5.

Table 3.5 Control factors and experimental condition levels

Factor	A	B	C
Level (i)	Nanoparticles Concentration (wt%)	Air Pressure (Bar)	Nozzle Orientation (Degree °)
Level 1 ($i=1$)	0%	1	15
Level 2 ($i=2$)	0.2%	2	30
Level 3 ($i=3$)	0.5%	3	45
Level 4 ($i=4$)	1.0%	4	60

In fuzzy logic approach, data from a similar combination of twelve experiments were utilized.

3.4 Experimental set up

3.4.1 Experimentation for optimization the cutting parameters in hard turning process

The turning experiments were carried out on hardened AISI4140 alloy steel round bars (55 to 56 HRC) with a diameter of 32 mm and length of 200 mm in an inclined bed type Okuma LB15 CNC lathe with Siemens 802D controller. The machining processes were accomplished using inserts which served as cutting tools made of the ceramic mixtures of Al_2O_3 and TiCN. The cutting tool was mounted on a rigid tool holder which was fixed at a Kristler three-component tool holder dynamometer and the cutting length was 150 mm as illustrated in Figure 3.4. In this study, all hard turning experiments were performed on the

inclined-bed type Okuma LB15 CNC lathe with Siemens 802D controller as shown in Figure 3.5. This machine has high rigidity, high static and dynamic stiffness which make it suitable for hard turning processes.

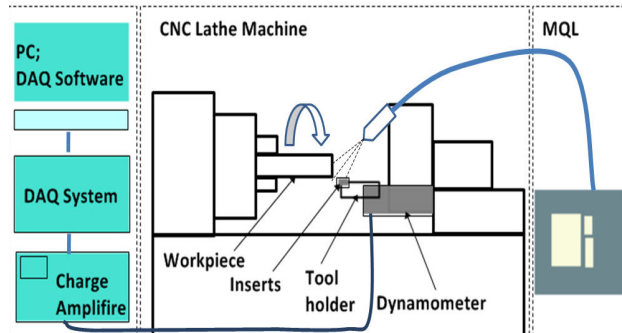


Figure 3.4 Experimental set up



Figure 3.5 Okuma LB15 CNC lathe

The cutting tools used were TaeguTec mixed ceramic inserts with the ISO designation of DNGA150608. The inserts were made from the mixture of Al_2O_3 and TiCN and the physical properties of the inserts are presented in Table 3.6. The inserts have the grade of AB20 designated by the tool manufacturer. The tools have high wear resistance with excellent cutting edge stability. The tool was recommended by the manufacturer for high speed finishing of hardened steels, cast iron and other hard materials. Analysis of the tool wear was performed on all inserts prior to machining to prevent ambiguous results due to manufacturing or handling damage.

Table 3.6 Physical properties of TaeguTec DNGA 150608 mixed ceramic tool

Grade		AB20
Composition		Al ₂ O ₃ , TiCN
Density (g/cm ³)		4.30
Hardness	HRA	94.5
	Vickers	2050
Bonding strength (Mpa)		650

The tools were mounted on a tool holder with the ISO designation of PDJNL25-25M-15 manufactured by Sandvik Coromant. Figure 3.6 and Figure 3.7 shows the insert tool and tool holder geometries respectively.

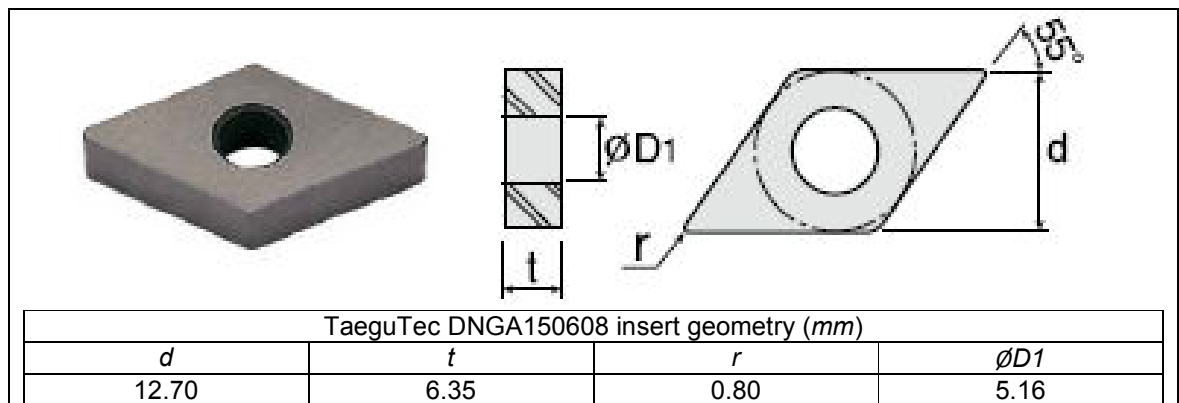


Figure 3.6 Geometries of TaeguTec mixed ceramic tool (TaeguTec, 2011)

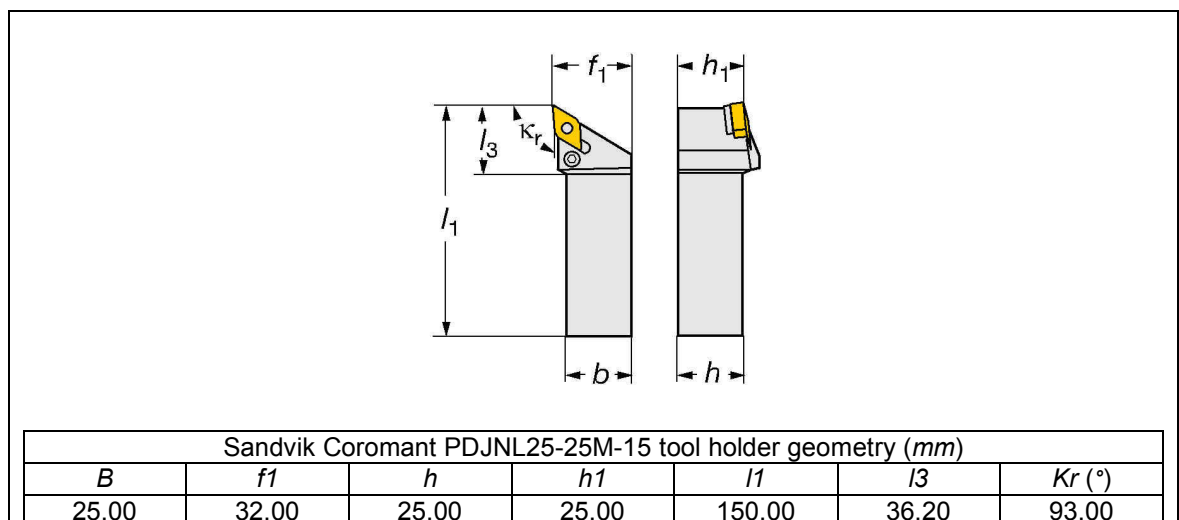


Figure 3.7 Geometries of Sandvik Coromant PDJNL25-25M-15 tool holder

(Sandvik Coromant, 2011)

The workpiece was AISI4140 medium carbon alloy steel and the chemical compositions of the workpiece is shown in Table 3.7.

Table 3.7 Chemical compositions of AISI4140 alloy steel

Material	Chemical composition (%)				
	C	Si	Mn	Cr	Mo
AISI4140	0.42	0.25	0.75	1.05	0.20

Flood cuttings were conducted by using soluble cutting fluid named Mobilcut 102 manufactured by Mobil. Following the recommendations from the manufacturer the cutting fluid was mixed with water to form a milky emulsion at a volumetric concentration of 1 part oil to 20 parts water. This type of cutting fluid has excellent emulsion stability, high resistance towards rust, outstanding lubricating properties and dependable heat transfer capacity. The details of the cutting fluid are shown in Table 3.8.

Table 3.8 Properties of Mobilcut 102 water soluble cutting fluid

Grade	Mobilcut 102
Colour	ASTM 2.0
Density at 15 °C (kg/L)	0.89
Emulsion stability	Excellent
Pour point (°C)	-6.00
Viscosity, cSt at 40 °C	34.00

The minimal quantity lubricant (MQL) mode of cutting was performed by using a developed fluid delivery system. The pulsing rate was 400 *pulse/min*, air pressure was 0.2 *MPa* and delivery rate was 2 *ml/min* which were reported as an optimal condition (Theponthi et al., 2009; Hamdan et al., 2012). The nozzle orientation was set at 45° for the horizontal and vertical angles which was found the most effective for the rake face temperature (Ueda et al., 2006). The MQL system has a pulsed jet nozzle having 1 *mm* orifice and controlled by a variable speed control drive. The nozzle was attached with a flexible holder for better delivery of cutting fluid and the holder was fastened at the tool turret to ensure continuous supply of cutting fluid throughout the cutting path.

The literature review shows that straight oil is suitable for MQL system. Therefore, the cutting fluid used was ECOCUT HSG 905 S produced by FUCHS which is designed for high speed heavy machining process. The characteristics of the straight oil are listed in Table 3.9. ECOCUT HSG 905 S has the benefits of outstanding anti-mist properties, chlorine free EP properties, good detergent and dispersing qualities.

Table 3.9 Characteristics of ECOCUT HSG 905 S

Properties	Value	Test method
Appearance	B & C	Visual
Colour	L0.5	ASTM D 1500
Specific gravity at 60/60 °F (°C)	0.828	ASTM D 1298
Flash point COC (°C)	152.0	ASTM D 92
Viscosity at 40 °C (cSt)	5.0	ASTM D 445
Copper corrosion/24 h at 100 °C	1a	ASTM D 130
Pour point (°C)	-15.0	ASTM D 97
Foam test seq. 1 (ml)	15/0	ASTM D 892
TAN (mgKOH/g)	0.2	ASM D 664

An adjustable spot cooler vortex tube with single point system manufactured by EXAIR was used to deliver chilled air which is one of the lubrication modes in experimental condition levels. The vortex tube was mounted firmly at the tool turret using the swivel magnetic base. The vortex tube supplied compressed air at 0.65 MPa and each experiment was started when the temperature at the nozzle outlet dropped to 0 ± 1 °C measured by K-type thermocouple. It can supply cold air instantly and provides maintenance free quiet operations. The specifications of the vortex tube are included in Table 3.10.

Table 3.10 Specifications of adjustable spot cooler vortex tube 3825

Model	Adjustable spot cooler 3825
Temperature range (°C)	-34 to +21
Air consumption (SLPM)	425 to 850
Cooling capacity (Kcal/hr)	Up to 504

3.4.2 Experimentation for SiO₂ nano base lubricant in hard turning process

To investigate the effects of SiO₂ nano base lubricant on tool wear and surface roughness, hard turning operation of hardened steel AISI4140 was carried out with coated carbide inserts. Cylindrical AISI4140 steel workpiece of 20×200mm² was selected as a case study. A new cutting inserts were adopted for each set of experiments. The workpiece material was heat treated (through-hardened) to achieve the hardness of 52±02HRC. This material is normally used to manufacture roller bearings and automotive components. The mechanical properties of hardened AISI4140 steel are shown in Table 3.11. The machine employed in this study was OKUMA LB15 Lathe Machine, 15hp. To measure the surface roughness (R_a), a calibrated portable surface meter (Mitutoyo SJ-201P) was applied with a cut off distance and sampling length of 1.2mm. In addition, polished granite surface was utilized for more stable and accurate measurement of surface roughness. Tool wear was measured at the end of each cut under an optical microscope at 450× magnification (Dinolite).

Table 3.11 Mechanical properties of AISI4140 steel

Properties		Conditions	
		T (°C)	Treatment
Density (×1000 kg/m ³)	7.7-8.03	25	
Poisson's Ratio	0.27-0.30	25	
Elastic Modulus (GPa)	190-210	25	
Tensile Strength (Mpa)	655.0	25	Annealed at 815°C more
Yield Strength (Mpa)	417.1		
Elongation (%)	25.7		
Reduction in Area (%)	56.9		

Experimentation was carried out with a thin pulsed jet nozzle developed in the laboratory and controlled by a variable speed control drive. The nozzle was equipped with an additional air nozzle to accelerate the lubricant entering the cutting zone and to reduce the oil consumption up to 25%. The nozzle system was attached to a flexible portable

fixture set located on the machining spindle. The flexible design allows the nozzle to set at any desired position without interfering the tool or workpiece during machining. The diameter of the nozzle orifice was 1mm and MQL pressure was set to 0.2 MPa with a delivery rate of 2ml/min. Table 3.12 presents the overall experimental conditions.

Table 3.12 Experimental conditions

Machine tool	OKUMA LB15 Lathe Machine, 15 hp
Instrumentation	
Surface Profilometer	Mitutoyo SJ-201, range (0~12.5mm)
Tool wear Microscope	Dino-Lite AM-4013ZT4 range (400X~470X)
Work material and cutting condition	
Work specimens	AISI4140 steel
Hardness	50 HRC
Size	D 30x200mm
Cutting insert	Coated carbide, Sandvik DNMG 150608 PM
Cutting velocity	120 m/min
Feed rate	0.15 mm/rev
Depth of cut	0.5 mm
Cutting fluid	MQL condition at 0.75 L/hr, FuchsECOCUT oil HSG 905 S,
Nanoparticles	Silicon dioxide, 5-15 nm particle size , 99.5% trace metals basis

3.4.3 Experimentation for SiO₂ and MoS₂ nano base lubricant in milling process

The experiments of SiO₂ and MoS₂ nano base lubricant in milling process are conducted by using the experimental set-up as shown in Figure 3.8. The machine contained a vertical type-machining center (Mitsui Seiki VT3A). The spindle has constant position preloaded bearings with oil-air lubrication system while the maximum rotational speed and power of the machine was 20,000 min⁻¹ and 15 kW, respectively. To investigate the cutting forces, the slot-milling test was carried out of a rectangular workpiece of aluminium AL6061-T6 having a dimension of 50×50×200 mm³. The mechanical properties of aluminium (AL6061-T6) are shown in Table 3.13.

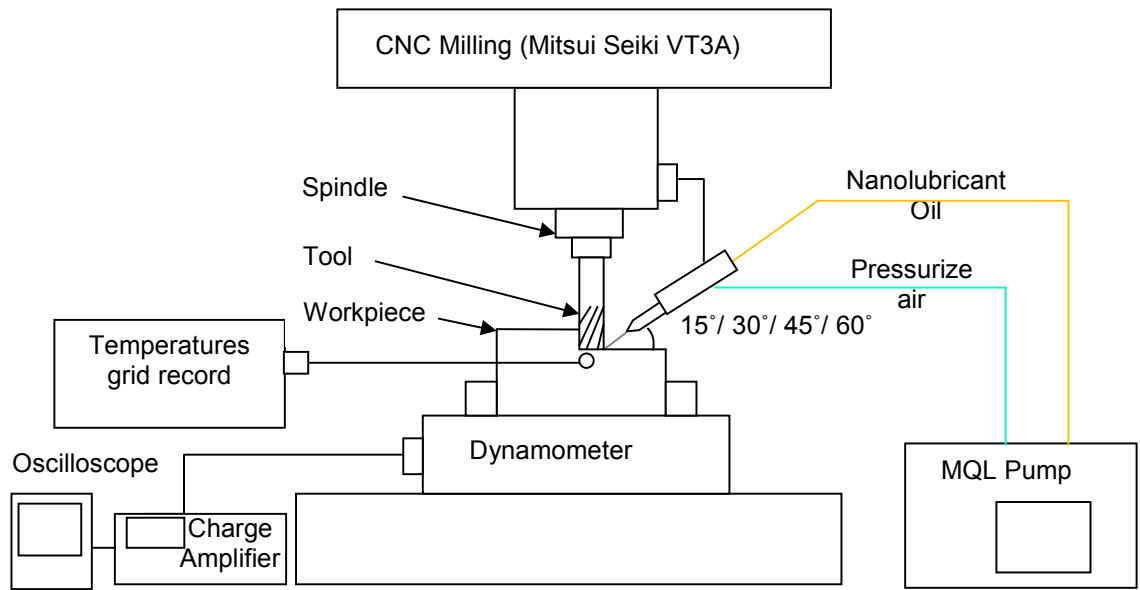


Figure 3.8 Experimental set-up

Table 3.13 Mechanical properties of aluminium (Al6061-T6)

Ultimate Tensile Strength (MPa)		0.2% Proof Stress (MPa)		Webster Hardness Tester (Model B)		Hardness Vickers, (HV) Typical
Min	Typical	Min	Typical	Min	Typical	
260	310	240	275	8'	15'	105

The cutting tool used in the experiment was high speed steel (HSS) with 2 flutes with 10 mm diameter. This is the most common tool used for milling in the industries. The tool moves in the +X direction to cut a stroke of 200 mm. Figure 3.9 shows the workpiece and its tool paths. The cutting speed, feed and depth of cut were 5000 min^{-1} , 100 mm/min and 5 mm respectively which was recommended by the manufacturer. The cutting forces were measured by using a Kistler three-axis dynamometer (type 9255B). The measured cutting force signals in X, Y, and Z directions were captured and filtered with low pass filters (10 Hz cut off frequency). The cutting temperature was measured by using K-Type Testo 925 thermocouple. All test measurements were repeated three times in order to reduce abrupt readings. The thermocouple was installed under the machining surface that reflects the amount of heat dissipation in the workpiece. This amount of dissipated heat is

an indication of the change in the coefficient of friction between tool and chip at cutting zone. During machining, the temperature was measured at every two minutes. The surface roughness of the workpiece was measured by using a surface profilometer (MarSurf PS1 Perthometer). The R_a values were used since they consider the averages of peaks and valleys on the surface and these values are more accurate than the R_t and R_z values. Three measurements were taken and the average is presented in this research.

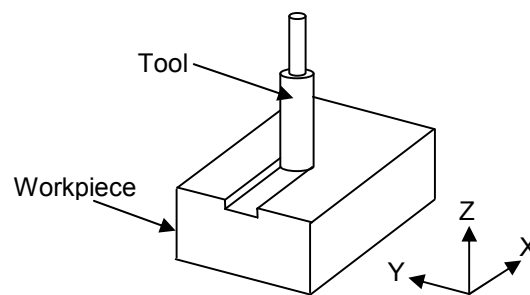


Figure 3.9 The workpiece and tool paths

Two different types of lubrication modes were used in this research. The ordinary lubricant oil and nano base lubricants were studied. To deliver the lubricant to the tool chip interface, MQL system was adopted. The experiment was carried out by using a thin-pulsed jet nozzle that is developed in laboratory and controlled by a variable speed control drive. In the case of using nanoparticles suspended lubrication system, the nozzle was equipped with an additional air nozzle to accelerate the lubricant into the cutting zone. This procedure also reduced the lubricant consumption up to 25%. The nozzle system was attached to a flexible portable fixture mounted on the machining spindle. The flexible design allows the injection nozzle to set at any desired position without interfering with the tool or workpiece during the machining process. The diameter of the nozzle orifices was 1 mm and the MQL oil pressure was set to 0.2 MPa with a delivery rate of 2 ml/min. Figure 3.10 presents the schematic drawing of the nozzle.

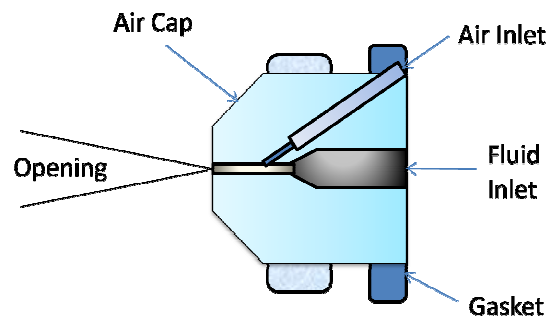


Figure 3.10 Schematic drawing of the nozzle

3.4.4 Experimental set up for carbon onion nano base lubricant in milling process

The experimental set-up used in this study is illustrated in Figure 3.11. The machine used in this experiment was a vertical-type machining centre (Sakai CNC MM-250 S3), in which the spindle has constant position preloaded bearings with oil-air lubrication and the maximum rotational speed was 5000 min^{-1} . The tool used in the experiments was SEC-ALHEM2S8 having a diameter of 8 mm as shown in Figure 3.12.

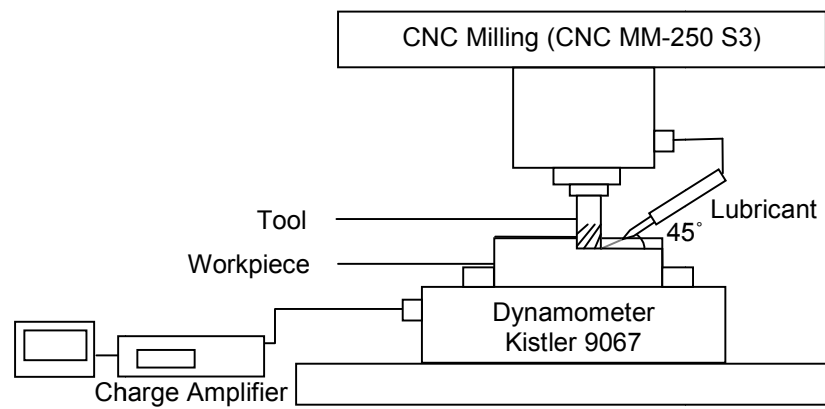


Figure 3.11 The experimental set up

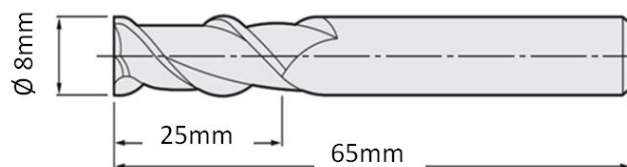


Figure 3.12 The tool geometry

The cutting process of a rectangular Duralumin AL-2017-T4 workpiece (118 HV) having a dimension of $50 \times 20 \times 10 \text{ mm}^3$ was selected as the case study. Table 3.14 shows the mechanical properties of Duralumin AL-2017-T4 and Figure 3.13 shows the workpiece and tool path in the cutting tests. The slot milling test was carried out and the tool moves in the + X direction to cut a stroke of 50 mm. The cutting speed, feed rates and depths of cut were set at 75.408 m/min, 100 mm/min and 1.0 mm respectively as it was recommended by the.

To ensure the consistent lubrication supply, lubricants were properly poured on the top of the workpiece during machining. The cutting force was measured by using Kistler three-axis dynamometer (type 9067) and Keyence NR-600 with Wave Logger Pro Software. The surface roughness (R_a) was measured by using Nanofocus roughness tester equipped with μ sufr software at a magnification of $10\times$, in accordance to the ISO 11562 standard with a 0.6 mm cut-off distance. After each cut, the surface roughness was measured by using stylus profilometer. Three fixed spots were chosen for measuring the surface roughness, where one of the spot was in the middle and the other two was at the edge. Following this, the mean of the three readings was recorded.

Table 3.14 The mechanical properties of Duralumin AL-2017

Mechanical properties	Value
Hardness, Vickers	118
Ultimate tensile strength	427 MPa
Tensile yields strength	276 MPa
Modulus elasticity	72.4 GPa
Poisson ratio	0.33
Fatigue strength	124 MPa
Shear Modulus	27 GPa
Shear Strength	262 MPa

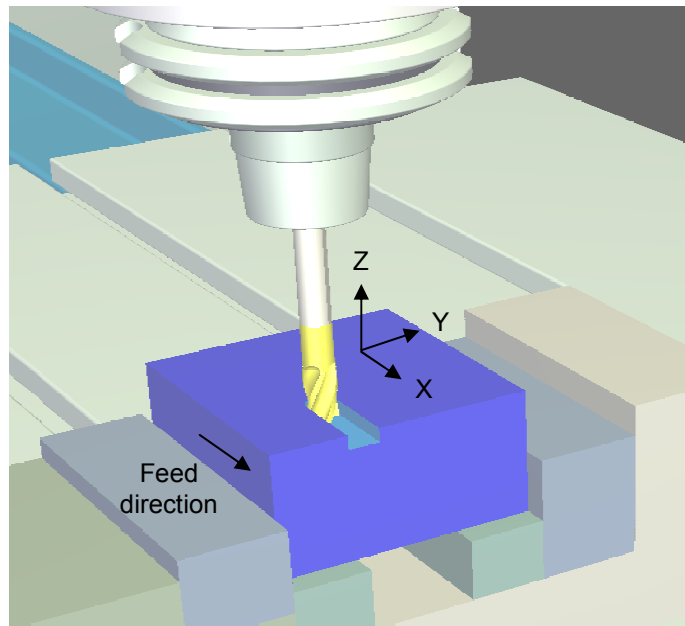


Figure 3.13 The workpiece and tool paths

3.5 Measuring Instrument

In order to evaluate the experimental response, the measuring instruments that were utilized in this research is tabulated in Table 3.15.

Table 3.15 Measuring instrument to evaluate the experimental response

Response	Measuring Instruments
Cutting force	Dynamometer – Kistler 9255B/9067
Surface roughness	Surface meter – Nanofocus + μ surf, Mitutoyo Perthometer
Cutting temperature	Thermocouple – K-Type(<i>Testo 925</i>), Infrared camera
Tool wear	Dinolite microscope
Surface morphology	FESEM <i>Field Emission Scanning Electron Microscope</i>
Surface morphology	EDX <i>Energy dispersive X-ray</i>

3.5.1 Measuring cutting force

For the SiO_2 and MoS_2 nano base lubricant, the cutting force components were measured and recorded by using a Kristler three component tool holder dynamometer (Type 9121). The output from the dynamometer was amplified through Kristler multichannel charge amplifier (Type 5019 A 141). The amplifier was connected to a data acquisition system (National Instruments) that stored all data into a computer installed with

LabVIEW 2011 SP1 software. The force components were radial force (F_x), feed force (F_y) and thrust force (F_z). Before conducting any experiments the dynamometer was calibrated by using the standard weight. The sampling frequency was set in such a way that allows 20 data points to be stored in every cycle.

For the carbon onion nano base lubricant, the cutting force was measured by using the Kistler three-axis dynamometer (type 9067). The measured cutting force signals (X and Y directions) were captured by the Keyence NR-600 equipped with Wave Logger Pro Software. The sampling frequency was set in such that 20 points can be obtained in per spindle revolution. The captured force signal was filtered by low-pass filters (10 Hz cutoff frequency). The dynamometer measured the F_x and F_y forces which are considered as the resultant of all the fluctuating tangential (F_t) and radial (F_r) forces. In this case, cutting force (F_c) was calculated based on the measured F_x and F_y which is equal to:

$$F_c = \sqrt{F_x^2 + F_y^2} \quad \dots \text{Equation 3.1}$$

3.5.2 Measuring surface roughness

Surface roughness of the workpieces was measured after each experiment in term of arithmetic mean value, R_a . Five specific points across the surface was used for measuring the surface roughness and averaged was taken for the sake of statistical significance. The surface roughness was measured using Mitutoyo Surftest SJ-201 profilometer and the surface profiles of the workpieces were generated by Mitutoyo Ver 4.00 software. Specifications used for the measurements are shown in Table 3.16. Surface roughness of cylindrical samples can be measured by using this device because the V-grooves designed at the bottom of detector which ensures stability during measuring. The surface roughness of the specimens was measured on a graphite table to ensure the flatness, stability and accuracy during measurements.

Table 3.16 Specifications for surface roughness measurements

Model	Mitutoyo SurfTest SJ201
Standard	ISO97
Profile	R
Filter	PC50
Unit	mm
Cut-off	0.80
Range	Auto

After machining, the surface roughness (R_a) was measured by using Nanofocus roughness tester equipped with μ sufr software following the ISO 11562 with 0.5 mm cut-off distance. The surface roughness was measured for three times at 10 \times magnification after every single machining run and the average was taken to present the result.

3.5.3 Measurement of cutting temperature

Table 3.17 shows the specification of K-Type Testo 925 thermocouple used to measure the relative cutting temperature during the experimental run.

Table 3.17 K-Type Testo 925 thermocouple specification

Specification	Range
Immersion tip measuring range	-200 to +1000 °C
Accuracy	$\pm(0.5\text{ }^{\circ}\text{C} + 0.3\% \text{ of mv})$ (-40 to +900 °C) $\pm(0.7\text{ }^{\circ}\text{C} + 0.5\% \text{ of mv})$ (remaining range)
Resolution	0.1 °C (-50 to +199.9 °C) 1 °C (remaining range)

The cutting temperature was also measured by using non-contact infrared thermometer produced by Raytek equipped with DataTemp Multidrop software as illustrated in Figure 3.14. The cutting temperature at the tool-work interface was measured by triggering on the laser towards the interface. This process is suitable for high temperature measurement especially for hard machining. The continuous measurements of the cutting temperature was recorded as discrete data by the software for easier analysis. The specifications of the device are shown in Table 3.18.



Figure 3.14 Raytek Infrared Thermometer

Table 3.18 Specifications of Raytek Infrared thermometer

Model	Raytek Infrared Thermometer MM1MH
Temperature range (°C)	540 to 3000
Optical resolution	300:1
Spectral response (μm)	1
Response time (ms)	1

3.5.4 Measuring Tool wear

Dino Lite digital USB microscope (AM413ZT) was used to observe the tool wear in this study as shown in Figure 3.15. This versatile microscope is convenient to obtain quick picture with computer aided measurement capability. The resolution of this microscope is 1280×1024 pixels and can be magnified up to 450×.

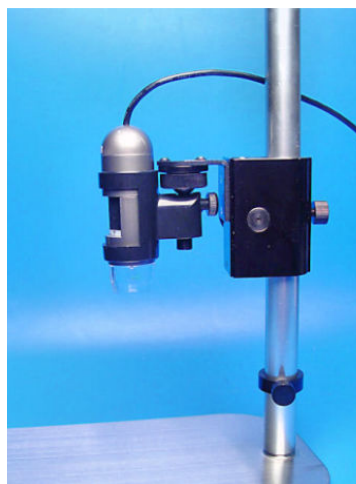


Figure 3.15 Dino Lite Digital microscope

The tool wear was also measured in terms of average tool flank wear. The tool flank wear before and after machining was observed and measured by using Somotech light microscope at a magnification of 100× as it is shown in Figure 3.16. The tool wear images were captured and measured by using measureIT software along with the wear land.



Figure 3.16 Tool flank wear measurement by using Somotech light microscope

3.5.5 Surface morphology

To measure the surface morphology, Zeiss Gemini field emission scanning electron microscope (FESEM) was used and it is shown in Figure 3.17. A field-emission cathode is used in the electron gun for providing narrower probe beams with low or high electron energy. This capacity of this machine provides better spatial resolution and minimizes the sample charging and damage.

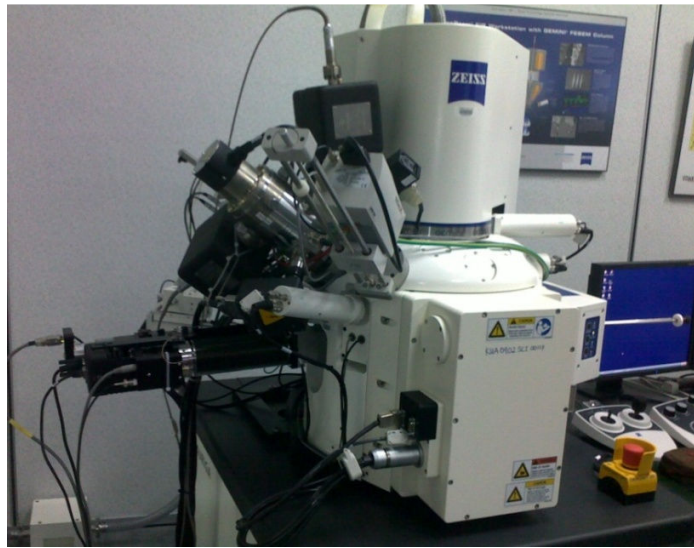


Figure 3.17 Zeiss Gemini field emission scanning electron microscope (FESEM)

CHAPTER 4 RESULTS, DATA ANALYSIS AND DISCUSSIONS

4.1 Introduction

The results of SiO₂, MoS₂ and carbon onion nano base lubricant in turning and milling processes is presented in this research work. To ensure the improvement of performance in machining process by using nano base lubricants, the analysis and discussion of the results are focused on optimizing the parameters in hard turning and milling process. The results, data analysis and discussions will be covered the following aspects:

- L₁₆(4)⁴ orthogonal array design of experiment machining parameter optimization in hard turning process
- L₁₆(4)³ orthogonal array design of experiment in hard turning with SiO₂ nano base lubricant
- Fuzzy logic approach in determining the effect of SiO₂ nano base lubricant on tool wear and surface roughness in hard turning
- L₁₆ (4)³ orthogonal array design of experiment in milling with SiO₂ nano base lubricant
- Fuzzy logic approach in determining the effect of SiO₂ nano base lubricant on cutting force and surface roughness in milling
- L₁₆(4)³ orthogonal array design of experiment in milling with MoS₂ nano base lubricant
- Carbon onion nano base lubricant in milling

4.2 $L_{16}(4)^4$ orthogonal array design of experiment for machining parameter optimization in hard turning process

To optimize the machining parameters in hard turning process, the $L_{16}(4)^4$ orthogonal array design of experiment were conducted. In this case, several response were measured such as cutting force and power consumption, surface roughness, chip thickness ratio and cutting temperatures.

4.2.1 Cutting force and power consumption

Figure 4.1 shows an example cutting forces in X, Y and Z directions for cutting speed of 50 m/min, feed rate of 0.15 mm/rev, depth of cut 0.4 mm and MQL lubrication modes. While, Table 4.1 is presenting TPM and S/N ratio for cutting force.

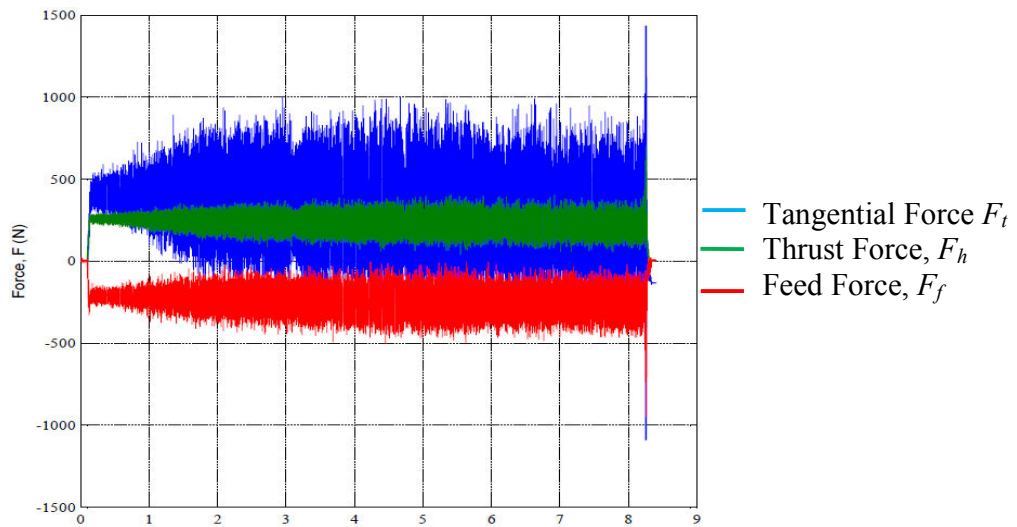


Figure 4.1 An example of measured cutting forces at cutting speed of 50 m/min, feed rate: 0.15 mm/rev and depth of cut 0.4 mm and MQL lubrication modes

Table 4.1 TPM and S/N ratio for cutting force

Exp. no.	Cutting force	TPM (N)	S/N ratio (dB)
1	97.96	97.96	-39.82
2	170.58	170.58	-44.64
3	304.73	304.73	-49.68
4	461.36	461.36	-53.28
5	121.28	121.28	-41.68
6	151.81	151.81	-43.63
7	440.41	440.41	-52.88
8	372.44	372.44	-51.42
9	137.36	137.36	-42.76
10	262.92	262.92	-48.40
11	159.44	159.44	-44.05
12	328.49	328.49	-50.33
13	190.29	190.29	-45.59
14	213.37	213.37	-46.58
15	208.38	208.38	-46.38
16	182.93	182.93	-45.25

The TPM and S/N response data for cutting force is shown in Table 4.2 where TPM is the target performance measurement, which is equal to the average of the measured cutting force at the same level of input parameters (*i*). The TPM and S/N response graph for cutting force is plotted in the Figure 4.2 and Figure 4.3, respectively. From the TPM response graph, the feed rate (factor B) is found to have the most significant effect on the cutting force which is similar to the finding found for surface roughness. The second most significant factor is the depth of cut (factor C), followed by the cutting speed (factor A) and the lubrication mode (factor D). The analysis proposed that the optimal cutting parameters for lowest cutting force should adhere to the lowest feed rate (B1, 0.05 mm/rev), the lowest depth of cut (C1, 0.20 mm), the highest cutting speed (A4, 245 m/min) and MQL cutting condition should be applied (D3). Therefore, the optimal machining parameters for the lowest cutting force are the combination of A4 B1 C1 D3.

Table 4.2 TPM and S/N Response data for cutting force

Factor and interaction	Level (i)	TPM response data (N)				S/N ratio response data (dB)			
		A _i	B _i	C _i	D _i	A _i	B _i	C _i	D _i
Summation at the level of input parameter	1	258.65	136.72	148.03	270.05	-46.85	-42.46	-43.18	-47.40
	2	271.48	199.67	207.18	223.18	-47.39	-45.81	-45.75	-46.42
	3	222.05	278.23	256.97	217.96	-46.38	-48.24	-47.60	-46.24
	4	198.74	336.30	338.74	239.72	-45.94	-50.06	-50.03	-46.51
Difference		72.74	199.58	190.70	52.09	1.45	7.60	6.84	1.15
Rank		3	1	2	4	3	1	2	4

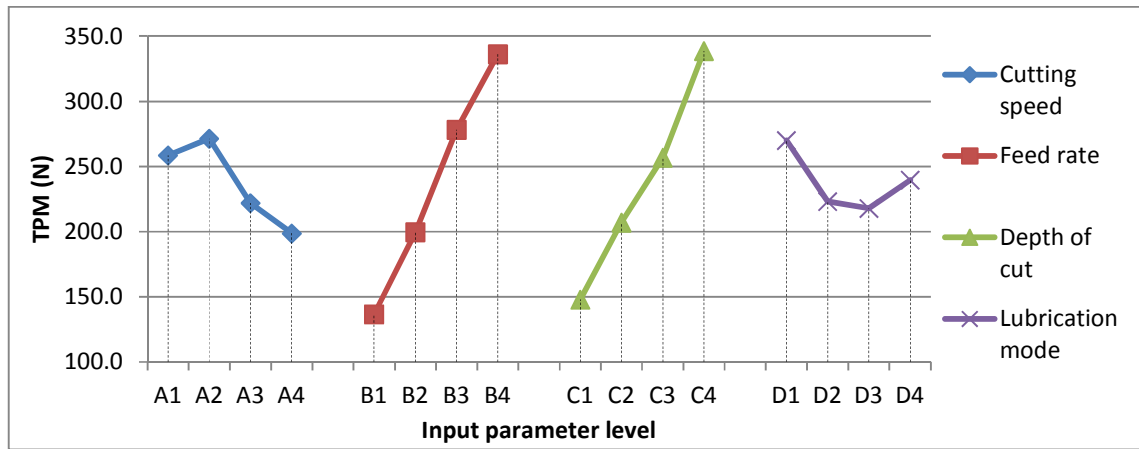


Figure 4.2 TPM response graph for cutting force

As depicted in Figure 4.3, the S/N ratio response reveals that the cutting force is heavily influenced by the feed rate (factor B), followed by the depth of cut (factor C), the cutting speed (factor A) and the lubrication mode (factor D). It is seen from the graph that the optimal cutting parameters for lowest cutting force is the lowest feed rate (B1, 0.05 mm/rev), the lowest depth of cut (C1, 0.20 mm), the highest cutting speed (A4, 245 m/min) and machined by adopting the MQL technique (D3). Thus, the combination for the optimal cutting parameters with lowest cutting force is A4 B1 C1 D3.

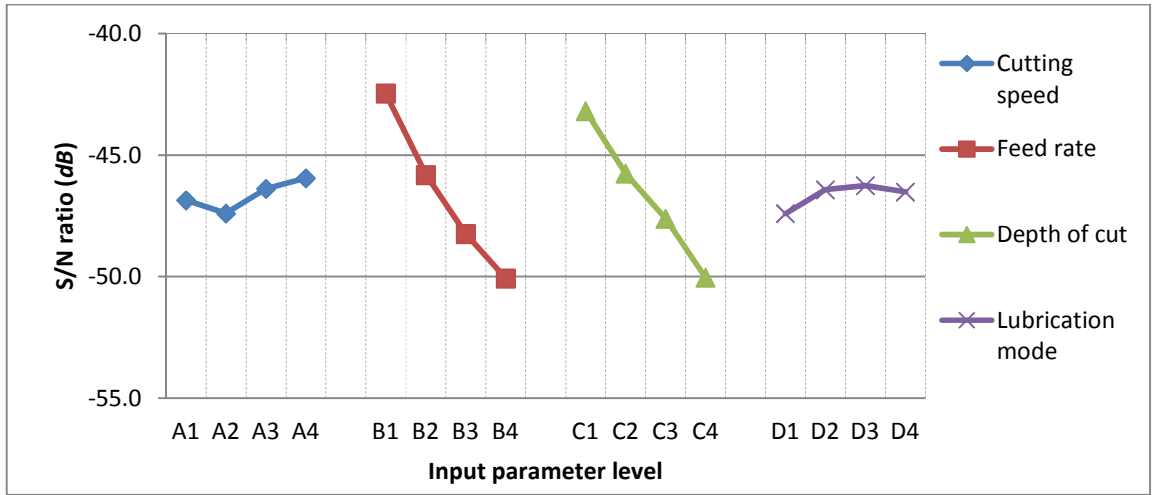


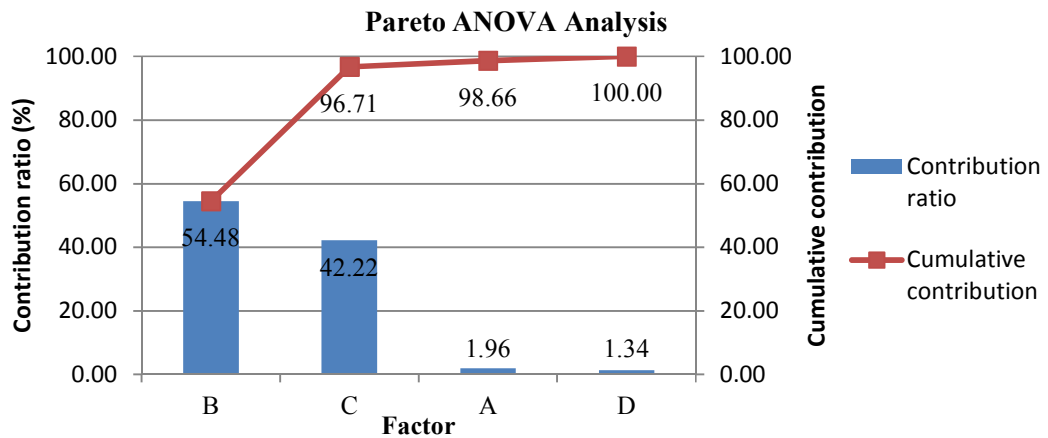
Figure 4.3 S/N response graph for cutting force

The analysis of variance by using Pareto ANOVA is an alternative method to analyze the data for the optimization process. The summation of the squares of differences (S) for each control factor is calculated. One such example for S_A can be obtained by the following equation 4.2:

$$S_A = (A_1 - A_2)^2 + (A_1 - A_3)^2 + (A_2 - A_3)^2 + (A_3 - A_4)^2 \quad \dots \text{Equation 4.1}$$

Similarly, S_B , and S_C are calculated. The contribution ratio for each factor is calculated as the percentage of summation of squares of differences for each factor (S) to the total summation of the squares of differences. The Pareto ANOVA analysis for cutting force is tabulated in Table 4.3. It is seen that the feed rate (factor B) and depth of cut (factor C) contributes 54.48% and 42.22% of the cutting parameters of cutting force. These two factors contribute most of the effect which is 96.71%. The cutting speed (factor A) contributes 1.96% which is almost identical to the contribution of the lubrication mode 1.34% (factor D). In other words, in Pareto ANOVA analysis similar combination (A4 B1 C1 D3) is obtained for the cutting force as it was seen for TPM and S/N ratio analysis.

Table 4.3 Pareto ANOVA analysis for cutting force

Factor and interaction		A_i	B_i	C_i	D_i																				
Summation at the level of input parameter	1	-46.85	-42.46	-43.18	-47.40																				
	2	-47.39	-45.81	-45.75	-46.42																				
	3	-46.38	-48.24	-47.60	-46.24																				
	4	-45.94	-50.06	-50.03	-46.51																				
Total summation at factor level		-186.11	-186.58	-186.58	-186.58																				
Summation of squares of differences (S)		4.66	129.98	100.72	3.19																				
Total of summation squares of differences $S_t= S_A+ S_B+ S_C+ S_D$		238.57																							
Contribution ratio (%)		1.96	54.48	42.22	1.34																				
Pareto diagram																									
<div><p>Pareto ANOVA Analysis</p><p>Contribution ratio (%)</p><table><thead><tr><th>Factor</th><th>Contribution ratio (%)</th></tr></thead><tbody><tr><td>B</td><td>54.48</td></tr><tr><td>C</td><td>42.22</td></tr><tr><td>A</td><td>1.96</td></tr><tr><td>D</td><td>1.34</td></tr></tbody></table><p>Cumulative contribution</p><table><thead><tr><th>Factor</th><th>Cumulative contribution (%)</th></tr></thead><tbody><tr><td>B</td><td>54.48</td></tr><tr><td>C</td><td>96.71</td></tr><tr><td>A</td><td>98.66</td></tr><tr><td>D</td><td>100.00</td></tr></tbody></table></div>						Factor	Contribution ratio (%)	B	54.48	C	42.22	A	1.96	D	1.34	Factor	Cumulative contribution (%)	B	54.48	C	96.71	A	98.66	D	100.00
Factor	Contribution ratio (%)																								
B	54.48																								
C	42.22																								
A	1.96																								
D	1.34																								
Factor	Cumulative contribution (%)																								
B	54.48																								
C	96.71																								
A	98.66																								
D	100.00																								
Cumulative contribution		54.48	96.71	98.66	100.00																				
Optimum combination		B1	C1	A4	D3																				
Overall optimum conditions for all factors		A4 B1 C1 D3																							

The analyses show that the feed rate and depth of cut are the most significant factors that influence the cutting force. The cutting force is directly proportional to the feed rate and depth of cut. The increase of these factors leads to an increase of cutting force because the combination of feed rate and depth of cut define the uncut chip section and determine the amount of energy required to remove a specific volume of material. The higher feed rate and depth of cut generate larger undeformed chip area and hence increase the cutting force to overcome the resistance of the workpiece (Ghani et al., 2004).

The highest cutting speed is found to promote the lower cutting force. This is because the cutting temperature increases with increasing cutting speed. Rise in temperature at the tool-chip interface reduces both of the shearing strength and friction forces (Bouacha et al., 2010). Moreover, machining at higher cutting speed avoids the formation of built up edge which has detrimental effect on cutting forces (Ebrahimi & Moshksar, 2009). Lower cutting force ensures lower distortion in the workpiece, which in turn improves the surface finish of the product (Senthil Kumar et al., 2003).

MQL is found the most suitable technique for lowering the cutting force. It is believed that the pulsed-jet application allows the cutting oil to penetrate into the tool-chip and tool-workpiece interfaces more efficiently. Lubricants take places even inside the minute capillaries and interfaces to reduce the friction force. Beside this, the penetration and adhesion of the lubricants to the workpiece can promote the plastic flow at the backside of the chip which relieves the compressive stress and promotes the formation of curl chip that reduces tool-chip contact length (Pusavec et al., 2011; Sharma et al., 2009).

As a consequence of changing the cutting force, the power consumption was investigated as well. The power consumption of the cutting tool is obtained as follows (Reddy & Rao, 2006).

$$P = F_c V_c \quad (\text{Watt}) \quad \dots \text{Equation 4.2}$$

Where, P represents the power consumption (kW), F_c is the cutting force (N) and V_c is the cutting speed (m/min). However, it should be noted that during turning process, the tangential force (F_t) is mainly responsible for shearing of the material while the radial force (F_r) is responsible for the feed force to perform cutting. F_t and F_r are frequently changed based on the engaged angle of cutting. However, the dynamometer is measuring F_x and F_y forces which are considered as the fluctuating tangential (F_t) and radial (F_r) forces.

The forces generated during metal cutting have a direct influence on cutting force and chip thickness ratio. The three components of force that occur during turning are shown in Figure 4.4. According to this figure, the feed force, thrust force and main cutting force is represented by F_f , F_t and F_c respectively. Cutting force is one of the most important characteristic variables in the cutting processes (Ghani et al., 2004). In this case, the cutting force (F_t) is represented based on the measured F_x , thrust force (F_h) is represented based on the measured F_z and radial force (F_r) is represented based on the measured F_y .

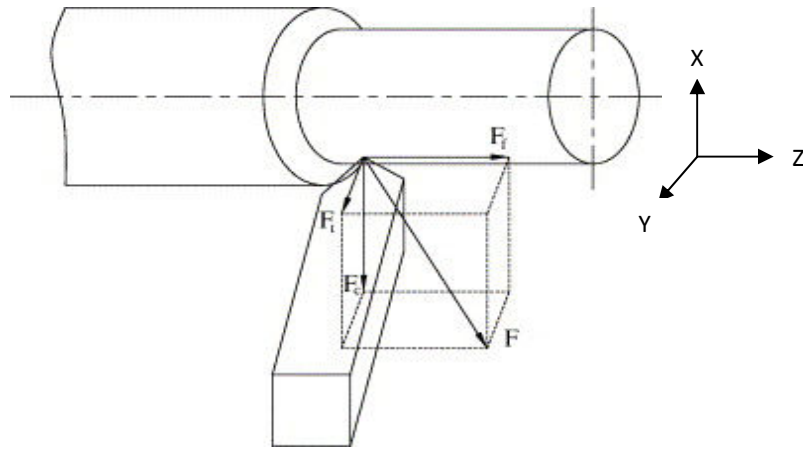


Figure 4.4 Cutting force components which occurs during metal cutting in turning
(Ghani et al., 2004)

Figure 4.5 shows the changes in power consumption during the cutting process. As it can be seen, the power consumption is reduced significantly at lowest feed rate (B1, 0.05 mm/rev), lowest depth of cut (C1, 0.20 mm), highest cutting speed (A4, 245 m/min) and applying MQL cutting (D3).

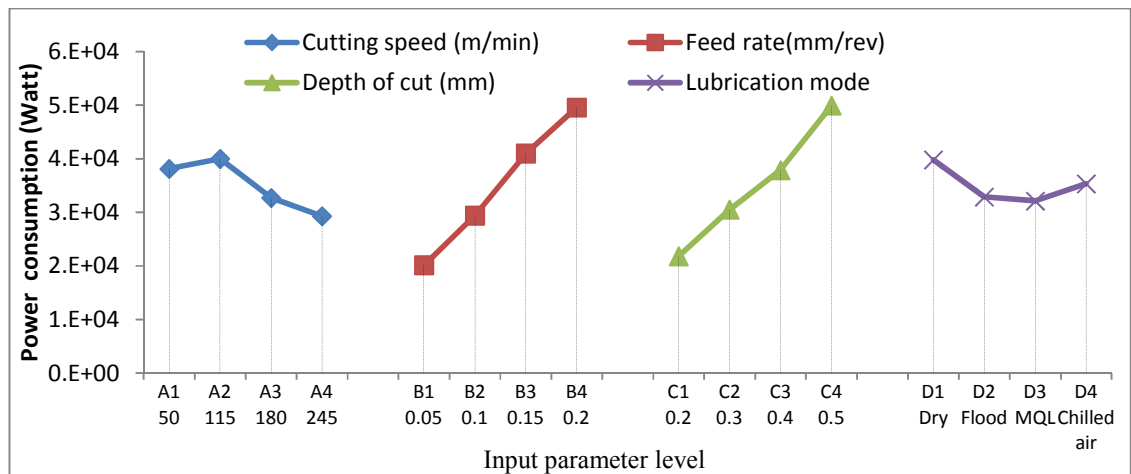


Figure 4.5 The power consumption of the cutting tool for both lubrication modes

The results from the seizure experiment can be explained by the fact that the deformation of the chip flowed over a tool leads to a localized intense shear region due to the friction at the rake face. This type of shear action is known as secondary shear. The results from seizure experiment shows that the feed rate is the most prominent factors affecting the cutting force followed by depth of cut, cutting speed, while the lubrication mode has a less significant effect. Thus for lower cutting force, the recommended setting are the lowest values of the depth of cut, feed rate and cutting speed in conjunction with the application of MQL. The experimental results show that the cutting force is lower at higher cutting speed and comparatively high at low cutting speed. The cutting force exhibits an almost linear increasing trend with cutting speed. The reason for the reduction of cutting force with increasing cutting speed is due to the decreasing in chip thickness. This means that at smaller speed, thinner chips are produced. It is also suggested that the drop in these forces is partly caused by the decrease in contact area of flow and partly caused by the drop in shear strength at the flow zone. As the cutting speed decreases, the chips become thinner and shear angle increases. Such an increment of shear angle decreases the chip reduction coefficient and chip strains. This indicates that the plastic deformation takes place with less strain, so the force and power consumptions are lowered. The coefficient of friction is

decreased and consequently main cutting force is also decreased, which in turn preserves the machining performance leading to smaller power consumption. Another possible reason is that when the spindle speed is increased, cutting energy generates compressive stresses leading to an increase in temperature at the tool-chip interface. The generated heat in the machining zone helps to soften the workpiece material which in turn reduces the cutting forces required to cut the material with better surface finish. However, it is believed that the spindle speed should be controlled to an optimum value, as the temperature significantly affect the cutting forces and power consumption especially for hard materials. Thus the implementation of cutting fluid as a coolant is very crucial.

In term of lubrication modes, MQL technique is found to be the most suitable for lowering the cutting force and power consumption. It is believed that the low viscosity of straight oil employed with pulsed-jet application allows the cutting oil to penetrate efficiently into the tool-chip and tool-work interfaces. Hence, the minute capillaries and interfaces are wetted by the lubricants and the friction force is reduced (Kumar & Ramamoorthy, 2007). Besides, the penetration and adhesion of lubricant to the work surface promotes the plastic flow at the backside of the chip which relieves the compressive stress and promotes the formation of curly chip that reduces tool-chip contact length (Sharma et al., 2009). The experimental results show that chilled air does not reduce the cutting force due to the fact that the blow of chilled air towards cutting zone increases the hardness and brittleness of the workpiece material which makes the chip formation more difficult to be accomplished. Additionally, the effect of cutting parameters is similar for both on cutting forces and chip thickness ratio. This observation further supports that the proposed combination of cutting parameters is capable to show good machining performances.

A verification test was performed by using the optimal parameters in order to ensure the results. To address this issue, the combination of A4 B1 C1 D3 was used to validate the recommendation. This test was repeated for sixteen times and the average TPM values are reported for the cutting forces and chip thickness. The result shows an improvement of 10.48% and 8.22% in cutting force and chip thickness respectively, compared to the values obtained from experiments shown in Table 4.1. Based on the results, the following conclusions are derived:

1. Lower power consumption during machining can be achieved with the set of the lowest feed rate (B1, 0.05 mm/rev), lowest depth of cut (C1, 0.20 mm), highest cutting speed (A4, 245 m/min) and applying MQL cutting condition (D3).
2. Thus for the recommended setting for lower cutting force are the lowest values of the depth of cut and feed rate with the highest values of the lubrication pressure and spindle speed.

4.2.2 Surface roughness

Table 4.4 shows the TPM and S/N ratio for surface roughness. The TPM and S/N response data for surface roughness are shown in Table 4.5. The TPM response graph is plotted based on the data taken from Table 4.5 as it is shown in Figure 4.6.

Table 4.4 TPM and S/N ratio for surface roughness

Exp. no.	Surface roughness	TPM (μm)	S/N ratio (dB)
1	0.17	0.17	15.08
2	0.40	0.40	7.96
3	0.93	0.93	0.66
4	1.34	1.34	-2.56
5	0.28	0.28	10.87
6	0.45	0.45	6.55
7	0.72	0.72	2.85
8	1.32	1.32	-2.44
9	0.18	0.18	14.58
10	0.24	0.24	12.34
11	0.78	0.78	2.11
12	1.35	1.35	-2.58
13	0.26	0.26	11.64
14	0.33	0.33	9.62
15	0.79	0.79	2.02
16	1.27	1.27	-2.10

It is clear from the figure that the feed rate (factor B) is the most significant factor affecting the surface roughness followed by the cutting speed (factor A), the depth of cut (factor C) and the lubrication mode (factor D). It is seen that the lowest feed rate (B1, 0.05 mm/rev), intermediate cutting speed (A3, 180 m/min), highest depth of cut (C4, 0.50 mm) and hard turning operation in the dry cutting condition (D1) is the best combination for the best surface finish. The optimal cutting parameters combination for best surface finish is A3 B1 C4 D1.

Table 4.5 TPM and S/N response data for surface roughness

Factor and interaction	Level (i)	TPM response data (μm)				S/N ratio response data (dB)			
		A _i	B _i	C _i	D _i	A _i	B _i	C _i	D _i
Summation at the level of input parameter	1	0.70	0.22	0.67	0.64	5.28	13.04	5.41	6.24
	2	0.69	0.35	0.70	0.69	4.45	9.11	4.56	4.81
	3	0.63	0.80	0.68	0.68	6.61	1.91	5.60	5.44
	4	0.66	1.32	0.64	0.69	5.29	-2.41	6.06	5.14
Difference		0.07	1.09	0.06	0.05	2.15	15.45	1.50	1.42
Rank		2	1	3	4	2	1	3	4

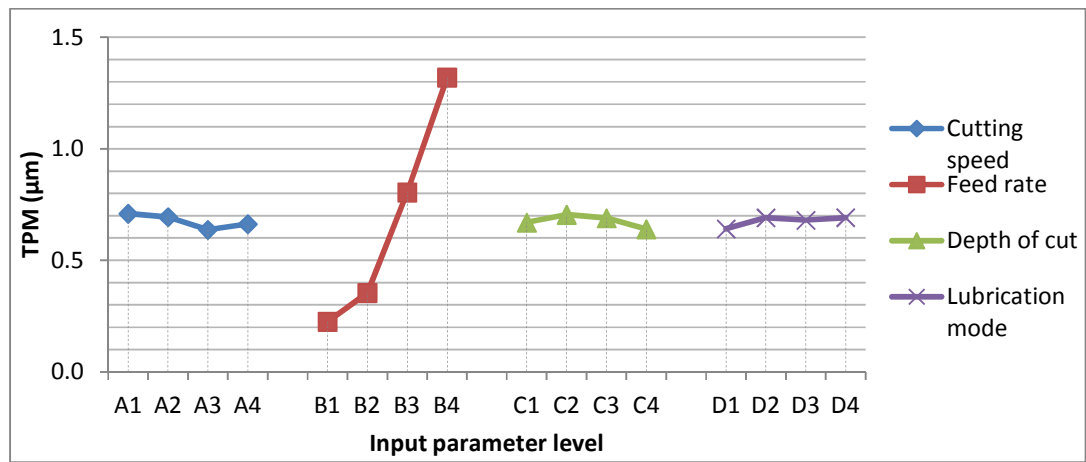


Figure 4.6 Graph of TPM response for surface roughness

The S/N ratio response graph for surface roughness is presented in Figure 4.7 which is constructed from the S/N ratio response data tabulated in Table 4.5. The highest S/N ratio indicates the best surface finish. The graph reveals that the feed rate (factor B) is the most influential factor for surface roughness, followed by the cutting speed (factor A), the depth of cut (factor C) and finally the lubrication mode (factor D). The lowest surface roughness can be achieved by using the lowest feed rate (B1, 0.05 mm/rev), intermediate cutting speed (A3, 180 m/min) and highest depth of cut (C4, 0.50 mm) with dry cutting condition (D1). Hence, the optimal parameters combination for best surface finish is A3 B1 C4 D1.

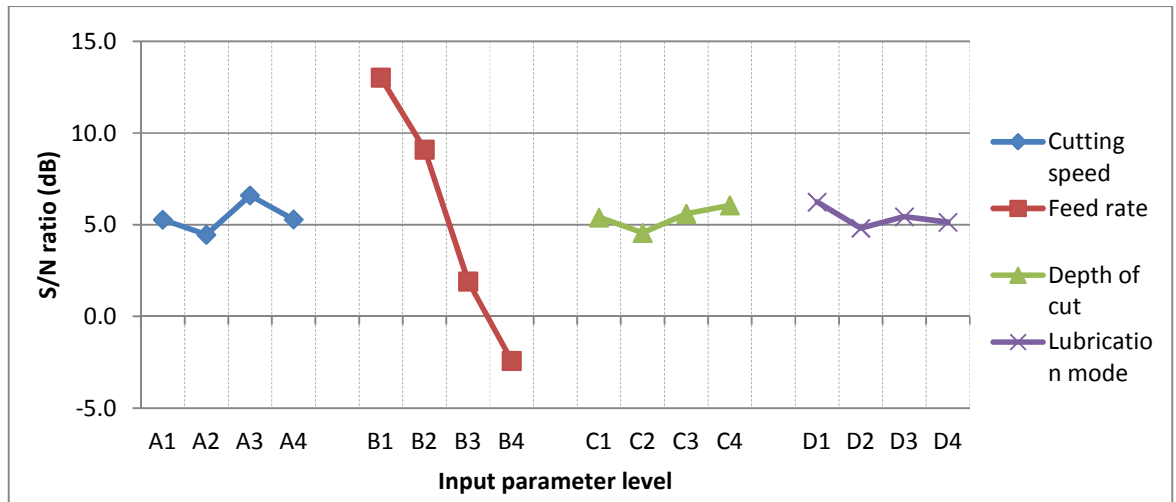
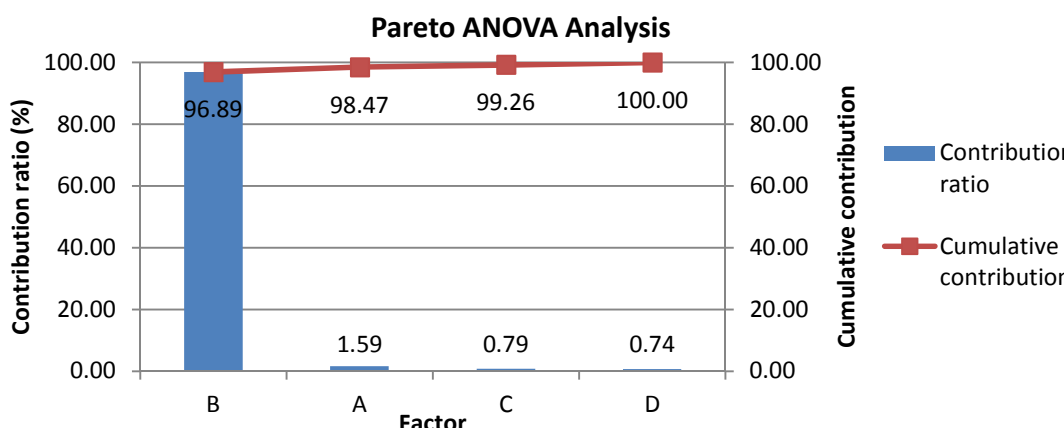


Figure 4.7 Graph of S/N ratio response for surface roughness

Table 4.6 proposes the best combination for surface roughness using the Pareto ANOVA analysis. It shows that the feed rate (factor B) has the most prominent effect which is 96.89%. The cutting speeds, the depth of cut and the lubrication mode have insignificant effect on surface roughness. The contribution of parameters for surface roughness is cutting speed (factor A) is 1.59%, depth of cut (factor C) 0.79 % and the lubrication mode (factor D) 0.74%. The best combination to achieve the lowest surface roughness is A3 B1 C4 D1 which is similar to the TPM and the S/N ratio response analysis. In addition, the cutting speed has weaker effect on the surface roughness which is identical from all analysis. Hence, highest cutting speed can be set to take the advantage of higher material removal without deteriorating the surface finish.

Table 4.6 Pareto ANOVA analysis for surface roughness

Factor and interaction		A_i	B_i	C_i	D_i															
Summation at the level of input parameter	1	5.28	13.04	5.41	6.24															
	2	4.45	9.11	4.56	4.81															
	3	6.61	1.91	5.60	5.44															
	4	5.29	-2.41	6.06	5.14															
Total summation at factor level		21.65	21.65	21.65	21.65															
Summation of squares of differences (S)		9.53	582.03	4.73	4.44															
Total of summation squares of differences $S_t= S_A+ S_B+ S_C+ S_D$		600.7445																		
Contribution ratio (%)		1.59	96.89	0.79	0.74															
Pareto diagram																				
<div><p>Pareto ANOVA Analysis</p><p>The chart displays the contribution ratio of factors B, A, C, and D. Factor B contributes 96.89%, A contributes 1.59%, C contributes 0.79%, and D contributes 0.74%. The cumulative contribution starts at 96.89% for B, reaches 98.47% for A, 99.26% for C, and finally reaches 100.00% for D.</p><table><thead><tr><th>Factor</th><th>Contribution ratio (%)</th><th>Cumulative contribution (%)</th></tr></thead><tbody><tr><td>B</td><td>96.89</td><td>96.89</td></tr><tr><td>A</td><td>1.59</td><td>98.47</td></tr><tr><td>C</td><td>0.79</td><td>99.26</td></tr><tr><td>D</td><td>0.74</td><td>100.00</td></tr></tbody></table></div>						Factor	Contribution ratio (%)	Cumulative contribution (%)	B	96.89	96.89	A	1.59	98.47	C	0.79	99.26	D	0.74	100.00
Factor	Contribution ratio (%)	Cumulative contribution (%)																		
B	96.89	96.89																		
A	1.59	98.47																		
C	0.79	99.26																		
D	0.74	100.00																		
Cumulative contribution		96.89	98.47	99.26	100.00															
Optimum combination		B1	A3	C4	D1															
Overall optimum conditions for all factors		A3 B1 C4 D1																		

The continuous increment of the cutting speed might deteriorate the surface roughness as well. It is known that high cutting speed results in higher cutting temperature. Moreover, the highest cutting speed can cause chattering to the machine tool that might affect the surface roughness negatively (Benga & Abrao, 2003). Therefore, it is believed that the cutting speed should be controlled at an optimum value to take the advantage of higher material removal with a good surface finish. Even though the analysis suggests that the depth of cut plays a minor role in affecting the surface roughness, it is worth to state that the highest depth of cut should be considered all the time. The reasons are the ability to

produce good surface finish and to compensate the low material removal attribute by low feed rate.

Comparison between lubrication modes it is found that the dry cutting mode is the best choice to improve the surface finish in hard turning process. Dry cutting increases the workpiece and tool tip temperature close to the cutting zone. Thus, the workpiece is annealed and softened. The thermal softening reduces shear strength and hardness of the material which makes the chip formation easier, reduces the cutting force and improves the surface finish (Bartarya & Choudhury, 2012; Diniz & Micaroni, 2002).

4.2.3 Chip thickness ratio

The TPM and S/N ratio for chip thickness ratio is shown in Table 4.7. While, the TPM responses for chip thickness are shown in Table 4.8.

Table 4.7 TPM and S/N ratio for chip thickness ratio

Exp. no.	Chip thickness ratio	TPM (μm)	S/N ratio (dB)
1	0.50	0.50	-6.04
2	0.63	0.64	-4.00
3	0.72	0.72	-2.85
4	0.82	0.83	-1.67
5	0.78	0.79	-2.17
6	0.88	0.88	-1.39
7	0.77	0.78	-2.25
8	0.97	0.98	-0.28
9	0.55	0.56	-5.13
10	0.79	0.80	-2.03
11	1.20	1.20	1.46
12	1.10	1.10	0.81
13	0.58	0.59	-4.75
14	0.88	0.88	-1.15
15	1.05	1.06	0.27
16	1.66	1.67	4.44

Table 4.8 TPM response for chip thickness ratio

Factor and interaction	Level (i)	TPM response data			
		A_i	B_i	C_i	D_i
Summation at the level of input parameter	$i = 1$	0.67	0.60	1.06	0.81
	$i = 2$	0.85	0.79	0.89	0.85
	$i = 3$	0.91	0.94	0.78	0.99
	$i = 4$	1.04	1.14	0.74	0.83

Figure 4.8 presents the TPM response graph for chip thickness ratio and it indicates that the feed rate (factor B) is the major factor that affects the chip thickness ratio. The cutting speed (factor A) and the depth of cut (factor C) are the significant cutting parameters in determining the chip thickness ratio. Meanwhile, the lubrication mode (factor D) has the least significant influence to the chip thickness ratio. The Figure 4.8 illustrates that the chip thickness ratio is increased with the high values of feed rate and cutting speed. On the contrary, the chip thickness ratio is increased with the low values of the depth of cut and machining using MQL lubrication mode. The larger TPM value is ideal because higher

chip thickness ratio signifies better the machining operation. The optimal cutting parameters are not proposed in this section because the chip thickness ratio acts as the indication to the machining operation.

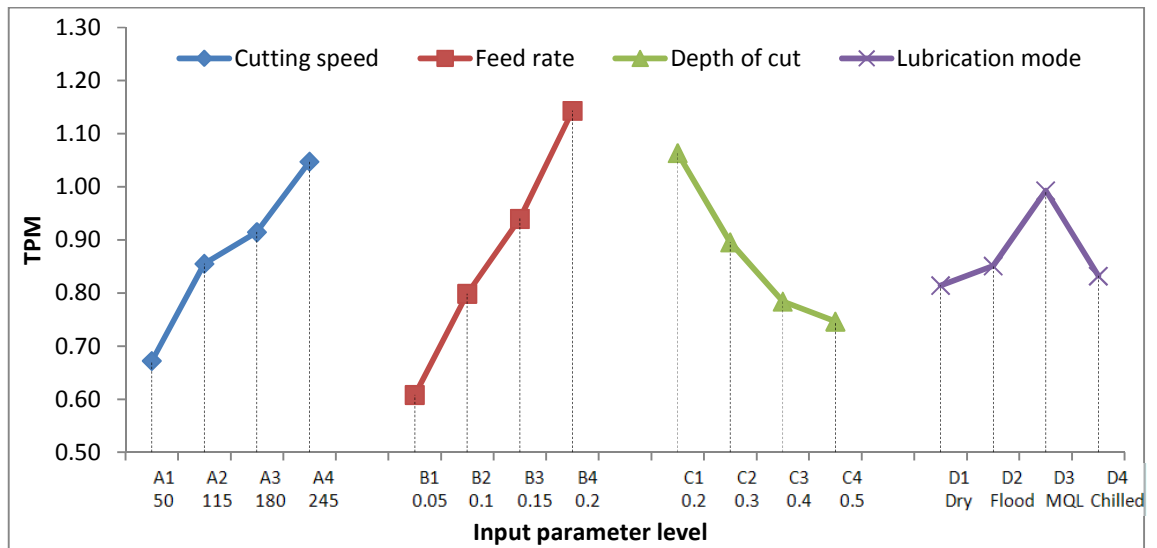


Figure 4.8 TPM response graph for chip thickness ratio

4.2.4 Cutting temperature

Table 4.9 shows the TPM and S/N ratio for cutting temperature. Figure 4.9 illustrates the TPM response for cutting temperature obtained from TPM and S/N response data shown in Table 4.10.

Table 4.9 TPM and S/N ratio for cutting temperature

Exp. no.	Cutting temperature, T (°C)	TPM (°C)	S/N ratio (dB)
1	662.23	662.23	-56.42
2	540.00	540.00	-54.65
3	577.23	577.23	-55.23
4	593.60	593.60	-55.47
5	583.63	583.63	-55.32
6	602.27	602.27	-55.60
7	730.03	730.03	-57.27
8	574.90	574.90	-55.19
9	589.90	589.90	-55.42
10	572.90	572.90	-55.16
11	608.33	608.33	-55.68
12	725.30	725.30	-57.21
13	540.00	540.00	-54.65
14	665.20	665.20	-56.46
15	549.30	549.30	-54.80
16	556.27	556.27	-54.91

From the figure, it is seen that the sequence of factors according to their significance towards cutting temperature are lubrication mode (factor D) followed by cutting speed (factor A), feed rate (factor B) and finally depth of cut (factor C). The combination of the level 2 (flood cutting mode) of the lubrication mode, the level 1 (50 m/min) of the cutting speed, the level 2 of the feed rate (0.10 mm/rev) and the level 2 (0.30 mm) of the depth of cut is found to be ideal for minimum cutting temperature. Hence, the optimum combination for cutting temperature is A1 B2 C2 D2.

Table 4.10 TPM and S/N response data for cutting temperature

Factor and interaction	Level (i)	TPM response data (°C)				S/N ratio response data (dB)			
		A _i	B _i	C _i	D _i	A _i	B _i	C _i	D _i
Summation at the level of input parameter	1	570.23	589.06	607.27	695.69	-55.03	-55.37	-55.65	-56.83
	2	622.70	572.05	576.52	537.90	-55.84	-55.06	-55.08	-54.55
	3	624.10	616.22	601.80	572.50	-55.86	-55.74	-55.57	-55.15
	4	572.81	612.51	604.25	583.76	-55.12	-55.69	-55.55	-55.31
Difference		53.87	44.16	30.75	157.79	0.83	0.68	0.56	2.28
Rank		2	3	4	1	2	3	4	1

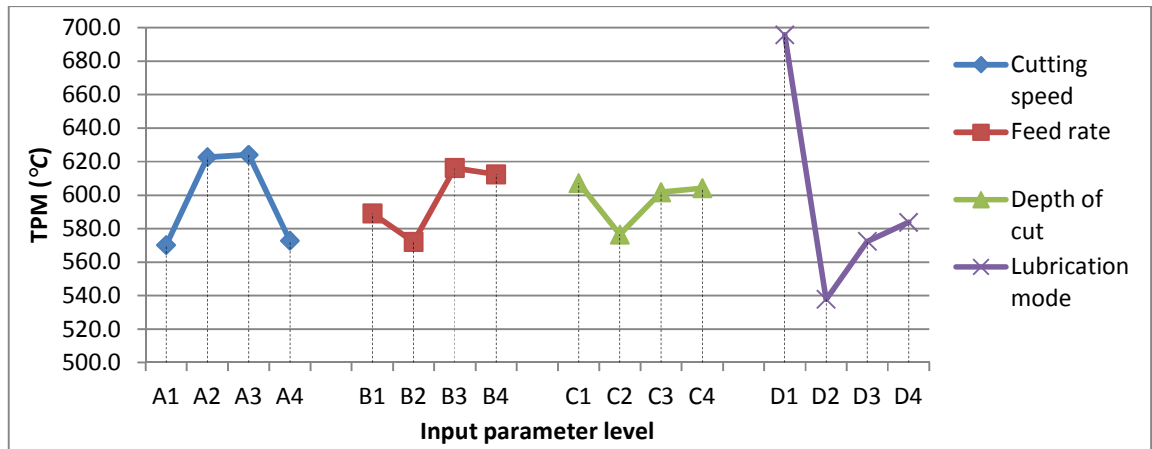


Figure 4.9 TPM response graph for cutting temperature

The lubrication mode (factor D) has the highest significance level towards cutting temperature whilst the cutting speed (factor A) has the second highest level. The variation of the feed rate (factor B) and the depth of cut (factor C) show less influence on the cutting temperature. These findings are graphically presented in Figure 4.10. Besides, the best combination for lowest cutting temperature is the level 2 (flood cutting mode) of the lubrication mode, the level 1 (50 m/min) of the cutting speed, the level 2 of the feed rate (0.10 mm/rev) and the level 2 (0.30 mm) of the depth of cut, which can be summarized as A1 B2 C2 D2.

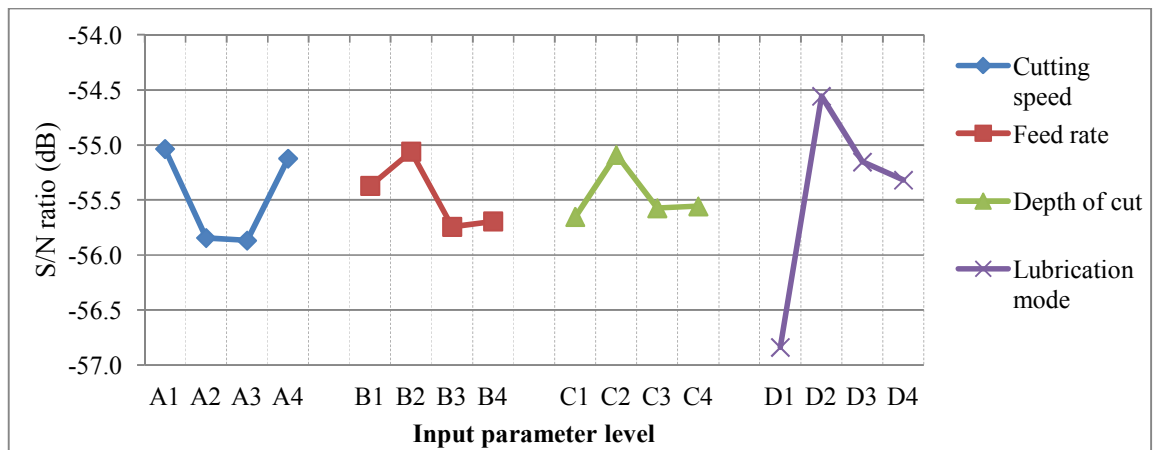
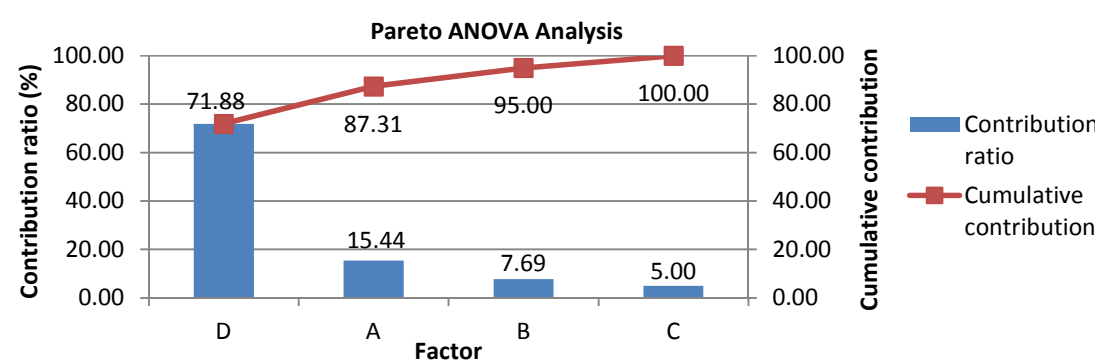


Figure 4.10 S/N ratio response graph for cutting temperature

The cutting temperature obtained from the Pareto ANOVA analysis is shown in Table 4.11. The best combination for lowest cutting temperature is the lubrication mode (factor D) 71.88%, the cutting speed (factor A) 15.44%, the feed rate (factor B) 7.69% and the depth of cut (factor C) 5.00%. The lubrication mode and the cutting speed have the essential roles in affecting the cutting temperature up to cumulative percentage of 87.31. In short, the best combination for lowest cutting temperature is A1 B2 C2 D2. Moreover, the analysis proved that the depth of cut has insignificant effects on the cutting temperature. Therefore, depth of cut can be increased without increasing temperature to facilitate the productivity needed in the industries.

Table 4.11: Pareto ANOVA analysis for cutting temperature

Factor and interaction		Ai	Bi	Ci	Di															
Summation at the level of input parameter	1	-55.03	-55.37	-55.65	-56.83															
	2	-55.84	-55.06	-55.08	-54.55															
	3	-55.86	-55.74	-55.57	-55.15															
	4	-55.12	-55.69	-55.55	-55.31															
Total summation at factor level		-221.87	-221.87	-221.87	-221.87															
Summation of squares of differences (S)		2.43	1.21	0.78	11.32															
Total of summation squares of differences $S_T= S_A+ S_B+ S_C+ S_D$		15.7501																		
Contribution ratio (%)		15.44	7.69	5.00	71.88															
Pareto diagram																				
<div><p>Pareto ANOVA Analysis</p><p>The chart displays the contribution ratio of four factors (D, A, B, C) to the total variation in cutting temperature. Factor D is the most significant, contributing 71.88% of the total. Factor A contributes 15.44%, B contributes 7.69%, and C contributes 5.00%. The cumulative contribution of the factors is shown as a red line with square markers, reaching 100.00% at factor C.</p><table><tr><th>Factor</th><th>Contribution ratio (%)</th><th>Cumulative contribution (%)</th></tr><tr><td>D</td><td>71.88</td><td>71.88</td></tr><tr><td>A</td><td>15.44</td><td>87.31</td></tr><tr><td>B</td><td>7.69</td><td>95.00</td></tr><tr><td>C</td><td>5.00</td><td>100.00</td></tr></table></div>						Factor	Contribution ratio (%)	Cumulative contribution (%)	D	71.88	71.88	A	15.44	87.31	B	7.69	95.00	C	5.00	100.00
Factor	Contribution ratio (%)	Cumulative contribution (%)																		
D	71.88	71.88																		
A	15.44	87.31																		
B	7.69	95.00																		
C	5.00	100.00																		
Cumulative contribution		71.88	87.31	95.00	100.00															
Optimum combination		D2	A1	B2	C2															
Overall optimum conditions for all factors		A1 B2 C2 D2																		

Analysis reveals that the combination of lubrication mode and cutting speed contributes 87.31% of the cutting temperature. The higher cutting speed increases the cutting temperature tremendously. It was seen that the cutting temperature increases linearly from the speed of 50 to 180 m/min. However, it is noticeable that the cutting temperature decreases if cutting speed continue to increase above 180 m/min. It is clear that the cutting speed is a function of heat generation during machining. On the other hand, the reduction of cutting temperature at the highest cutting speed ensures higher material removal. Higher material removal results in more heat dissipation to the surroundings by forced convection and heat carried away by the chip. Furthermore, flood cutting mode is

the best solution for reducing the cutting temperature. The higher specific heat capacity of water present in the emulsions makes it a very effective coolant during cutting operation.

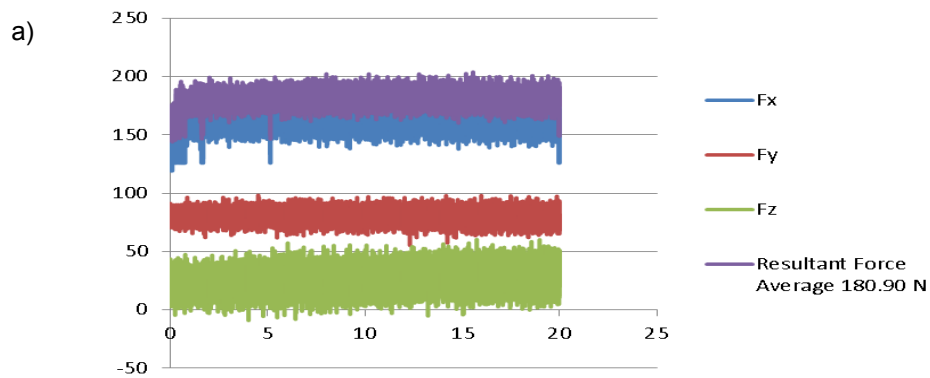
In this study, all types of analyses on surface roughness show similar results. Analyses show that the feed rate is the most prominent factor influencing the surface roughness in hard turning. The surface roughness decreases with the decreasing of feed rate. Similar results were obtained by other researchers as well (Hamdan et al., 2011). On the other hand, the cutting speed has the second highest importance in affecting the surface roughness although its sole contribution is insignificant. The analysis shows that the preferable cutting speed for better surface roughness is level 3 which is regarded as high cutting speed in this study. At high cutting speed, the velocity of chips flow is faster. Thus, the contact time between the chips and machined surface is short which reduces the possibility of the chip wrapping back to the newly generated surface (Ghani et al., 2004). Since the chip is harder than the workpiece, high cutting speed reduces the tendency of the chips entering into cutting zone to avoid scratches on the finished surface (Thepsonthi et al., 2009). Furthermore, at increased cutting speed the lateral plastic flow of the material can be avoided to reduce uneven surface profile (Bouacha et al., 2010; Rech & Moisan, 2003).

4.3 $L_{16}(4)^3$ orthogonal array design of experiment in hard turning with SiO₂ nano base lubricant

4.3.1 Cutting force and power consumption

The hard turning test was carried out as a case study of the cutting process of AISI4140 steel workpiece. The cutting force was measured periodically at every 5 minute intervals and six readings were taken in the continuous cutting process. Two different lubrication modes were used in this research, namely, ordinary lubrication and SiO₂ nano base lubricant. To deliver the lubricant to the tool-chip interface, the MQL system with a thin-pulsed jet nozzle was adopted for the both lubrication modes. In the SiO₂ nano base lubricant, the nozzle is equipped with an additional air nozzle to accelerate the lubricant into the cutting zone and to reduce the oil consumption up to 25%.

During the hard turning of AISI4140 steel with coated carbide tools, the effect of different lubrication modes was studied. Figures 4.11 (a) and (b) show an example of measured cutting forces in X, Y and Z-axis direction by using ordinary lubrication and SiO₂ nano base lubricant after 20 seconds of cutting (speed: 120 m/min, feed rate: 0.15 mm/rev, 0.5 mm). Results depict that the lower cutting force can be obtained by using lubricants containing 0.2 wt% SiO₂ compared to normal lubrication system at similar cutting parameters.



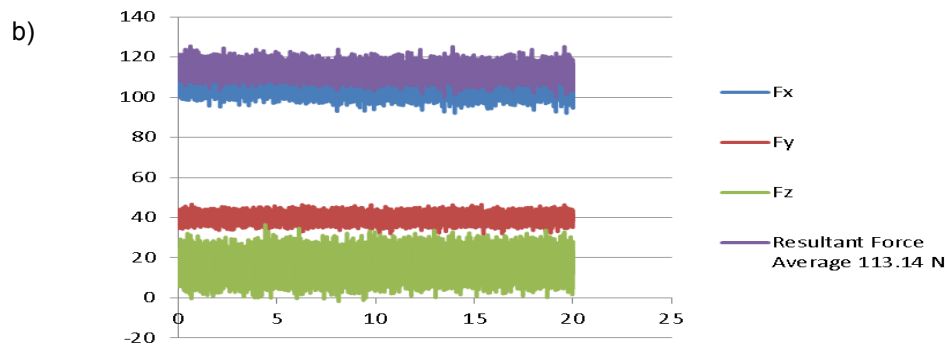


Figure 4.11 An example of measured cutting forces in X, Y and Z-axis direction after 20 seconds of cutting at a speed of 120 m/min, feed rate of 0.15 mm/rev and depth of cut of 0.5 mm by using (a) ordinary lubrication system and (b) SiO₂ nano base lubricant

The variation of cutting force with different concentration of SiO₂ is shown in Figure 4.12. Results depict that the lower cutting force is obtained by using SiO₂ nano base lubricant containing 0.2 wt% nanoparticles compared to normal lubrication system at similar cutting parameters. Figure 4.13 is presenting the Variation in cutting forces for both modes of lubrication

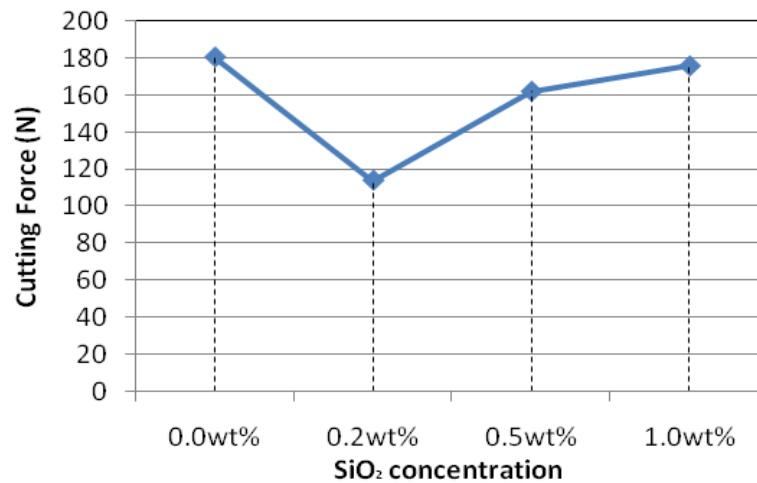


Figure 4.12 Variation of cutting performance at different concentration of SiO₂

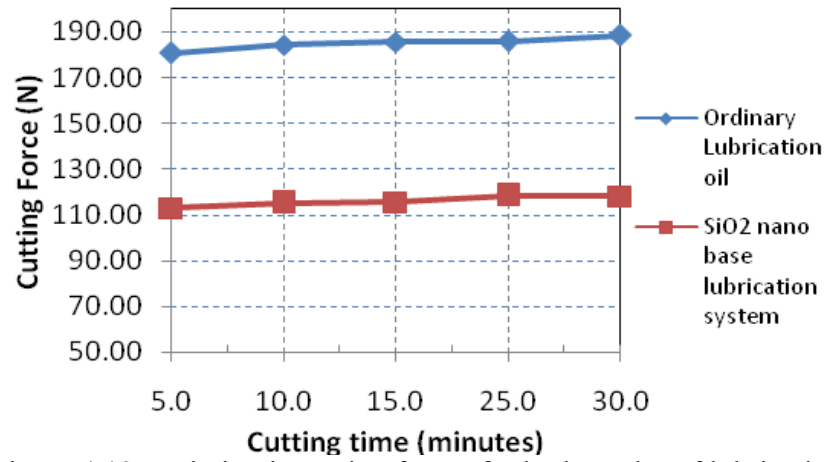


Figure 4.13 Variation in cutting forces for both modes of lubrication

As a consequence in the change of cutting force, the specific energy (E_c) and the power consumption is investigated as well. The specific energy of the cutting tool is obtained as follows (Reddy & Rao, 2006):

$$E_c = \frac{F_c V_c}{f d_a d_r} \quad (\text{J/mm}^3) \quad \text{Equation 4.3}$$

where E_c is the specific energy, F_c is the cutting force (Newton), V_c is the cutting speed (m/min) of the tool, f is the work feed (mm/min), d_a is the axial depth of cut (mm), and d_r is the radial depth of cut (mm).

Figure 4.14 and 4.15 shows the changes in specific energy and power requirement of the cutting tool for both lubrication modes respectively. As it can be seen in Figure 4.14 and 4.15, the specific energy and power consumption is reduced significantly for the nano base lubricant compared to the ordinary lubrication system. As an example, the reduction in power consumption reduction is 37.19%.

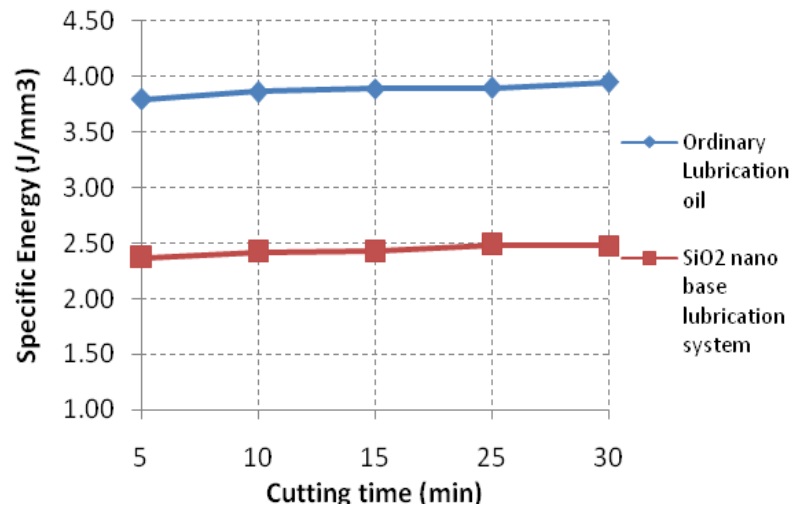


Figure 4.14 The specific energy required at the cutting tool for both lubrication modes

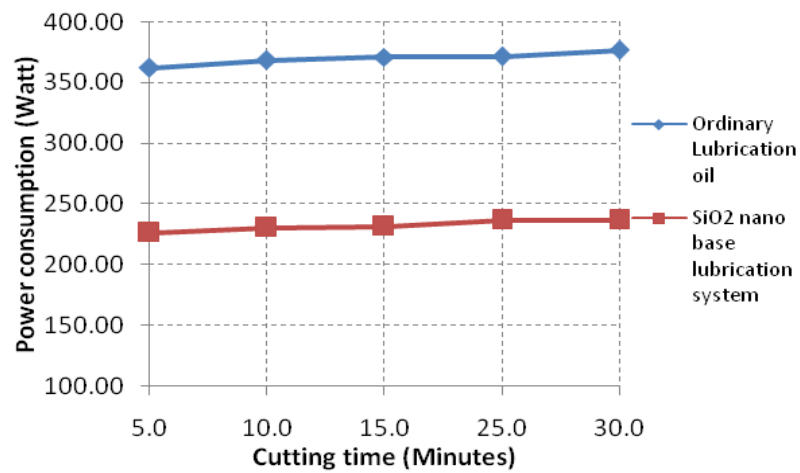


Figure 4.15 The power required at the cutting tool for both lubrication modes

In this research, the development of SiO₂ nano base lubricant is investigated in machining process for less power consumption and pollution. From the Figures 4.13, 4.14 and 4.15 it is seen that the cutting forces, specific energy and power requirement is reduced considerably by using the SiO₂ nano base lubricant. Overall, SiO₂ nano base lubricant is an eco-friendly alternative since it requires less force, energy and power compared to normal lubrication system. Based on the results obtained, the following conclusions can be derived:

1. SiO₂ nanoparticles dispersed in mineral oil improve the machining performance by reducing the coefficient of friction and cutting forces compared to ordinary lubrication system.

2. The specific energy and power requirement is reduced during the machining process with the application of SiO₂ nano base lubricant compared to the ordinary lubrication system.
3. The effectiveness of SiO₂ nano base lubricant is high compared to the ordinary lubrication system because SiO₂ nanoparticles in the mineral oil roll and slide at the tool chip interface to reduce the coefficient of friction.

4.3.2 Surface roughness

Figures 4.16 provide examples of surface roughness respectively at 120 m/min cutting speed, 15mm/rev feed and 0.5mm depth of cut. 0.0 wt% SiO₂ nanoparticles were added to the lubricant and 1 bar air pressure was applied with a nozzle angle of 15°. Table 4.12 shows the measured value for surface roughness.

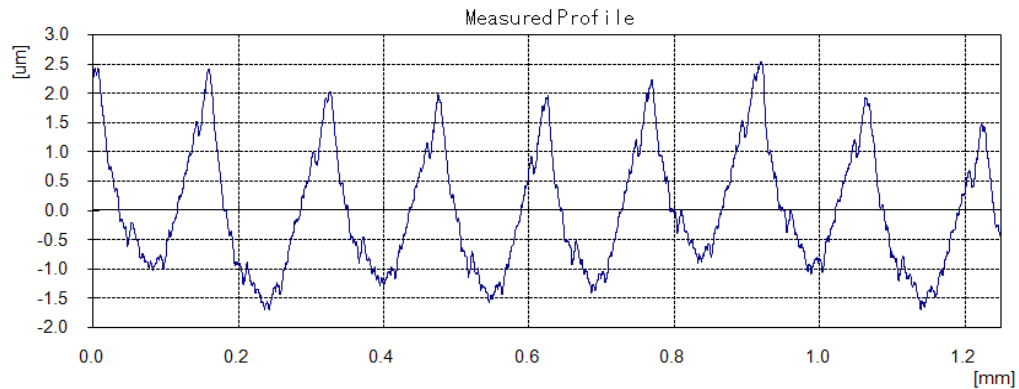


Figure 4.16 An example of surface roughness at 120 m/min cutting speed, 15 mm/rev feed and 0.5 mm depth of cut (nanoparticle concentration: 0.0 wt%, air pressure: 1 bar and nozzle angle 15°)

Table 4.12 Measured value of surface roughness

Exp. No.	Control factors and Levels (<i>i</i>)			Measured Parameters				
	SiO ₂ concentration (A)	Air Pressure (B)	Nozzle Orientation (C)	Surface roughness				
				Reading			TPM(μm)	S/N (dB)
				1	2	3		
1	<i>i</i> =1	1	1	0.75	0.70	0.83	0.76	1.17
2	<i>i</i> =1	2	2	0.65	0.67	0.65	0.66	1.80
3	<i>i</i> =1	3	3	0.75	0.76	0.81	0.77	1.10
4	<i>i</i> =1	4	4	0.85	0.88	0.88	0.87	0.59
5	<i>i</i> =2	1	2	0.70	0.74	0.74	0.73	1.37
6	<i>i</i> =2	2	1	0.89	0.92	0.92	0.91	0.39
7	<i>i</i> =2	3	4	0.71	0.69	0.71	0.70	1.51
8	<i>i</i> =2	4	3	0.77	0.79	0.78	0.78	1.06
9	<i>i</i> =3	1	3	0.56	0.61	0.59	0.59	2.29
10	<i>i</i> =3	2	4	0.69	0.66	0.69	0.68	1.65
11	<i>i</i> =3	3	1	0.76	0.75	0.70	0.74	1.31
12	<i>i</i> =3	4	2	0.62	0.64	0.69	0.65	1.85
13	<i>i</i> =4	1	4	0.83	0.85	0.92	0.87	0.60
14	<i>i</i> =4	2	3	0.83	0.80	0.84	0.82	0.83
15	<i>i</i> =4	3	2	0.81	0.79	0.81	0.80	0.93
16	<i>i</i> =4	4	1	0.74	0.75	0.75	0.75	1.23

Figures 4.17 (a) and (b) provide the examples of measured surface roughness for both lubrication systems at 120m/min cutting speed, 15mm/rev feed and 0.5mm depth of cut. Results depict that the lower surface roughness is obtained by using 0.2 wt% SiO₂ in the lubricants (0.62 μ m) compared to normal lubrication system (0.81 μ m) at similar machining parameters.

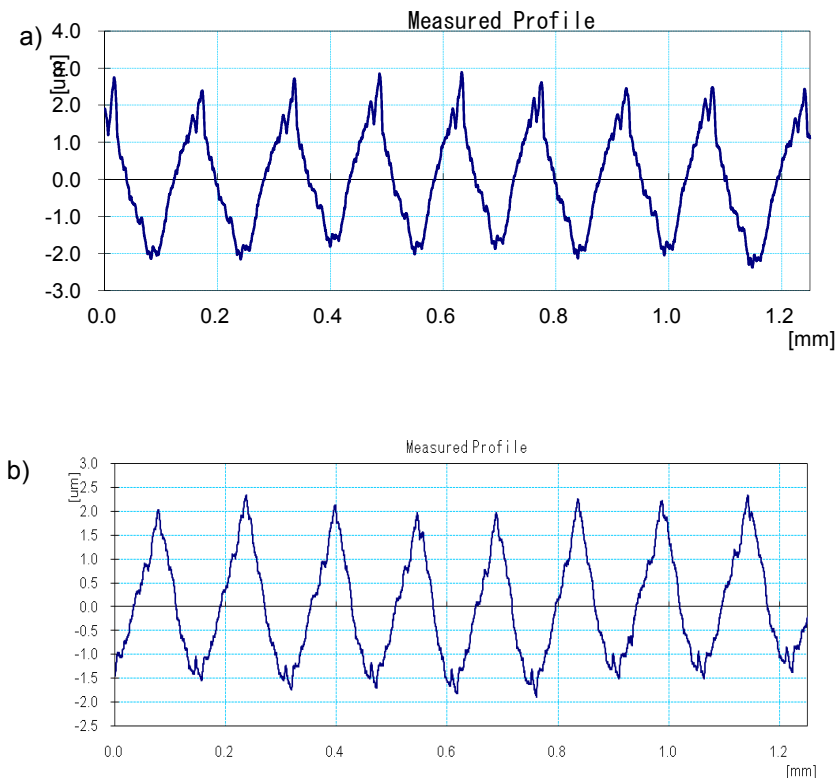


Figure 4.17 An example of measured surface roughness at 120m/min cutting speed, 15mm/rev feed rate and 0.5 mm depth of cut by using (a) ordinary lubricant and (b) nano base lubricant containing 0.2 wt% SiO₂

These results are supported by the stereoscopic photographs for three-dimensional views of machined surface at different lubrication modes as it is shown in Figure 4.18 (a) and (b). It is clearly shown that the smaller surface roughness is obtained by using 0.2 wt% SiO₂ nano base lubricant.

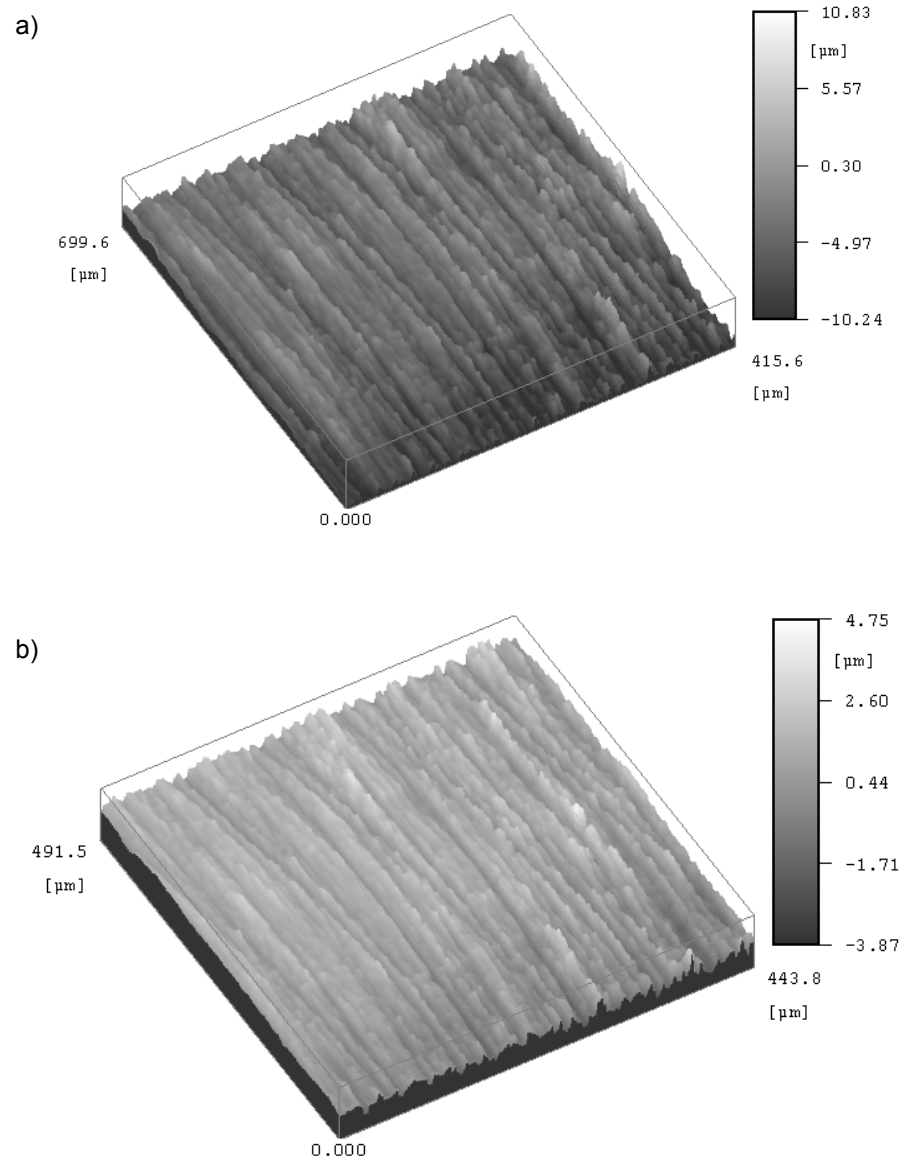


Figure 4.18 An example of measured surface roughness for both lubrication modes at 120m/min cutting speed, 15mm/rev feed and 0.5 mm depth of cut by using (a) ordinary lubricant and (b) nano base lubricant containing 0.2 wt% SiO₂

The calculated TPM and S/N response data for surface roughness are listed in Table 4.13 and it has been plotted in Figure 4.19. From Figure 4.19 (a) and (b), nanoparticles concentration of 0.5 wt% (A3), air pressure of 1 bar (B1) and nozzle angle of 30° (C2) are deemed to be the best choices for attaining the lowest surface roughness. In conclusion, the optimal parameter for attaining the lowest tool wear and surface roughness are A3 B2 C4 and A3 B1 C2 respectively.

Table 4.13 The calculated S/N and TPM response for surface roughness

Response Table for Signal to Noise (S/N) Ratios				Response Table for Means (TPM)			
Level	SiO ₂ Concentration (wt%)	Air Pressure (bar)	Nozzle Orientation (°)	Level	SiO ₂ Concentration (wt%)	Air Pressure (bar)	Nozzle Orientation (°)
1	2.33	2.71	2.05	1	0.76	0.73	0.79
2	2.16	2.33	2.97	2	0.78	0.77	0.71
3	3.55	2.42	2.63	3	0.66	0.75	0.74
4	1.79	2.36	2.17	4	0.81	0.76	0.78
Delta	1.75	0.37	0.92	Delta	0.14	0.03	0.08
Rank	1	3	2	Rank	1	3	2

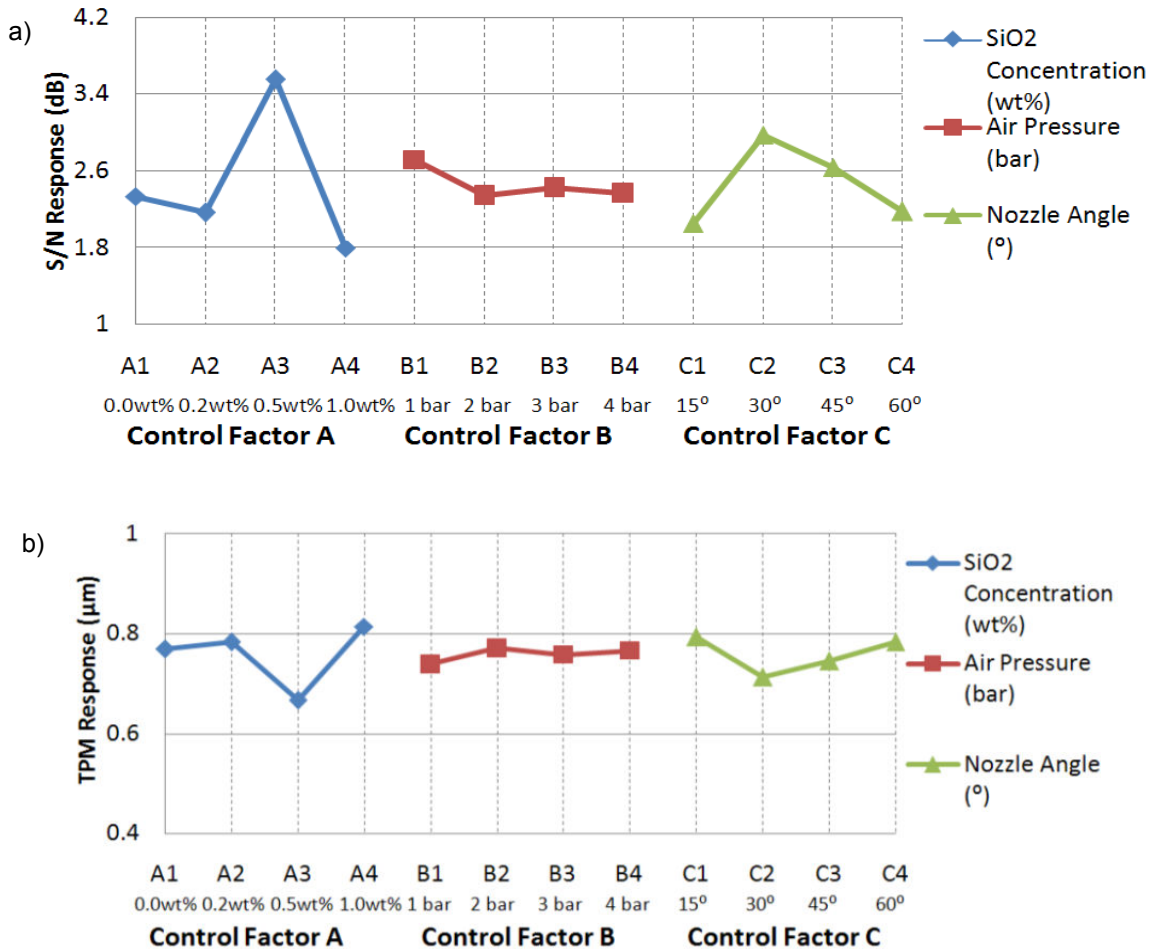


Figure 4.19 Surface roughness at different control factors (a) S/N response graph and (b) TPM response graph

These observation further supports that the application of SiO₂ nano base lubricant is capable to show good machining performances.

4.3.3 Tool wear

Figure 4.20 provides examples of tool wear measured at 120 m/min cutting speed, 15mm/rev feed and 0.5mm depth of cut. 0.0 wt% SiO₂ nanoparticles were added to the lubricant and 1 bar air pressure was applied with a nozzle angle of 15°. Table 4.14 presents the responses of tool wear for the selected array of experiments.

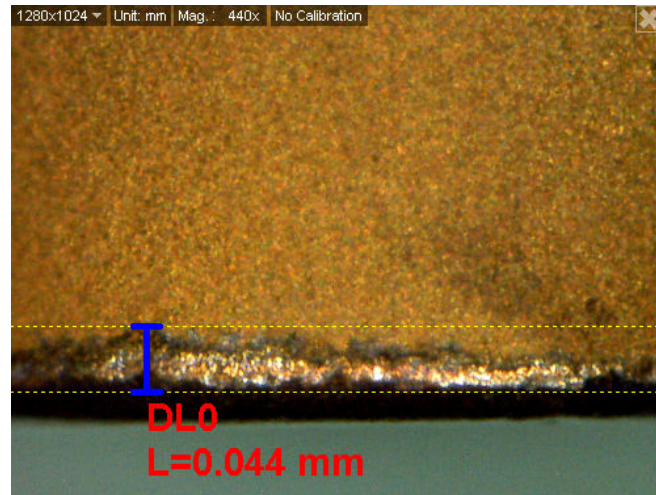


Figure 4.20 An example of tool wear at 120 m/min cutting speed, 15 mm/rev feed and 0.5 mm depth of cut (Concentration: 0.0 wt%, air pressure: 1 bar and nozzle angle 15°)

Table 4.14 The response of tool wear

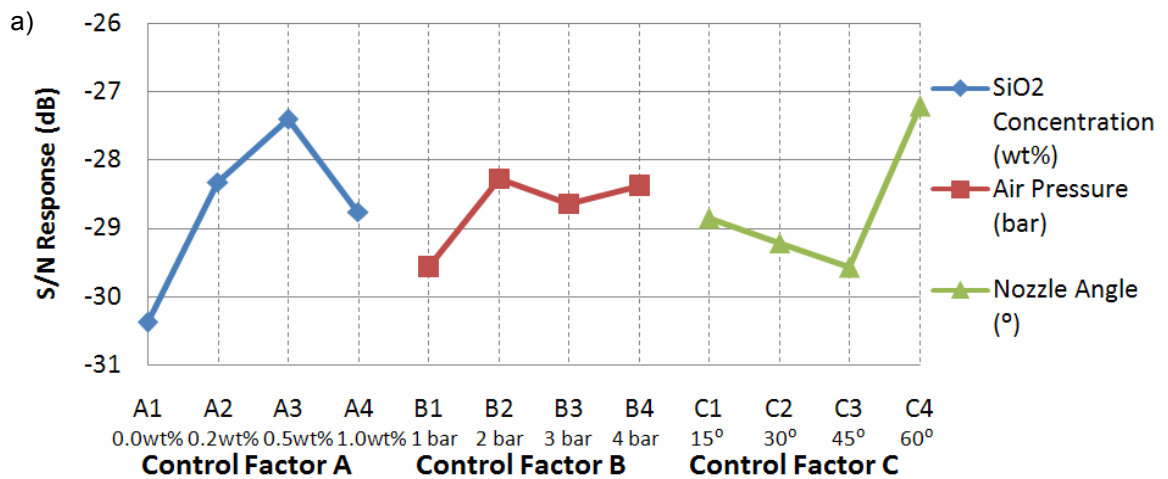
Exp. No.	Tool wear				
	Reading			TPM	S/N
	1	2	3		
1	43.50	45.60	43.80	44.30	-32.93
2	27.20	26.50	24.30	26.00	-28.30
3	40.80	38.50	38.60	39.30	-31.89
4	27.60	26.80	24.50	26.30	-28.40
5	36.30	35.90	33.70	35.30	-30.96
6	24.10	23.80	22.00	23.30	-27.35
7	22.20	22.50	20.40	21.70	-26.73
8	25.80	26.50	25.70	26.00	-28.30
9	26.30	26.80	24.90	26.00	-28.30
10	23.90	23.40	24.70	24.00	-27.60
11	19.40	20.70	19.90	20.00	-26.02
12	23.70	24.80	24.40	24.30	-27.71
13	19.90	20.90	20.10	20.30	-26.15
14	30.40	30.80	31.80	31.00	-29.83
15	31.90	31.50	30.50	31.30	-29.91
16	27.70	29.20	29.20	28.70	-29.16

For calculating the S/N ratio for tool wear and surface roughness, smaller values are always preferred. The calculated S/N and TPM responses data for tool wear and surface roughness are presented in Table 4.15.

Table 4.15 The calculated of S/N and TPM response data for tool wear

Response Table for Signal to Noise (S/N) Ratios				Response Table for Means (TPM)			
Level	SiO ₂ Concentration (wt%)	Air Pressure (bar)	Nozzle Orientation (°)	Level	SiO ₂ Concentration (wt%)	Air Pressure (bar)	Nozzle Orientation (°)
1	-30.38	-29.58	-28.86	1	33.98	31.47	29.07
2	-28.33	-28.27	-29.22	2	26.57	26.07	29.22
3	-27.41	-28.64	-29.58	3	23.57	28.07	30.57
4	-28.76	-28.39	-27.22	4	27.82	26.32	23.07
Delta	2.97	1.31	2.36	Delta	10.4	5.4	7.5
Rank	1	3	2	Rank	1	3	2

Figure 4.21 (a) and (b) shows the TPM and S/N responses of the tool wear. From Figure 4.21 (a) and (b) and based on the criteria of smaller TPM and larger S/N response, the nanoparticles concentration of 0.5 wt% (A3), air pressure of 2 bar (B2), and nozzle angle of 60° (C4) are determined to be the best choices for obtaining the lowest tool wear.



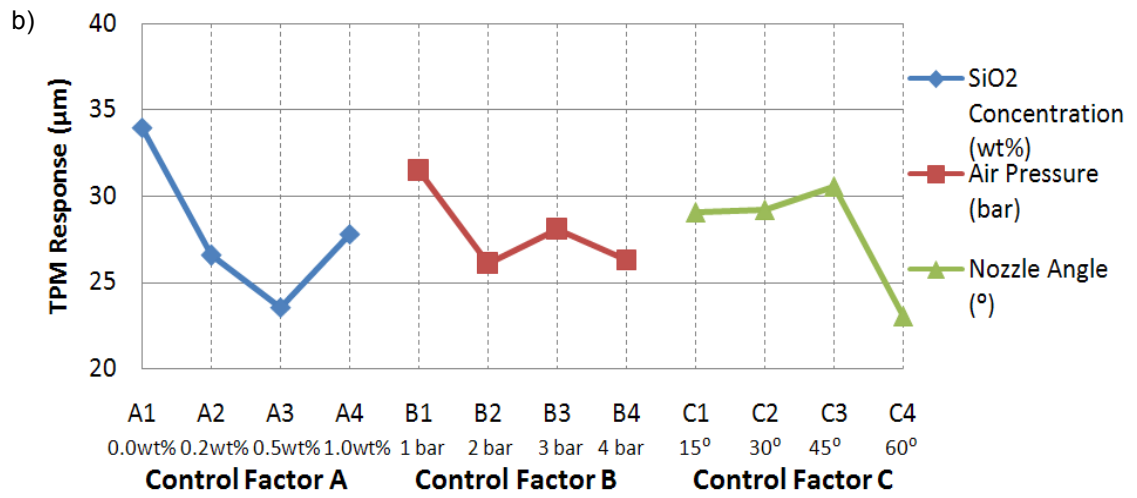


Figure 4.21 Tool wear at different control factors (a) S/N response graph and (b) TPM response graph

4.4 Fuzzy logic approach in determining the effect of SiO₂ nano base lubricant on tool wear and surface roughness in hard turning

4.4.1 Fuzzy Logic Analysis

The relationship between the input parameters, namely concentration of nanoparticles in the lubricant, air pressure and nozzle orientation is investigated with the output parameters namely tool wear and surface roughness of AISI4140 steel during hard turning operation. Each input parameter was varied for four membership functions: low, medium, high, and very high. The output variables (tool wear and surface roughness) also divided into four membership functions: best, good, average and bad. The characteristics of the input and output variables are given in Table 4.16.

Table 4.16 Fuzzy linguistic and abbreviation of variables for each parameter

Inputs		Range
Parameters	Linguistic variables	
A - Nanoparticle concentration (wt %)	Low (L), medium (M), high (H), very high (VH)	0.0-1.0 wt%
B- Air pressure (bar)		1-4 bar
C - Nozzle orientation (degree °)		15°-60°
Output		
Tool wear (µm)	Best, Good, Average, Bad	20.0 µm – 44.3 µm
Surface Roughness (µm)	Best, Good, Average, Bad	0.34µm – 3.14µm

4.4.1 (i) Membership functions for input and output fuzzy variables

The event and type of membership functions for fuzzification are mainly dependent upon the relevant event (Jaya et al., 2010). In this model, each input and output parameter has four membership functions. The Gauss shape of membership function is employed to describe the fuzzy sets for input variables. In the output set of fuzzy variables, the triangular shape of membership functions is considered. Triangular membership function generally possesses increasing and decreasing characteristics with only one definite value (Jaya et al., 2010). The input variables were partitioned according to the parameter ranges from the experiment. Membership functions for fuzzy input variables are shown in Figure

4.22 (a-c). Moreover, Figure 4.23 (a) and (b) illustrates the membership functions of fuzzy set for the output tool wear and surface roughness.

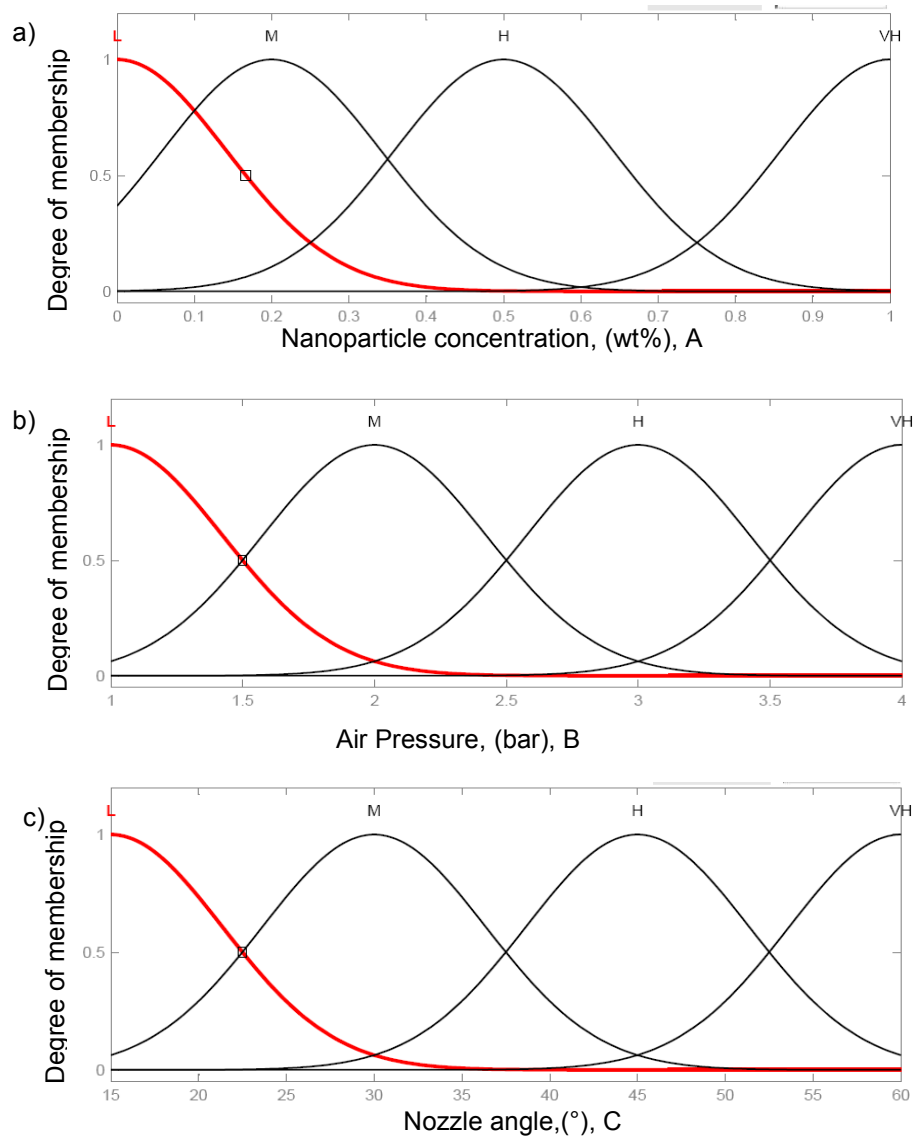


Figure 4.22 Membership function for the input variables (a) nanoparticle concentration, (b) air pressure and (c) nozzle angle

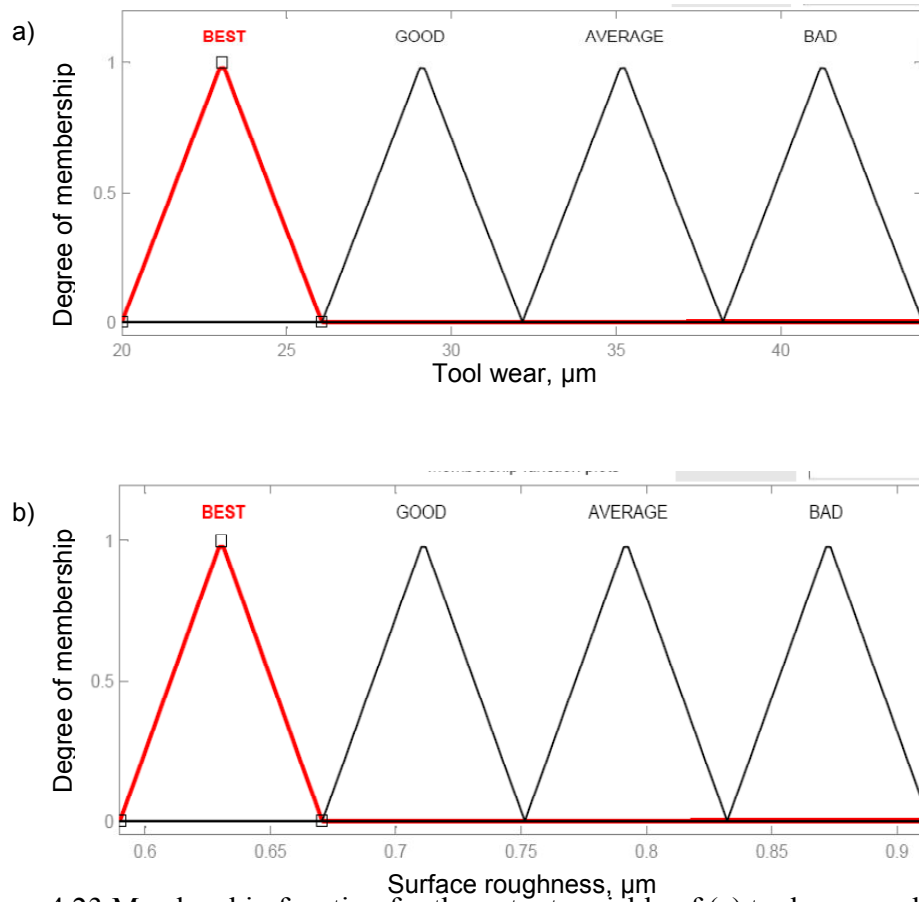


Figure 4.23 Membership function for the output variable of (a) tool wear and (b) surface roughness

4.4.1(ii) Structure of fuzzy rules

A set of 12 rules was constructed based on the actual experiment for tool wear and surface roughness during hard turning operation of AISI4140 steel by using SiO_2 nano base lubricants. Experimental results were simulated in Matlab software on the basis of Mamdani fuzzy logic (Table 4.17).

Table 4.17 The basis of Mamdani Fuzzy logic

Tool wear	Surface roughness
1. If (A is LOW) and (B is L) and (C is L) then (Tool wear is BAD)	1. If (A is LOW) and (B is L) and (C is L) then (Surface roughness is AVERAGE)
2. If (A is LOW) and (B is M) and (C is M) then (Tool wear is BEST)	2. If (A is LOW) and (B is M) and (C is M) then (Surface roughness is BEST)
3. If (A is LOW) and (B is H) and (C is H) then (Tool wear is BAD)	3. If (A is LOW) and (B is H) and (C is H) then (Surface roughness is AVERAGE)
4. If (A is MEDIUM) and (B is L) and (C is M) then (Tool wear is AVERAGE)	4. If (A is MEDIUM) and (B is L) and (C is M) then (Surface roughness is GOOD)
5. If (A is MEDIUM) and (B is M) and (C is L) then (Tool wear is BEST)	5. If (A is MEDIUM) and (B is M) and (C is L) then (Surface roughness is BAD)
6. If (A is MEDIUM) and (B is H) and (C is VH) then (Tool wear is BEST)	6. If (A is MEDIUM) and (B is H) and (C is VH) then (Surface roughness is GOOD)
7. If (A is HIGH) and (B is L) and (C is H) then (Tool wear is BEST)	7. If (A is HIGH) and (B is L) and (C is H) then (Surface roughness is BEST)
8. If (A is HIGH) and (B is M) and (C is VH) then (Tool wear is BEST)	8. If (A is HIGH) and (B is M) and (C is VH) then (Surface roughness is GOOD)
9. If (A is HIGH) and (B is H) and (C is L) then (Tool wear is BEST)	9. If (A is HIGH) and (B is H) and (C is L) then (Surface roughness is GOOD)
10. If (A is VERY_HIGH) and (B is L) and (C is VH) then (Tool wear is BEST)	10. If (A is VERY_HIGH) and (B is L) and (C is VH) then (Surface roughness is BAD)
11. If (A is VERY_HIGH) and (B is M) and (C is H) then (Tool wear is GOOD)	11. If (A is VERY_HIGH) and (B is M) and (C is H) then (Surface roughness is AVERAGE)
12. If (A is VERY_HIGH) and (B is H) and (C is M) then (Tool wear is GOOD)	12. If (A is VERY_HIGH) and (B is H) and (C is M) then (Surface roughness is AVERAGE)

4.4.1 (iii) Defuzzification

In this model, the centroid of area (COA) defuzzification method was called due to its wide acceptance and capability for giving more accurate results compared to other methods (Leung et al., 2003; Oktem et al., 2006). In this method, the resultant membership functions are developed by uniting the output of each rule. In other words the overlapping area of the fuzzy output set is counted as one, providing more results (Chandrasekaran et al., 2010; Hashmi et al., 2003).

The output of the tool wear and surface roughness were constructed from the fuzzy logic as shown in Figure 4.24 and 4.25, respectively. Figure 4.24 (a) and (b) presents the relation between the input parameters and tool wear of AISI4140 steel during hard turning operation as predicted by a fuzzy based model. As presented in Figure 4.24 (a), the lowest tool wear is obtained at 0.5 wt% of SiO₂ and significantly rises with increasing SiO₂

concentration. Meanwhile, the tool wear is minimal at 2 bar lubricant pressure whereas, it increases at 3bar lubrication pressure. From Figure 4.25 (b) it is clearly seen that the tool wear is reduced at the nozzle angle of 60°. In Figure 4.25 (a), surface roughness is minimal at 0.5 wt% of SiO₂ and significantly goes up with increasing SiO₂ concentration. The surface roughness is minimal at 30° nozzle angle. Obviously, in Figure 4.25 (b), the increment of lubrication pressure increases the surface roughness during machining.

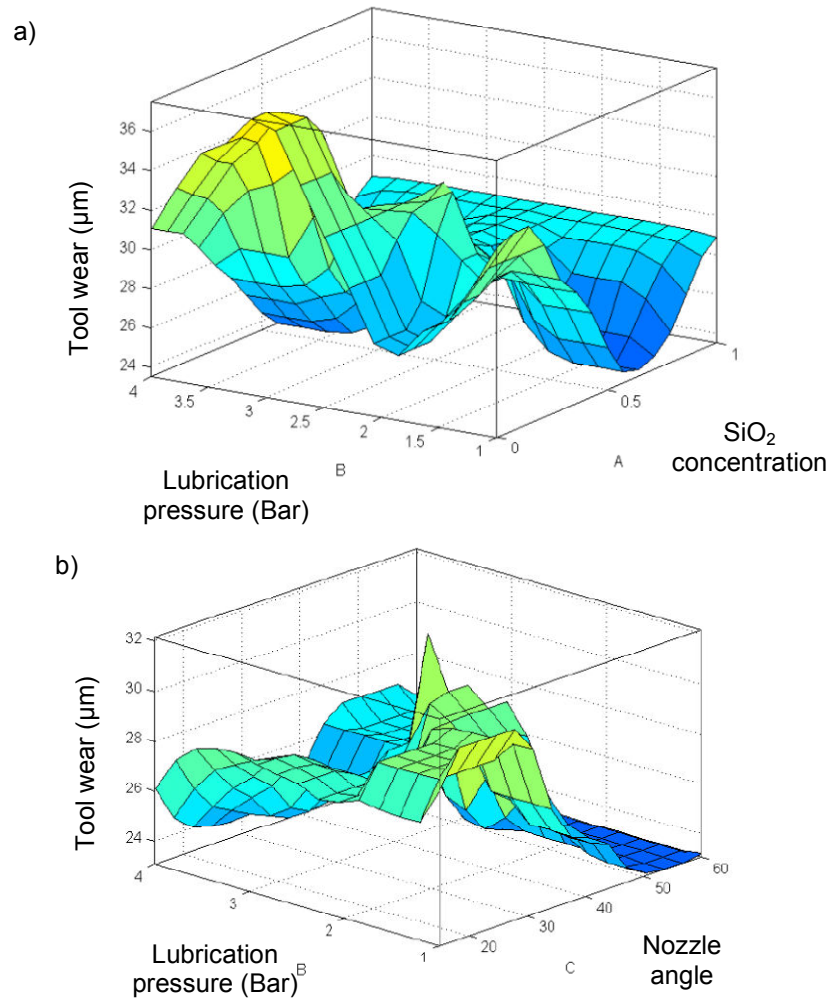


Figure 4.24 The predicted tool wears obtained by fuzzy logic in relation to (a) change of lubrication pressure and SiO₂ concentration and (b) nozzle angle and lubrication pressure

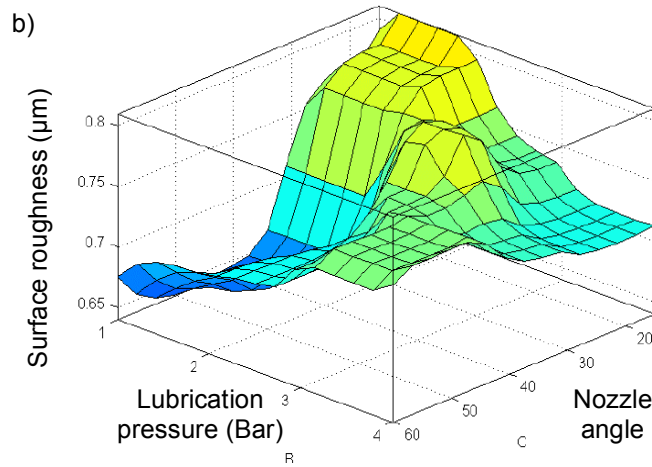
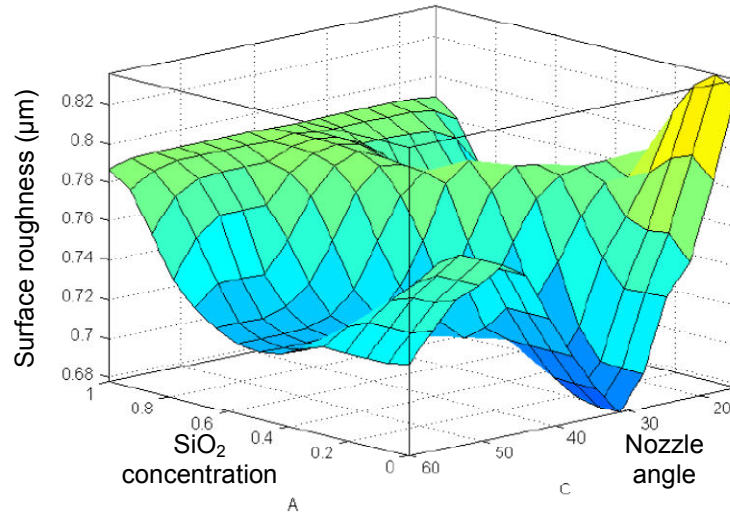


Figure 4.25 The predicted surface roughness obtained by fuzzy logic in relation to (a) change of SiO₂ concentration and nozzle angle and (b) lubrication pressure and nozzle angle

4.4.1 (iv) Investigating fuzzy model accuracy and error

Four new separate experiments were carried out to investigate the accuracy of fuzzy model. The individual error percentage was obtained by dividing the absolute difference of the predicted and measured values by the measured value as shown in equation 4.4 where e_i is individual error; R_m is measured value and R_p is predicted value.

$$e_i = \left(\frac{|R_m - R_p|}{R_m} \right) \times 100\% \quad \text{Equation 4.4}$$

Meanwhile, accuracy is calculated to measure the closeness of the predicted value to the measured value. The accuracy of the model is the average of individual accuracy as shown in equation 4.5 where A is the model accuracy and N is the total number of data set.

$$A = \frac{1}{N} \sum_{i=1}^N \left(1 - \frac{|R_m - R_p|}{R_m} \right) \times 100\% \quad \dots \text{Equation 4.5}$$

To investigate the accuracy of the fuzzy model, four new experimental tests were carried out on tool wear and surface roughness. Tool wear and surface roughness results are tabulated in Table 4.18, then compared with the prediction from fuzzy model. For tool wear and surface roughness, the highest error percentages are 8.06% and 4.35% respectively. The low level of error indicates that the fuzzy prediction for tool wear and surface roughness are very close to the actual experimental values. Accuracy of the values indicates that the proposed model can be used to predict the tool wear and surface roughness of a machined surface of AISI4140 steel during hard turning operation by using SiO₂ nano base lubricants. Thus, the proposed fuzzy logic model provides a promising solution for predicting the roughness and tool wear during hard turning operation with a specific range of parameters.

Table 4.18 The accuracy and error of the fuzzy logic model prediction

	Tool wear (output)				Surface roughness (output)			
	Measured	Predicted (fuzzy)	Error, %	Accuracy %	Measured	Predicted (fuzzy)	Error, %	Accuracy, %
1	16.9	17.5	3.42	96.57	0.44	0.46	4.35	95.65
2	31.0	28.5	8.06	91.93	0.82	0.80	2.50	97.50
3	31.3	29.1	7.02	92.8	0.80	0.78	2.56	97.44
4	28.7	29.1	1.37	98.63	0.75	0.72	4.00	96.00

In this study, SiO₂ nanoparticles were mixed with ordinary mineral oil at different concentrations to investigate the tool wear and surface roughness in CNC hard turning operation of AISI4140 steel. The experimental results, fuzzy logic approach and response analyses lead to similar conclusions. Clearly, mode 3 with 0.5 wt% of SiO₂ nanoparticles in ordinary mineral oil produces the lowest tool wear and best surface quality.

A verification test was carried out to check the reliability of the results. The verification test was conducted by using the following combinations of optimal parameter: A3 B2 C4 for tool wear and A3 B1 C2 for surface roughness. These combinations were repeated up to sixteen times and the average TPM values were measured for tool wear and surface roughness. The results from the confirmation test for tool wear and surface roughness are 0.44 µm and 16.9 µm respectively. The results indicates an improvement of 15% and 23% in surface roughness and tool wear respectively compared to the smallest values obtained from the initial experiments. Based on fuzzy logic approach and response analysis obtained from the Taguchi optimization, the following conclusions can be drawn:

1. The lowest tool wear is obtained at 0.5 wt% of SiO₂ nanoparticles in the mineral oil with 2 bar air pressure and 60° nozzle angle.
2. Surface roughness is reduced at 0.5 wt% of SiO₂ nanoparticles suspended in mineral oil, with less air pressure and 30° nozzle angle.
3. The excellent performance and reduction in consumption of the nano base lubricant leads to the conclusion that suspending SiO₂ nanoparticles in the mineral oil is a feasible way to improve the machining process. With the low cost, outstanding properties and eco-friendly characteristics of SiO₂ nanoparticles, it is an innovative and effective alternative for flood lubrication as well.

4.5 L₁₆ (4)³ orthogonal array design of experiment in milling with SiO₂ nano base lubricant

4.5.1 Cutting force and power consumption

After all the experiments were done, the Taguchi optimization method was employed to analyze the data, optimize the parameters and identify the most statistically significant parameter. The data were analyzing by using signal to noise (S/N) response analysis, interaction analysis and analysis of variance (Pareto ANOVA).

The calculated S/N ratio and TPM values are summarized in Table 4.19, where TPM is the target performance measurement factor which is equal to the average of the measured cutting forces, cutting temperature and surface roughness at the same level of input parameters (*i*). Furthermore, the TPM and S/N response data are calculated and summarized in Table 4.20 for cutting force.

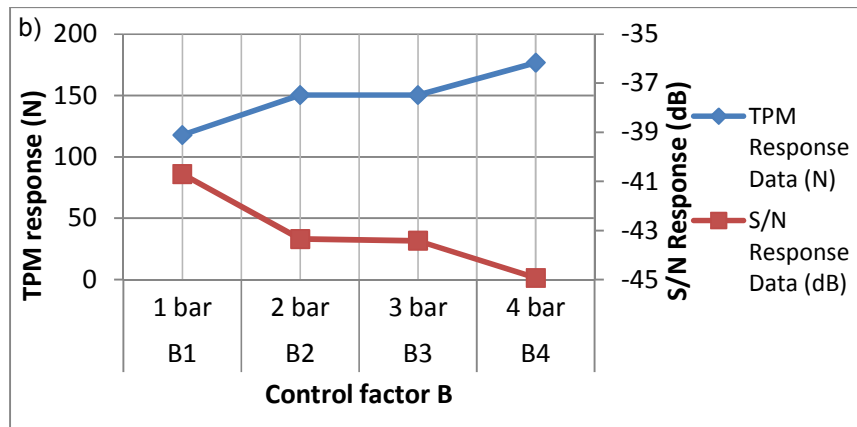
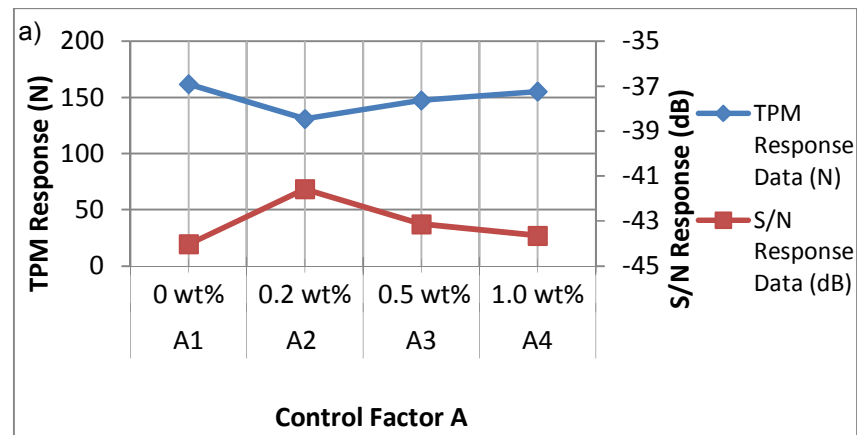
Table 4.19 The TPM and S/N ratio values for cutting force

Test Levels	Cutting Force	
	TPM (N)	S/N Ratio (dB)
1	134.16	-42.55
2	197.91	-45.93
3	130.78	-42.33
4	184.43	-45.32
5	53.81	-34.62
6	150.31	-43.54
7	161.99	-44.19
8	157.63	-43.95
9	171.81	-44.70
10	107.70	-40.64
11	121.92	-41.72
12	188.04	-45.49
13	111.43	-40.94
14	145.66	-43.27
15	186.76	-45.43
16	177.31	-44.97

Table 4.20 The TPM and S/N response data for cutting force

Level of input parameters (<i>i</i>)	TPM Response (N)			S/N Response (dB)		
	A_i	B_i	C_i	A_i	B_i	C_i
Level 1	161.82	117.80	145.93	-44.03	-40.70	-43.20
Level 2	130.94	150.40	156.63	-41.57	-43.35	-42.86
Level 3	147.37	150.36	151.47	-43.14	-43.42	-43.56
Level 4	155.29	176.85	141.39	-43.65	-44.93	-42.77
Difference	30.88	59.05	15.24	2.46	4.23	0.79
Rank	2	1	3	2	1	3

Figure 4.26 show TPM and S/N response graphs of cutting force at different control factors. From Figure 4.26 (a-c) and based on the criteria of smaller TPM and larger S/N ratio, the air pressure of 1 bar (B1), nano base lubricant containing 0.2 wt% nanoparticles (A2) and highest nozzle angle of 60° (C4) are determined to be the best choices for obtaining the lowest cutting force.



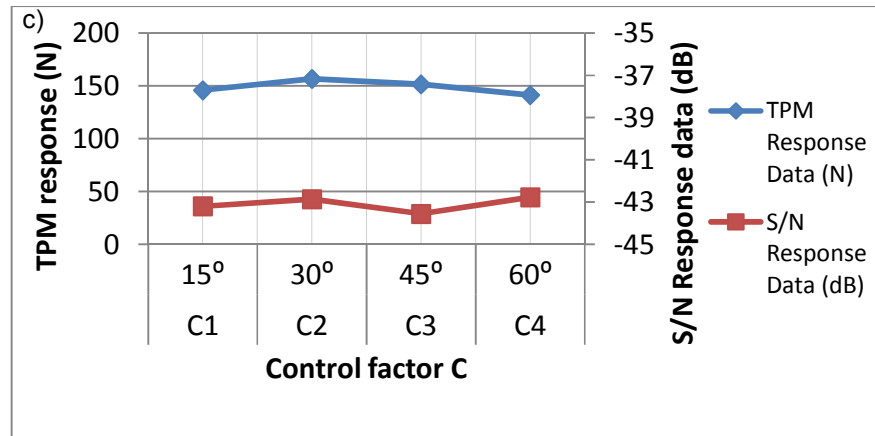


Figure 4.26 TPM and S/N response graphs of cutting force at different control factors (a) concentration of the nanoparticles, control factor A, (b) air pressure, control factor B and (c) nozzle orientation, control factor C

The interaction analysis is an alternative method to analyze the data for the optimization process. Interaction data analysis for cutting force, are presented in Table 4.21. The data is constructed from the S/N response data tabulated in the Table 4.20. From the calculated two-way table it can be seen that the optimum parameters for the lowest cutting force is A2 B1 C4. It can be noted that these results are found to be similar with the others obtained using the S/N and TPM analysis.

Table 4.21 Interaction data analysis for cutting force

AXB	B1	B2	B3	B4	Total	Highest total response
A1	-42.55	-45.93	-42.33	-45.32	-176.13	A2
A2	-34.62	-43.54	-44.19	-43.95	-166.30	
A3	-44.70	-40.64	-41.72	-45.49	-172.55	
A4	-40.94	-43.27	-45.43	-44.97	-174.61	
Total	-162.81	-173.38	-173.67	-179.73		
Highest total response	B1					
AXC	C1	C2	C3	C4	Total	Highest total response
A1	-42.55	-45.93	-42.33	-45.32	-176.13	A2
A2	-43.54	-34.62	-43.95	-44.19	-166.30	
A3	-41.72	-45.49	-44.70	-40.64	-172.55	
A4	-44.97	-45.43	-43.27	-40.94	-174.61	
Total	-172.79	-171.46	-174.25	-171.09		
Highest total response	C4					
BXC	C1	C2	C3	C4		Highest total response
B1	-42.55	-34.62	-44.70	-40.94	-162.81	B1
B2	-43.54	-45.93	-43.27	-40.64	-173.38	
B3	-41.72	-45.43	-42.33	-44.19	-173.67	
B4	-44.97	-45.49	-43.95	-45.32	-179.73	
Total	-172.79	-171.46	-174.25	-171.09		
Highest total response	C4					

The significant factors are chosen from the left-hand side of the Pareto diagram. From Table 4.22, it can be seen that the air pressure (B), nano base lubricant (A) and nozzle angle (C) contributes 70.44%, 26.62% and 2.94% respectively for the lowest cutting force. The air pressure and nano base lubrication are considered the prominent factors, having a cumulative contribution of 95.07%. The Pareto ANOVA analysis recommends that the combination of A2 B1 C4 is the best parameters to obtain the lowest cutting force.

Table 4.22 Pareto ANOVA analysis for cutting force

S/N	S/N Response data (dB)		
Control Factor levels (i)	<i>A_i</i> Nanoparticle concentration	<i>B_i</i> Air pressure	<i>C_i</i> Nozzle angle
Level 1	-44.03	-40.70	-43.20
Level 2	-41.57	-43.35	-42.86
Level 3	-43.14	-43.42	-43.56
Level 4	-43.65	-44.93	-42.77
Total summation	-172.40	-172.40	-172.40
Square of Differences (S)	$S_A = 14.00$	$S_B = 37.06$	$S_C = 1.55$
Total summation of squares of differences $St = S_A + S_B + S_C$	52.61		
Contribution Ratio (%)	26.62	70.44	2.94

Pareto Diagram			
<p>Pareto ANOVA</p> <p>Contribution ratio (%)</p> <p>Cumulative contribution (%)</p> <p>Factor</p> <p>Contribution Ratio (%)</p> <p>Cumulative Contribution</p>			
Cumulative Contribution	70.44	97.06	100.00
Optimum Combination	A2	B1	C4
Overall optimum conditions for all factors	A2 B1 C4		

Figure 4.27 shows the cutting force for both ordinary and nano base lubrication modes. Figure 4.28 shows the reduction in cutting force by the use of nano base lubricant. From Figures 4.27 and 4.28, it is clearly seen that the cutting forces are reduced significantly up to 40.22%-42.13% by the use of nano base lubricant compared with the ordinary lubrication system.

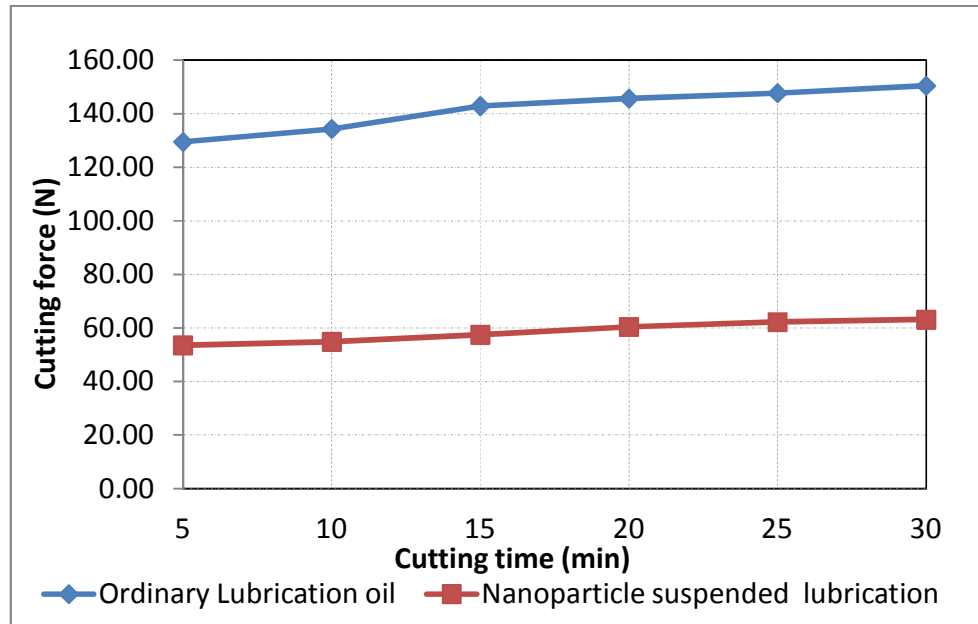


Figure 4.27 The cutting forces for both modes of lubrication

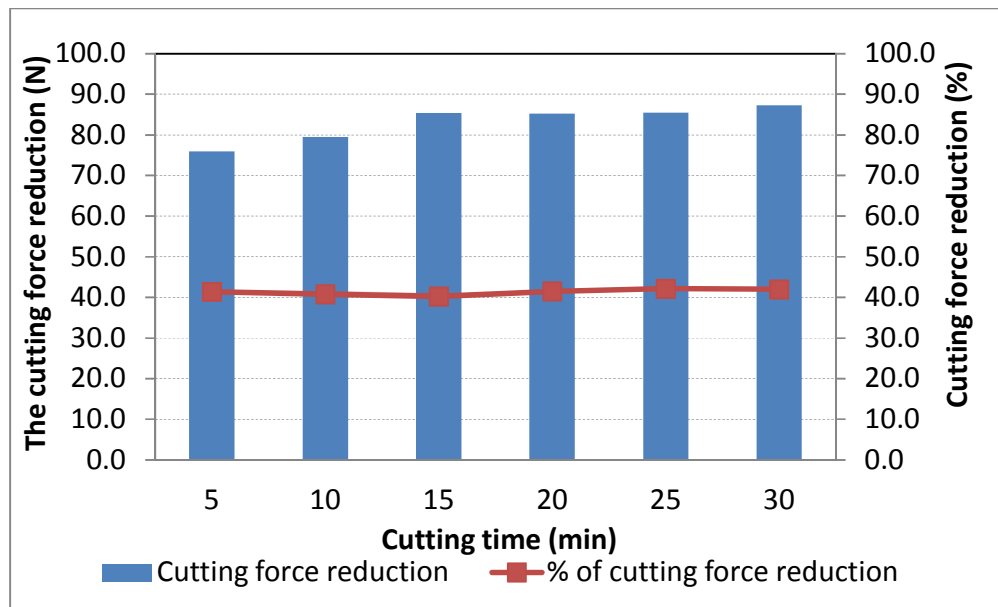


Figure 4.28 Reduction in cutting force

The required specific energy and power consumption of the cutting tool is reduced with the reduction of cutting force. Figure 4.29 represents the change in specific energy during cutting process for both modes of lubrication.

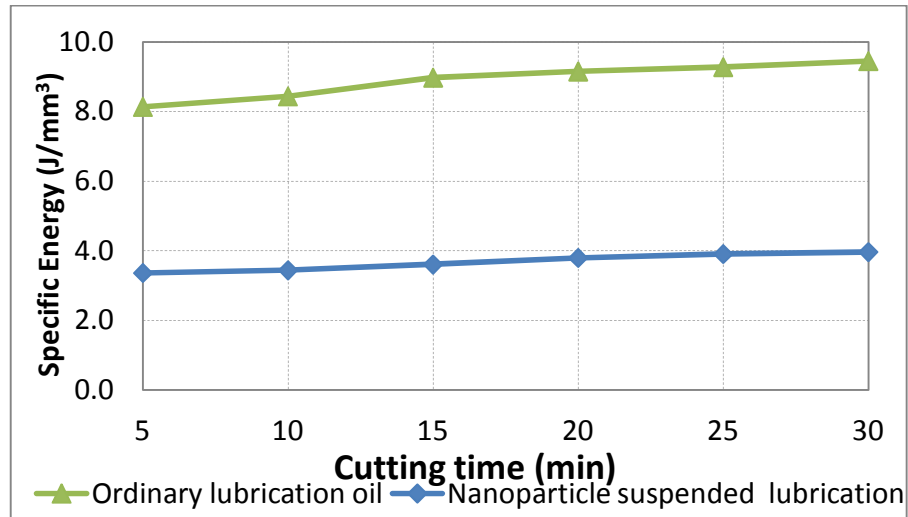


Figure 4.29 Changes in specific energy during the cutting process for both modes of lubrication

Figure 4.30 compares the reduction in power and Figure 4.31 shows the reduction in power by using nano base lubricant. As it can be seen from Figure 4.31, the power consumption is reduced significantly up to 40.22%-42.13% by the use of nano base lubricant.

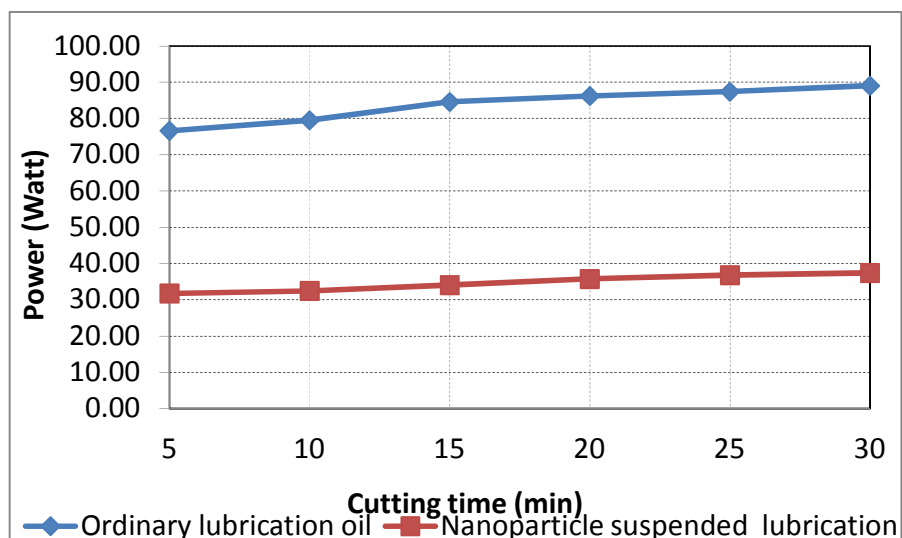


Figure 4.30 Requirement of power at the cutting tool for both lubrication modes

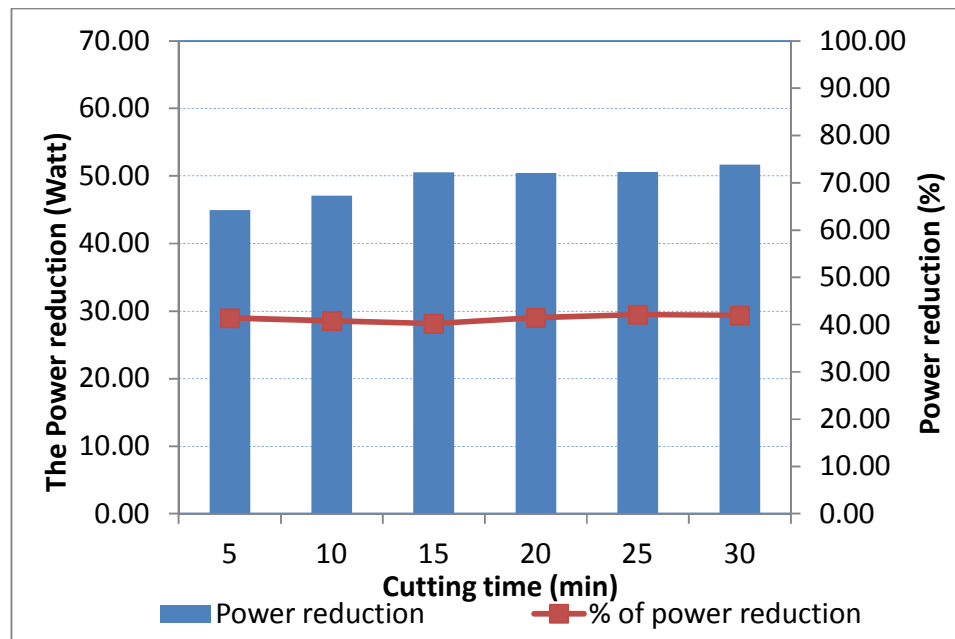


Figure 4.31 Reduction in power consumption for both lubrication modes

Figure 4.30 and 4.31 shows that the cutting forces and the power requirement for the cutting tool are reduced considerably by using nano base lubricant. Applying the nano base lubricant at the tool chip interface reduces the friction coefficient which leads to lower cutting force with less power consumption. However, introducing nano base lubricant reduces the cutting force and power consumption. Based on the results obtained, the following conclusions can be derived:

1. SiO_2 nanoparticles suspended mineral oil improves the machining performance by reducing the coefficient of friction and cutting forces compared to the ordinary lubrication system.
2. Lower specific energy and power consumption is achieved during machining with the application of nano base lubricant compared to the ordinary lubrication system.
3. The cutting force is reduced with the application of nano base lubricant compared to ordinary lubrication system.

4.5.2 Surface roughness

The calculated TPM and S/N ratio values for surface roughness are summarized in Table 4.23, where TPM is the target performance measurement factor which is equal to the average of the surface roughness at the same level of input parameters. Furthermore, the TPM and S/N response data are calculated and summarized in Table 4.24 for surface roughness.

Table 4.23 The calculated (S/N) ratio and TPM values for surface roughness.

Test Levels	Surface Roughness (Ra)	
	Calculated TPM Values	Calculated S/N Ratio (dB)
1	3.14	-9.94
2	0.75	2.48
3	1.42	-3.02
4	1.53	-3.67
5	0.74	2.64
6	1.62	-4.17
7	0.88	1.10
8	1.34	-2.54
9	1.07	-0.60
10	0.93	0.64
11	0.80	1.97
12	1.58	-3.97
13	0.75	2.50
14	0.68	3.38
15	0.34	9.47
16	0.74	2.57

Table 4.24 The TPM and S/N response data for surface roughness

Level of input parameters (<i>i</i>)	TPM Response (μm)			S/N Response (dB)		
	A_i	B_i	C_i	A_i	B_i	C_i
Level 1	1.71	1.42	1.57	-3.54	-1.35	-2.39
Level 2	1.14	0.99	0.85	-0.74	0.58	2.65
Level 3	1.09	0.86	1.13	-0.49	2.38	-0.69
Level 4	0.63	1.30	1.02	4.48	-1.90	0.14
Difference	1.08	0.57	0.72	8.01	4.28	5.05
Rank	1	3	2	1	3	2

Based on the same TPM and S/N criteria, Figure 4.32 (a-c) suggests that the highest concentration of nanoparticles (1.0 wt%) in the lubricant (A4), nozzle angle of 30° (C2) and air pressure of 3 bar (B3) are determined to be the best choices for obtaining the lowest surface roughness.

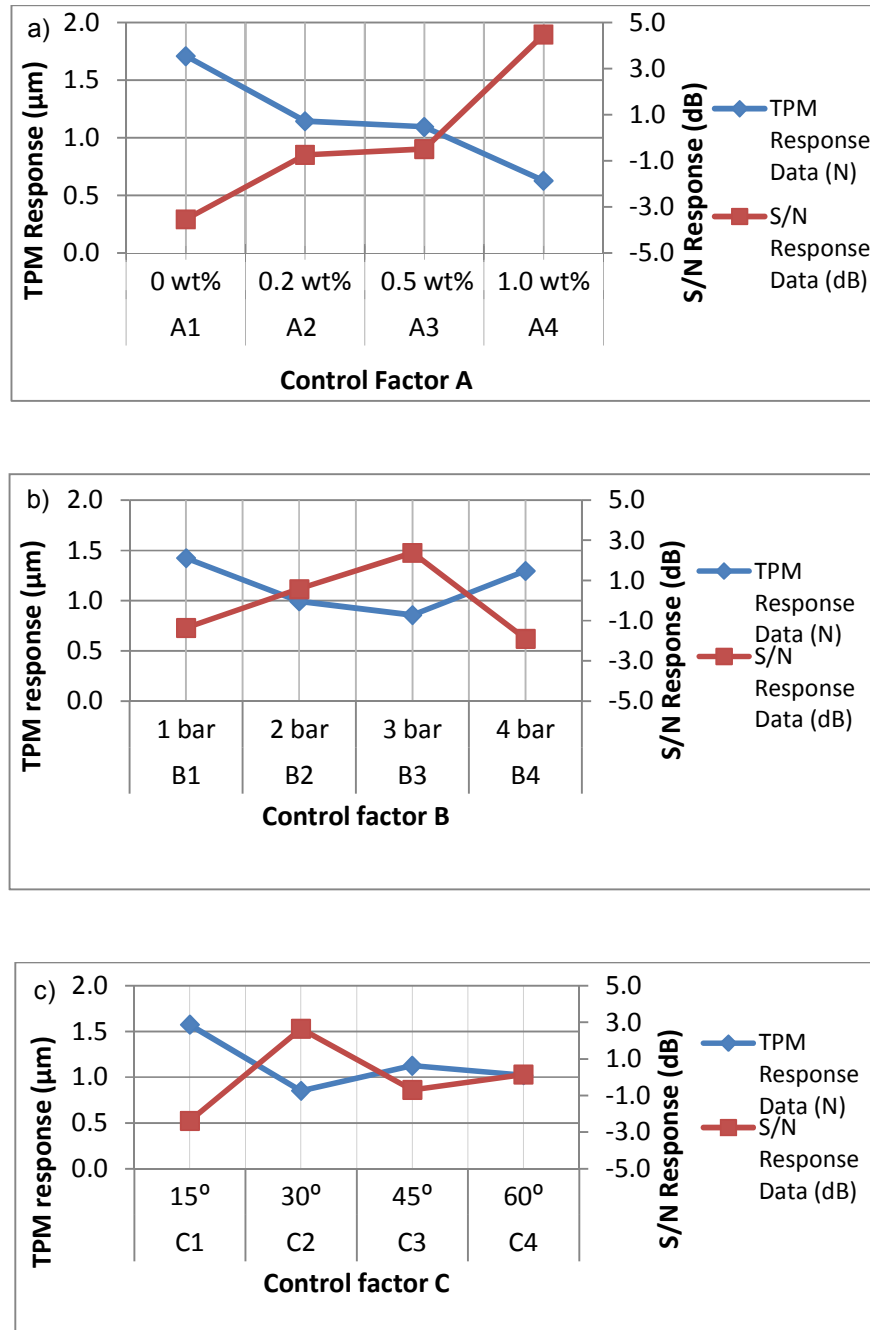


Figure 4.32 TPM and S/N response graphs of surface roughness at different control factors (a) concentration of the nanoparticles, control factor A, (b) air pressure, control factor B and (c) nozzle orientation, control factor C

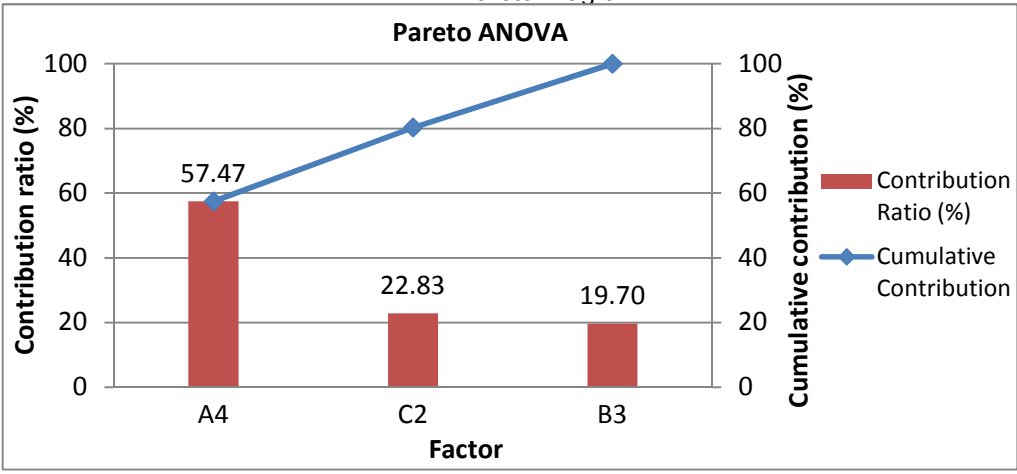
Interaction data analysis for surface roughness are presented in Table 4.25 respectively. The data is constructed from the S/N response data tabulated in the Table 4.24. From the calculated two-way table it can be seen that the optimum parameters for the lowest surface roughness is A4 B3 C2. It can be noted that these results are found to be similar with the others obtained using the S/N and TPM analysis.

Table 4.25 Interaction data analysis for surface roughness

AXB	B1	B2	B3	B4	Total	Highest total response
A1	-9.94	2.48	-3.02	-3.67	-14.14	A4
A2	2.64	-4.17	1.10	-2.54	-2.97	
A3	-0.60	0.64	1.97	-3.97	-1.96	
A4	2.50	3.38	9.47	2.57	17.92	
Total	-5.40	2.32	9.53	-7.61		
Highest total response	B3					
AXC	C1	C2	C3	C4	Total	Highest total response
A1	-9.94	2.48	-3.02	-3.67	-14.14	A4
A2	-4.17	2.64	-2.54	1.10	-2.97	
A3	1.97	-3.97	-0.60	0.64	-1.96	
A4	2.57	9.47	3.38	2.50	17.92	
Total	-9.57	10.61	-2.77	0.57		
Highest total response	C2					
BXC	C1	C2	C3	C4	Total	Highest total response
B1	-9.94	2.64	-0.60	2.50	-5.40	B3
B2	-4.17	2.48	3.38	0.64	2.32	
B3	1.97	9.47	-3.02	1.10	9.53	
B4	2.57	-3.97	-2.54	-3.67	-7.61	
Total	-9.57	10.61	-2.77	0.57		
Highest total response	C2					

In the case of all parameters (air pressure, nanoparticle concentration and nozzle angle) are considered as prominent factors, having a cumulative contribution of 100% as shown by the Pareto ANOVA analysis for surface roughness in Table 4.26. The Pareto ANOVA analysis recommends that A4 B3 C2 is the best combination to obtain the lowest surface roughness.

Table 4.26 Pareto ANOVA analysis for surface roughness

S/N	S/N Response data (dB)		
Control Factor levels (i)	A_i Nanoparticle concentration	B_i Air pressure	C_i Nozzle angle
Level 1	-3.54	-1.35	-2.39
Level 2	-0.74	0.58	2.65
Level 3	-0.49	2.38	-0.69
Level 4	4.48	-1.90	0.14
Total summation	-0.29	-0.29	-0.29
Square of Differences (S)	$S_A = 133.33$	$S_B = 45.71$	$S_C = 52.97$
Total summation of squares of differences $St = S_A + S_B + S_C$	52.61		
Contribution Ratio (%)	57.47	19.70	22.83
<p style="text-align: center;">Pareto Diagram</p>  <p style="text-align: center;">Pareto ANOVA</p> <p>Contribution ratio (%)</p> <p>Cumulative contribution (%)</p> <p>Contribution Ratio (%)</p> <p>Cumulative Contribution</p> <p>Factor</p> <p>A4 C2 B3</p>			
Cumulative Contribution	57.47	80.3	100.00
Optimum Combination	A4	B3	C2
Overall optimum conditions for all factors	A4 B3 C2		

4.5.3 Cutting temperature

Table 4.27 is presenting the calculated TPM and S/N ratio for cutting temperature. The TPM and S/N response data for cutting temperature are then calculated and summarized in Table 4.28.

Table 4.27 The calculated TPM and S/N ratio for cutting temperature

Test Levels	Cutting Temperature	
	Calculated TPM Values (°C)	Calculated S/N Ratio (dB)
1	57.20	-35.15
2	71.20	-37.05
3	56.10	-34.98
4	48.80	-33.77
5	43.50	-32.77
6	53.50	-34.57
7	73.10	-37.28
8	69.70	-36.86
9	67.80	-36.62
10	61.50	-35.78
11	51.30	-34.20
12	65.00	-36.26
13	58.10	-35.28
14	56.90	-35.10
15	65.50	-36.32
16	68.20	-36.68

Table 4.28 The TPM and S/N response data for cutting temperature

Level of input parameters (<i>i</i>)	TPM Response (°C)			S/N Response (dB)		
	A_i	B_i	C_i	A_i	B_i	C_i
Level 1	58.33	56.65	57.55	-35.24	-34.96	-35.15
Level 2	59.95	60.78	61.30	-35.37	-35.62	-35.60
Level 3	61.40	61.50	62.63	-35.72	-35.70	-35.89
Level 4	62.18	62.93	60.38	-35.85	-35.89	-35.53
Difference	3.85	6.28	5.08	0.61	0.94	0.74
Rank	3	1	2	3	1	2

From Figure 4.33 (a-c), the air pressure of 1 bar (B1), lubricant containing no nanoparticles (A1) and lowest nozzle angle of 15° (C1) are determined to be the best choices for obtaining the lowest cutting temperature.

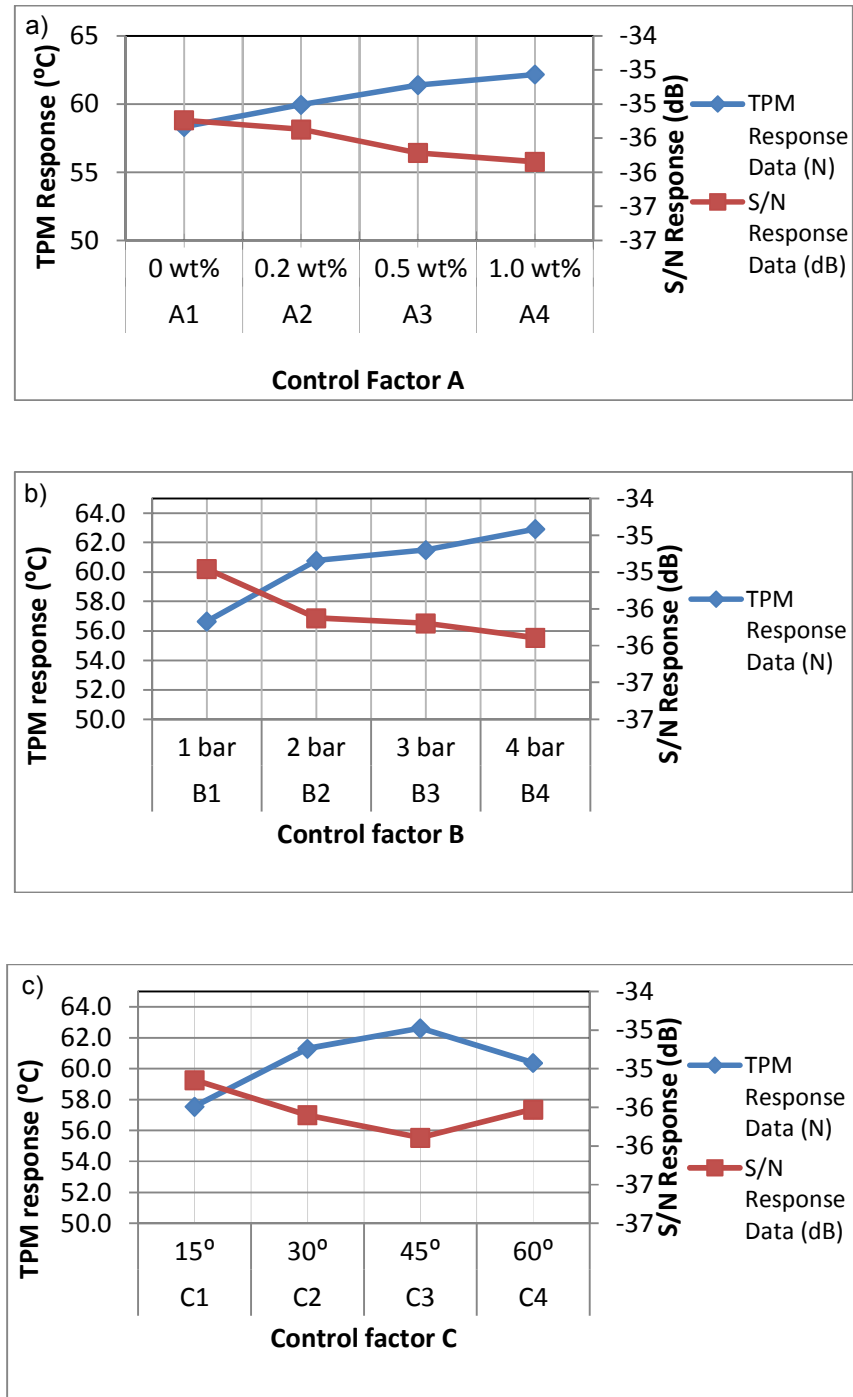


Figure 4.33 TPM and S/N response graphs of cutting temperature at different control factors (a) concentration of the nanoparticles, control factor A, (b) air pressure, control factor B and (c) nozzle orientation, control factor C

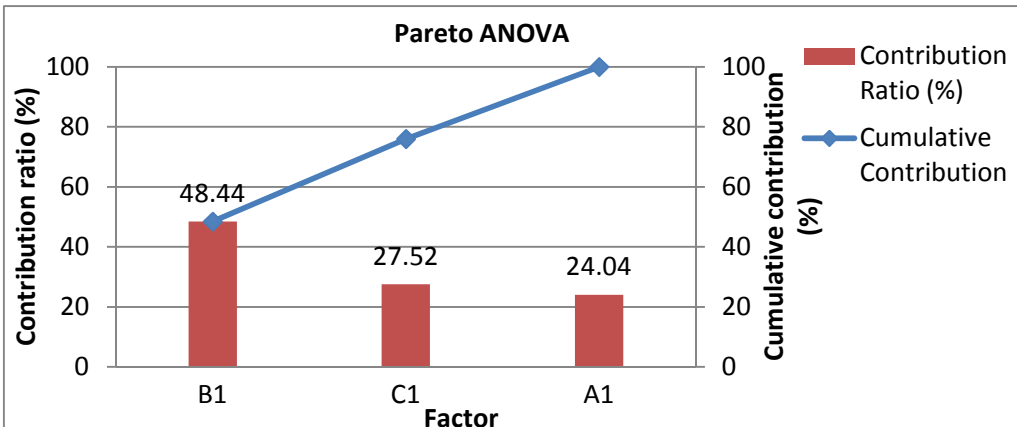
Interaction data analysis for cutting temperature is presented in Table 4.29 The data is constructed from the S/N response data tabulated in the 4.31. From the calculated two-way table it can be seen that the optimum parameters for the lowest cutting temperature is A1 B1 C1. It can be noted that these results are found to be similar with the others obtained using the S/N and TPM analysis.

Table 4.29 Interaction data analysis for cutting temperature

AXB	B1	B2	B3	B4	Total	Highest total response
A1	-35.15	-37.05	-34.98	-33.77	-140.95	A1
A2	-32.77	-34.57	-37.28	-36.86	-141.48	
A3	-36.62	-35.78	-34.20	-36.26	-142.86	
A4	-35.28	-35.10	-36.32	-36.68	-143.39	
Total	-139.83	-142.50	-142.78	-143.57		
Highest total response	B1					
AXC	C1	C2	C3	C4	Total	Highest total response
A1	-35.15	-37.05	-34.98	-33.77	-140.95	A1
A2	-34.57	-32.77	-36.86	-37.28	-141.48	
A3	-34.20	-36.26	-36.62	-35.78	-142.86	
A4	-36.68	-36.32	-35.10	-35.28	-143.39	
Total	-140.59	-142.40	-143.57	-142.11		
Highest total response	C1					
BXC	C1	C2	C3	C4	Total	Highest total response
B1	-35.15	-32.77	-36.62	-35.28	-139.83	B1
B2	-34.57	-37.05	-35.10	-35.78	-142.50	
B3	-34.20	-36.32	-34.98	-37.28	-142.78	
B4	-36.68	-36.26	-36.86	-33.77	-143.57	
Total	-140.59	-142.40	-143.57	-142.11		
Highest total response	C1					

From Table 4.30, the air pressure (B), nano base lubricants (A) and nozzle angle (C) contributes 48.44%, 27.52% and 24.04% respectively for obtaining lowest cutting temperature. In this case all parameters (air pressure, nanoparticle concentration and nozzle angle) are considered as prominent factors, having a cumulative contribution of 100%. The Pareto ANOVA analysis recommends that A1 B1 C1 is the best combination to obtain the lowest cutting temperature. Finally from Table 4.30, the nano base lubricant (A), nozzle angle (C) and air pressure (B) contributes 57.47%, 22.83% and 19.70% respectively.

Table 4.30 Pareto ANOVA analysis for cutting temperature

S/N	S/N Response data (dB)		
Control Factor levels (i)	Ai Nanoparticle concentration	Bi Air pressure	Ci Nozzle angle
Level 1	-35.24	-34.96	-35.15
Level 2	-35.37	-35.62	-35.60
Level 3	-35.72	-35.70	-35.89
Level 4	-35.85	-35.89	-35.53
Total summation	-142.17	-142.17	-142.17
Square of Differences (S)	$S_A = 0.98$	$S_B = 1.98$	$S_C = 1.13$
Total summation of squares of differences $St = S_A + S_B + S_C$	52.61		
Contribution Ratio (%)	24.04	48.44	27.52
<div style="text-align: center;">Pareto Diagram</div> 			
Cumulative Contribution	48.44	75.96	100.00
Optimum Combination	A1	B1	C1
Overall optimum conditions for all factors	A1 B1 C1		

In this study, three techniques were used for the purpose of the analyses. All techniques deliver similar results. Extensive dispersion of SiO₂ nanoparticles in cutting oil

facilitated by high pressure stream air at cutting zone shows better performance by reducing the cutting force, temperature and surface roughness. The atomized mist of the nano base lubricant exhibits more efficient feeding into the cutting zone compared to the flood lubrication method. The splash off by the rotating cutting tool during flood lubrication reduces the efficiency, while the atomized mist sticks to the tool-workpiece interface to assist the cutting operation. The presence of nanoparticles in the lubricant also acts as a polisher at the tool-workpiece interface. An interacting force is induced at the interface between the nanoparticles and tool surface (Yan et al., 2011). This interacting force travels upon the tool surface with a certain speed and then emits power to the surface. Tu-Chieh and Yaw-Terng found a large interacting force acting between the particles and workpiece reduces the surface energy of workpiece which is basically the binding strength between the surface and sub-surface atoms of the workpiece. The breaking process requires certain amount of energy to break the weak asperities of workpiece and generates new surface with lower roughness. The nanoparticles transfer the potential energy from tool, then it is converted into kinetic energy of surface atoms and dissipates heat (Tu-Chieh & Yaw-Terng, 2006). Consequently, with increasing the nanoparticles concentration to the lubricant, more and more nanoparticles will be able to transfer kinetic energy to the workpiece surface and thus heat dissipation will be increased. The low friction behavior of the nanoparticles effectively minimizes the frictional effects at tool-workpiece interface and thus reduces the cutting force. For large amount of nanoparticles present in cutting oil collides and impedes by the asperities on work surface and generate higher cutting force.

The viscosity of cutting oil can be increased by introducing nanoparticles in the base lubricant. More nanoparticles also work as spacer between tool-workpiece interfaces which eliminates the tool-workpiece contact. In high speed machining process, the large amount of heat generation changes the elastohydrodynamic lubrication into boundary

lubrication where spherical nanoparticles act as a roller between the rubbing surfaces and thus reduces the coefficient of friction (Kao & Lin, 2009; Wu et al., 2007). Beside this, the porous nature of spherical SiO_2 nanoparticles impart high elasticity which augments their resilience in a specific loading range and further enhance the gap in tool-workpiece interface (Rapoport et al., 2002). Therefore, with the extreme pressure of additives in cutting oil and the existence of gap between tool-workpiece interface, there is a high contact resistance which induces the formation of chemical reaction film on the workpiece surface (Lin & So, 2004). This gap will result the formation of thin protective film on the surfaces. The increase in nanoparticles in the lubricant will increase the growth of thin protective film on the machined surface. Due to the breakage of more asperities, the more workpiece surface comes in contact with the cutting oil and thus strong chemical interaction is formed between nano base lubricant and new surface. This process definitely increase the quality of the machined surface by reducing coefficient of friction (Kwangho Lee et al., 2009).

During the cutting process, the consumed energy is transformed into heat at deformation zones. With increasing the amount of nanoparticles the heat generation is increased and it may reach to the melting temperature of the workpiece. Another reason for increasing the temperature may due to the formation of thin film which prevents the heat dissipation from the machined surface. It is suspected that raising of temperature softens the material aiding grain boundary dislocation which makes it easier the cutting operation at lower the cutting force (Reddy & Rao, 2006).

During cutting, variation in air pressure affects the formation of protective film (Hirata et al., 2004). It is believed that the protective film is the mixture of chemically reacted lubricant and Al_2O_3 which is produced on the surface of Al6061-T6 alloy. The formation of Al_2O_3 is the natural properties of aluminium alloy in air. Therefore, high air

pressure increases the oxygen content which adsorbs onto aluminium to form Al_2O_3 (Wakabayashi et al., 2007). The Al_2O_3 layer possesses higher hardness and cause higher cutting force during machining. The higher cutting force might be due to smaller rake angle induced by hard protective film which increases the friction at the rake face of tool. This causes the temperature of some thin layers on the back face of the chip adjacent to rake face of the tool to reach close to melting temperature. High temperature effect the strain energy of the workpiece in the presence of extreme pressure of additive in cutting oil. The film formations are enhanced on the machined surface at high temperature (Lin & So, 2004). Due to high temperature the film is welded with the workpiece. This welded zone of Al_2O_3 has slightly higher hardness compared to pure Al_2O_3 layer (Prado et al., 2001). Therefore, higher cutting force is required to overcome the hardness of the welded protective film. However, the results on surface roughness show that the surface roughness decreases initially but drastically increases when air pressure is beyond 2 bar. This may due to the formation of welded region at higher air pressure. This welded layer can act as peeler which might pull away some workpiece material mechanically (Thepsonthi et al., 2009). The appropriate air pressure helps the nano base lubricant to penetrate into the deep of cutting zone and assist in polishing the machined surface. Moreover, appropriate air pressure do not raise the cutting temperature to high level and therefore leads to intensive formation of protective film to reduce surface roughness.

In high speed machining process, nozzle orientation is an important factor, but very few literatures reported on the detail study of the most appropriate nozzle orientation. For lowest cutting temperature, nozzle angle of 15° shows the optimum result. Since tertiary deformation zone contributes most of the heat evolution, therefore nozzle orientation at 15° successfully withdraw heat from the tertiary zone. However, 30° nozzle angle shows optimum result for best surface roughness and chip thickness ratio. It may be due to the fact

that this angle accelerates the cutting oil to the machining zone in order to obtain better surface quality. Again, as mentioned before, the cutting oil at tool-chip interface has negligible effect on the cutting force, therefore 60° nozzle angle may not be the optimum for chip thickness ratio as cutting force shows optimum in 60° nozzle angle.

During the process of polishing, the particles can be partially embedded into the machined surface. When the particles collided with the asperities, the particle may shear and change their shape due to the extreme pressure at the cutting zone. The sheared off particles is expected to assist the cutting process but the rolling action of the spherical nanoparticles is reduced. Usage of higher amount of nanoparticles helps to plough off the partially embedded particles by new nanoparticles and both of these particles contributes to polish the surface. The plough off particles leave a thin exfoliated film on the machined surface due to the damage for high loading (Rapoport et al., 2005). Meanwhile, with increasing the nanoparticles, they may impregnate into the pore of the surface and can be sheared by other coming nanoparticles. The rolling action of nanoparticles leads to the formation of an easy sheared lubrication film as well as asperities and thus the quality of surface polishing is enhanced (Rapoport et al., 2002). Thus, the impact of SiO₂ particles encountered on intermetallic particles increases the cutting force. Therefore, this is the reason why improper feeding of nano base lubricant causes negative effect on the cutting operation.

After the optimal levels of all control factors are identified, the last step was to conduct a verification test using these optimal parameters of A2 B1 C4 for cutting force, A1 B1 C1 for cutting temperature and A4 B3 C2 for surface roughness to validate the recommendation. This test was repeated for sixteen times and the average TPM values of cutting forces, cutting temperature and surface roughness were measured. The result shows an improvement of 25.02%, 29.34% and 26.28% in cutting force, cutting temperature and

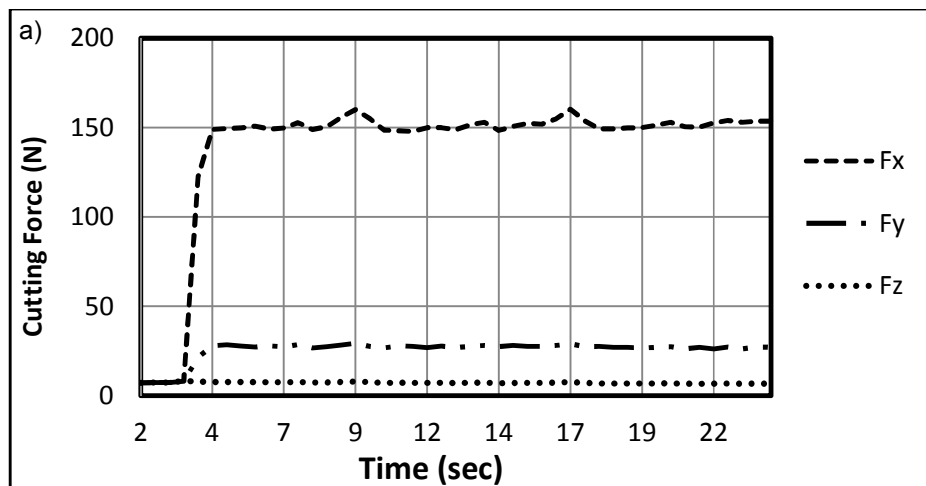
surface roughness respectively compared to the values obtained from initial experiments. Based on the results obtained from the Taguchi optimization method, the following conclusions can be made:

1. Lubricant containing 0.2 wt% SiO₂ nanoparticles with high stream air pressure and nozzle angle of 60° reduces the cutting force.
2. The lowest cutting temperature is obtained by using lowest amount of nanoparticles in the mineral oil with high air pressure and nozzle angle of 15°.
3. The best surface roughness is obtained with higher nanoparticles concentration, air pressure of 2 bar and nozzle angle of 30°.

The excellent performance over pure oil and the drastic reduction of consumption leads to the conclusion that MQL nano base lubricant is a feasible way to improve the machining process. The low cost and excellent properties of SiO₂ nanoparticles create an opportunity for the nano base lubricants to be a new effective alternative for flood lubrication due to the environmental issue.

4.5.4 Morphological analysis

The slot milling test was carried out with the proposed experimental setup to examine the morphology of machined surface. Figure 4.34 (a) and (b) illustrates an example of the cutting forces in the X, Y and Z-axis directions and surface roughness at 5000 min^{-1} cutting speed, 100 mm/min feed rate and 5 mm depth of cut respectively containing 0.2 wt% nanoparticles in the lubricant. Figure 4.35 (a-c) shows the variation in cutting force, cutting temperature and surface roughness at different concentration of SiO_2 nanoparticles respectively. As it is seen in Figure 4.35, the lowest cutting force, cutting temperature and surface roughness were obtained at 0.2, 0 and 1.0 wt% of SiO_2 concentrations in mineral oil, respectively.



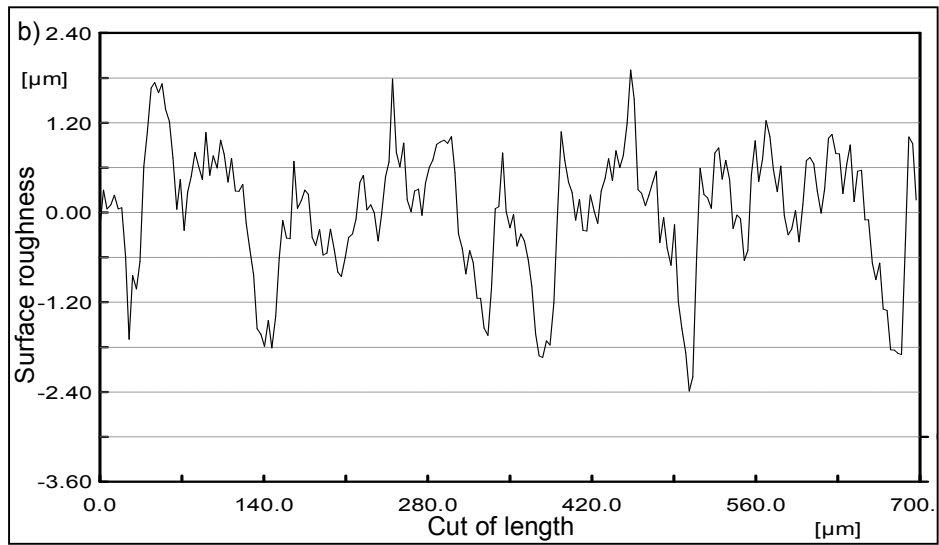
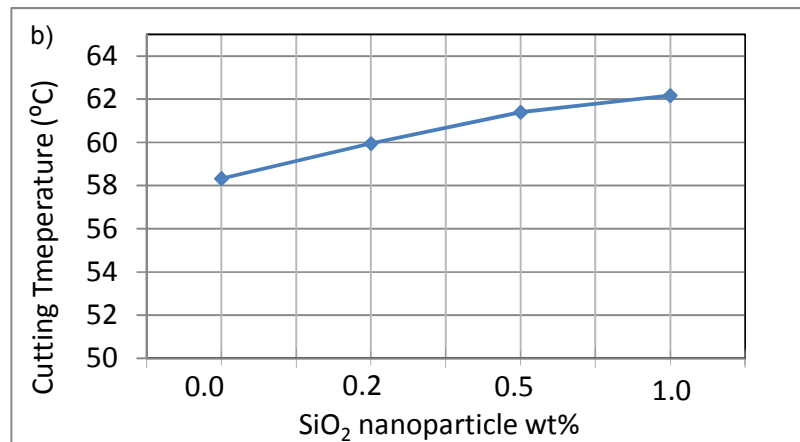
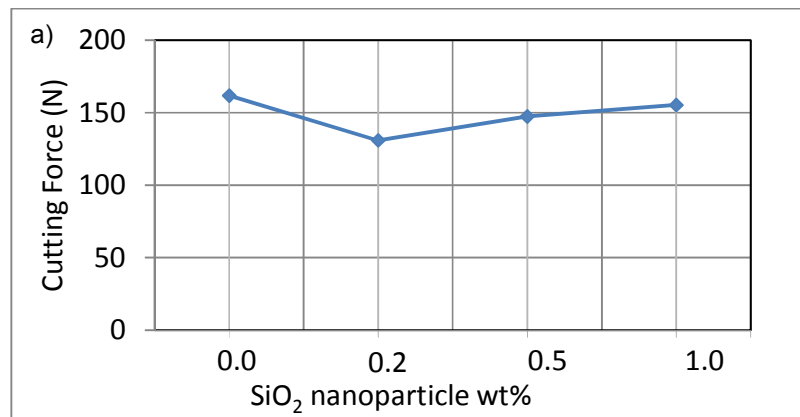


Figure 4.34 Illustration of (a) cutting forces in the X, Y and Z-axis directions and (b) surface roughness at 5000 min^{-1} cutting speed, 100 mm/min feed rate and 5 mm depth of cut using 0.2 wt\% nanoparticles in the lubricant



c)

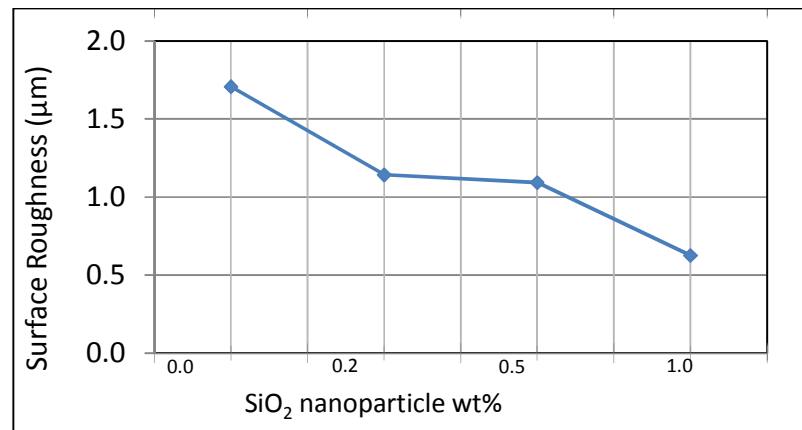


Figure 4.35 Effects of SiO₂ nanoparticles on (a) cutting force, (b) cutting temperature and (c) surface roughness

The mechanism behind such phenomena is due to the increment of SiO₂ concentration, which increases the number of nanoparticles at the tool-workpiece interface. These nanoparticles serve as spacers, eliminating the contact between the tool and workpiece. In high speed machining processes, the generated heat converts the elastohydrodynamic lubrication into boundary lubrication. The nanoparticles in the lubricant act as a fluid film bearing and thus reduces the coefficient of friction at the tool-workpiece interface by the rolling action of nanoparticles (Shenoy et al., 2012). Nanoparticles in the base oil collide with each other and are impeded by the asperities which increases the cutting forces.

In contrast, a high pressure air stream in the cutting zone facilitates the dispersion of SiO₂ nanoparticles in the cutting oil which enhances the performance during machining. The atomized mist mixed with SiO₂ nanoparticles suspended lubricant exhibits more efficient feeding properties at the cutting zone compared to flood lubrication process. Nanoparticles at the tool-workpiece interface act as a polisher as an interacting force is induced by the nanoparticles.

Furthermore, the nanoparticles transfer an increased amount of kinetic energy to the workpiece. Hence, during the cutting process, the energy that is consumed is transformed to

heat energy at the deformation zones (Hamdan et al., 2011). The heat generation raises with increasing the nanoparticles concentration in the lubricant and it may reach as high as the melting temperature of the workpiece material. Another reason for the drastic increase in temperature may be due to the formation of a protective SiO_2 thin film that prevents heat dissipation from the machined surface. According to the work by Suresh and Venkateswara et al the machinability of AISI1045 steel is increased by using molybdenum disulphide as a solid lubricant (Suresh Kumar Reddy & Venkateswara Rao, 2006). Solid lubricants raise the temperature and soften the material by promoting the movement of grain boundary dislocations. Thus, temperature seems to play a very important role that affects the cutting force.

4.5.4 (i) The morphology of the machined surface

Field emission scanning electron microscopy (FESEM) equipped with energy dispersive X-ray (EDX) were utilized to examine the morphology of the machined surface. The surface of the workpiece was initially cleaned to remove all unwanted contamination. The workpiece was etched by hot sodium hydroxide solution to remove minor surface imperfections. The surface oxides (combination of intermetallic, metal and metal oxides) are removed by using an aqueous solution of phosphoric acid, sulfuric acid, simple and complex fluoride ions, organic carboxylic acid and manganese in its oxidation state. The formation and growth of the protective SiO_2 thin film on the machined surface as well as the migration of metal during machining were examined through surface elemental mapping analysis.

4.5.4 (ii) The formation and growth of the protective SiO₂ thin film on the machined surface

Figure 4.36 shows the FESEM image of the surfaces after machining with four different SiO₂ concentrations in the lubricant. Clearly, several thin protective films are developed on the machined surface containing billions of SiO₂ nanoparticles (Figures 4.36 (b-d)). These regular thin films are expanded when SiO₂ concentration is increased from 0.2 wt% to 1.0wt%. Small exfoliations or shedding of thin film is also occurred at high concentration of nanoparticles (Figure 4.36(d)). The increment of nanoparticles concentration in the nano base lubricant might increase the viscosity of the cutting oil. In this case, more nanoparticles at the tool-workpiece interface serve as spacers, eliminating tool-workpiece contact friction. Moreover, the porous nature and high elasticity of SiO₂ nanoparticles could increase the resilience in a specific loading range along with the gap at the tool-workpiece interface. This phenomenon was also observed in the tribological properties of hydrosilicate powders when they are used as lubricant additives for steel-steel contacts (Zhang et al., 2011). Therefore, the extreme pressure of additives and the presence of a gap between the tool and workpiece results high contact resistance at the interface. This high contact resistance is responsible for film formation through chemical reaction. In addition, generation of higher heat in the cutting zone transforms the elastohydrodynamic lubrication into boundary lubrication. The result is the formation of thin protective films over the surfaces, as seen in Figure 4.36. The increment of nanoparticles content in the lubricant boosts the growth of thin protective film on machined surfaces. In other words, throughout the machining process the nanoparticles rub against the asperities at the workpiece surface and the newly created surface is exposed to cutting oil. Consequently, strong chemical interactions take place between the nano base lubricant and newly created surface, and a more intensive protective film is formed. This process certainly increases the

quality of the machined surface by reducing the coefficient of friction. These results were obtained by Lee et al (Lee et al., 2009) gives the basic understanding about the role of nanoparticles in nano base lubricant.

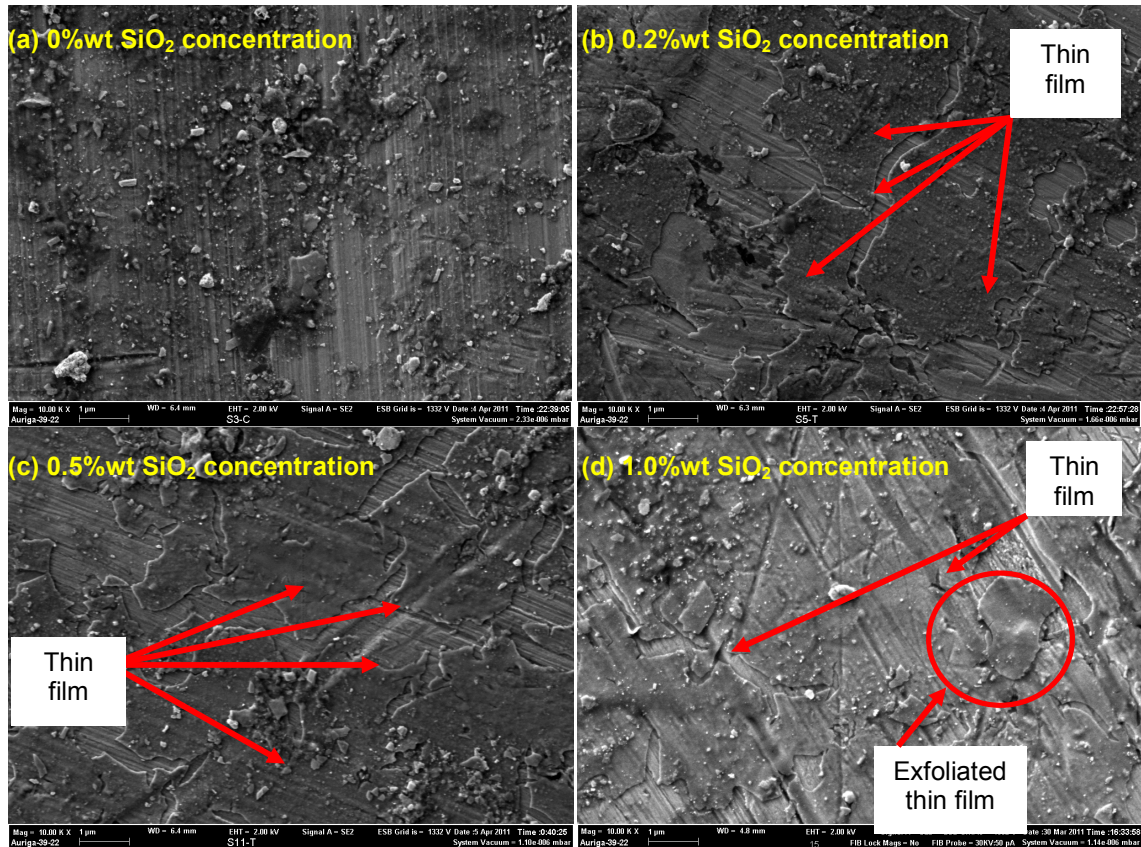


Figure 4.36 FESEM image on the surface machined by nano base lubricants containing SiO₂ nanoparticles of (a) 0 wt%, (b) 0.2 wt%, (c) 0.5 wt% and (d) 1.0 wt%

In additional exploration, the machine surface was analyzed by using energy dispersive X-ray (EDX) as it is shown in Figure 4.37. The results on elemental compositions are summarized in Table 4.31. It is seen from Table 4.31 in conjunction with Figure 4.37 that with increasing the SiO₂ content in the lubricant increases the oxygen (O) and silicon (Si) content on the machined surface. However, when the SiO₂ content in the lubricant ranges in between 0.5 to 1.0 wt%, the O and Si content stabilizes on the machined surface. Iron (Fe) and carbon (C) is also seen in the EDX spectrum when SiO₂ content is

above 0.5 wt% in the lubricant. Iron and carbon is originated on the machine surface from the cutting tool wear.

Table 4.31 Elemental composition of the surfaces machined by nano base lubricants containing different amount of SiO₂ nanoparticles

	SiO ₂ nanoparticle concentration	Oxygen (O)	Silicone (Si)
a	0 wt%	0.045	0.025
b	0.2 wt%	0.175	0.098
c	0.5 wt%	0.368	0.175
d	1.0 wt%	0.34	0.17

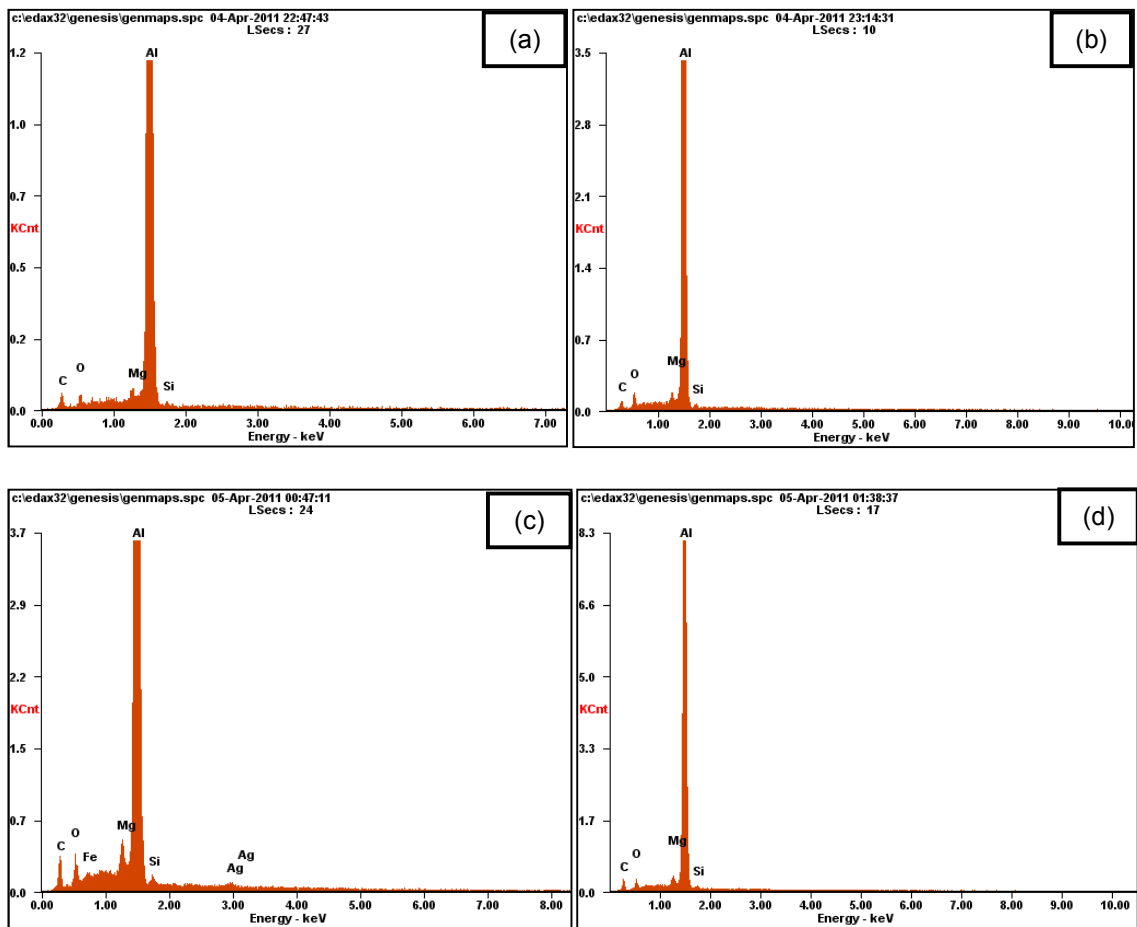


Figure 4.37 Energy dispersive X-Ray (EDX) analysis on the surface machined by nano base lubricants containing SiO₂ nanoparticles of (a) 0 wt%, (b) 0.2 wt%, (c) 0.5 wt% and (d) 1.0 wt%

4.5.4 (iii) Surface elemental mapping

Surface elemental mapping was employed to determine the surface quality, orientation and distribution of SiO_2 nanoparticles over the machined surface. The elemental mapping of the surfaces machined by nano base lubricants containing 0.2, 0.5 and 1 wt% SiO_2 is shown in Figure 4.38 (a-c) respectively.

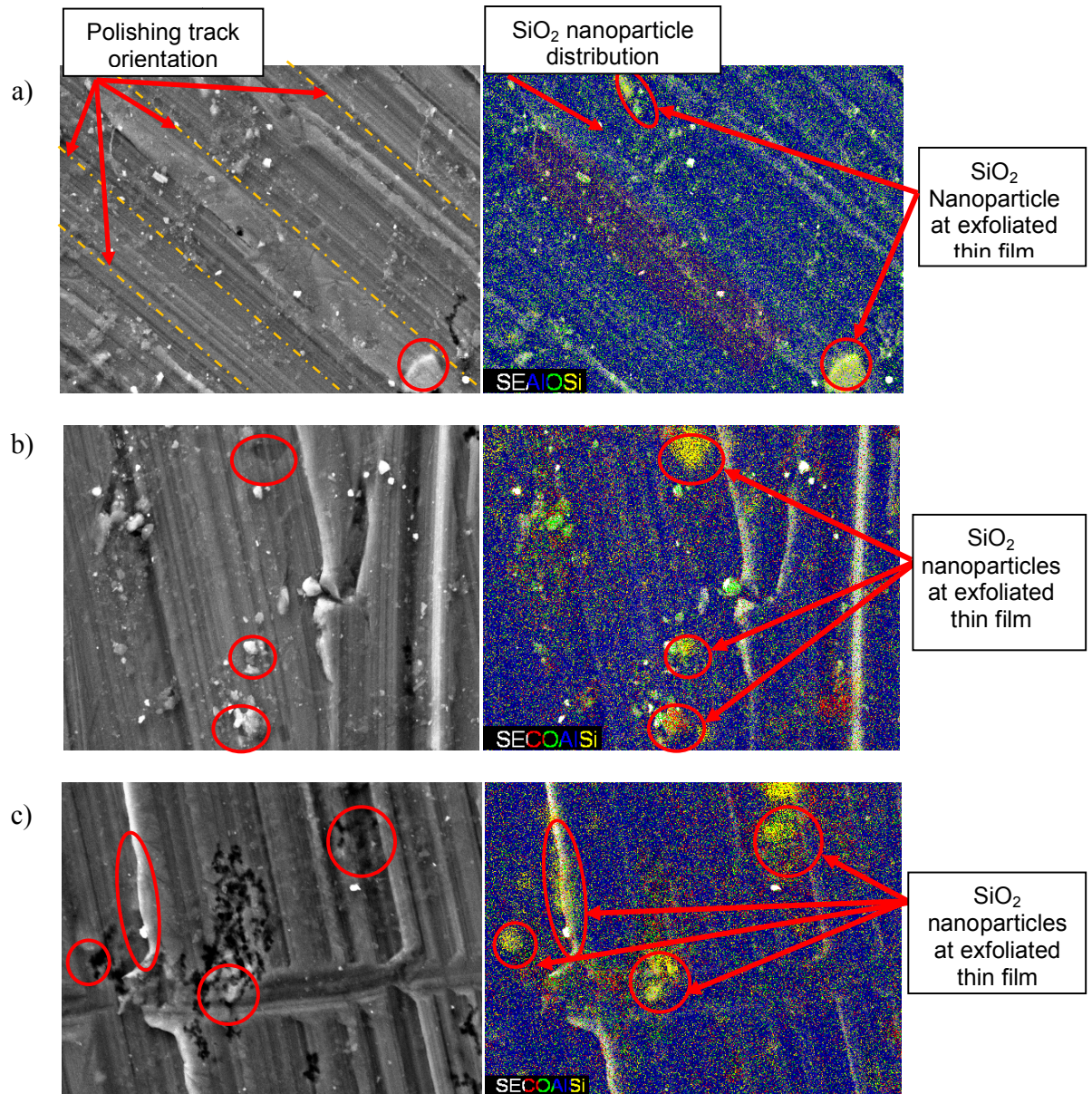


Figure 4.38 Surface elemental mapping of the samples machined by nano base lubricants containing SiO_2 nanoparticle of (a) 0.2 wt%, (b) 0.5 wt% and (c) 1.0 wt%

Figure 4.38 (a) demonstrates that at lower concentration of SiO₂ nanoparticles (0.2 wt%), the polishing track orientation matches with the distribution of SiO₂ nanoparticles, particularly on the exfoliated thin film. At the SiO₂ concentration of 0.5 wt%, more SiO₂ nanoparticles are present compared to the on the exfoliated thin film (Figure 4.38 (b)). At 0.5 wt% of SiO₂ nanoparticles, the track of embedded nanoparticles onto the machined surface is evident. Eventually, nanoparticles can be ploughed off but some debris of nanoparticles is remained on the surface. When the SiO₂ nanoparticle concentration is raised to 1.0 wt%, higher amounts of SiO₂ nanoparticles are embedded onto the machined surface compared to the instances of 0.2 and 0.5 wt% nanoparticles (Figure 4.38 (c)). It is obvious that the nanoparticles are burnished on the surface of porous alumina. Several SiO₂ nanoparticles are partially embedded into the surface and some tracks of ploughed off is seen, while additional nanoparticle debris are left behind as it can be seen in Figure 4.38(c).

Considering the results from elemental mapping, the nanoparticles seem to assist the cutting operation. The assisting mechanism of the nanoparticles can be categorized into three levels. At the first level, the particles are partially embedded onto the machined surface due to the collision with the asperities at extremely high pressure in the cutting zone. Here, the particles are sheared and the shape of the particles is changed due to compression. The sheared off the debris continues to assist the cutting process, but the rolling capacity of nanoparticles is reduced. At the second level, the partially embedded nanoparticles are ploughed off by new nanoparticles and the particles continue to polish the surface. The thin exfoliated film is left on the surface due to the ploughed off the particles (Williams, 2005). At the third stage, the concentration of the nanoparticles is increased by the upcoming new particles. The nanoparticles impregnate into the surface pores, after which they get shaved off by other incoming nanoparticles. The rolling of nanoparticles produces surface asperities and a lubrication film is formed which can be sheared easily.

The phenomenon enhances the surface polishing and improves the machining quality. According to the results, the 1.0 wt% of SiO₂ nanoparticles in the lubricant offers the best surface finishing compared to other concentrations.

4.5.4 (iv) Material migration during machining

To explore migration of elements during machining at extreme conditions, the depth of cut was increased to 8 mm by using nano base lubricant containing 0.2 wt% nanoparticles. Element mapping on the machined surfaces shows the formation of intermetallic containing iron (Fe), carbon (C) and copper (Cu) atoms. These elements are originated from the HSS M35 cutting tool. Similar observations were seen in the EDX analysis given in Figure 4.39. Since aluminium alloys exhibit high adhesive characteristics, material transfer between the tool-workpiece interfaces might be promoted. Inappropriate feeding of nano base lubricant into the cutting zone results unsuccessful cutting operation. This leads to higher cutting temperatures and a larger layer is normally found to adhere with the tool flank and work surface. This also indicates strong abrasion force between the tool tip and work surface. For this reason, Fe and C were smeared on the surface of aluminium. The present aluminium alloy consists of Mg-Si-O elements and Fe and Cu adheres only to the areas where Mg-Si-O binder is exposed. Similar findings were revealed in the research conducted by (Jha et al., 1989). Elemental mapping also clearly illustrates that Fe and Cu adheres only to the regions where Mg-Si-O exists. Material transfer is associated to conditions of high stress in addition with elevated temperature during machining. Due to inter-diffusion of elements between the tool and workpiece, intermetallic particles are formed on the workpiece surface. The melting point of these intermetallic particles is much higher compared to the substrate aluminium alloy and a built-up layer is formed on the substrate by thermal-mechanical mechanisms. Consequently, there is the possibility of forming a built-up aluminium layer on the cutting

tool tip because the cutting tool (HSS M35) consists of 5 wt% Co binder. However, this layer might be detrimental to the quality of the machined surface. Meanwhile, the hardness of SiO₂ nanoparticles is greater than other intermetallics formed on the aluminium surface. The impact of SiO₂ nanoparticles on the intermetallics can increase the cutting force. For this reason the feeding of nano base lubricant is crucial and improper feeding might result negative affect during the cutting operation.

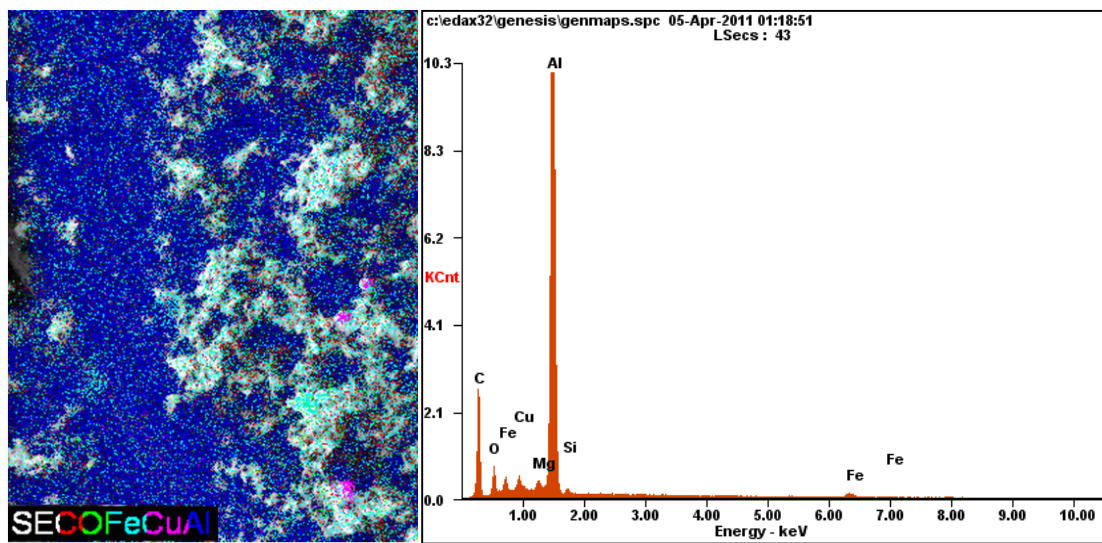


Figure 4.39 Elemental mapping and EDX spectroscopy on a machined surface at 8 mm depth of cut, 5000 min⁻¹ cutting speed and 100 mm/min feed rate

The excellent performance of nano base lubricant over mineral oil lead to the conclusion that using nano base lubricant containing SiO₂ nanoparticles is feasible for improving the machining process and surface morphology. The presence of SiO₂ nanoparticles in the tool-workpiece interface enhances the surface finishing due to the rolling action and impregnation of nanoparticles. Therefore, addition of SiO₂ nanoparticles in the lubricant is a novel and effective means to improve the machining process as well as an alternative to flood lubrication due to the excellent surface finish and environmental concerns.

4.6 Fuzzy logic approach in determining the effect of SiO₂ nano base lubricant on cutting force and surface roughness in milling process

4.6.1 Introduction

Due to the complexity and uncertainty of the machining processes, soft computing techniques are preferred to physics-based models for predicting and optimizing the performance of the machining processes. In this research work, a new approach based on fuzzy logic is used to predict the performance of the machining of Al-6061-T6 by using SiO₂ nano base lubricant. The parameters for SiO₂ nano base lubrication includes the determination of SiO₂ concentration, nozzle angle and air pressure are investigated to improve the milling of Al6061-T6 alloy to achieve the correct lubrication conditions for the lowest cutting force, cutting temperature and surface roughness. Four membership functions are allocated to connect with each input of the model. The predicted results achieved via fuzzy logic approach are compared with the experimental result. The result demonstrated by fuzzy logic approach for cutting force, cutting temperature and surface roughness showed 96.195%, 98.27% and 91.37% accuracy with the experimental results respectively.

4.6.2 Data analysis and discussions

The relationships between the input parameters (nanoparticles concentration in the lubricant, air pressure and nozzle angle) with the output parameters (cutting force, cutting temperature and surface roughness) during the milling operation of Al-6061-T6 alloy were referred to construct the rules. Fuzzy linguistic variables and fuzzy expressions for input and output parameters are shown in Table 4.32. For each input variable, four membership functions were used which are low, medium, high and very high. The output parameters (cutting force, surface roughness and cutting temperature) also used four membership functions of best, good, average and bad.

Table 4.32 Fuzzy linguistic and abbreviation of variables for each parameter

Inputs		Range
Parameters	Linguistic variables	
A - Nanoparticle concentration (wt %)	Low (L), medium (M), high (H), very high (VH)	0.0-1.0 wt%
B- Air pressure (bar)		1-4 bar
C - Nozzle orientation (degree °)		15°-30°
Output		
Cutting Force (N)	Best, Good, Average, Bad	58.3 – 179.9
Cutting Temperature (°C)		43.5 – 73.1
Roughness (µm)		0.34 – 3.14

4.6.2 (i) Membership functions for input and output fuzzy variables

In choosing the membership functions for fuzzification, the event and type of membership functions are mainly depend on the relevant event (Jaya et al., 2010). In this model, each input and output parameter has four membership functions. Gauss shape of membership function was employed to describe the fuzzy sets for input variables. In the output variables of fuzzy set, triangular shape of membership functions were used. Triangular membership function possesses gradually increasing and decreasing characteristics with only one definite value (Jaya et al., 2010). The input variables were partitioned according to the parameter ranges from the experiment. Membership functions of the fuzzy set of input variables are shown in Figure 4.40 (a-c). Moreover, Figure 4.41 shows the membership functions for the output cutting force, cutting temperature and surface roughness fuzzy set.

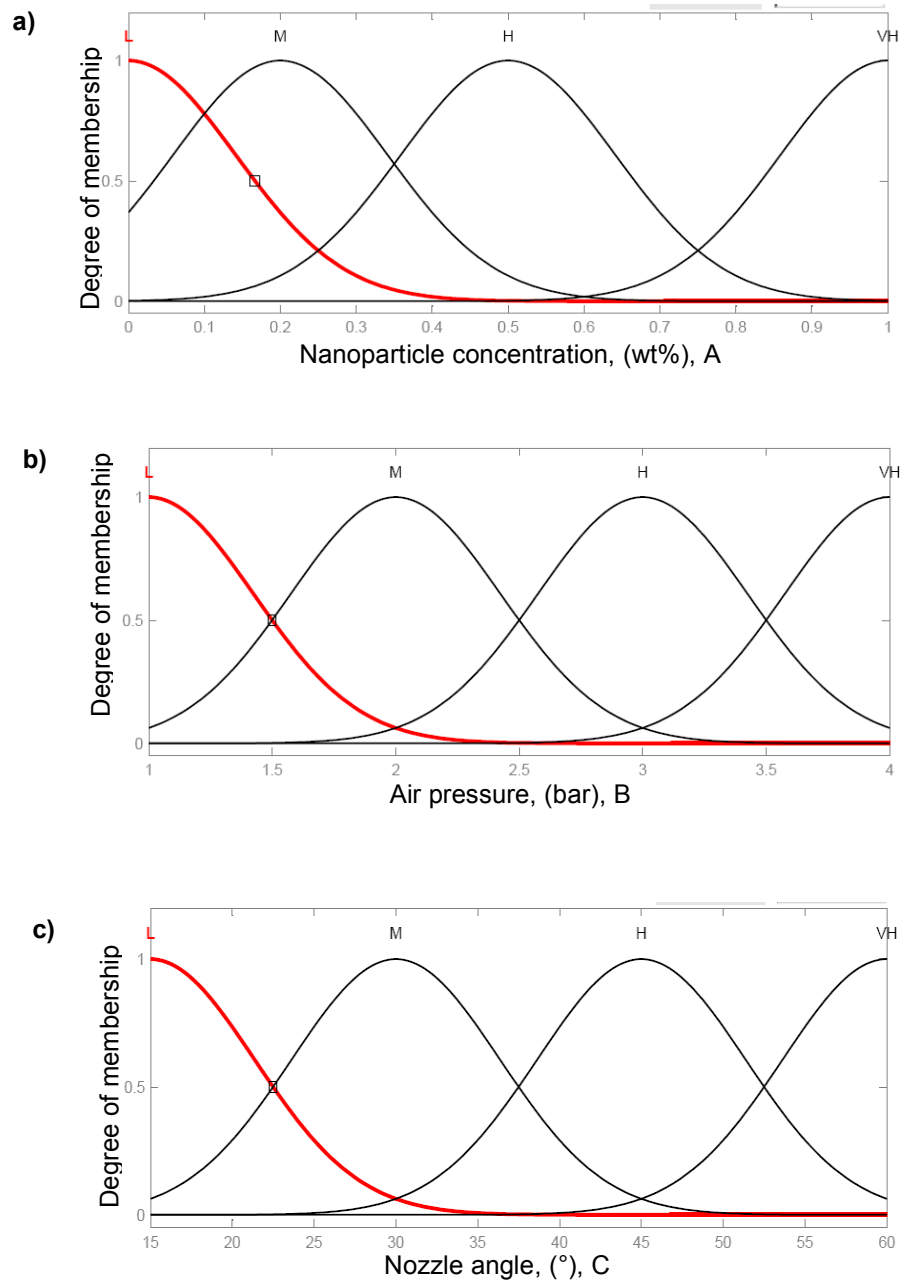


Figure 4.40 Membership function for inputs variables (a) nanoparticle concentration, (b) air pressure and (c) Nozzle angle

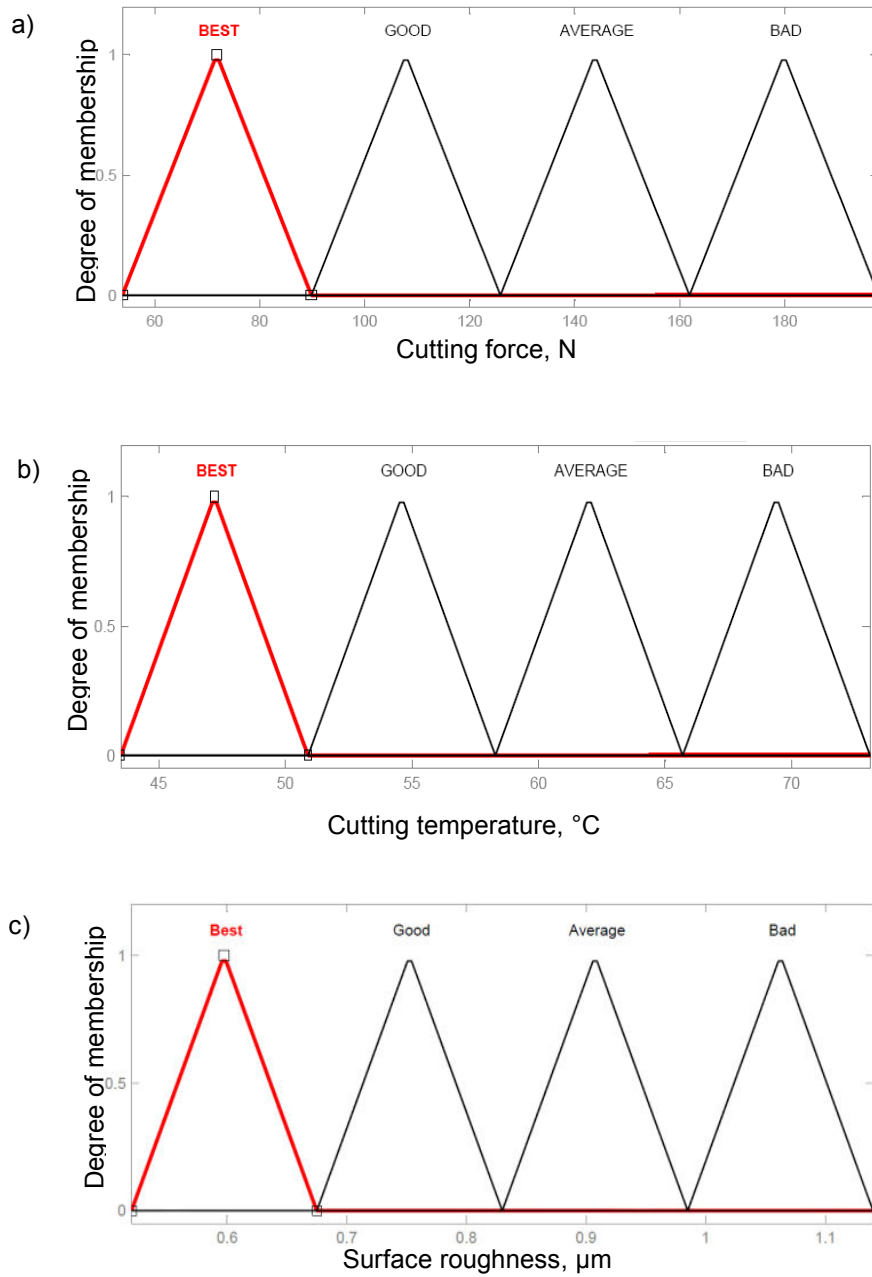


Figure 4.41 Membership function for the output variables of (a) cutting force, (b) cutting temperature and (c) surface roughness

4.6.2 (ii) Structure of Fuzzy Rules

A set of 12 rules were constructed based on the actual experiments for cutting force, cutting temperature and surface roughness of Al-6061-T6 alloy during milling operation by

using SiO₂ nano base lubricant. Experimental results were simulated in the Matlab software on the basis of Mamdani fuzzy logic which is shown in Table 4.33.

Table 4.33 Basis of Mamdani fuzzy logic for cutting force, cutting temperature and surface roughness

Cutting force	Cutting temperature	Surface roughness
1. IF (A is L) and (B is L) and (C is L) then (Cutting force is Average)	1. IF (A is L) and (B is L) and (C is L) then (Cutting temperature is Good)	1. IF (A is L) and (B is L) and (C is L) then (Surface roughness is Bad)
2. IF (A is L) and (B is M) and (C is M) then (Cutting force is bad)	2. IF (A is L) and (B is M) and (C is M) then (Cutting temperature is bad)	2. IF (A is L) and (B is M) and (C is M) then (Surface roughness is Best)
3. IF (A is L) and (B is H) and (C is H) then (Cutting force is Average)	3. IF (A is L) and (B is H) and (C is H) then (Cutting temperature is Good)	3. IF (A is L) and (B is H) and (C is H) then (Surface roughness is Good)
4. IF (A is L) and (B is VH) and (C is VH) then (Cutting force is Bad)	4. IF (A is L) and (B is VH) and (C is VH) then (Cutting temperature is Best)	4. IF (A is L) and (B is VH) and (C is VH) then (Surface roughness is Good)
5. IF (A is M) and (B is L) and (C is M) then (Cutting force is Best)	5. IF (A is M) and (B is L) and (C is M) then (Cutting temperature is Best)	5. IF (A is M) and (B is L) and (C is M) then (Surface roughness is Best)
6. IF (A is M) and (B is M) and (C is L) then (Cutting force is Average)	6. IF (A is M) and (B is M) and (C is L) then (Cutting temperature is Good)	6. IF (A is M) and (B is M) and (C is L) then (Surface roughness is Good)
7. IF (A is M) and (B is H) and (C is VH) then (Cutting force is Bad)	7. IF (A is M) and (B is H) and (C is VH) then (Cutting temperature is Bad)	7. IF (A is M) and (B is H) and (C is VH) then (Surface roughness is Best)
8. IF (A is M) and (B is VH) and (C is H) then (Cutting force is Average)	8. IF (A is M) and (B is VH) and (C is H) then (Cutting temperature is Bad)	8. IF (A is M) and (B is VH) and (C is H) then (Surface roughness is Good)
9. IF (A is H) and (B is L) and (C is H) then (Cutting force is Bad)	9. IF (A is H) and (B is L) and (C is H) then (Cutting temperature is Bad)	9. IF (A is H) and (B is L) and (C is H) then (Surface roughness is Good)
10. IF (A is H) and (B is M) and (C is VH) then (Cutting force is Good)	10. IF (A is H) and (B is M) and (C is VH) then (Cutting temperature is Average)	10. IF (A is H) and (B is M) and (C is VH) then (Surface roughness is Best)
11. IF (A is H) and (B is H) and (C is L) then (Cutting force is Good)	11. IF (A is H) and (B is H) and (C is L) then (Cutting temperature is Good)	11. IF (A is H) and (B is H) and (C is L) then (Surface roughness is Best)
12. IF (A is H) and (B is VH) and (C is M) then (Cutting force is Bad)	12. IF (A is H) and (B is VH) and (C is M) then (Cutting temperature is Average)	12. IF (A is H) and (B is VH) and (C is M) then (Surface roughness is Good)

4.6.2 (iii) Defuzzification

Figure 4.42 (a) and (b) are the examples to show the relation between input parameters and cutting force during milling of Al-6061-T6 alloy by fuzzy based model. As it can be seen from Figure 4.42(a), the cutting force is lowest for the addition of 0.2 wt% SiO₂ nanoparticles in the lubrication system. The cutting force significantly increases with

increasing SiO_2 content in the lubricant. While, from the Figure 4.42(b), it is clearly seen that nozzle angle has less significance to change the cutting force. The higher air pressure and nozzle angle leads to constant cutting force at certain value.

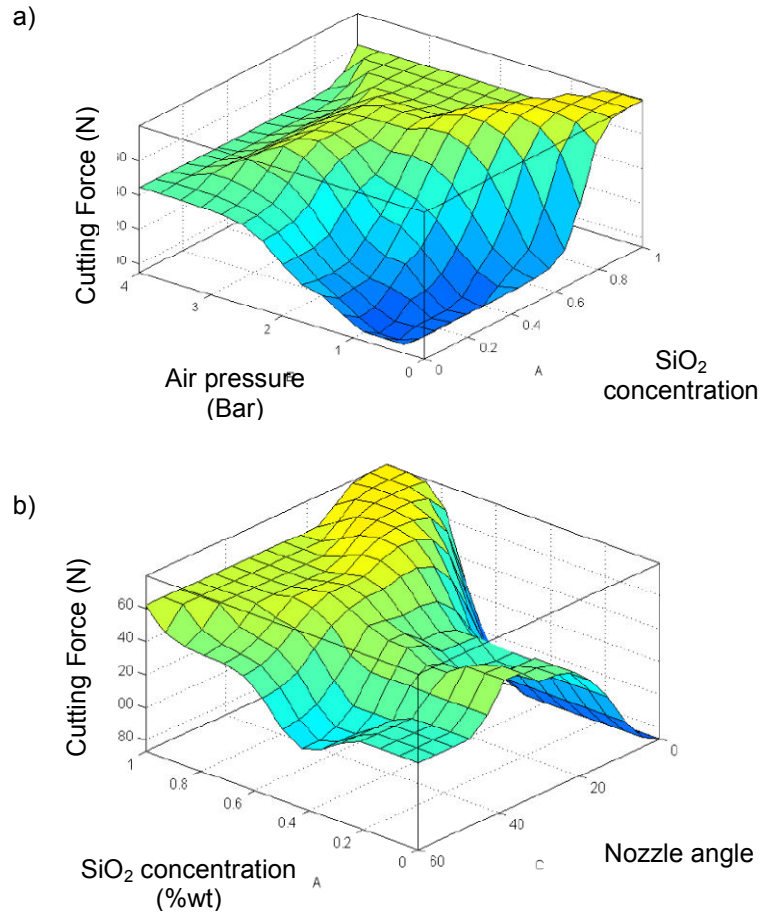


Figure 4.42 The predicted cutting force by fuzzy logic in relation to lubrication parameters (a) air pressure and SiO_2 concentration and (b) SiO_2 concentration and nozzle angle

Figure 4.43 (a) and (b) shows the relationship between input parameters and cutting temperature of Al-6061-T6 alloy during milling operation as predicted by fuzzy logic approach. It is seen from Figure 4.43(a) that the temperature increases significantly with increasing the air pressure with the SiO_2 concentration of 0.5 wt%. From Figure 4.40(b), it is clearly seen that the nozzle angle and SiO_2 concentration are very significant to change

the cutting temperature. It appears that the higher nozzle angle and SiO₂ concentration produces the higher cutting temperature.

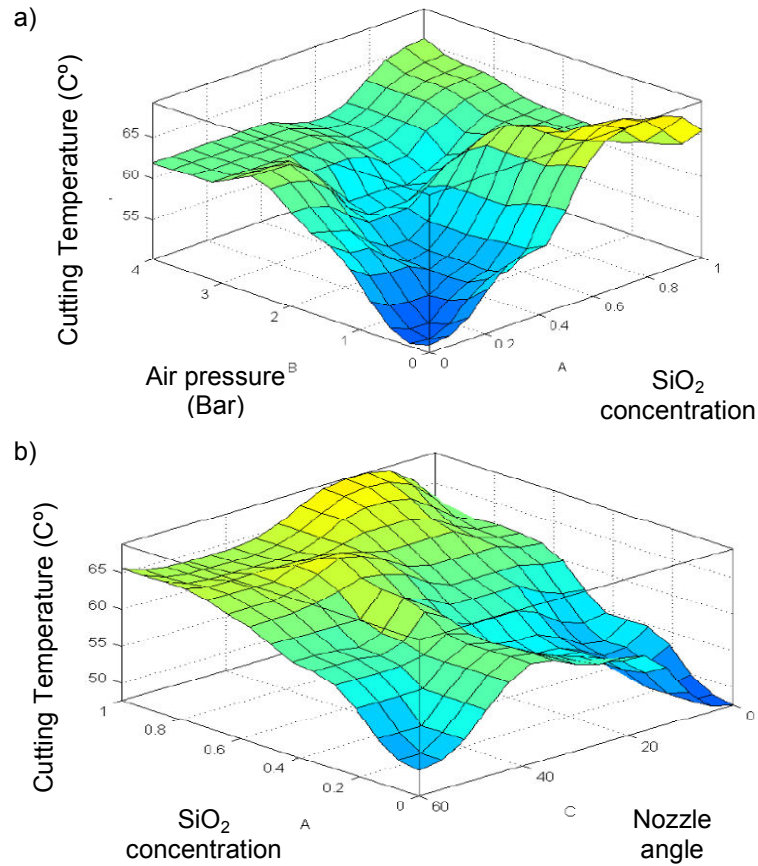


Figure 4.43 The predicted cutting temperature by fuzzy logic in relation to lubrication parameters (a) air pressure and SiO₂ concentration and (b) SiO₂ concentration and nozzle angle

Figure 4.44 (a) and (b) are shows the example of the relationship between input parameters and surface roughness of Al-6061-T6 alloy during milling operation as predicted by fuzzy based model. The surface roughness is found to increase significantly with increasing the air pressure and SiO₂ concentration. From Figure 4.44(b), it is clearly seen that surface roughness is minimum at 0.2wt% SiO₂ concentration. In general the higher nozzle angle and SiO₂ concentration will produce the higher surface roughness.

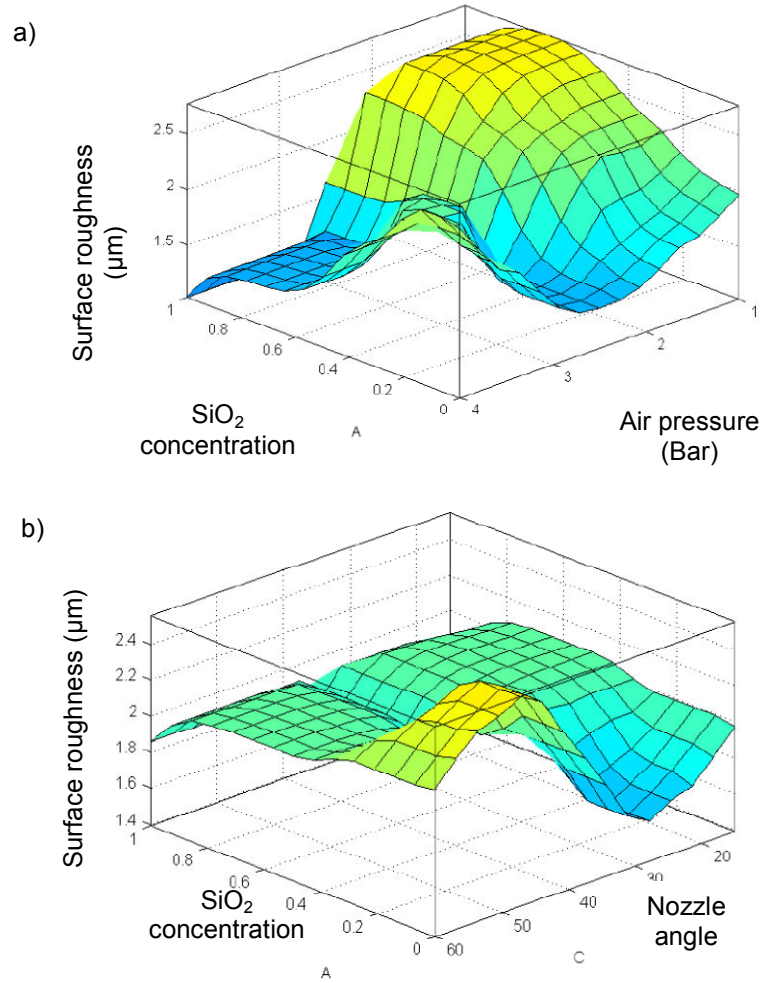


Figure 4.44 The predicted surface roughness by fuzzy logic in relation to lubrication parameters (a) SiO₂ concentration and air pressure and (b) SiO₂ concentration and nozzle angle

4.6.2 (iv) Investigate the accuracy of the fuzzy model

Table 4.34 presents the input parameters for the prediction of the accuracy while Table 4.35 presents the accuracy and error of the fuzzy logic. The error was calculated from the data set and the accuracy of the model was determined. The measured and predicted results for cutting force, cutting temperature and surface roughness are shown in Figure 4.45 (a-c) respectively. For cutting force, the highest error in fuzzy prediction is 8.97%. While for cutting temperature, the highest error is 3.5%. Meanwhile for surface roughness, the highest error for fuzzy model prediction is 16.42%. The low level of errors

shows that the fuzzy logic predicts the surface roughness very well close to the actual experimental surface roughness values.

Table 4.34 The input parameters for the accuracy and error prediction of the fuzzy logic model

No of Exp.	Parameters (Inputs)			
	A	B	C	D
1	2	4	3	2
2	3	4	2	1
3	4	4	1	3
4	4	4	1	1

Table 4.35 The prediction of the accuracy and error of the fuzzy logic model

	Cutting Force (N)				Cutting temperature ($^{\circ}$ C)				Surface roughness (μ m)			
	Measured	Predicted (fuzzy)	Error, %	Accuracy, %	Measured	Predicted (fuzzy)	Error, %	Accuracy %	Measured	Predicted (fuzzy)	Error, %	Accuracy, %
1	145.66	144	1.1	98.9	56.9	56.7	0.35	99.65	0.68	0.693	1.91	98.09
2	186.76	170	8.97	91.03	65.5	62	3.5	96.5	0.64	0.694	7.78	92.21
3	177.31	179	0.95	99.05	68.2	67.3	1.32	98.68	0.74	0.781	5.54	94.46
4	100.01	108	7.41	92.59	57.2	56.2	1.75	98.25	0.63	0.697	9.62	90.38

The low level of errors is seen in the fuzzy logic approach for cutting force, cutting temperature and surface roughness compared with the actual experimental values. The accuracy of this approach shows that the proposed model can be used to predict the cutting force, cutting temperature in the milling operation of Al-6061-T6 alloy by using SiO₂ nano base lubricant. Thus the proposed fuzzy logic model gives promising solution to predict the value in the specific range of parameters.

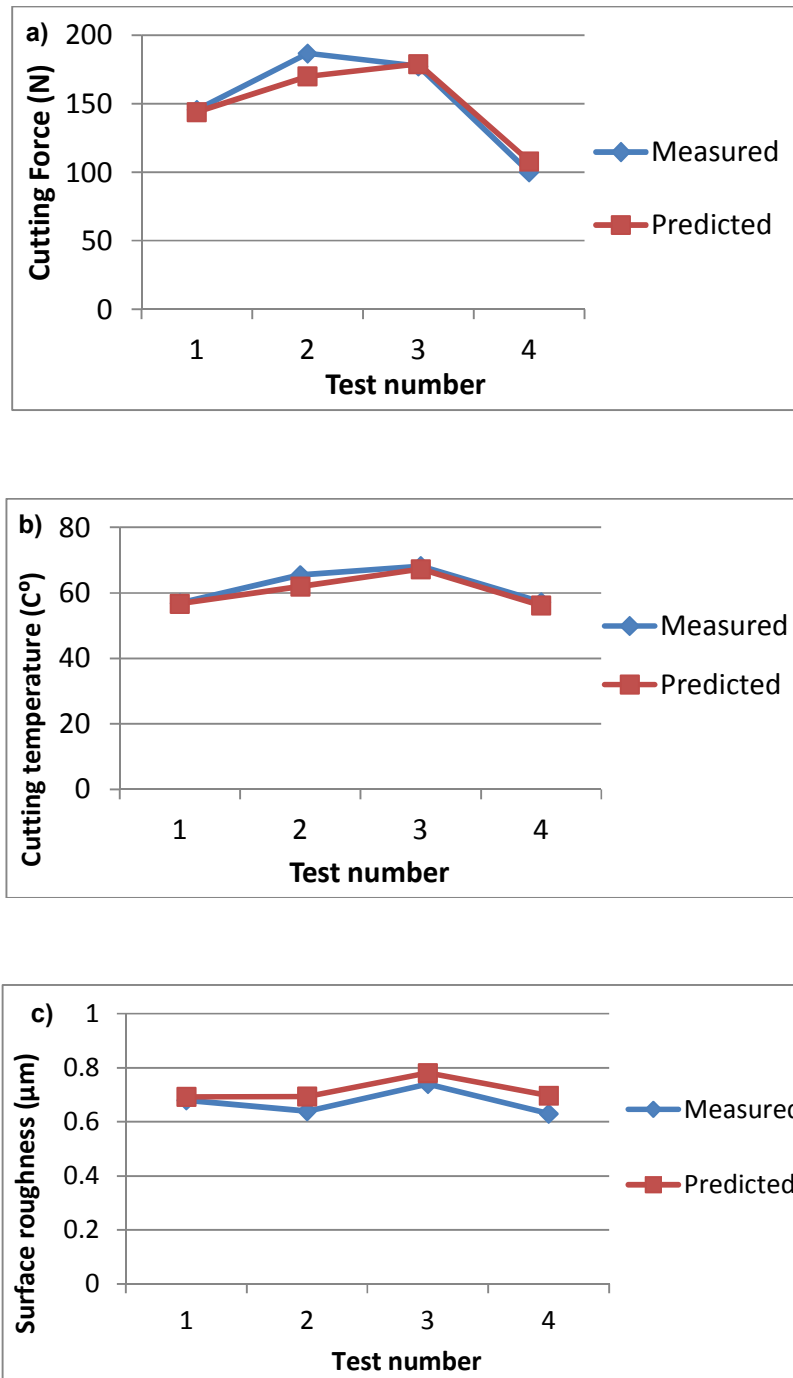


Figure 4.45 Comparison of the predicted and measured values of Al-6061-T6 alloy during milling operation (a) cutting force, (b) cutting temperature and (c) surface roughness

In this study, fuzzy logic based model is used to predict the cutting force, cutting temperature and surface roughness of Al-6061-T6 alloy during milling operation by using SiO₂ nano base lubricant. The result demonstrates very close accuracy between the fuzzy model and experimental results. The model accuracy is found to be 96.195%, 98.27% and

91.37% for cutting force, cutting temperature and surface roughness, respectively. The close agreement of the experimental results and predicted values clearly indicates that the fuzzy model can be used to predict the cutting force, cutting temperature and surface roughness within the range of input parameters.

It is seen from the fuzzy logic approach that extensive dispersion of SiO₂ nanoparticles in cutting oil facilitated by high air pressure reduces the cutting force. Tu-Chieh and Yaw-Terng (Tu-Chieh & Yaw-Terng, 2006) found that interacting force between particles and workpiece reduces the surface energy of the workpiece which means that the binding strength between the surface and sub-surface atoms of workpiece is weakened. Certain amount of energy is required to break the weekend asperities of the workpiece to generate new surface having lower roughness. The nanoparticles transfer potential energy from the tool and then converted into kinetic energy of the surface atoms to dissipate heat (Tu-Chieh & Yaw-Terng, 2006). So, with the increasing the nanoparticles concentration in the nano base lubricant, higher amount of kinetic energy is transferred to the workpiece surface and increase the heat dissipation. The low friction behavior of nanoparticles effectively reduces the frictional effects between the tool-workpiece interfaces and thus reduces cutting force. Presence of the nanoparticles in cutting oil collides with each other and impedes by the asperities and increase the cutting force. Another possible reason is that when the spindle speed is increased, cutting energy from the machining tool imposes compressive stress to the workpiece which increases the tool-chip interface temperatures. The generated heat at the machining zone helps to soften the workpiece material, reducing cutting forces leading to better surface quality. However, it is believed that the spindle speed should be controlled at an optimum value especially for those materials having lower thermal conductivity such as Al-6061-T6. The influence of

temperature significantly affects the chip formation mode, cutting forces, tool life and surface quality of the low conductive material.

Investigating the cutting temperature, the fuzzy logic modeling results is almost similar to the experimental results. In conjunction, nozzle orientation might be an important factor during high speed machining which is not addressed properly in the literatures. From the experiment it is seen that nozzle angle of 15° is optimum. The major contribution of heat in the workpiece material comes from tertiary deformation zone, therefore nozzle orientation at 15° successfully withdraw the heat from the tertiary zone. However, nozzle angle of 30° shows optimum result for surface roughness and chip thickness ratio. This may be attributed from the fact that the lubricant may accelerates better to the cutting zone at this nozzle orientation to obtain better surface quality. Again, as mentioned before, the lubricant has negligible effect on the cutting force and stress in cutting edge, therefore nozzle angle of 60° may not be the optimum for chip thickness ratio. During cutting process, the consumed energy is converted into heat at the deformation zones. The heat generation is increased with increasing the nanoparticles concentration in the lubricant and it may reach to the melting temperature of the workpiece material. Another reason for drastic increasing of temperature might be due to the formation of thin film which refrain the dissipation of heat from the machined surface. The higher temperature softens the workpiece material aiding grain boundary dislocation and hence the cutting force is reduced (Reddy & Rao, 2006; Yousefi & Ichida, 2000). The temperature of some thin layers on the back face of the chip adjacent to rake face of the tool reaches close to melting temperature. Associate with the higher temperature, the strain energy is effected and due to the extreme pressure of additives in cutting oil chemical reaction films are formed on the machined surface (Lin & So, 2004).

As illustrated by the fuzzy logic modeling, the surface roughness is possible to predict by using soft computing techniques. It is seen that the surface roughness decreases initially and then increases drastically when air pressure exceeds 2 bar. The higher air pressure leads to formation of welded surface. This welded surface can act as a peeler which may pull away some of the workpiece material mechanically (Thepsonthi et al., 2009). Again increasing air pressure helps to accelerate the nano base lubricant to penetrate deep inside of the cutting zone to assist the polishing with lower cutting temperature. Due to this reason a protective film is formed which reduces the surface roughness.

For better control and understanding of machining process, the knowledge of cutting force, cutting temperature and surface roughness as a function of machined surface quality has crucial importance. It is not economical to conduct surface quality test for the combination of different factors and parameters. The laboratory experiments consume a lot of time and most of the time is not sufficient for online controls. It is possible to develop a scheme to carry out the control with online learning. This approach would be helpful for predicting the process parameters in real time machining.

4.6.3 Summary

In this study, a fuzzy logic based model was established to predict the cutting force, cutting temperature and surface roughness of Al-6061-T6 alloy during milling operation by using SiO₂ nano base lubricant. The result demonstrates a good agreement between the fuzzy logic approach and experimental results. The fuzzy logic approach shows the accuracy of 96.195%, 98.27% and 91.37% for cutting force, cutting temperature and surface roughness respectively. The close agreement between the model and experimental results clearly indicates that the fuzzy logic approach can be implemented to predict the cutting force, cutting temperature and surface roughness within the range of input parameters during machining.

4.7 $L_{16}(4)^3$ orthogonal array design of experiment in milling with MoS₂ nano base lubricant

4.7.1 Cutting force

The milling of Al6061-T6 alloy was carried out to investigate the machining performance by using the suggested experimental setup. Table 4.36 presents the measured values of cutting force.

Table 4.36 The measured values of cutting force

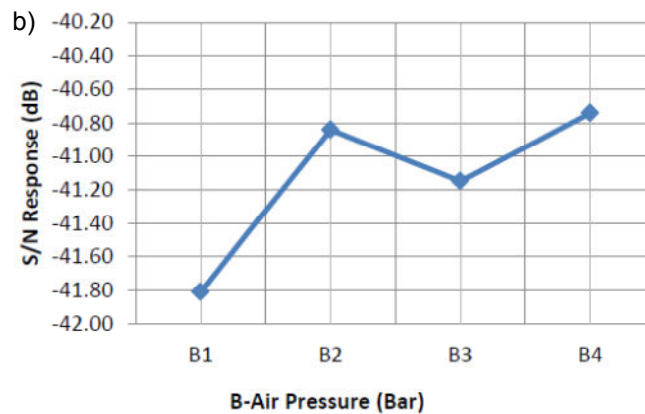
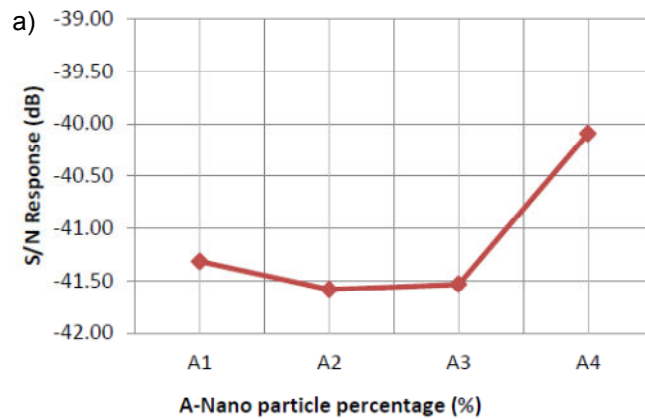
Exp. No.	Measured Values				
	Cutting Force (N)				
	Reading			Average	S/N Ratio (dB)
	1	2	3		
1	126.31	130.08	130.31	128.9	-42.21
2	103.21	116.96	103.73	107.96	-40.68
3	107.56	95.08	111.92	104.85	-40.43
4	130.61	118.94	125.90	125.15	-41.95
5	133.07	124.55	133.80	130.47	-42.31
6	111.66	112.81	106.22	110.23	-40.85
7	139.03	133.67	145.80	139.50	-42.90
8	104.32	106.07	99.50	103.30	-40.28
9	133.92	142.94	118.92	130.93	-42.43
10	113.89	126.95	103.71	114.85	-41.23
11	117.68	130.97	121.19	123.28	-41.83
12	111.15	110.48	101.62	107.75	-40.66
13	101.71	104.75	103.35	103.27	-40.28
14	109.68	101.13	110.38	107.26	-40.60
15	88.37	94.87	97.65	93.63	-39.44
16	99.73	103.68	98.88	100.77	-40.07

To optimize the parameters and to identify the most significant process parameters three types of analysis namely the noise (S/N) response analysis, interaction analysis and analysis of variance (Pareto ANOVA) were used. Additionally, Table 4.37 show the S/N response for cutting force.

Table 4.37 The S/N response data for cutting force

Level of parameter	S/N response data (dB)		
	<i>Ai</i>	<i>Bi</i>	<i>Ci</i>
Level 1	-41.32	-41.81	-41.24
Level 2	-41.59	-40.84	-40.77
Level 3	-41.54	-41.15	-40.94
Level 4	-40.10	-40.74	-41.59
Difference	1.49	1.07	0.82

Figures 4.46 shows the S/N response graphs for selecting the best combination to obtain the lowest cutting forces, cutting temperature and surface roughness respectively. The largest S/N response would reflect the best response which results in the lowest noise. This is the criteria employed to determine the optimal parameters. Based upon the criteria of larger S/N response, it is seen from Figure 4.46 that the nanoparticle concentration of 1 wt% (A4) with the air pressure of 1 bar (B4) and nozzle orientation at 30° angle (C2) are determined to be the best choices for obtaining the lowest cutting force.



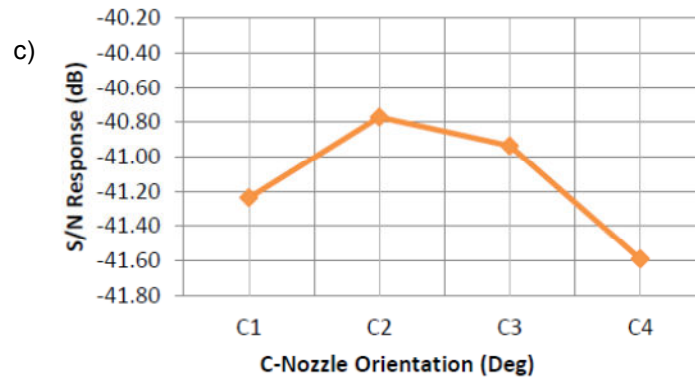


Figure 4.46 S/N response graphs of cutting force for (a) nanoparticles concentration A , (b) air pressure B and (c) nozzle orientation C

As an expression of the relation or association between two or more independent variables, a statistical interaction was defined in quantitative data analysis. This relation or association would be able to predict the effects of each independent variable upon a dependent variable. If an interaction exists, the effect of each independent variable will vary depending upon the other independent variable(s). In this study to optimize the process, the interaction analysis was used as an alternative method of analysis. The cutting force obtained from the S/N ratio data were presented in Table 4.38 It can be seen that $A4$ $B4$ $C2$ are the optimal combination of parameters to obtain the lowest cutting force.

Table 4.38 Interaction data analysis for cutting force

AxB	B1	B2	B3	B4	Total	Highest total response
A1	-42.21	-40.68	-40.43	-41.95	-165.27	
A2	-42.31	-40.85	-42.90	-40.28	-166.35	
A3	-42.43	-41.23	-41.83	-40.66	-166.15	
A4	-40.28	-40.60	-39.44	-40.07	-160.38	A4
Total	-167.23	-163.36	-164.59	-162.96		
Highest total response				B4		
AxC	C1	C2	C3	C4	Total	Highest total response
A1	-42.21	-40.68	-40.43	-41.95	-165.27	
A2	-40.85	-42.31	-40.28	-42.90	-166.35	
A3	-41.83	-40.66	-42.43	-41.23	-166.15	
A4	-40.07	-39.44	-40.60	-40.28	-160.38	A4
Total	-164.95	-163.09	-163.75	-166.36		
Highest total response		C2				
BxC	C1	C2	C3	C4	Total	Highest total response
B1	-42.21	-42.31	-42.43	-40.28	-167.23	
B2	-40.85	-40.68	-40.60	-41.23	-163.36	
B3	-41.83	-39.44	-40.43	-42.90	-164.59	
B4	-40.07	-40.66	-40.28	-41.95	-162.96	B4
Total	-164.95	-163.09	-163.75	-166.36	-162.96	
Highest total response		C2				

The analysis of variance using Pareto ANOVA was used as an alternative method to analyze the data for the optimization process. The Table 4.39 present the data obtained from Pareto ANOVA analysis for cutting force. These data were obtained by using the *S/N* response data from Table 4.37. The cumulative contribution and contribution ratio of all parameters for cutting force was plotted in Figures 4.46.

From Table 4.39 in conjunction with Figure 4.47, it can be seen that the nanoparticle concentration (*A*), air pressure (*B*) and nozzle orientation (*C*) contributes 47.85%, 35.55% and 16.60% respectively for the lowest cutting force. The nanoparticles concentration and air pressure are considered the prominent factors for affecting the cutting force, having a cumulative contribution of 83.40%. The Pareto ANOVA analysis

recommends that the combination of (A4 B4 C2) is the best parameters to achieve the lowest cutting force.

Table 4.39 Pareto ANOVA analysis for cutting force

S/N response data (dB)			
Control factor level (i)	Nanoparticles concentration (A)	Air pressure (B)	Nozzle angle (C)
Level 1	-41.32	-41.81	-41.24
Level 2	-41.59	-40.84	-40.77
Level 3	-41.54	-41.15	-40.94
Level 4	-40.10	-40.74	-41.59
Total Summation	-164.54	-164.54	-164.54
Square of differences (S)	$S_A=2.20$	$S_B=1.63$	$S_C=0.76$
Total summation of squares of differences $S_t=S_A+S_B+S_C$	4.59		
Contribution ratio (%)	47.85	35.55	16.60
Optimum combination	A4	B4	C2
Overall optimum conditions for all actors		A4, B4, C2	

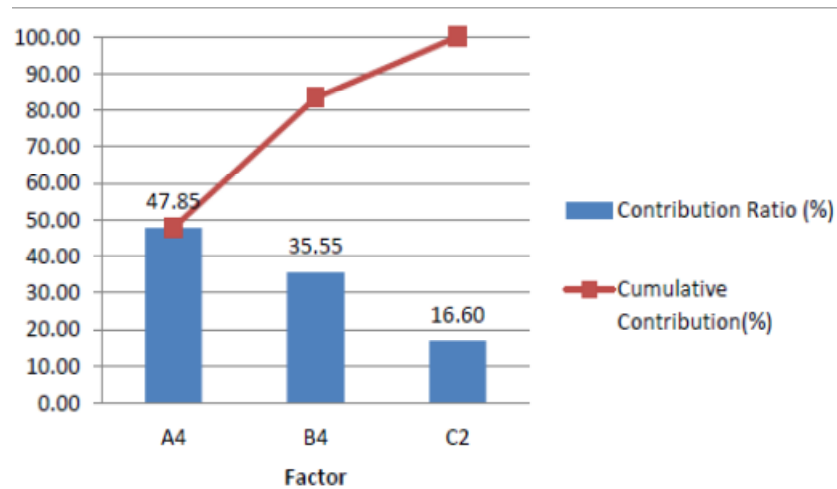


Figure 4.47 The contribution diagram and cumulative contribution for cutting force

In conclusion, the optimal parameters obtained from Pareto ANOVA analysis for lowest cutting force is the combination of A4 B4 C2.

4.7.2 Surface roughness

Table 4.40 presents the measured values of surface roughness. To optimize the parameters and to identify the most significant process parameters three types of analysis namely the noise (S/N) response analysis, interaction analysis and analysis of variance (Pareto ANOVA) were used. Table 4.41 shows the S/N response data for surface roughness.

Table 4.40 The measured values of surface roughness

Exp. No.	Measured Values				
	Surface Roughness(μm)				
	Reading			Average	S/N Ratio (dB)
	1	2	3		
1	2.12	1.92	1.66	1.9	-5.61
2	3.03	4.68	3.25	3.65	-11.42
3	0.36	0.76	0.54	0.55	4.81
4	1.29	0.84	0.89	1.01	-0.24
5	1.17	0.86	0.84	0.96	0.28
6	1.19	1.27	1.19	1.22	-1.71
7	1.13	1.17	1.34	1.21	-1.70
8	0.96	0.97	0.98	0.97	0.26
9	0.90	1.01	0.95	0.95	0.39
10	0.41	0.35	0.41	0.39	8.15
11	1.52	1.48	1.43	1.48	-3.38
12	1.23	1.20	1.03	1.15	-1.26
13	0.77	0.78	1.13	0.89	0.82
14	0.95	0.99	0.91	0.95	0.45
15	1.19	1.10	1.09	1.13	-1.04
16	0.86	0.82	0.76	0.81	1.80

Table 4.41 The S/N response data for surface roughness

Level of parameter	S/N response data (dB)		
	A_i	B_i	C_i
Level 1	-3.11	-1.03	-2.23
Level 2	-0.72	-1.13	-3.36
Level 3	0.98	-0.33	1.48
Level 4	0.51	0.14	1.76
Difference	4.09	1.28	5.12
Rank	2	3	1

On the other hand, it can be seen from Figure 4.48 that the nanoparticle concentration of 0.5 wt% (A3) and air pressure of 4 bars (B4) with the nozzle angle of 60° (C4) are the best choices for obtaining the lowest surface roughness.

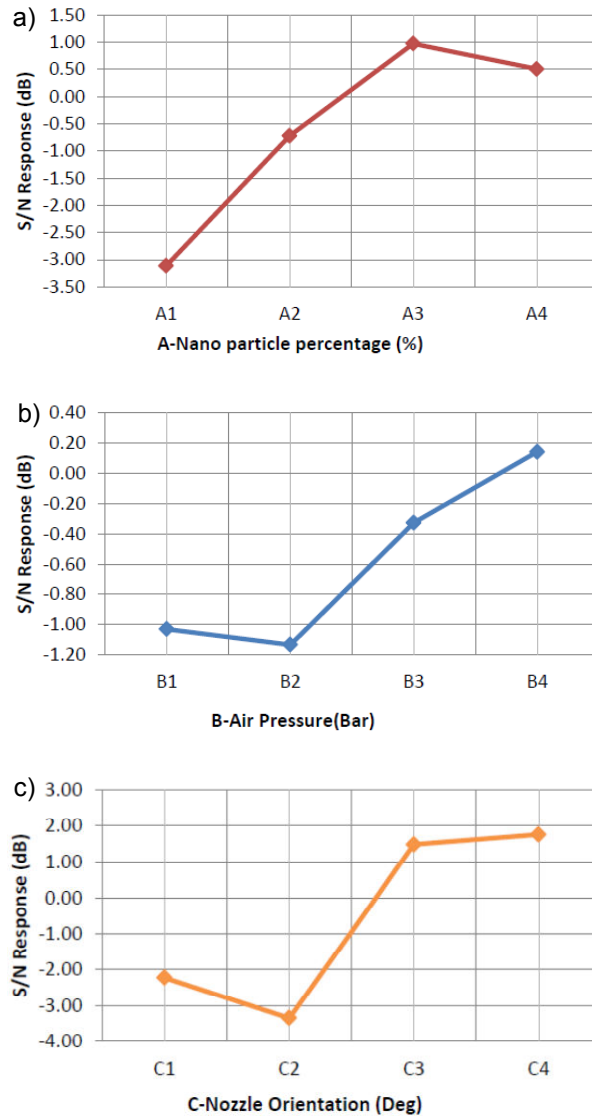


Figure 4.48 S/N response graphs of surface roughness for (a) nanoparticles concentration A , (b) air pressure B and (c) nozzle orientation C

The surface roughness obtained from the S/N ratio data was presented in Table 4.42. It can be seen that $A3$ $B4$ $C4$ are the optimal combination of parameters to obtain the lowest surface roughness.

Table 4.42 Interaction data analysis for surface roughness

AxB	B1	B2	B3	B4	Total	Highest total response
A1	-5.61	-11.42	4.81	-0.24	-12.45	
A2	0.28	-1.71	-1.70	0.26	-2.87	
A3	0.39	8.15	-3.38	-1.26	3.91	A3
A4	0.82	0.45	-1.04	1.80	2.03	
Total	-4.12	-4.53	-1.31	0.57		
Highest total response				B4		
AxC	C1	C2	C3	C4	Total	Highest total response
A1	-5.61	-11.42	4.81	-0.24	-12.45	
A2	-1.71	0.28	0.26	-1.70	-2.87	
A3	-3.38	-1.26	0.39	8.15	3.91	A3
A4	1.80	-1.04	0.45	0.82	2.03	
Total	-8.91	-13.43	5.92	7.03		
Highest total response				C4		
BxC	C1	C2	C3	C4	Total	Highest total response
B1	-5.61	0.28	0.39	0.82	-4.12	
B2	-1.71	-11.42	0.45	8.15	-4.53	
B3	-3.38	-1.04	4.81	-1.70	-1.31	
B4	1.80	-1.26	0.26	-0.24	0.57	B4
Total	-8.91	-13.43	5.92	7.03		
Highest total response				C4		

Lastly from Table 4.43 with Figure 4.49, the best combination for minimum surface roughness are found to be (*A3 B4 C4*). The nanoparticles concentration and nozzle orientation are considered as prominent factors, having a cumulative contribution of 97.9%.

Table 4.43 Pareto ANOVA analysis for surface roughness

S/N response data (dB)			
Control factor level (i)	Nanoparticle concentration (A)	Air pressure (B)	Nozzle angle (C)
Level 1	-3.11	-1.03	-2.23
Level 2	-0.72	-1.13	-3.36
Level 3	0.98	-0.33	1.48
Level 4	0.51	0.14	1.76
Total summation	-2.35	-2.35	-2.35
Square of differences (S)	$S_A=25.56$	$S_B=1.37$	$S_C=38.52$
Total summation of squares of differences $S_T=S_A+S_B+S_C$		65.46	
Contribution ratio (%)	39.05	2.10	58.85
Optimum combination	A3	B4	C4
Overall optimum conditions for all factors		A3, B4, C4	

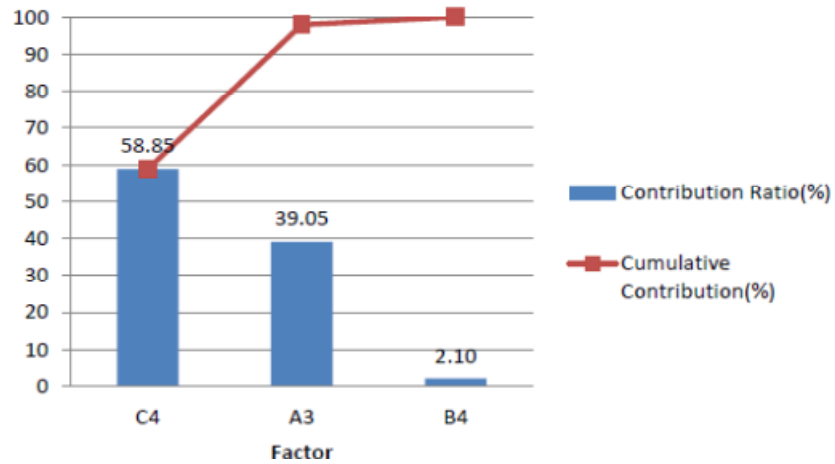


Figure 4.49 The contribution diagram and cumulative contribution for surface roughness

In conclusion, the optimal parameters obtained from Pareto ANOVA analysis for lowest surface roughness is the combination of *A3 B4 C4*.

4.7.3 Cutting temperature

The milling of Al6061-T6 alloy was carried out to investigate the machining performance by using the suggested experimental setup. Table 4.44 presents the measured values of cutting temperature.

Table 4.44 The measured values of cutting temperature

Exp. No.	Measured Values				
	Cutting Temperature (°C)				
	Reading			Average	S/N Ratio (dB)
	1	2	3		
1	34.20	39.00	35.00	36.07	-31.16
2	30.20	31.50	31.50	31.07	-29.85
3	53.50	37.50	37.90	42.97	-32.79
4	36.10	35.50	36.60	36.07	-31.14
5	35.70	38.00	38.20	37.30	-31.44
6	33.00	35.90	35.90	34.93	-30.87
7	36.80	38.10	38.70	37.87	-31.57
8	33.50	34.00	34.20	33.90	-30.60
9	34.20	35.30	34.70	34.73	-30.82
10	39.70	37.40	43.30	40.13	-32.09
11	33.70	35.20	35.20	34.70	-30.81
12	30.00	29.90	31.10	30.33	-29.64
13	33.00	35.40	34.60	34.33	-30.72
14	48.00	52.30	52.50	50.93	-34.15
15	33.80	34.60	35.00	34.47	-30.75
16	33.50	34.50	34.60	34.20	-30.68

To optimize the parameters and to identify the most significant process parameters for cutting temperature three types of analysis namely the noise (*S/N*) response analysis, interaction analysis and analysis of variance (Pareto ANOVA) were used. Table 4.45 shows the *S/N* response data for cutting temperature.

Table 4.45 The *S/N* response data for cutting temperature

Level of parameter	<i>S/N</i> response data (dB)		
	<i>A_i</i>	<i>B_i</i>	<i>C_i</i>
Level 1	-31.23	-31.03	-30.88
Level 2	-31.12	-31.74	-30.42
Level 3	-30.84	-31.48	-32.09
Level 4	-31.57	-30.52	-31.38
Difference	0.74	0.96	1.67
Rank	3	2	1

While, from Figure 4.50, the nanoparticle concentration of 0.5 wt% (A3) with the air pressure of 4 bars (B4) and nozzle orientation at 30° angle (C2) are determined to be the best choices for obtaining the lowest cutting temperature.

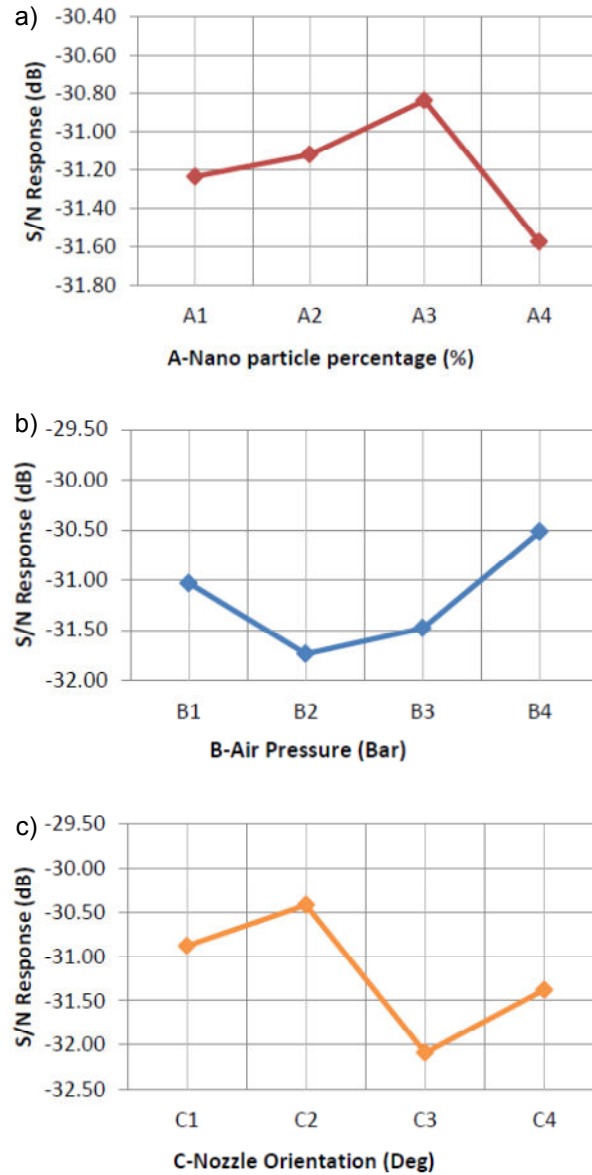


Figure 4.50 *S/N* response graphs of cutting temperature for (a) nanoparticles concentration *A*, (b) air pressure *B* and (c) nozzle orientation *C*

The cutting temperature obtained from the *S/N* ratio data (Table 4.45) was presented in interaction data analysis in Table 4.46. It can be seen that *A3 B4 C2* are the optimal combination of parameters to obtain the lowest cutting temperature.

Table 4.46 Interaction data analysis for cutting temperature

AxB	B1	B2	B3	B4	Total	Highest total response
A1	-31.16	-29.85	-32.79	-31.14	-124.94	
A2	-31.44	-30.87	-31.57	-30.60	-124.48	
A3	-30.82	-32.09	-30.81	-29.64	-123.35	A3
A4	-30.72	-34.15	-30.75	-30.68	-126.30	
Total	-124.13	-126.95	-125.92	-122.07		
Highest total response				B4		
AxC	C1	C2	C3	C4	Total	Highest total response
A1	-31.16	-29.85	-32.79	-31.14	-124.94	
A2	-30.87	-31.44	-30.60	-31.57	-124.48	
A3	-30.81	-29.64	-30.82	-32.09	-123.35	A3
A4	-30.68	-30.75	-34.15	-30.72	-126.30	
Total	-123.52	-121.67	-128.36	-125.51		
Highest total response		C2				
BxC	C1	C2	C3	C4	Total	Highest total response
B1	-31.16	-31.44	-30.82	-30.72	-124.13	
B2	-30.87	-29.85	-34.15	-32.09	-126.95	
B3	-30.81	-30.75	-32.79	-31.57	-125.92	
B4	-30.68	-29.64	-30.60	-31.14	-122.07	B4
Total	-123.52	-121.67	-128.36	-125.51		
Highest total response		C2				

From Table 4.47 in addition with Figure 4.51, it is found that the nozzle orientation (*C*), air pressure (*B*) and nanoparticles concentration (*A*) contributes 66.7% 22.66% and 10.63% respectively for obtaining lowest cutting temperature. The Pareto ANOVA analysis recommends that combination of (*A3 B4 C2*) is the finest parameters to obtain the lowest cutting temperature.

Table 4.47 Pareto ANOVA analysis for cutting temperature

S/N response data (dB)			
Control factor level (i)	Nanoparticles concentration (A)	Air pressure (B)	Nozzle angle (C)
Level 1	-31.23	-31.03	-30.88
Level 2	-31.12	-31.74	-30.42
Level 3	-30.84	-31.48	-32.09
Level 4	-31.57	-30.52	-31.38
Total summation	-124.77	-124.77	-124.77
Square of differences (S)	$S_A=0.79$	$S_B=1.69$	$S_C=4.97$
Total summation of squares of differences $S_t=S_A+S_B+S_C$		7.46	
Contribution ratio (%)	10.63	22.66	66.70
Optimum combination	A3	B4	C2
Overall optimum conditions for all actors		A3, B4, C2	

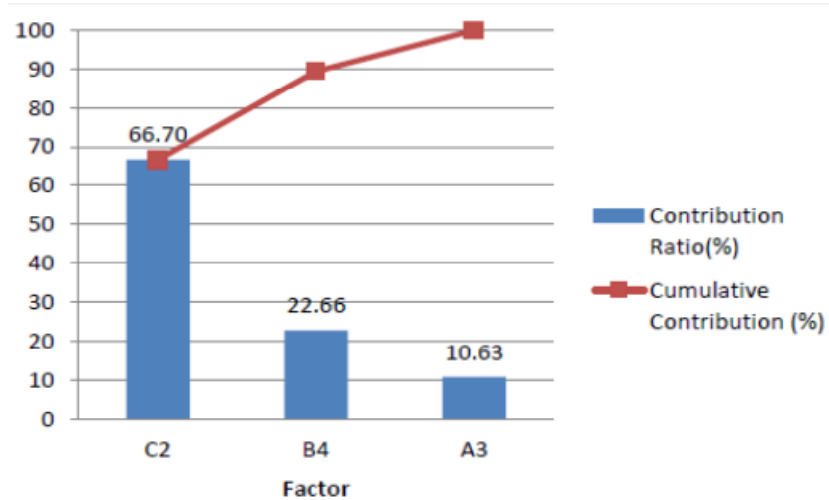


Figure 4.51 The contribution diagram and cumulative of contribution for cutting temperature

In conclusion, the optimal parameters obtained from Pareto ANOVA analysis for lowest cutting temperature is the combination of *A3 B4 C2*. The last stage in the Taguchi optimization method was to conduct a confirmation test by using the optimal parameters of *A4 B4 C2* for cutting force, *A3 B4 C2* for cutting temperature and *A3 B4 C4* for surface roughness. The confirmation test was repeated sixteen times and the average *S/N* ratio of the measured cutting forces, cutting temperature and surface roughness were calculated. The consequence represents the improvement of 2.62%, 0.04% and 2.56% in cutting force,

cutting temperature and surface roughness respectively compared to the values obtained from initial experiments.

In this present study, three techniques were used to investigate the optimal milling parameters of Al6061-T6 alloy by using nano-lubricants. All three processes gave similar results for obtaining optimal parameters. Suspending of MoS₂ nanoparticles in cutting oil facilitated by pressurized air decreases the cutting force, cutting temperature and surface roughness. The gaps between the tool and chip and other surfaces are often filled by only nanoparticles. Present and future applications of cutting require high-speed relative motion, high load, and high duty of cycles. It is known that the surface to volume ratio of nanoparticles are very high and for this reason the surface forces become the dominant forces governing the contact behavior. The atomized spray of nano-lubricant exhibits more efficient feeding into the cutting zone than the flood lubrication method (Liew, 2010). This may be due to splash off of the oil by the rotating cutting tool during flood lubrication, while spray of lubricant adheres at the tool-workpiece interface and thus assist during cutting operation.

The presence of nanoparticles in oil imposes a burnish effect at the tool-workpiece interface. An interacting force is induced at the interface between the particles and tool surface (Zhang et al., 2011). This interacting force travels upon the tool surface with a certain speed and then emits power to the surface. The breaking process of the asperities requires certain amount of energy to break the weekend parts for generating new surface with lower roughness. The nanoparticles transfer the potential energy from tool, and then it is converted into kinetic energy of surface atoms and dissipates heat (Tu-Chieh & Yaw-Terng, 2006). With increasing the nanoparticles concentration in the nano-lubricant, more kinetic energy is transferred to the workpiece surface and increases the heat dissipation.

Due to the low friction properties of nanoparticles, a significant reduction of friction is seen between tool and workpiece and consequently the cutting force is reduced.

Increasing the nanoparticles concentration in the lubricant increases the viscosity of cutting oil and therefore more nanoparticles stays in between the tool and workpiece. This eliminates the contact between tool and workpiece. In high speed machining process, the high generation of heat changes the elastohydrodynamic lubrication into boundary lubrication. The spherical nanoparticles reduce the coefficient of friction of the rubbing surfaces by the rolling effect of nanoparticles (Wu et al., 2007). Increasing the nanoparticles in the lubricant increases the growth of thin protecting film on machined surface, where more nanoparticles rub the asperities during machining and exposes more surfaces to cutting oil. Thus a strong chemical interaction is formed between the nano-lubricant and newly formed surface, and hence more intensive protective film is formed. This process definitely increases the quality of the machined surface by reducing coefficient of friction (Lee et al., 2009).

The consumed energy changes into heat in the deformation zones during the cutting process. The heat generation increases the cutting temperature. With increasing the nanoparticles concentration in the lubricant the cutting temperature can be as high as the melting temperature of the workpiece material. The other reason of drastic increase of temperature might be due to the formation of thin film which refrain the temperature dissipation from the machined surface. It is supposed that increment of temperature softens the material aiding grain boundary dislocation, and hence ease the cutting operation with lower cutting force (Suresh Kumar Reddy & Venkateswara Rao, 2006). During cutting process, pressurizes stream of air facilitates the feeding of nano-lubricant to the cutting zone which affect the formation of protective film (Hirata et al., 2004).

In combination, the nozzle orientation is an important factor during high speed machining operation. For obtaining the lowest cutting temperature, nozzle angle at 30° orientation shows the best result. It is found that nozzle angle at 30° orientation successfully withdraw heat from the workpiece surface. However, nozzle angle at 30° orientation shows the highest surface roughness and chip thickness ratio. This orientation might not be suitable for accelerating the cutting oil to the cutting zone and does not assist in machining to achieve better surface quality. As mentioned before, the cutting oil at tool-chip interface has negligible effect on the cutting force and stress at the cutting edge. Therefore 30° nozzle angle might be the optimum for cutting force. From the Taguchi optimization method and based on the results achieved, the following deductions are prepared:

1. The cutting force is minimized by using nano-lubricants containing 1 wt% of MoS₂ nanoparticles with 4 bars of air stream pressure at 30° nozzle angle.
2. The lowest cutting temperature is achieved by using nano-lubricants containing 0.5 wt% of MoS₂ nanoparticles with 4 bars of air stream pressure at 30° nozzle angle.
3. The best surface roughness is achieved with 0.5 wt% of MoS₂ nanoparticles in oil, 4 bar air pressure and nozzle orientation at 60° angle.

4.7.4 Morphological analysis

The FESEM and X-ray diffraction (XRD) were employed to examine the morphology and phase of the machined surface. Surface cleaning was necessary to remove all undesirable surface particles. To remove minor surface contamination the surface was etched by hot solutions of sodium hydroxide. The remaining surface oxides, which was a combination of inter metallic, metal and metal oxides were removed by using an aqueous solution containing an oxidizing inorganic acid, phosphoric and sulfuric acids, simple and complex fluoride ions, organic carboxylic acid, and manganese in its oxidation state.

4.7.4 (i) FESEM analysis

The FESEM images of the machined surfaces are shown in Figure 4.52 for four different MoS₂ concentrations. The results show that MoS₂ nanoparticles were dispersed at cutting zone by the high pressure of stream air. This technique improved the morphology of the machined surface. The atomized mist of MoS₂ nanoparticles ensured efficient feeding of the nano-lubricant into the cutting zone compared with conventional lubrication method. As it can be seen in Figure 4.52(b-d) that protective thin films were produced on the feed marks of the machined surface which contained billions of MoS₂ nanoparticles. These protective films provided much less friction and thermal deformation compared to the bared surface. The formation of thin film was increased when the concentration of MoS₂ nanoparticles was increased from 0.2 wt% to 0.5 wt%. However, further increase of the concentration up to 1.0 wt% lead less protective films compared to 0.5 wt% concentrations. This result is totally in agreement with the results for lowest surface roughness obtained at 0.5 wt% of MoS₂ nanoparticles. However, when the nanoparticles concentration was increased to 1 wt% the surface quality was declined.

The increment of nanoparticles concentration in the lubricant increased the viscosity of cutting oil. In this case, more nanoparticles were existed in between the tool-workpiece

interface and these nanoparticles served as spacers, which eliminate the friction between the tool and workpiece. The nanoparticles suspended lubricants have filler and polisher effect. Because of these effects nano-lubricant results the best surface finishes. Moreover, it was also proposed that the nanoparticles may roll like micro-spheres at the tool-workpiece interface which leads to the reduction of the frictional coefficient (Liu et al., 2004). The appearance and specifications of the nanoparticles such as the size, shape and concentration are the factors that control the frictional behaviors. It is worthy to note that the size of nanoparticles was in the range of 2–60 nm. Smaller nanoparticles are more effective to reduce the friction by forming protective film at the surface.

Other researchers showed that in thin film contacts, colloidal nanoparticles penetrate into the elastohydrodynamic contacts by a mechanism of mechanical entrapment (Wu et al., 2007). The high contact resistance in addition with extreme pressure at the cutting zone induces the formation of chemical reaction layer on the workpiece surface. The generation of large amount of heats at the cutting zone changes the elastohydrodynamic lubrication to boundary lubrication. This phenomenon results the formation of thin protective films on the surfaces as it can be seen in Figure 4.52.

It is believed that nanoparticles deposited on the friction surface and compensate for the loss of mass, which is called “mending effect” (Liu et al., 2004). Due to the porous nature of spherical MoS₂ nanoparticles, it could impart high elasticity, which augments their resilience in a specific loading range and enhances the gap at the tool-workpiece interface (Zhang et al., 2011). When nano base lubricant is dispersed at cutting zone, some particles embedded into the machined surfaces during machining process. Some particles have rolling effect and some particles are sheared due to very high pressure at cutting zone. The shape of the nanoparticles was changed due to high compression as it is shown in Figure 4.53. With increasing the concentration of MoS₂ nanoparticles the degree of shape

changing and shearing was increased. Also some of the nanoparticles were partially ejected by other nanoparticles that left the nozzle into the cutting zone. Consequently, nanoparticles can be supplied to the contact spots without being broken. The plough off nanoparticles left thin exfoliated film on its contact spot due to damage from high loading (Rapoport et al., 2005).

However, when nanoparticle concentrations continued to increase up to 1.0 wt%, the surface finish was reduced compared to 0.5wt% concentrations. Nanoparticles were impregnated into the pore of the surface with increasing the nanoparticles. These nanoparticles were then sheared by other incoming nanoparticles and more plough off particles left on the thin exfoliated film. Therefore, the 1.0 wt% concentration provided less surface quality compared to 0.5 wt% concentrations. Consequently, the concentration of 0.5 wt% provided the best machined surface morphology when the nano-lubricant was used during machining process. The machining of AL6061-T6 alloy with nano-lubricants containing 0.5 wt% of MoS₂ improved the surface roughness of 3.87% compared with the pure oil in ordinary machining process. For additional investigation, the substrate surface was analyzed by X-ray diffraction (XRD) as it is shown in Figure 4.54.

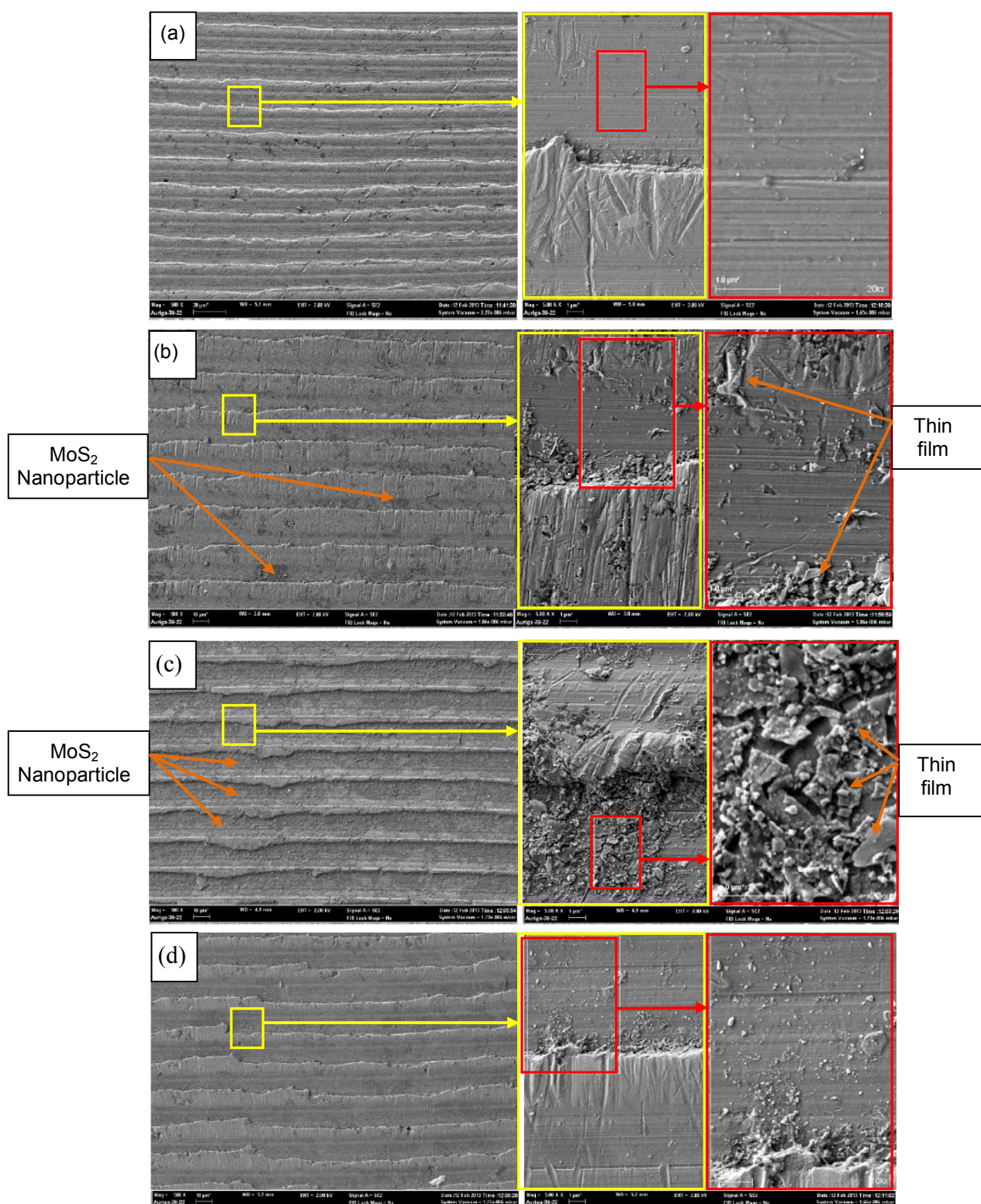


Figure 4.52 FESEM on samples (a), (b), (c) and (d) which machined with 0, 0.2, 0.5 and 1.0 wt% concentration of MoS₂ respectively

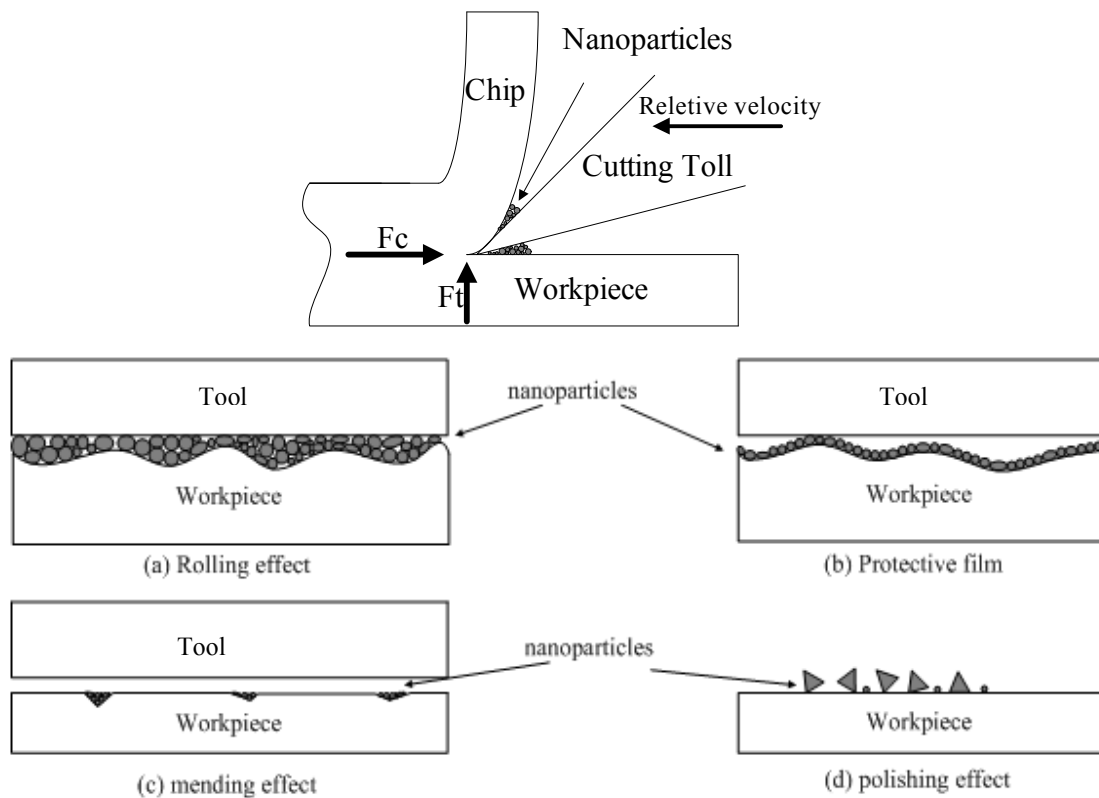


Figure 4.53 The presence of nanoparticle reduce the tool-workpiece in contact

4.7.4 (ii) XRD analysis

The XRD analysis (Figure 4.54) showed the existence of 1.1, 3.3 and 0.5 wt% of MoS_2 nanoparticles on the machined surface when the workpiece was milled by nano-lubricants containing 0.2, 0.5 and 1 wt% MoS_2 respectively. These results fully support the results obtained from the FESEM as the highest percentage of the residual MoS_2 was obtained from the workpiece that was milled by nano-lubricants containing 0.5 wt% MoS_2 nanoparticles. It is also seen that when nanoparticles concentrations was continued to increase up to 1.0 wt%, the residual content of MoS_2 is lowest.

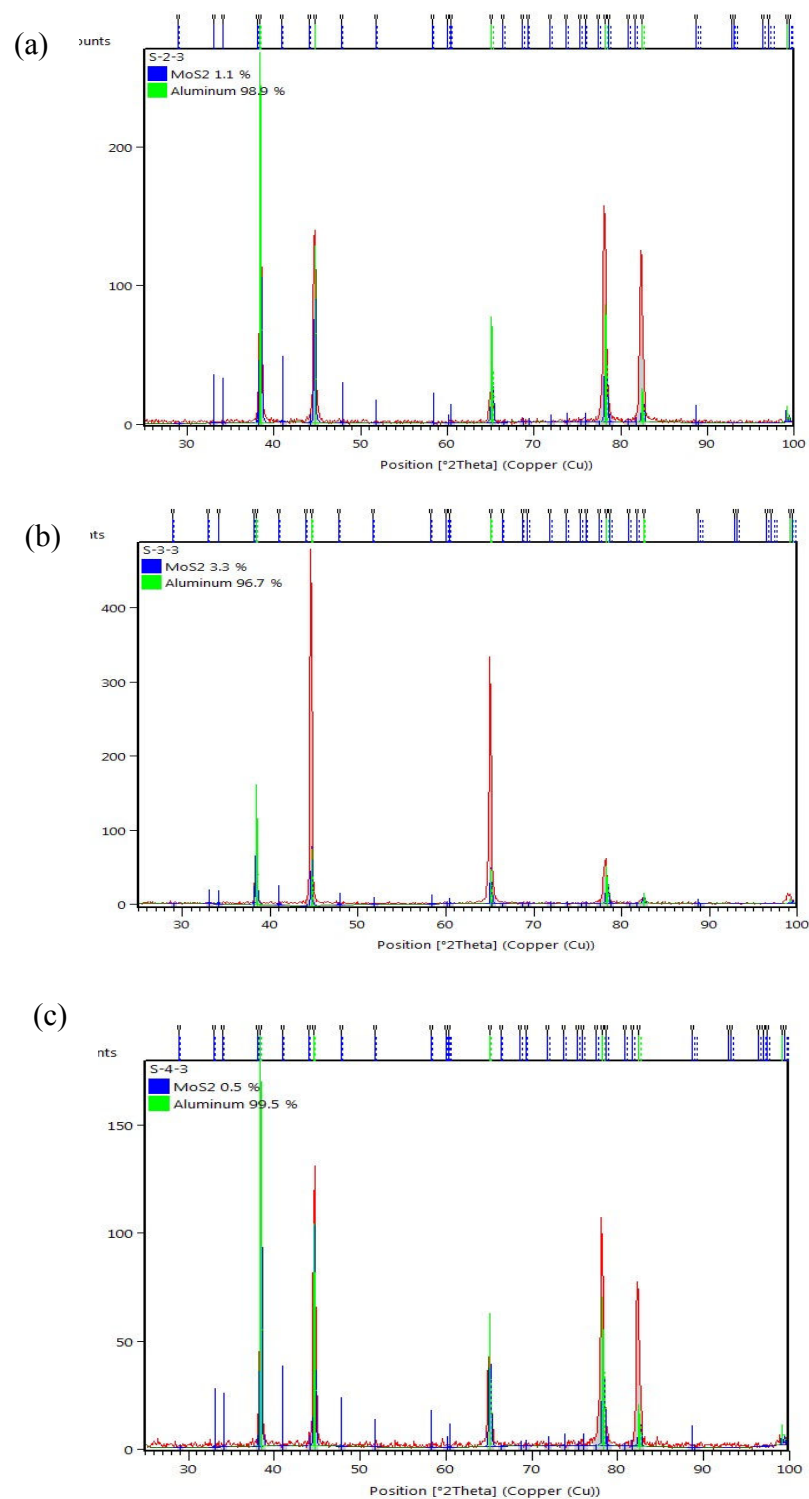


Figure 4.54 X-ray Diffraction (XRD) on samples (a), (b) and (c) under machining with 0.2, 0.5 and 1 wt % concentration of MoS₂ nanoparticles ,respectively

From the results, the existence of MoS₂ nanoparticles between the tool-workpiece interfaces improved the quality of machined surface. The MoS₂ nanoparticles impart their effects by rolling, filling and polishing action at the tool-workpiece interfaces. Finally, it can be conclude that MoS₂ suspended nano-lubricant is an excellent alternative for achieving the perfect surface quality.

4.8 Reduction in cutting force and surface roughness of Al-2017-T4 alloy by using carbon onion nano base lubricant

4.8.1 Introduction

The carbon onion nanoparticles were mixed with ordinary mineral oil at different concentration to investigate the cutting force and the surface roughness of Al-2017-T4 alloy during machining in CNC end milling. From the results it is seen that the cutting force and surface roughness are reduced by 21.99% and 46.32% respectively by using carbon onion nano base lubricant. This could be attributed from the tribological properties of the carbon onion which can reduce the coefficient of friction at the tool-chip interface during machining.

4.8.2 Data analysis and discussions

The slot-milling test was carried out to investigate the cutting force and the surface quality of Duralumin (Al-2017-T4) after machining with nano base lubricant containing carbon onion. Figure 4.55 (a-d) and Figure 4.56 (a-d) show the cutting forces and surface roughness for machining Al-2017-T4 alloy by using nano base lubricants containing different concentration of carbon onion. The average cutting force and surface roughness of the Al-2017-T4 alloy machined by nano base lubricants containing different concentration of carbon onion is summarized in Table 4.48.

Table 4.48 The average cutting force and surface roughness of Al-2017-T4 alloy machined by carbon onion nano base lubricant

Modes of lubrications	Carbon onions concentration	Cutting force (N)	Surface roughness R_a (μm)
Mode 1	0 wt%	53.51	0.380
Mode 2	0.5 wt%	46.58	0.324
Mode 3	1.0 wt%	43.64	0.248
Mode 4	1.5 wt%	41.74	0.204

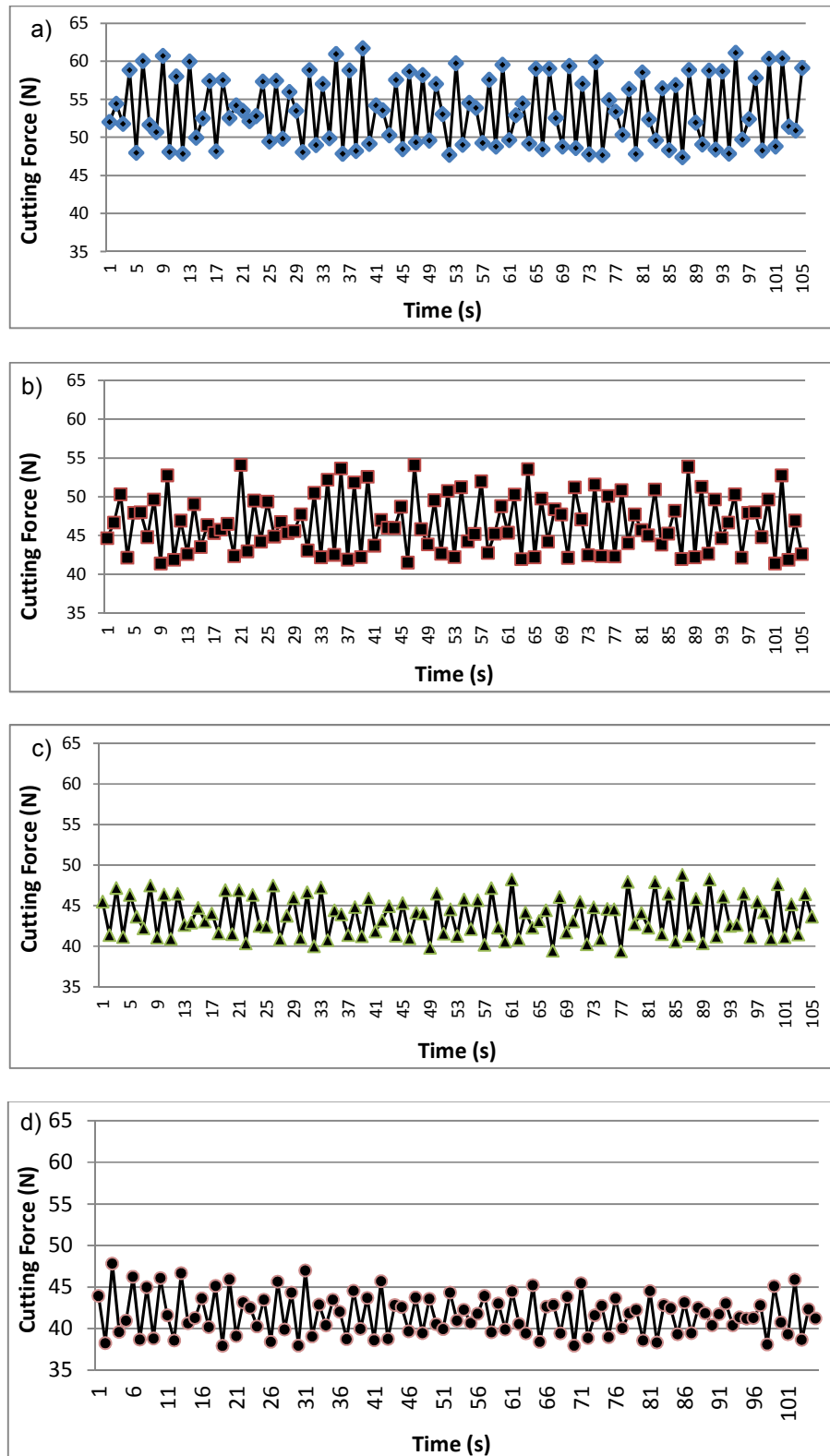
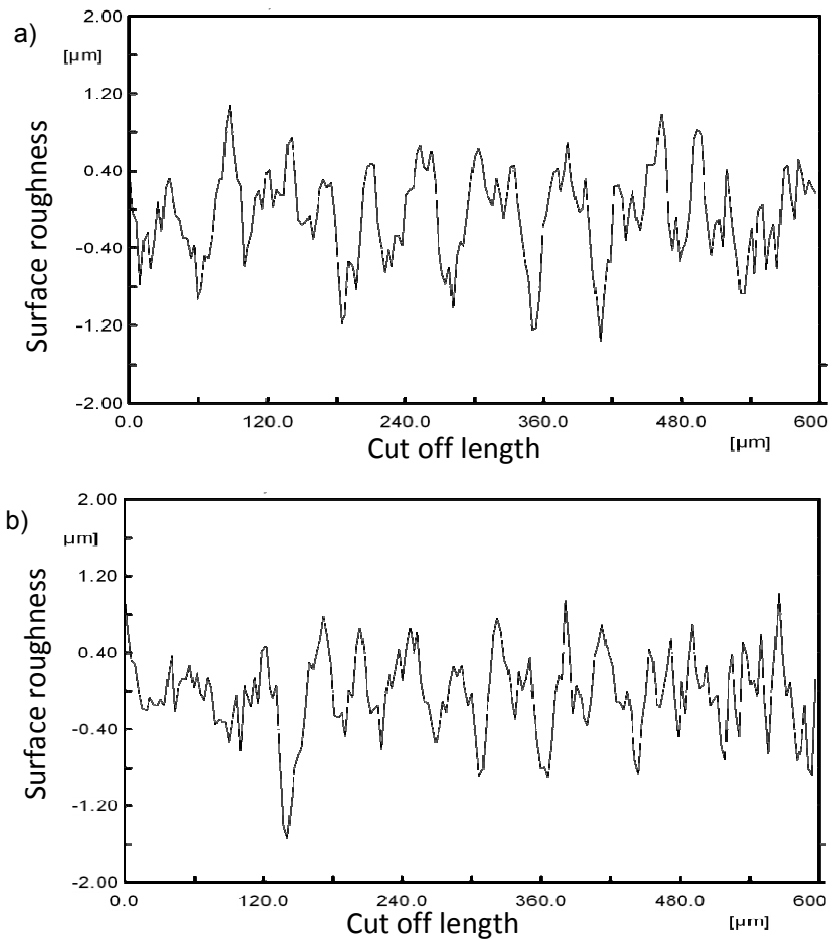


Figure 4.55 Cutting force of the Al-2017-T4 alloy machined nano base lubricants containing carbon onion (a) 0 wt%, (b) 0.5 wt%, (c) 1.0 wt% and (d) 1.5 wt%

The cutting force and surface roughness were examined for milling operations by using nano base lubricants containing carbon onion nanoparticles. The results from the experimentations require several analyses to ensure:

1. The surface quality is improved by using carbon onion nano base lubricant during machining process.
2. The cutting force, surface roughness, power consumption and oil consumption is reduced by implementing nano base lubricants containing carbon onion nanoparticles.



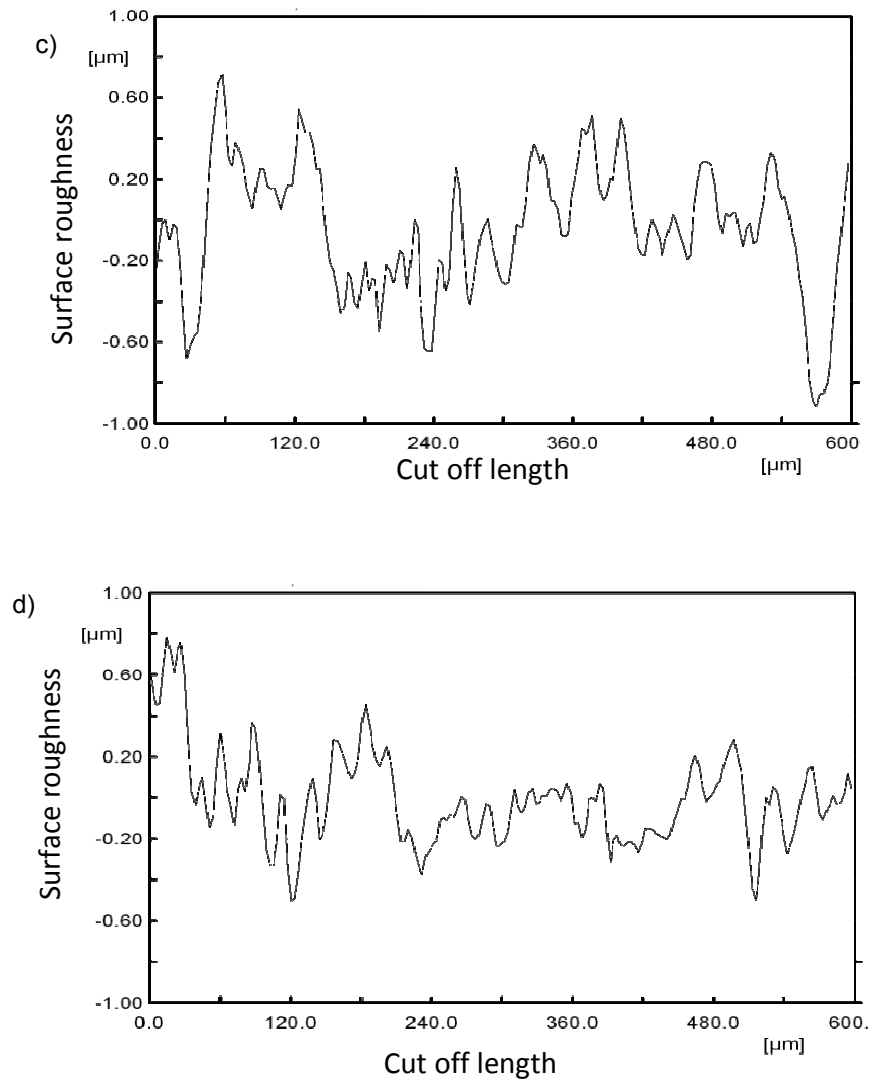


Figure 4.56 Surface roughness of the Al-2017-T4 alloy machined nano base lubricants containing carbon onion (a) 0 wt%, (b) 0.5 wt%, (c) 1.0 wt% and (d) 1.5 wt%

Carbon onion nanoparticles were mixed with ordinary mineral oil at different concentrations in order to investigate the cutting force and surface roughness during CNC end milling of Al-2017-T4 alloy. Figure 4.57 presents the cutting forces and surface roughness at different concentration of carbon onion nanoparticles in the base lubricant. As it can be seen from Figure 4.57, the lowest cutting force and surface roughness are obtained at the highest concentration of carbon onion nanoparticles (1.5 wt%) in the lubricant. In addition, reduction in the cutting force and surface roughness are found to be 21.99% and 46.32% respectively compared with ordinary lubrication system. These results are

supported by the Figure 4.58 (a-d) where stereoscopic three dimensional photographs of machined surface are shown for different modes of carbon onion concentration. It is clearly seen that the lowest surface roughness is obtained at the highest concentration of carbon onion nanoparticles (1.5 wt%) in the lubricant.

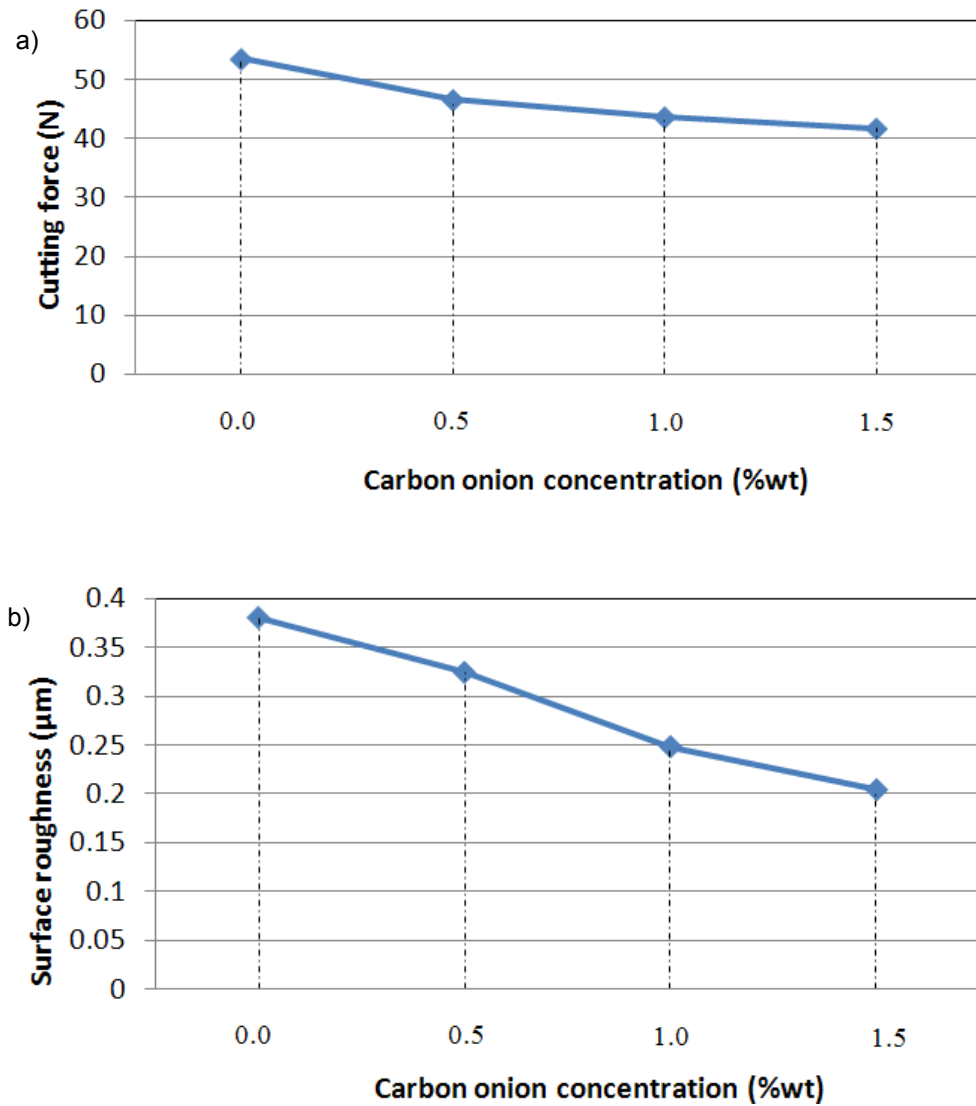
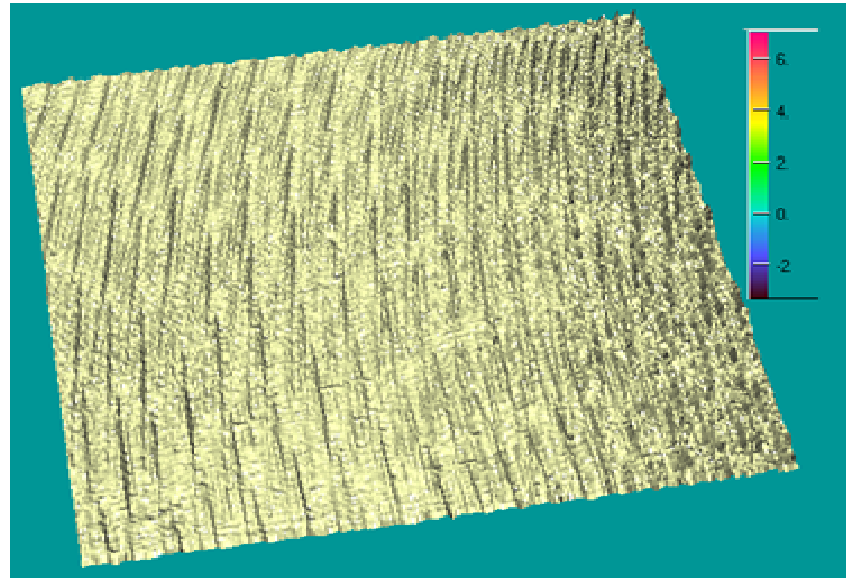
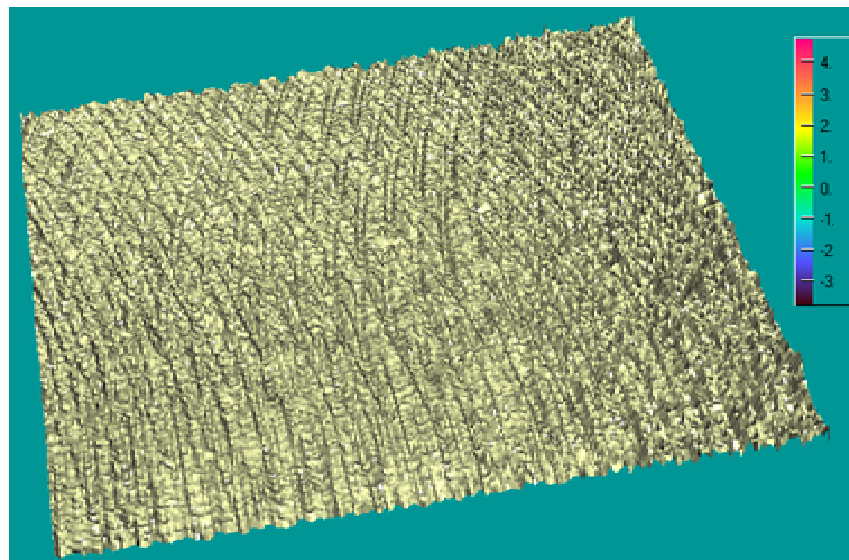


Figure 4.57 Effects of carbon onion nanoparticles in the lubricant during CNC end milling of Al-2017-T4 alloy (a) cutting force and (b) surface roughness

a)



b)



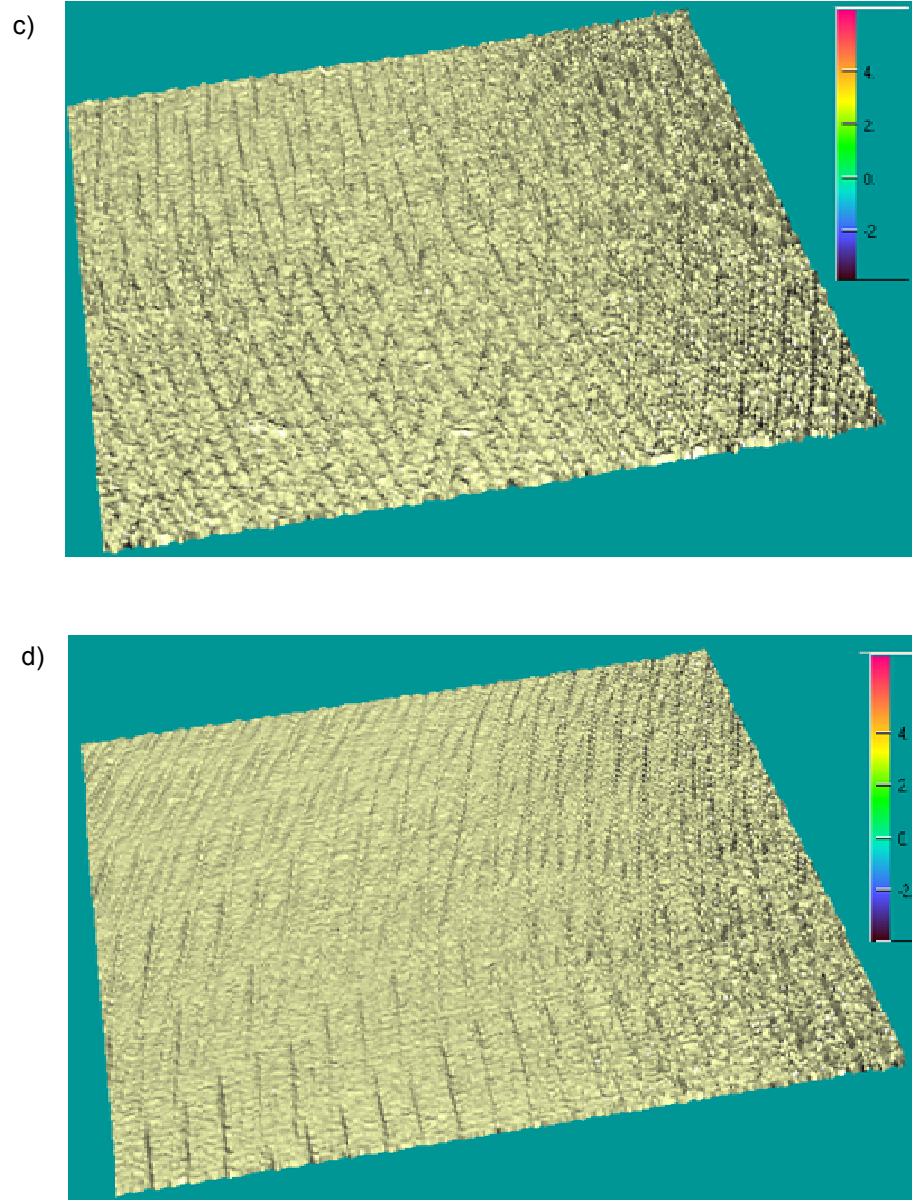


Figure 4.58 Stereoscopic three dimensional photographs of the Al-2017-T4 alloy surface during CNC end milling by using nano base lubricant containing carbon onion of (a) 0 wt%, (b) 0.5 wt%, (c) 1.0 wt% and (d) 1.5 wt%

4.8.3 Summary

In this study, the cutting force and surface roughness of Al-2017-T4 alloy is investigated during CNC end milling. Based on the results obtained, the highest concentration of carbon onion (1.5 wt%) results the lowest cutting force and best surface quality. In addition, the cutting force and surface roughness are found to be reduced by

21.99% and 46.32% respectively with the presence of optimum carbon onion in the lubrication system. The results are attributed from the tribological properties of the carbon onion which act as billions of quasi-spherical nanostructure rolling elements at the tool-chip interface. Consequently, the coefficient of friction at tool-chip interface is reduced significantly by the use of nano base lubricants containing carbon onion.

4.6 Discussions

Introducing carbon onion nano base lubricant to the machining system results less friction at the tool-chip interface with better surface quality. This phenomenon is mainly attributed from the tribological properties of carbon onion nano base lubricant. The outermost shell of the carbon onion nanoparticles scarcely contains defects as no dangling bonds exist on the surface when carbon atoms are perfectly arranged. Beside this, carbon onion nano base lubricant reduces the coefficient of friction which reduces the tool wear and cutting temperature as well.

Friction and wear of cutting tools plays significant roles during machining process. The complexity of a machining process makes it difficult to systematically analyze the friction and wear at the tool-chip interface (Weinert et al., 2004). Certainly, when the coefficient of friction is greater than 0.5, the sticky friction and flow occurs only within the workpiece, not at the tool-workpiece interface. Consequently, the thickness of the deformed chip is increased, leading to a decrease in cutting ratio and shear angle with an increase in shear length. Hence, the force and power required to remove the chip increases significantly, as it is shown in Figure 4.59 (Trent & Wright, 2000).

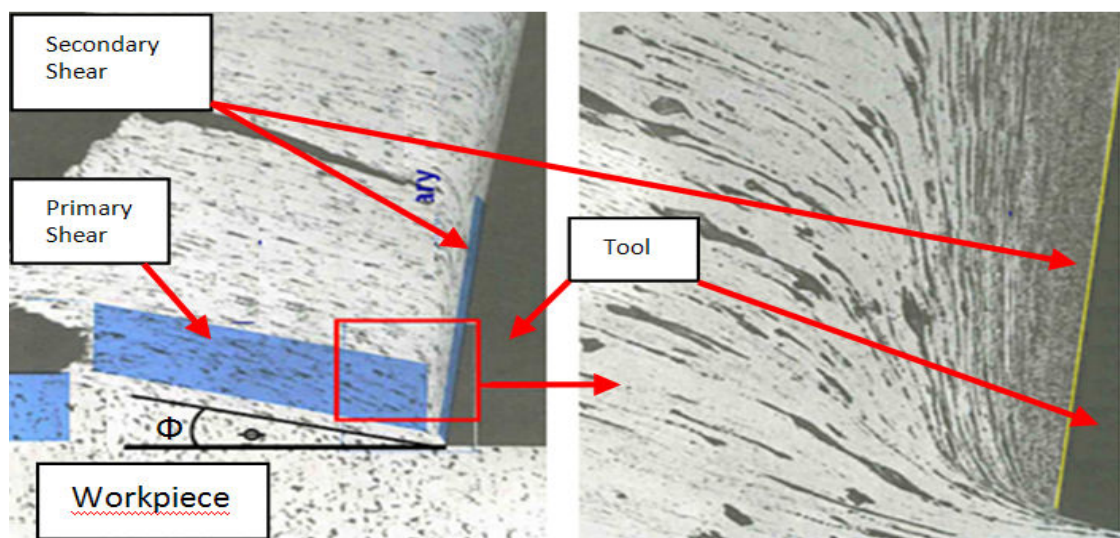


Figure 4.59 Primary and secondary shear zone

In other words, coefficient of friction greater than 0.5 results higher frictional force component F_f , leading to sticky friction. At this stage the chip flow occurs within the workpiece but not at the tool-workpiece interface as shown in the merchant circle presented in Figure 4.60. Consequently, the deformed chip thickness is increased, thus decreasing the cutting ratio and shear angle Φ with increasing the shear length. Hence, the cutting force component F_c is required to remove the chip (Sarhan & Matsubara, 2011). Furthermore, at higher plastic deformation, the chips are welded with the tool face which effectively changes the tool geometry and rake steepness. This results poor surface finish since the bits of the welded chip is broken off and sticks to the workpiece. These bits are problematic due to their inherent work-hardening properties.

Machining results reveal that coefficient of friction is reduced at the tool-chip interface by using nano base lubricants containing SiO_2 , MoS_2 and carbon onion nanoparticles. Reduction of coefficient of friction results lower cutting force. Due to tool wear an increment in cutting force (F_c) and friction force (F_f) is normally observed as presented from Merchant circle as in the Figure 4.60 (Alabi et al., 2010).

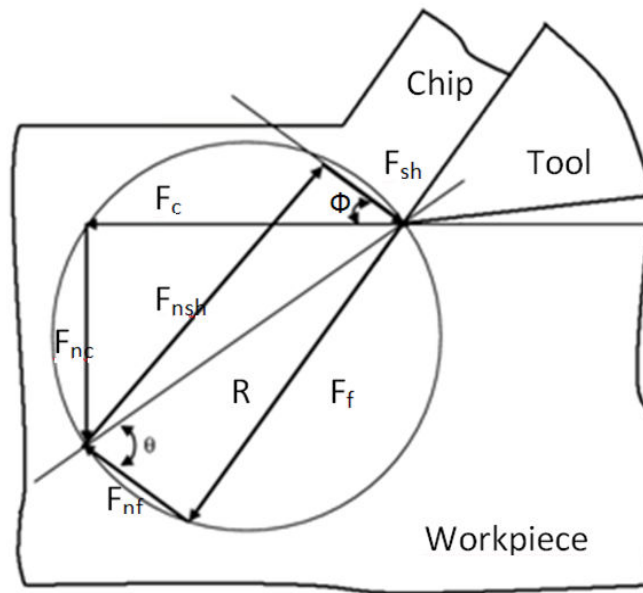


Figure 4.60 Merchant circle of cutting mechanism

Similarly, the deformation of the chip creates a localized region of intense shear due to the friction at the rake face which is known as secondary shear as it is presented in Figure 4.61-4.63.

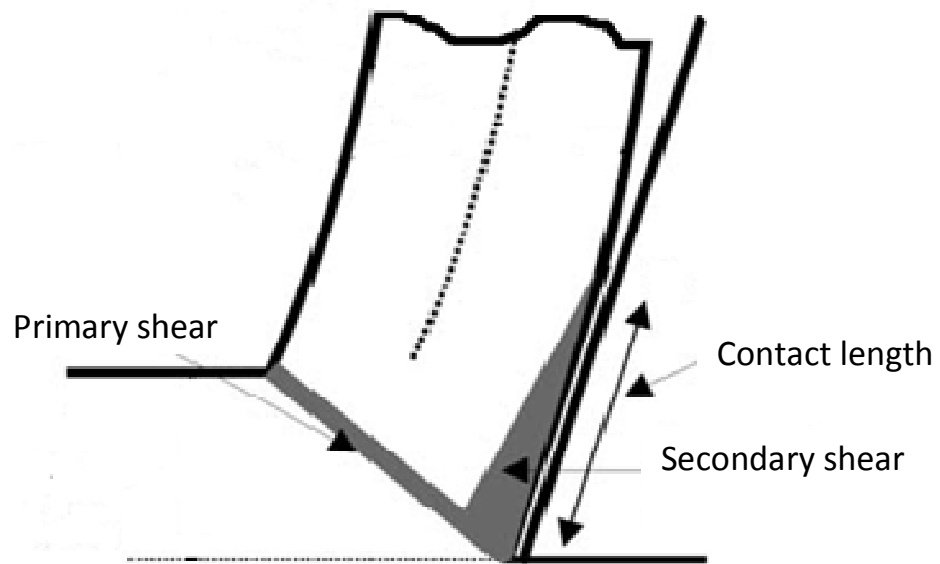


Figure 4.61 Shear zones distribution metal cutting process

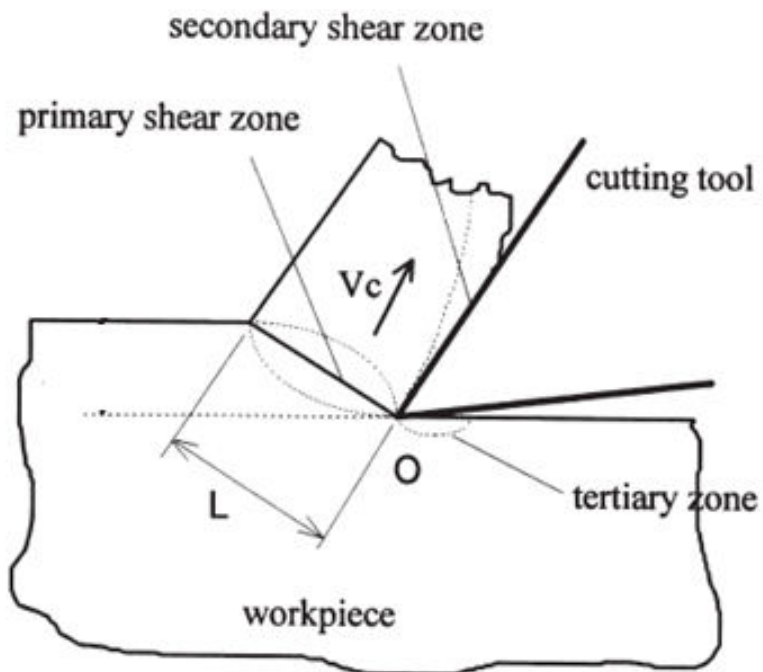


Figure 4.62 Shear zones area in metal cutting process

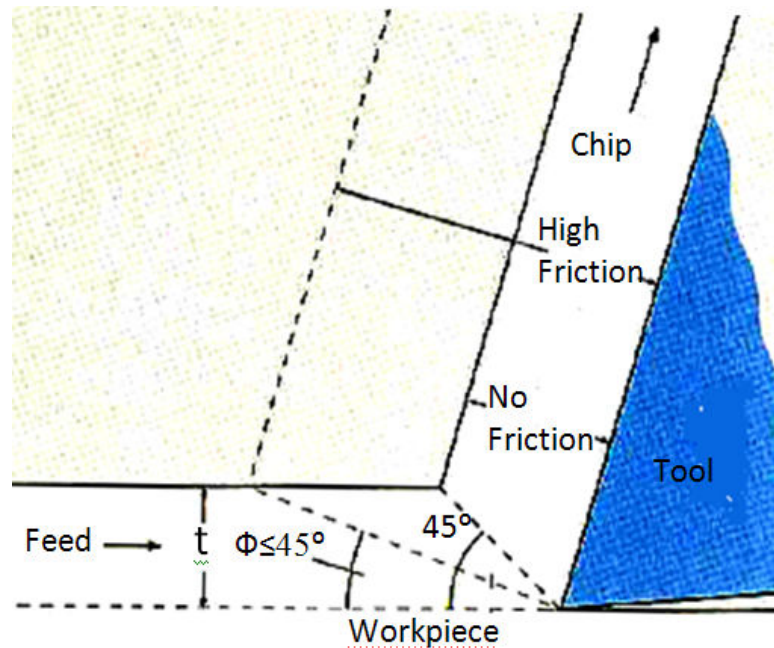


Figure 4.63 Friction in cutting mechanism

The friction force at the tool-chip interface normally increases due to tool wear which leads to an increment in cutting force and friction force (F_c) component. It is worthy to note that, by adopting the nano base lubricant at the tool-chip interface, the coefficient of friction can be reduced. For this reason, nano base lubrication is capable to reduce the cutting force with less power consumption. Nanoparticles in the mineral oil impart their effect by the combined action of rolling and sliding bearings at the tool chip interface. The rolling and sliding action of the nanoparticles reduces the coefficient of friction significantly. Therefore, the cutting force of the workpiece is reduced by the use of nano base lubricant. The reduction of cutting force leads to a reduction of specific energy and power consumption during the machining process. However, introducing the SiO_2 , MoS_2 and carbon onion nano base lubricant provides much less friction and superior surface quality due to the tribological properties of these nanoparticles as it is illustrated in Figure 4.64.

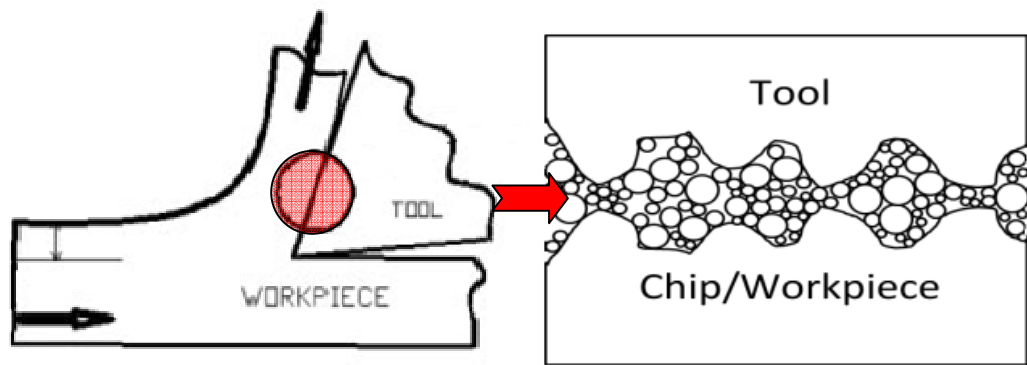


Figure 4.64 Rolling and sliding action of the nanoparticles at the tool-chip interface

Additionally, the findings for the lowest cutting forces are similar to the findings of better surface roughness. Hence, the observation further supports that the proposed nano base lubricant for lowest cutting force is capable to show good machining performances. Additionally, it is believed that the temperature at the cutting zone diminishes as well, resulting lower tool wear and consequently improves the surface quality. A higher concentration of nanoparticles has detrimental effects because more and more nanoparticles transfer kinetic energy to the workpiece surface and dissipate more heat. The low friction behavior of the nanoparticles is effective to minimize the frictional effects at the tool-workpiece interface and reducing cutting force.

CHAPTER 5 CONCLUSIONS AND FUTURE WORKS

5.1 Conclusions

In this research, SiO₂, MoS₂ and carbon onion nano-based lubricants for the metal cutting operation were successfully produced and developed. Several machining tests were carried out as a case study on the cutting process. Based on the results obtained, the following conclusions can be derived:

1. With the $L_{16}(4)^4$ orthogonal array experimental design for machining parameter optimization in the hard turning process, the improvement values of power consumption, surface roughness, chip thickness and cutting temperature obtained were 10.48%, 8.52%, 8.22% and 10.55%, respectively, compared to the minimum values attained from the initial experiments.
2. It appears that by implementing the $L_{16}(4)^3$ orthogonal array experimental design in the hard turning process with SiO₂ nano-based lubricant, the power consumption was reduced by 37.19% as opposed to an ordinary lubrication system. By using the Fuzzy logic approach, the surface roughness and tool wear seemed to be diminished by 23% and 15% when applying SiO₂ nano-based lubricant to the hard turning process compared with regular lubrication.
3. The implementation of the $L_{16}(4)^3$ orthogonal array experimental design with SiO₂ nano-based lubricant for the milling process diminished cutting force, surface roughness and cutting temperature by 25.02%, 26.28% and 29.34% respectively, compared with an ordinary lubrication system. A morphological analysis indicates that the presence of SiO₂ nanoparticles in the tool-workpiece interface enhances the surface finish due to the rolling action and impregnation with nanoparticles.

4. The $L_{16}(4)^3$ orthogonal array experimental design was carried out with MoS_2 nano-based lubricant to investigate the effect of various types of nano-based lubricant on the milling process. The results signify 2.62%, 2.56% and 0.04% improvement in cutting force, surface roughness and cutting temperature respectively, over the smallest values obtained from the initial experiments. Morphologically, the presence of MoS_2 nanoparticles in the tool-workpiece interfaces enhanced the machined surface quality. MoS_2 nanoparticles impart their effects by the actions of rolling, filling and polishing at the tool-workpiece interfaces.
5. The application of carbon onion nano-based lubricant in the milling process to attain performance improvement was investigated owing to its tribological properties. According to the results, cutting force and surface roughness seemed to be reduced by 21.99% and 46.32% respectively, in the presence of optimum carbon onion in the lubrication system compared with ordinary lubrication.

5.2 Future works

The future works should be focused on:

1. To improve the suspension of nanoparticles in the nano base lubricant system so it can be used for longer time.
2. To investigation the effect of the size of nanoparticles during machining process-To investigate the effects of; the amount of nano particles, their size, continuous homogeneity in oil and the method of applying lubricants in machining process.
3. To investigate the effects of cost, environmental and other technical aspects when analyzing the optimal nano lubricant for various machining processes.
4. To investigate the effects of nano lubricants on reduction of frictional heat (reduction of heat generated due to friction), work piece and tool temperature.

REFERENCES

- Alabi, A. G. F., Ajiboye, T. K., & Olusegun, H. D. (2010). Investigating the cutting forces in heat treated medium carbon steel when turning on a lathe machine. *Journal of Engineering, Design and Technology*, Vol. 8(No. 1), pp. 80-93.
- Alberts, M., Kalaitzidou, K., & Melkote, S. (2009). An investigation of graphite nanoplatelets as lubricant in grinding. *International Journal of Machine Tools & Manufacture*, 49, 966-970.
- Aoyama, T. (2002). Development of a Mixture Supply System for Machining with Minimal Quantity Lubrication. *CIRP Annals - Manufacturing Technology*, 51(1), 289-292. doi: [http://dx.doi.org/10.1016/S0007-8506\(07\)61519-4](http://dx.doi.org/10.1016/S0007-8506(07)61519-4)
- Attanasio, A., Gelfi, M., Giardini, C., & Remino, C. (2006). Minimal quantity lubrication in turning: Effect on tool wear. *Wear*, 260 333-338.
- Bartarya, G., & Choudhury, S. K. (2012). State of the art in hard turning. *International Journal of Machine Tools and Manufacture*, 53(1), 1-14. doi: <http://dx.doi.org/10.1016/j.ijmachtools.2011.08.019>
- Benga, G. C., & Abrao, A. M. (2003). Turning of hardened 100Cr6 bearing steel with ceramic and PCBN cutting tools. *Journal of Materials Processing Technology*, 143–144(0), 237-241. doi: [http://dx.doi.org/10.1016/S0924-0136\(03\)00346-7](http://dx.doi.org/10.1016/S0924-0136(03)00346-7)
- Bhaduri, D., Kumar, R., Jain, A. K., & Chattopadhyay, A. K. (2010). On tribological behaviour and application of TiN and MoS₂-Ti composite coating for enhancing performance of monolayer cBN grinding wheel. *Wear*, 268, 1053-1065.
- Bouacha, K., Yallese, M. A., Mabrouki, T., & Rigal, J.-F. (2010). Statistical analysis of surface roughness and cutting forces using response surface methodology in hard turning of AISI 52100 bearing steel with CBN tool. *International Journal of Refractory Metals and Hard Materials*, 28(3), 349-361. doi: <http://dx.doi.org/10.1016/j.jirmhm.2009.11.011>
- Budak, E. (2006). Analytical models for high performance milling. Part 1: Cutting forces, structural deformations and tolerance integrity. *International Journal of Machine Tools & Manufacture*, 46(1478-1488).
- Chandrasekaran, M., Muralidhar, M., Krishna, C., & Dixit, U. (2010). Application of soft computing techniques in machining performance prediction and optimization: a literature review. *The International Journal of Advanced Manufacturing Technology*, 46(5), 445-464. doi: 10.1007/s00170-009-2104-x
- Chang, L., Zhang, Z., Zhang, H., & Schlarb, A. K. (2006). On the sliding wear of nanoparticle filled polyamide 66 composites. *Composites Science and Technology*, 66, 3188-3198.
- Choi, Y., & Liu, C. R. (2009). Performance of nano/micro CBN particle coated tools in superfinish hard machining. *International Journal of Machine Tools & Manufacture* 49.
- Damera, N. R., & Pasam, V. K. (2008). Performance Profiling of Boric Acid as Lubricant in Machining. *J. of the Braz. Soc. of Mech. Sci. & Eng.*, Vol. XXX(No. 3).
- Demas, N., Timofeeva, E., Routbort, J., & Fenske, G. (2012). Tribological Effects of BN and MoS₂ Nanoparticles Added to Polyalphaolefin Oil in Piston Skirt/Cylinder Liner Tests. *Tribology Letters* 47(1), 91-102. doi: 10.1007/s11249-012-9965-0
- Deng, J., Cao, T., Yang, X., & Liu, J. (2006). Self lubrication of sintered ceramic tools with CaF₂ addition in dry cutting. *International Journal of Machine Tool & Manufacture*, 46(9), 957-963.

- Deshmukh, S. D., & Basu, S. K. (2006). *Significance of solid lubricants in metal cutting*. Paper presented at the 22nd AIMTDR.
- Dhar, N. R., Ahmed, M. T., & Islam, S. (2007). An experimental investigation on effect of minimum quantity lubrication in machining AISI 1040 steel. *International Journal of Machine Tools & Manufacture*, 47, 748-753.
- Dilbag, S., & Rao, P. V. (2008). Performance improvement of hard turning with solid lubricants. *Int J Adv Manuf Technol* 38, 529-535.
- Diniz, A. E., & Micaroni, R. (2002). Cutting conditions for finish turning process aiming: the use of dry cutting. *International Journal of Machine Tools and Manufacture*, 42(8), 899-904. doi: [http://dx.doi.org/10.1016/S0890-6955\(02\)00028-7](http://dx.doi.org/10.1016/S0890-6955(02)00028-7)
- Dixit, U. S., Sarma, D. K., & Davim, J. P. (2012). *Machining with Minimal Cutting Fluid Environmentally Friendly Machining* (pp. 9-17): Springer US.
- Ebrahimi, A., & Moshksar, M. M. (2009). Evaluation of machinability in turning of microalloyed and quenched-tempered steels: Tool wear, statistical analysis, chip morphology. *Journal of Materials Processing Technology*, 209(2), 910-921. doi: <http://dx.doi.org/10.1016/j.jmatprotec.2008.02.067>
- Erdemir, A. (1991). Tribological properties of boric acid and boric-acid-forming surfaces: part I, crystal chemistry and mechanism of self lubrication of boric acid", . *Lubricant Engineering*, 47, 168-178.
- Erdemir, A., eryilmaz, O. L., & Fenske, G. R. (1999). Self-replenishing solid lubricant films on boron carbide. *Surface Engineering*, 15(4), 291-295.
- Erdemir, A., Fenske, G. R., Erck, R. A., Nicholas, F. A., & Bush, D. E. (1991). Tribological properties of boric acid and boric-acid-forming surfaces. Part II, mechanisms of formation and self-lubrication films on boron and boric oxide-containing surfaces. *Lubr. Eng*, 47, 179-183.
- Erdemir, A., Halter, M., & Fenske, G. R. (1997). Preparation of ultra low-friction surface films on vanadium diboride. *Wear*, 205, 236-239.
- Fratila, D. (2009). Evaluation of near-dry machining effects on gear milling process efficiency. *Journal of Cleaner Production*, 17(9), 839-845. doi: <http://dx.doi.org/10.1016/j.jclepro.2008.12.010>
- Ghani, J. A., Choudhury, I. A., & Hassan, H. H. (2004). Application of Taguchi method in the optimization of end milling parameters. *Journal of Materials Processing Technology*, 145(1), 84-92. doi: [http://dx.doi.org/10.1016/S0924-0136\(03\)00865-3](http://dx.doi.org/10.1016/S0924-0136(03)00865-3)
- Ginzburg, B. M., Shibaev, L. A., Kireenko, O. F., Shepelevskii, A. A., Baidakova, M. V., & Sitnikova, A. A. (2002). Antiwear effect of fullerene C60 additives to lubricating oils. *Russ. J. Appl. Chem.*, 75(8), 1330-1335.
- Gopal, A. V., & Rao, P. V. (2004). Performance improvement of grinding in SiC using graphite as a solid lubricant. *Materials and manufacturing processes*, 19(2), 177-186.
- Greenberg, R., Halperin, G., Etsion, I., & Tenne, R. (2003). The effect of WS₂ nanoparticles on friction reduction in various lubrication regimes. *Tribology Letters*, 17(2), 179-186.
- Guleryuz, C. G., Krzanowski, J. E., Veldhuis, S. C., & Fox-Rabinovich, G. S. (2009). Machining performance of TiN coatings incorporating indium as a solid lubricant. *Surface & Coatings Technology* 203, 3370-3376.
- Hadad, M. J. (2010). *Minimum Quantity Lubrication-MQL in grinding: Process & Investigation of Surface Quality*. Tarbiat Modares University, Tehran, Iran.
- Hamdan, A., Sarhan, A. A. D., & Hamdi, M. (2011). An Optimization Method of the Machining Parameters in High Speed Machining of Stainless Steel Using Coated

- Carbide Tool for Best Surface Finish. *The International Journal of Advanced Manufacturing Technology*, 58(Issue 1), 81-91. doi: DOI: 10.1007/s00170-011-3392-5
- Hashmi, K., Graham, I. D., & Mills, B. (2003). Data selection for turning carbon steel using a fuzzy logic approach. *Journal of Materials Processing Technology* 135(1), 44-58. doi: [http://dx.doi.org/10.1016/S0924-0136\(02\)01011-7](http://dx.doi.org/10.1016/S0924-0136(02)01011-7)
- He, H.-B., Li, H.-Y., Xu, Z.-Z., Kim, D., & Lyu, S.-K. (2010). Effect of MoS₂-based composite coatings on tribological behavior and efficiency of gear. *International Journal of Precision Engineering and Manufacturing*, 11(6), 937-943. doi: 10.1007/s12541-010-0114-0
- Hirata, A., Igarashi, M., & Kaito, T. (2004). Study on solid lubricant properties of carbon onions produced by heat treatment of diamond clusters or particles. *Tribology International*, 37, 899-905.
- Hsiao, Y. F., Tarng, Y. S., & Huang, W. J. (2008). Optimization of Plasma Arc Welding Parameters by Using the Taguchi Method with the Grey Relational Analysis. *Materials and Manufacturing Processes*, 23(1), 51 - 58.
- Hu, K., Huang, F., Hu, X., Xu, Y., & Zhou, Y. (2011). Synergistic Effect of Nano-MoS₂ and Anatase Nano-TiO₂ on the Lubrication Properties of MoS₂/TiO₂ Nano-Clusters. *Tribology Letters* 43(1), 77-87. doi: 10.1007/s11249-011-9789-3
- Hwang, Y., Park, H. S., Lee, J. K., & b, W. H. J. (2006). Thermal conductivity and lubrication characteristics of nanofluids. *Current Applied Physics* 6S1, e67-e71.
- Jaya, A. S. M., Hashim, S. Z. M., & Rahman, M. N. A. (2010, Nov. 29 2010-Dec. 1 2010). *Fuzzy logic-based for predicting roughness performance of TiAlN coating*. Paper presented at the Intelligent Systems Design and Applications (ISDA), 2010 10th International Conference on.
- Jha, A. K., Prasad, S. V., & Upadhyaya, G. S. (1989). Dry sliding wear of sintered 6061 aluminium alloy— graphite particle composites. [doi: 10.1016/0301-679X(89)90147-3]. *Tribology International*, 22(5), 321-327.
- Jianxin, D., Lili, L., Xuefeng, Y., Jianhua, L., Junlong, S., & Jinlong, Z. (2007). Self-lubrication of Al₂O₃/TiC/CaF₂ ceramic composites in sliding wear tests and in machining processes. *Materials & Design*, 28 757-764.
- JX, D., TK, C., & ZL, D. (2006). Tribological behaviors of hot-pressed Al₂O₃/TiC ceramic composites with addition of CaF₂ solid lubricants. *Journal of the European Ceramic society*, 26(8).
- Kalita, P., Malshe, A. P., Arun Kumar, S., Yoganath, V. G., & Gurumurthy, T. (2012). Study of specific energy and friction coefficient in minimum quantity lubrication grinding using oil-based nanolubricants. *Journal of Manufacturing Processes*, 14(2), 160-166. doi: <http://dx.doi.org/10.1016/j.jmapro.2012.01.001>
- Kalita, P., Malshe, A. P., & Rajurkar, K. P. (2012). Study of tribo-chemical lubricant film formation during application of nanolubricants in minimum quantity lubrication (MQL) grinding. *CIRP Annals - Manufacturing Technology*, 61(1), 327-330. doi: <http://dx.doi.org/10.1016/j.cirp.2012.03.031>
- Kao, M.-J., & Lin, C.-R. (2009). Evaluating the role of spherical titanium oxide nanoparticles in reducing friction between two pieces of cast iron. *Journal of Alloys and Compounds* 483(1-2), 456-459. doi: <http://dx.doi.org/10.1016/j.jallcom.2008.07.223>
- Kelly, J. F., & Cotterell, M. G. (2002). Minimal lubrication machining of aluminium alloys. *Journal of Materials Processing Technology*, 120, 327-334.

- Khettabi, R., Fatmi, L., Masounave, J., & Songmene, V. (2013). On the micro and nanoparticle emission during machining of titanium and aluminum alloys. *CIRP Journal of Manufacturing Science and Technology* 6(3), 175-180. doi: <http://dx.doi.org/10.1016/j.cirpj.2013.04.001>
- Krajnik, P., Pusavec, F., & Rashid, A. (2011). Nanofluids: Properties, Applications and Sustainability Aspects in Materials Processing Technologies. In G. Seliger, M. M. K. Khraisheh & I. S. Jawahir (Eds.), *Advances in Sustainable Manufacturing* (pp. 107-113): Springer Berlin Heidelberg.
- Krishna, P. V., & Rao, D. N. (2008). Performance evaluation of solid lubricants in terms of machining parameters in turning. *International Journal of Machine Tools & Manufacture*, 48, 1131-1137.
- Krishna, P. V., Rao, D. N., & Srikant, R. R. (2009). Predictive modelling of surface roughness and tool wear in solid lubricant assisted turning of AISI 1040 steel. *Technical Note, Proc. IMechE J. Engineering Tribology*, 223, 929-934.
- Kwangho Lee, Yujin Hwang, Seongir Cheong, Youngmin Choi, Laeun Kwon, Jaekeun Lee, & Kim, S. H. (2009). Understanding the role of nanoparticles in Nano-oil Lubrication. *Tribol Lett*, 35, 127-131.
- Lathkar, G. S., & Bas, U. S. K. (2000). *Clean metal cutting process using solid lubricants*,. Paper presented at the proceeding of the 19th AIMTDR Conference.
- Lee, C.-G., Hwang, Y.-J., Choi, Y.-M., Lee, J.-K., Choi, C., & Oh, J.-M. (2009). A study on the tribological characteristics of graphite nano lubricants. *International Journal of Precision Engineering and Manufacturing*, 10(1), 85-90. doi: 10.1007/s12541-009-0013-4
- Lee, J., Cho, S., Hwang, Y., Cho, H.-J., Lee, C., Choi, Y., . . . Kim, S. H. (2009). Application of fullerene-added nano-oil for lubrication enhancement in friction surfaces. *Tribology International*, 42, 440-447.
- Lee, K., Hwang, Y., Cheong, S., Choi, Y., Kwon, L., Lee, J., & Kim, S. (2009). Understanding the Role of Nanoparticles in Nano-oil Lubrication. *Tribology Letters* 35(2), 127-131. doi: 10.1007/s11249-009-9441-7
- Lee, K., Hwang, Y., Cheong, S., Choi, Y., Kwon, L., Lee, J., & Kim, S. H. (2009). Understanding the Role of Nanoparticles in Nano-oil Lubrication. *Tribol Lett*, 35(127-131).
- Leung, R. W. K., Lau, H. C. W., & Kwong, C. K. (2003). An expert system to support the optimization of ion plating process: an OLAP-based fuzzy-cum-GA approach. *Expert Systems with Applications* 25(3), 313-330. doi: [http://dx.doi.org/10.1016/S0957-4174\(03\)00071-X](http://dx.doi.org/10.1016/S0957-4174(03)00071-X)
- Li, C. H., & Peterson, G. P. (2007). Mixing effect on the enhancement of the effective thermal conductivity of nanoparticle suspensions (nanofluids). *International Journal of Heat and Mass Transfer*, 50, 4668-4677.
- Liew, W. Y. H. (2010). Low-speed milling of stainless steel with TiAlN single-layer and TiAlN/AlCrN nano-multilayer coated carbide tools under different lubrication conditions. *Wear*, 268, 617-631.
- Lin, Y. C., & So, H. (2004). Limitations on use of ZDDP as an antiwear additive in boundary lubrication. *Tribology International*, 37, 25-33.
- Lin, Y. C., & So, H. (2004). Limitations on use of ZDDP as an antiwear additive in boundary lubrication. *Tribology International* 37(1), 25-33. doi: [http://dx.doi.org/10.1016/S0301-679X\(03\)00111-7](http://dx.doi.org/10.1016/S0301-679X(03)00111-7)

- Liu, G., Li, X., Qin, B., Xing, D., Guo, Y., & Fan, R. (2004). Investigation of the mending effect and mechanism of copper nano-particles on a tribologically stressed surface. *Tribol. Left*, 17(4), 961-966.
- Mukhopadhyay, D., Banerjee, S., & Reddy, N. S. K. (2007). Investigation to study the application of solid lubricant in turning AISI 1040 steel. *Transaction of the ASME Journal of Manufacturing Science and Engineering*, 129, 520-526.
- Nageswara Rao, D., & Vamsi Krishna, P. (2008). The influence of solid lubricant particle size on machining parameters in turning. [doi: DOI: 10.1016/j.ijmachtools.2007.07.007]. *International Journal of Machine Tools and Manufacture*, 48(1), 107-111.
- Nakamura, T., Tanaka, S., Hayakawa, K., & Fukai, Y. (2000). A study of the lubrication behavior of solid lubricants in the upsetting process. *Journal Tribology* 122, 803-808.
- Nasir., A. (1998). *General comments on ecological and dry machining*. Paper presented at the In Network Proceedings "Technical Solutions to Decrease Consumption of Cutting Fluids," Sobotin-Sumperk, Czech Republic.
- Oktem, H., Erzurumlu, T., & Erzincanli, F. (2006). Prediction of minimum surface roughness in end milling mold parts using neural network and genetic algorithm. [doi: 10.1016/j.matdes.2005.01.010]. *Materials & Design*, 27(9), 735-744.
- Peng, D. X., Kang, Y., Hwang, R. M., Shyr, S. S., & Chang, Y. P. (2009). Tribological properties of diamond and SiO₂ nanoparticles added in paraffin. *Tribology International*, 42, 911-917.
- Prabhu, S., & Vinayagam, B. (2012). AFM investigation in grinding process with nanofluids using Taguchi analysis. *The International Journal of Advanced Manufacturing Technology*, 60(1-4), 149-160. doi: 10.1007/s00170-011-3599-5
- Prado, R. A., Murr, L. E., Shindo, D. J., & Soto, K. F. (2001). Tool wear in the friction-stir welding of aluminium alloy 6061 + 20% Al₂O₃: a preliminary study. *Scripta Materialia*, 45, 75-80.
- Prihandana, G. S., Mahardika, M., Hamdi, M., Wong, Y. S., & Mitsui, K. (2009). Effect of micro-powder suspension and ultrasonic vibration of dielectric fluid in micro-EDM processes - Taguchi Approach. *International Journal of Machine Tool & Manufacture*, 49, 1035-1041.
- Pusavec, F., Hamdi, H., Kopac, J., & Jawahir, I. S. (2011). Surface integrity in cryogenic machining of nickel based alloy—Inconel 718. *Journal of Materials Processing Technology*, 211(4), 773-783. doi: <http://dx.doi.org/10.1016/j.jmatprotec.2010.12.013>
- Qiu, S., Zhou, Z., Dong, J., & Chen, G. (2001). Preparation of Ni nanoparticles and evaluation of their tribological performance as potential additives in oils. *J. Tribol.*, 123, 441-443.
- Rahman, M., Kumar, A. S., & Salam, M. U. (2002). Experimental evaluation on the effect of minimal quantities of lubricant in milling. *International Journal of Machine Tools & Manufacture*, 42, 539-547.
- Rao, D. N., & Srikant, R. R. (2006). Influence of emulsifier content on cutting fluid properties. *Proceedings of the IMechE Part B: Journal of Engineering Manufacture*, 220, 1803-1806.
- Rapoport, L., Leshchinsky, V., Lvovsky, M., Nepomnyashchy, O., Volovik, Y., & Tenne, R. (2002). Mechanism of friction of fullerenes. *Industrial Lubrication and Tribology*, 54, 171-176.

- Rapoport, L., Leshchinsky, V., Lvovsky, M., Nepomnyashchy, O., Volovik, Y., & Tenne, R. (2002). Mechanism of friction of fullerenes. *Industrial Lubrication and Tribology*, 54(2002), 171-176.
- Rapoport, L., Leshchinsky, V., M. Lvovskya, I. L., Volovik, Y., Feldman, Y., Popovitz-Biro, R., & Tenne, R. (2003). Superior tribological properties of powder materials with solid lubricant nanoparticles. *Wear*, 255, 794-800.
- Rapoport, L., Nepomnyashchy, O., Lapsker, I., Verdyan, A., Moshkovich, A., Feldman, Y., & Tenne, R. (2005). Behavior of fullerene-like WS₂ nanoparticles under severe contact conditions. *Wear*, 259(1-6), 703-707. doi: <http://dx.doi.org/10.1016/j.wear.2005.01.009>
- Rapoport, L., Nepomnyashchy, O., Lapsker, I., Verdyan, A., Moshkovich, A., Feldman, Y., & Tenne, R. (2005). Behavior of fullerene-like WS₂ nanoparticles under severe contact conditions. *Wear*, 259, 703-707.
- Rech, J., & Moisan, A. (2003). Surface integrity in finish hard turning of case-hardened steels. *International Journal of Machine Tools and Manufacture*, 43(5), 543-550. doi: [http://dx.doi.org/10.1016/S0890-6955\(02\)00141-4](http://dx.doi.org/10.1016/S0890-6955(02)00141-4)
- Reddy, N. S. K., & Nouari, M. (2011). The influence of solid lubricant for improving tribological properties in turning process. *Lubrication Science*, 23(2).
- Reddy, N. S. K., Nouari, M., & Yang, M. (2010). Development of electrostatic solid lubrication system for improvement in machining process performance. *International Journal of Machine Tools & Manufacture*, 50, 789-797.
- Reddy, N. S. K., & Rao, P. V. (2005). A genetic algorithmic approach for optimization of surface roughness prediction model in dry milling. *An international Journal of Machining Science and Technology*, 9(1), 63-84.
- Reddy, N. S. K., & Rao, P. V. (2006). Experimental investigation to study the effect of solid lubricants on cutting forces and surface quality in end milling. *International Journal of Machine Tools & Manufacture*, 46, 189-198.
- Reddy, N. S. K., & Rao, P. V. (2006). Experimental Investigation to study the effect of solid lubricants on cutting forces and surface quality in end milling. *International Journal of Machine Tool & Manufacture*, 46, 189-198.
- Reddy, S. K. N., & Rao, O. V. (2005). Performance improvement of end milling using graphite as a solid lubricant. *Material Manufacturing Process*, 20(2), 1-14.
- S.Shaji, & V.Radhakrishnan. (2002). Investigations on the application of solid lubricants in grinding. *Proc.Inst.Mech.Eng.P.BJ.Eng.Manuf.*, 216, 1325-1343.
- Sadeghi, M. H., Hadad, M. J., Tawakoli, T., Vesali, A., & Emami, M. (2010). An investigation on surface grinding of AISI 4140 hardened steel using minimum quantity lubrication-MQL technique. *International Journal of Material Forming* 3(4), 241-251. doi: 10.1007/s12289-009-0678-3
- Sarhan, A., Sayed, R., Nassr, A. A., & El-Zahry, R. M. (2001). Interrelationships between cutting force variation and tool wear in end-milling. *Journal of Materials Processing Technology*, 109, 229-235.
- Sarhan, A. A. D., M.Sayuti, & Hamdi, M. (2011). Reduction of power and lubricant oil consumption in milling process using a new SiO₂ nanolubrication system. *International Journal of Advanced Manufacturing Technology*, DOI: 10.1007/s00170-00012-03940-00177.
- Sarhan, A. A. D., & Matsubara, A. (2011). Compensation Method of the Machine Tool Spindle Thermal Displacement for Accurate Monitoring of Cutting Forces. *International Journal of Materials and Manufacturing Processes*, 26(12), 1511-1521. doi: DOI: 10.1080/10426914.2010.544825

- Sarhan, A. A. D., & Matsubara, A. (2011). Compensation Method of the Machine Tool Spindle Thermal Displacement for Accurate Monitoring of Cutting Forces. *International Journal of Materials and Manufacturing Processes*, Volume 26(Issue 12), 1511-1521 DOI: 1510.1080/10426914.10422010.10544825. doi: DOI: 10.1080/10426914.2010.544825
- Sayuti, M., Sarhan, A. A. D., Fadzil, M., & Hamdi, M. (2011). Enhancement and verification of a machined surface quality for glass milling operation-using CBN grinding tool- Taguchi approach. *International Journal of Advanced Manufacturing Technology*. doi: DOI: 10.1007/s00170-011-3657-z
- Sayuti, M., Sarhan, A. A. D., & Hamdi, M. (2011). Experimental Study on Minimizing the Edge Chipping in Glass Milling Operation using an Internal CBN Grinding Tool. *International Journal of Materials and Manufacturing Processes*, , 26(8), 969-976. doi: DOI: 10.1080/10426914.2010.530533
- Senthil Kumar, A., Raja Durai, A., & Sornakumar, T. (2003). Machinability of hardened steel using alumina based ceramic cutting tools. *International Journal of Refractory Metals and Hard Materials*, 21(3-4), 109-117. doi: [http://dx.doi.org/10.1016/S0263-4368\(03\)00004-0](http://dx.doi.org/10.1016/S0263-4368(03)00004-0)
- Shaji, S., & Radhakrishnan, V. (2002). An investigation on surface grinding using graphite as lubricant. *International Journal of Machine Tool & Manufacture*, 42(6), 733-740.
- Shaji, S., & Radhakrishnan, V. (2003). An investigation on solid lubricant moulded grinding wheels. *International Journal of Machine Tool & Manufacture*, 43(9), 965-972.
- Sharma, V. S., Dogra, M., & Suri, N. M. (2009). Cooling techniques for improved productivity in turning. [doi: DOI: 10.1016/j.ijmachtools.2008.12.010]. *International Journal of Machine Tools and Manufacture*, 49(6), 435-453.
- Shen, B. (2008). *Minimum Quantity Lubrication Grinding using Nanofluids*. Doctor of Philosophy, The University of Michigan.
- Shen, B., Kalita, P., Malshe, A., & Shih, A. (2008). Performance of novel MoS₂ nanoparticles based grinding fluids in minimum quantity lubrications grinding. *Trans. NAMRI/SME*, 36, 357-364.
- Shenoy, B. S., Binu, K. G., Pai, R., Rao, D. S., & Pai, R. S. (2012). Effect of nanoparticles additives on the performance of an externally adjustable fluid film bearing. [doi: 10.1016/j.triboint.2011.10.004]. *Tribology International*, 45(1), 38-42.
- Singh, D., & Rao, P. V. (2008). Performance improvement of grinding of SiC using graphite as solid lubricant. *The International Journal of Advanced Manufacturing Technology*, 38, 529-535.
- Sreejith, P. S., & Ngoi, B. K. A. (2000). Dry machining: Machining of the future. [doi: DOI: 10.1016/S0924-0136(00)00445-3]. *Journal of Materials Processing Technology*, 101(1-3), 287-291.
- Street, K. W., Marchetti, M., Wal, R. L. V., & Tomasek, A. J. (2004). Evaluation of the tribological behavior of nano-onions in Krytox 143AB. *Tribology Letters*, 16, 143-149.
- Suresh Kumar Reddy, N., & Venkateswara Rao, P. (2006). *Enhancement of machinability of AISI1045 steel using molybdenum disulphide as a solid lubricant*. Paper presented at the 2006 ASME International Mechanical Engineering Congress and Exposition, IMECE2006, November 5, 2006 - November 10, 2006, Chicago, IL, United states.

- Tan, X. C., Liu, F., Cao, H. J., & Zhang, H. (2002). A decision-making framework model of cutting fluid selection for green manufacturing and a case study. [doi: DOI: 10.1016/S0924-0136(02)00614-3]. *Journal of Materials Processing Technology*, 129(1-3), 467-470.
- Tawakoli, T., Hadad, M. J., Daneshi, A., Sadeghi, M. H., & Sadeghi, B. (2011). Study on the effects of abrasive and coolant-lubricant types on minimum quantity lubrication-MQL grinding. *Advanced Materials Research*, 325, 231-237.
- Tawakoli, T., Hadad, M. J., & Sadeghi, M. H. (2010). Influence of oil mist parameters on minimum quantity lubrication – MQL grinding process. *International Journal of Machine Tools and Manufacture* 50(6), 521-531. doi: <http://dx.doi.org/10.1016/j.ijmachtools.2010.03.005>
- Tawakoli, T., Hadad, M. J., & Sadeghi, M. H. (2010). Investigation on minimum quantity lubricant-MQL grinding of 100Cr6 hardened steel using different abrasive and coolant–lubricant types. *International Journal of Machine Tools and Manufacture* 50(8), 698-708. doi: <http://dx.doi.org/10.1016/j.ijmachtools.2010.04.009>
- Tawakoli, T., Hadad, M. J., Sadeghi, M. H., Daneshi, A., Stöckert, S., & Rasifard, A. (2009). An experimental investigation of the effects of workpiece and grinding parameters on minimum quantity lubrication—MQL grinding. *International Journal of Machine Tools and Manufacture* 49(12–13), 924-932. doi: <http://dx.doi.org/10.1016/j.ijmachtools.2009.06.015>
- Thepsonthi, T., Hamdi, M., & Mitsui, K. (2009). Investigation into minimal-cutting-fluid application in high-speed milling of hardened steel using carbide mills. [doi: DOI: 10.1016/j.ijmachtools.2008.09.007]. *International Journal of Machine Tools and Manufacture*, 49(2), 156-162.
- Thepsonthi, T., Hamdi, M., & Mitsui, K. (2009). Investigation into minimal-cutting-fluid application in high-speed milling of hardened steel using carbide mills. *International Journal of Machine Tools & Manufacture*, 49(2009), 156-162.
- Thottackad, M., Perikinalil, R., & Kumarapillai, P. (2012). Experimental evaluation on the tribological properties of coconut oil by the addition of CuO nanoparticles. *International Journal of Precision Engineering and Manufacturing*, 13(1), 111-116. doi: 10.1007/s12541-012-0015-5
- Tönshoff, H., & Denkena, B. (2013). *Cooling Lubrication Basics of Cutting and Abrasive Processes* (pp. 371-396): Springer Berlin Heidelberg.
- Trent, E. M., & Wright, P. K. (2000). *Metal Cutting* (Fourth ed.): Butterworth-Heinemann.
- Tu-Chieh, H., & Yaw-Terng, S. (2006). A method for reducing tool wear in a polishing process. *International Journal of Machine Tools & Manufacture*, 46, 413-423.
- Tu-Chieh, H., & Yaw-Terng, S. (2006). A method for reducing tool wear in a polishing process. *International Journal of Machine Tools & Manufacture*, 46, 413-423.
- Ueda, T., Hosokawa, A., Oda, K., & Yamada, K. (2001). Temperature on Flank Face of Cutting Tool in High Speed Milling. *CIRP Annals - Manufacturing Technology*, 50(1), 37-40. doi: [http://dx.doi.org/10.1016/S0007-8506\(07\)62065-4](http://dx.doi.org/10.1016/S0007-8506(07)62065-4)
- Vamsi Krishna, P., Srikant, R. R., Padmini, R., & Parakh, B. (2012). Basic Properties and Performance of Vegetable Oil-Based Boric Acid Nanofluids in Machining. In S. Sathiyamoorthy, B. E. Caroline & J. G. Jayanthi (Eds.), *Emerging Trends in Science, Engineering and Technology* (pp. 197-206): Springer India.
- Venkata Rao, R. (2011). Environmental Aspects of Manufacturing Processes *Advanced Modeling and Optimization of Manufacturing Processes* (pp. 339-360): Springer London.

- Wakabayashi, T., Suda, S., Inasaki, I., Terasaka, K., Musha, Y., & Toda, Y. (2007). Tribological Action and Cutting Performance of MQL Media in Machining of Aluminium. *Annals of the CIRP*, 56/1.
- Weinert, K., Inasaki, I., Sutherland, J. W., & Wakabayashi, T. (2004). Dry Machining and Minimum Quantity Lubrication. [doi: DOI: 10.1016/S0007-8506(07)60027-4]. *CIRP Annals - Manufacturing Technology*, 53(2), 511-537.
- Williams, J. A. (2005). Wear and wear particles—some fundamentals. [doi: 10.1016/j.triboint.2005.03.007]. *Tribology International*, 38(10), 863-870.
- Wu, Y. Y., Tsui, W. C., & Liu, T. C. (2007). Experimental analysis of tribological properties of lubricating oils with nanoparticle additives. [doi: DOI: 10.1016/j.wear.2006.08.021]. *Wear*, 262(7-8), 819-825.
- Wu, Y. Y., Tsui, W. C., & Liu, T. C. (2007). Experimental analysis of tribological properties of lubricating oils with nanoparticle additives. *Wear*, 262(7-8), 819-825. doi: <http://dx.doi.org/10.1016/j.wear.2006.08.021>
- X.Tao, Z.Jiazheng, & Kang, X. (1996). The ball-bearing effect of diamond nanoparticles as an oil additive. *J.Phys. D Appl. Phys.*, 29, 2932-2937.
- Xiaodong, Z., Xun, F., Huaqiang, S., & Zhengshui, H. (2007). Lubricating properties of Cynex 302-modified MoS₂ microsphere in base oil 500SN. . *Lubrication Science*, 19, 71-79.
- Yan, J., Zhang, Z., & Kriyagawa, T. (2010). Effect of nano-particle lubrication in diamond turning of reaction-bonded SiC.
- Yan, J., Zhang, Z., & Kriyagawa, T. (2011). Effect of nano-particle lubrication in diamond turning of reaction-bonded SiC. *International Journal of Automation Technology*, Vol.5(No.3), pp. 307-312.
- Yousefi, R., & Ichida, Y. (2000). A study on ultra - high-speed cutting of aluminium alloy: Formation of welded metal on the secondary cutting edge of the tool and its effects on the quality of finished surface. *Journal of the International Societies for precision Engineering and Nanotechnology*, 24, 371-376.
- Zhang, B.-S., Xu, B.-S., Xu, Y., Gao, F., Shi, P.-J., & Wu, Y.-X. (2011). CU nanoparticles effect on the tribological properties of hydrosilicate powders as lubricant additive for steel-steel contacts. [doi: 10.1016/j.triboint.2011.03.002]. *Tribology International*, 44(7-8), 878-886.
- Zhang, J. Z., Chen, J. C., & Kirby, E. D. (2007). Surface roughness optimization in an end-milling operation using the Taguchi design method. *Journal of Materials Processing Technology* 184(1-3), 233-239. doi: <http://dx.doi.org/10.1016/j.jmatprotec.2006.11.029>
- Zhang, Z., Yan, J., & Kuriyagawa, T. (2011). Study on tool wear characteristics in diamond turning of reaction-bonded silicon carbide. *International Journal of Advanced Manufacturing Technology*, 57, 117-125.
- Zhou, J., Yang, J., Zhang, Z., Liu, W., & Xue, Q. (1999). Study on the structure and tribological properties of surface-modified Cu nanoparticles. *Mater. Res. Bull.*, 34(9), 1361-1367.

LIST OF PUBLICATION

1. M. Sayuti, Ahmed A. D. Sarhan, Tomohisa Tanaka, M. Hamdi, Yoshio Saito, Cutting force reduction and surface quality improvement in machining of aerospace duralumin AL-2017-T4 using carbon onion nanolubrication system, International Journal of Advanced Manufacturing Technology, 2012 "Published" (*ISI-Cited Publication*)
2. Ahmed A. D. Sarhan, M. Sayuti, M. Hamdi. Reduction of power and lubricant oil consumption in milling process using a new SiO₂ nanolubrication system -International Journal of Advanced Manufacturing Technology, 2012 "Published" (*ISI-Cited Publication*)
3. Sayuti, M., Sarhan, A. D., & Hamdi, M. An investigation of optimum SiO₂ nanolubrication parameters in end milling of aerospace Al6061-T6 alloy. The International Journal of Advanced Manufacturing Technology, 2012. "Published" (*ISI-Cited Publication*)
4. Mohd Sayuti Ab Karim, Ahmed Aly Diaa Mohammed Sarhan, Mohd Hamdi Abd Shukor, Surface quality improvement in CNC end milling of aluminium alloy using nanolubrication system, IAENG Transactions on Engineering Technologies, 2012, Springer Publication
5. M. Sayuti, Tomohisa Tanaka, Ahmed A. D. Sarhan, Yoshio Saito, M. Hamdi, Surface quality improvement in CNC end milling of aerospace AL-2017-T4 alloy using carbon onion nanolubrication with DLC cutting tool, July 4-6, World Congress Engineering 2012, London, U.K (WCE 2012)
6. M. Sayuti, Tomohisa Tanaka. An investigation of onion like carbon lubrication performance for cutting force in end milling process – 3rd Multidisciplinary International Student Workshop, August 4-5, 2011, Tokyo Institute Technology, Tokyo, Japan. (MISW 2011)
7. M. Sayuti, Ahmed A. D. Sarhan, M. Hamdi, M. E. Ooi. Development of nanoparticle suspended lubrication system in machining process for less power consumption and pollution, United Kingdom-Malaysia-Ireland Engineering Science Conference 2011(UMIES 2011).
8. M. Sayuti, Ahmed. A. D. Sarhan, M. Hamdi "Effect of SiO₂ nano base lubrication system on the tool wear and surface roughness in hard turning process of hardened steel AISI4140, Machining Science and Technology, "Under review" (*ISI-Cited Publication*)
9. M. Sayuti, Ahmed. A. D. Sarhan, M. Hamdi "Investigate the machining performance in end milling of aerospace AL 6061-T6 using SiO₂ nanolubrication Fuzzy logic base approach, Machining Science and Technology, "Under review" (*ISI-Cited Publication*)
10. Bizhan Rahmati, Ahmed A. D. Sarhan, M. Sayuti, Investigation the optimum molybdenum disulfide (MoS₂) nanoparticle suspended lubrication parameters for machining AL6061-T6 operating CNC High speed milling machine process, International Journal of Advanced Manufacturing Technology, "Under review" (*ISI-Cited Publication*)
11. M. Sayuti, Ahmed. A. D. Sarhan, M. Hamdi "Investigate the possibility of using carbon onion nanolubrication with DLC cutting to reduce the machining power consumption" International Journal of Advanced Manufacturing Technology, "Under review" (*ISI-Cited Publication*)

PATENTS

1. A Nano Liquid Lubrication Composition and its Preparation Method (PI2012701070)

AWARDS

1. Gold Medal - An Inorganic Nano Base Lubrication System to be Used in Heavy Duty Industrial Machining , Malaysian Technology Expo (MTE 2013), 21-23 feb 2013, PWTC Kuala Lumpur.
2. Best Student Paper Award of The 2012 International Conference of Manufacturing Engineering and Engineering Management (ICMEEM 2012), “Surface Quality Improvement in CNC End Milling Machined Aerospace AL-2017-T4 Alloy using Carbon Onion Nanolubrication with DLC Cutting Tool”, World Congress Engineering (WCE 2012), 4-6th July 2012, London.
3. Consolation Award - Engineering Invention & Innovation Exhibition, Newly Nanolubrication System in CNC Machining Processes for Better Product Quality, More Power Savings and Less Oil Consumption and Pollution, EINIX 2012.